INVESTIGATING THE EFFECT OF CRYO TREATED TOOL AND WORK MATERIAL IN ULTRASONIC MACHINING OF TITANIUM ALLOYS.

A THESIS

Submitted in fulfillment of the requirements
for the award of the degree of

DOCTOR OF PHILOSOPHY

in

MECHANICAL ENGINEERING

By

GAURAV KUMAR DHURIA
Registration. No. 950808008

THAPAR INSTITUTE OF ENGINEERING & TECHNOLOGY
(Deemed to be University)
PATIALA-147004, INDIA

PREFACE

This research work was carried out by the author under the guidance of Dr. Ajay Batish, Professor, Department of Mechanical Engineering, Thapar University, Patiala and Dr. Rupinder Singh, Professor, Department of Production Engineering, Guru Nanak Dev Engineering College, Ludhiana.

The experimentation for the presented work was carried out on Ti-6Al-4V titanium alloy to explore the effect of six process parameters on machining response variables such as material removal rate, tool wear rate, surface roughness and dimensional accuracy. Sonic Mill 500W Ultrasonic Machine Tool available in the Mechanical Engineering Department at Thapar University, Patiala was used for experimentation.

Following articles have been published from the presented work:

1. Gaurav Kumar Dhuria, Rupinder Singh, Ajay Batish (2016) Predictive modeling of surface roughness in ultrasonic machining of cryogenic treated Ti-6Al-4V. *Engineering Computations,* 33 (8) 2377 – 2394 (SCIE - Impact Factor 0.691).
2. Gaurav Kumar Dhuria, Rupinder Singh, Ajay Batish,(2016) Application of a hybrid Taguchi-entropy weight-based GRA method to optimize and neural network approach to predict the machining responses in ultrasonic machining of Ti–6Al–4V. *J Braz. Soc. Mech. Sci. Eng.,* 39 (7) 2619-2634 (SCIE – Impact Factor 0.963).
3. Rupinder Singh, Gaurav Kumar Dhuria, Ajay Batish (2017) Effect of Cryogenic Treatment on Ultrasonic Machining of Titanium and Its Alloys: A Review, *Reference Module in Materials Science and Materials Engineering,* http://dx.doi.org/10.1016/B978-0-12-803581-8.04157-6.
4. Gaurav Kumar Dhuria, Rupinder Singh, Ajay Batish (2016) Process capability study in ultrasonic drilling of Ti-6Al-4. *Proc. of Internatonal Conference on Production and Industrial Engineering,* Dec 19-21, 2016 NIT Jalandhar.
5. Gaurav Kumar Dhuria, Rupinder Singh, Ajay Batish (2011) Ultrasonic machining of titanium and its alloys: a state of art review and future prospective. *Int. J. of Machining and Machinability of Materials,* 10 (4) 326 – 355.

CERTIFICATE

Certified that the thesis entitled "**Investigating the effect of cryo treated tool and work material in ultrasonic machining of Titanium alloys**" being submitted by Gaurav Kumar Dhuria, (Univ. Regn. No. 950808008) to Mechanical Engineering Department, Thapar Institute of Engineering & Technology (Deemed to be University), Patiala in fulfillment of the requirement for award of degree of Doctor of Philosophy, is an authentic record of research work carried out by him under our guidance and supervision. The matter presented in the thesis has not been submitted in part or full to any other University or Institute for award of any degree.

Dr. Ajay Batish
Professor
Mechanical Engineering Department
TIET, Patiala

Dr. Rupinder Singh
Professor
Department of Production Engineering
GNDEC, Ludhiana

ACKNOWLEDGEMENT

I take this opportunity to express my sincere, heartfelt gratitude and adulation to my supervisors **Dr. Ajay Batish**, Professor, Department of Mechanical Engineering and Dean, Partnerships and Accreditation, Thapar University, Patiala and **Dr. Rupinder Singh**, Professor, Department of Production Engineering and Dean, Academics, Guru Nanak Dev Engineering College, Ludhiana for their invaluable guidance, persistent inspiration and immense cooperation in accomplishing the present work. The work would not have been possible without their constant motivation, constructive suggestions and thought provoking discussions. In the times of adversities they were always there to uplift the morale and ensured my focus on the target. It has been a blessing to work under their mentoring and I thank the Almighty for providing me the opportunity for the same.

No work is possible without the blessings of parents and I am lucky to have such affectionate and caring revered parents who motivated and showered their unconditional love and blessings that were instrumental in completion of the work.

I express my sincere gratitude to Prof. Prakash Gopalan, Director, Thapar University, Patiala, for providing the required institutional and infrastructure facilities and supporting the work. I am extremely thankful to Dr. O. P. Pandey, Dean, Research and Sponsored Projects, Thapar University, Patiala, Dr. S. K. Mohapatra, Head, Mechanical Engineering Department, Dr. Vinod Kumar, Associate Prof., Mechanical Engineering Department and Dr. Tarun Nanda, Ph. D. Coordinator for their continuous encouragement, invaluable suggestions and kind support during the course of the work.

I am highly indebted to Dr. Manoj Kumar, Principal, DAVIET, Jalandhar for his continuous support at the work place. I am extremely grateful to Prof. C. L. Kochher, former Director, DAVIET, Jalandhar for inspiring and supporting me to complete the work.

I express my sincere gratitude to Sh. Narinder Singh and Sh. Sukhbir Singh, Mechanical Engineering Department, Thapar University for their cooperation and assistance during the work. I am also thankful to Sh. Trilok Singh, Retd. Lab Superintendent, Thapar University Patiala, for his technical inputs.

I take this opportunity to express my profound gratitude to Sh. Riyaz Amin, Proprietor, Cryonet, Surat, Mr. Nitin Joshi, Bhukhanwala Industries Pvt. Ltd., Mumbai, Mr. H.S.K. Alva, Manager, Snam Abrasives, Hosur, Mr. Vivek Aggarwal, Krishna Micro Abrasives for material and processing support to accomplish the work.

I am extremely indebted to Mr. Charlie Wilhite, Mr. Clyde Treadwell and Mr. Bill Brenn from Sonic Mill, Albuquerque for their technical advice and support during the work.

The work would have been very difficult without the technical support and guidance of my friend Sh. M. R. Sallan, Assistant Director, CIHT, Jalandhar. I also express my heartfelt gratitude to Sh. Bachittar Singh for technical advice and support.

A special mention and admiration needs to be made of my wife Mrs. Puja Dhuria for her continuous inspiration and unconditional support that enabled me complete the work. Our new born, Vardaan, has been the best gift of the Almighty and I am thankful to the mother and the baby for their support and understanding. I am extremely grateful to my sister Mrs. Suman Girdhar and brother-in-law Dr. Akshay Girdhar for their immense support and for inspiring and motivating me to complete the work.

I want to express my sincere thanks to all those who directly or indirectly helped me during the course of research work.

Above all, I bow before the **Almighty God**, whole heartedly thanking and expressing my indebtedness for all His blessings, kindness and for not letting me down at the time of crisis.

(Gaurav Kumar Dhuria)

CONTENTS

LIST OF FIGURES

LIST OF TABLES

LIST OF ABBREVIATIONS

Adj. MS	Adjusted Mean of Square
AHP	Analytical Hierarchical Process
ANN	Artificial Neural Network
ANOVA	Analysis of Variance
ASTM	American Society for Testing and Materials
BP	Back Propagation
CT	Cryogenic Treatment
DCT	Deep Cryogenic Treatment
DOE	Design of Experiments
DOF or dof	Degrees of Freedom
F	Variance Ratio
GRA	Grey Relational Analysis
GRG	Grey Relational Grade
HCS	High Carbon Steel
HOS	Hole Oversize
LM	Levenberg Marquadt
MRR	Material Removal Rate
OA	Orthogonal Array
OFAT	One Factor at a Time
RUM	Rotary Ultrasonic Machining
S/N	Signal to Noise
SCT	Shallow Cryogenic Treatment
SEM	Scanning Electron Microscopy
Seq. SS	Sequential Sum of Squares
SR	Surface Roughness
SS	Stainless Steel
TG	Tolerance Grade
TWR	Tool Wear Rate
USM	Ultrasonic Machining
UT	Untreated

ABSTRACT

Ultrasonic machining is a non-traditional, but established mechanical material removal process, generally suitable for hard and brittle materials such as quartz, ceramics, glass, semiconductors etc., carried out using shaped tools, high frequency mechanical motion and an abrasive slurry. USM neither involves chemical reaction nor is of thermal type and is also suitable for machining of electrically non-conductive and brittle work piece materials which are generally difficult to machine by conventional machining methods.

Titanium is the fourth most abundant structural metal and ninth most abundant element in the earth's crust. Titanium has been recognized as an element (Symbol Ti; atomic number 22; and atomic weight 47.9) for at least 200 years. Despite of being a difficult to machine material due to high chemical reactivity, tendency to weld to cutting tool, poor thermal conductivity that leads to accumulation of heat near the cutting edge of the tool, high retained strength and hardness at elevated temperature and low modulus of elasticity, titanium and its alloys find wide applications in aerospace, chemical, automotive, petroleum, medical and sporting goods industry. Commercially pure titanium alloys (ASTM Grades 1–4, 7, 11) are used mainly for their corrosion resistance properties in applications requiring adequate strength while high-strength alloyed forms are sub graded into three main groups: α – alloys, β- alloys and αβ – alloys and are used mostly for their superior strength-to-weight ratios and good corrosion resistance for applications in aerospace, automotive, and biomedical sector. The most popular of these, accounting for more than 50% of titanium usage worldwide and extensively used in aircraft construction for parts under low thermal stress, is Ti-6Al-4V that belongs to αβ- alloys. Using appropriate cutting tools with high hot hardness, good thermal conductivity, chemical inertness and high strength in conventional machining and use of non-conventional methods such as EDM can offer solution to these problems. Machining of Titanium with USM has also been reported by some authors.

Cryogenic treatment is an inexpensive, one time, permanent treatment affecting the entire section of component unlike coatings. Cryogenic treatment is an add on process over conventional heat treatment wherein samples are cooled down to prescribed cryogenic temperature level at slow rate, maintained at this temperature for a long time and then brought back to room temperature. Depending upon the lowest temperature to which the

material is carried, cryogenic treatment is classified as Shallow Cryogenic Treatment (SCT) or Deep Cryogenic Treatment (DCT). The lowest temperature in the former is 193K which is near to temperature of dry ice while for the later it is 77K that is at the liquefying temperature of nitrogen.

The current study was envisaged to explore the effect of cryogenic treatment together with other machining parameters on response variables such as MRR, TWR, SR, HOS and Tolerance Grades in ultrasonic machining of Ti-6Al-4V alloy. A preliminary pilot experimentation was carried out wherein various input factors were varied at several levels with one factor at a time approach. Finally the experimentation was carried out with the use of Design of Experiments (DOE) using Taguchi's L_{18} Orthogonal Array. Based on the results of pilot experimentation and the objectives of the study, six factors comprising of USM power, abrasive slurry type, slurry grit size, tool material and type of cryogenic treatment given to tool and work material were selected for investigation in the DOE phase for measurement of five response variables viz Material Removal Rate (MRR), Tool Wear Rate (TWR), Surface Roughness (SR), Hole Oversize (HOS) and Tolerance Grades (TG). Whereas MRR was a higher the better characteristic, TWR, HOS and SR were lower-the-better characteristics in the measurement of response variables.

Among the five response variables, MRR was found to increase with increase in USM power and size of abrasive particles in the slurry owing to larger momentum associated with higher power and coarser particles. Stainless steel tool was found to form the best combination with the work material for maximum MRR. Harder abrasive slurry of boron carbide was also the most superior for increased MRR. USM power rating, type of abrasive slurry, tool material and abrasive grit size were found to be the significant parameters affecting material removal rate in ultrasonic machining of Ti-6Al-4V in the order of percentage contribution starting from highest. The optimum combination resulted from the design of experiments for maximum MRR corresponded to 400W of USM power, Boron Carbide Slurry, Stainless Steel tool material with #220 abrasive grit size using untreated tool material and cryogenic treated work material. However, tool wear was also found to increase at most of the points of maxima for MRR and was also found to be strongly determined by relative tool work-piece hardening. Increased power, coarser abrasive particles and harder slurry caused higher tool wear on the similar lines as with MRR. Titanium was found to minimize the tool wear while cryogenic treatment also significantly reduced the tool wear in USM. The optimum setting for minimum tool wear rate was thus obtained corresponding to aluminium oxide slurry, titanium tool, 100W power, #500 abrasive grit size, deep cryogenic treated tool material and untreated work material.

Surface roughness was significantly affected by abrasive particle size wherein the coarser particles led to bigger indentations causing poor surface finish. Higher power rating and harder tool were also associated with increased surface roughness which improved marginally with cryogenic treatment of the workpiece. Minimum surface roughness, and hence the best surface quality, was obtained when machining with aluminium oxide slurry, titanium tool, 20W power rating, #500 grit size and deep cryogenic treated tool and work-piece. Abrasive particle size was the dominating factor in establishing the hole oversize and hence tolerance grades. Bigger particle size led to bigger gap between tool and workpiece on the hole entrance causing oversize. Hole oversize was found to depend on rate of machining as well. Factors such as high power and coarser abrasives that lead to increased MRR also resulted in increased HOS. On the other hand HOS was also relatively more corresponding to lower power rating as compared to little higher values due to slow rate of machining. This means an optimum machining rate is essential to obtain minimum HOS. Accordingly, coarse grains, high power and hard tool material were associated with poor tolerance grades as well. The obtained tolerance grades ranged from IT 12 to IT 15. SEM Micrographs have been used to identify fracture at machined surface that comprised of brittle as well as ductile mode.

The four responses have been modeled using ANN with appropriate network architecture. The correlation coefficient and deviation of ANN predicted results from the experimental results has been shown using appropriate graphs. Single hidden layer 6-7-1 neural network architecture based on LM algorithm using log-sigmoid and pure linear activation function for hidden and output layer respectively was able to effectively model the MRR, TWR and SR. The developed model exhibited reasonable accuracy of prediction within the range of the varied parameters.

Entropy weight based Grey Relational Analysis hybridized with Taguchi's methodology was used to optimize MRR and TWR. Subsequently, Analytical Hierarchical Process (AHP) for optimization was used to optimize the four responses together (MRR, TWR, SR and HOS). Weights were generated, firstly for the four responses and subsequently for the experimental outputs of all the responses as per the underlying theories of AHP.

CHAPTER – 1

INTRODUCTION

There has been a constant endeavor, propelled by the need though, ever since the evolution of mankind, to convert available resources into useful ones be it in form of food articles or energy conversion or use of tools to create articles that are essential for easy and smooth life. Over the years both the tools and the energy sources to power these tools have been reincarnated and re-designed to meet the challenging demand associated with complexity of jobs desired by the mankind. From the era when the tools were powered by muscular power of man and animals to the present day of automated machine tools, indeed the human race has traversed a huge distance largely due to developments in energy sources and technology in a broader view. If the maiden universal milling machine developed in 1862 by J. R. Brown for cutting helical flutes of twist drills and the turret lathe of nineteenth century for automatic production of screws were a revolution in manufacturing sector, the introduction of technology in Numerical Control during 1953 opened the doors towards enhanced product accuracy and uniformity [1]. Due to rapid growth in electronics and computer industry several developments have continued in machining processes and related machine tools during the last 50 years.

With the advancements in new engineering materials possessing improved thermal, chemical and mechanical properties, low rigidity structures and production of complex shapes and micromachined components with high tolerances and fine surface quality, traditional machining methods often become ineffective. Advancements in aviation and aerospace industry in particular have sought the development of new materials and composites with superior strength to weight ratio. Need of bio-materials where compatibility with body tissues and life of insertion are the critical issues has also led to development of several such new materials. Machining and drilling requirements of these materials with requisite quality in terms of surface generated and tolerances and in terms of productivity and economic viability pose serious challenges for conventional available methods. Mishra [2] has highlighted the limitations of conventional machining with several case studies of manufacturing sectors such as those of making blind square holes with high surface finish, circular through holes with very large L/D ratio (greater than 30) and contour machining in hard die block materials like WC or stellite. Conventional machining in such cases becomes either un-economical due to increased production times or incapable because of inability to achieve required shape and accuracy. A number of ceramics and composite materials have been developed but the high cost and damage generated during their machining is major obstacle in the implementation of these materials [1]. Fortunately though an equal amount of research has also been carried out in developing the methods suitable for these requirements. The relatively new set of processes, though are existing for more than 50 years, have been termed as non-traditional machining methods owing to their nature of basic operational difference from conventional methods. Whereas in conventional methods the tool material needs to be harder than work material, in some of the non-traditional method machining can be done even in the absence of a physical tool. High cost associated with machining ceramics and composites together damage generated during conventional machining hinders the implementation of these materials. Volumetric wear of grinding wheel of the order of 50-200 times have restricted the use of classical grinding to very limited use for manufacturing of Polycrsyatlline Diamond (PCD) based tools [1]. To meet such demands, these non-traditional processes which have been categorized into Mechanical, Thermal, Chemical and Electrochemical processes based on the inherent method employed to transfer energy required for machining, are being used extensively these days. Each process within these categories has its own characteristic attributes and limitations, hence no one process is the best for all manufacturing situations.

Currently non-traditional processes possess virtually unlimited capabilities compared to conventional processes, except for volumetric material removal rates. Though over the years great advances have been made in increasing the same as well [3]. While in some cases these non-traditional machining processes are applied to increase productivity by reducing the number of overall manufacturing operations required to produce a product, in other cases, these are used to reduce the number of rejects experienced by the traditional manufacturing method by increasing repeatability, reducing in-process breakage of fragile work pieces, or by minimizing detrimental effects on work piece properties.

Usage and applications of non-traditional manufacturing processes will continue to grow in the years to come as manufacturing engineers, product designers, and metallurgical engineers become increasingly aware of the unique capabilities and advantages offered by these processes.

1.1 CLASSIFICATION OF NON-TRADITIONAL PROCESSES

As specified in previous section, non-traditional processes are classified according to source of energy employed to carry out material removal from the work surface. Thus there are four major categories:

- Mechanical Energy Based Processes: Machining in these processes takes place by mechanical abrasion of abrasive particles energized by ultrasonic vibrations, as in ultrasonic machining (USM), or by high pressure stream of gas or air, as in Abrasive Jet Machining (AJM). Use of water stream and abrasive particles entrained in water stream is also very popular and forms the basis of Water Jet Machining (WJM) and Abrasive Water Jet Machining (AWJM) respectively. Magnetic Abrasive Finishing (MAF), which makes use of magnetic field controlled machining forces through a brush of magnetic abrasives is used for finish machining.
- Thermal Energy Based Processes (Thermo-electric processes): These processes involve melting or vaporizing of workpiece material under the effect of immense localized heating. The resultant heat energy is the result of conversion of kinetic energy of electron beam (Electron Beam Machining, EBM) or energized photons as in case of Laser Beam Machining. However arguably the most popular process of this category is Electric Discharge Machining (EDM) which uses plasma channel through dielectric media between electrically conductive tool and workpiece to raise the temperature at workpiece surface to thousands of degree Celsius.
- Chemical Processes: Chemical dissolution of the exposed material in chemical machining (CHM) and photochemical machining (PCM) under the action of strong etchants forms the basis of these processes. Selective material removal is the key feature of these processes wherein material to be protected is covered with maskants.
- Electrochemical Processes: High current passed through electrolyte between tool and workpiece across small potential difference results in electrochemical dissolution due to ion displacement. These processes work on Faraday’s Law of electrolysis. Electrochemical Machining (ECM), Electrochemical Drilling (ECDR) and Electrochemical Deburring (ECD) are some of the common variants of these processes.

All the aforesaid processes involve only one kind of machining action for removal of material from work surface. Technological improvements in these processed have been accomplished by combining two or more machining actions to evolve hybrid machining processes [1]. The combination infuses advantages of two different mechanisms thereby improving the machining prospects. Some of the common hybrid machining processes are

Laser Assisted Electrochemical Machining, Ultrasonic assisted Electric Discharge Machining, Electro Discharge Erosion etc.

Some of these non-traditional processes such as EDM, USM, ECM, LBM are being used extensively on otherwise difficult to machine materials by conventional methods. The selection of a particular process for a given application is based on several criterion those including desired accuracy, finish and production volumes. Accordingly a comparison with regard to process capability, operational characteristics, compatibility with work material and overall economic considerations are weighed against each other before arriving at decision of process selection.

The current work was aimed at ultrasonic machining of titanium using cryogenic treatment of tool and workpiece. Accordingly the focus of write-up in following section is solely on Ultrasonic Machining Process.

1.2 ULTRASONIC MACHINING (USM)

Ultrasonic machining is a non-traditional, but established mechanical material removal process generally suitable for hard and brittle materials such as quartz, ceramics, glass, semiconductors etc. with the use of shaped tools, high frequency mechanical motion and an abrasive slurry. USM neither involves chemical reaction nor is of thermal type and is also suitable for machining of electrically non-conductive and brittle work piece materials which are generally difficult to machine by conventional machining methods. The process involves conversion of low frequency electrical energy to a high frequency electrical signal using a suitable power generator and then converting this high frequency electrical signal into high frequency mechanical vibrations of the order of 20 kHz using a magnetostrictive or piezoelectric transducer. The vibrations are amplified and transmitted through a horn to the tool [4,5]. The tool vibrates in parallel direction to the axis of tool feed and the total excursion being only a few hundredths of a millimeter [3]. Abrasive slurry composed of an abrasive material like silicon carbide, boron carbide, alumina etc suspended in oil or water is pumped around the cutting zone and a controlled static load is applied to the tool. The material removal takes place in form of micro chipping by the action of abrasive particles held in slurry between tool and work piece under the impact of vibrating tool with static load [5]. The abrasive particles under this impact from the tool strike the work piece with a force which is upto 150000 times their weight. Each impact site by the individual abrasive particle creates a small crater in brittle materials and under the shaped tool when thousands of abrasives impinge upon the workpiece, the desired profile is created by removal of microchips from the surface. This is precisely the reason that the process is also referred to as Ultrasonic Impact Grinding [3]. Holes as small as 76μm in diameter can be machined with USM, however the depth to diameter ratio is generally limited to 3:1 [6]. Micro-USM could be a good alternative to micro machining or micro-EDM in metallic glass without causing any heat generation or light emission, crystallization and formation of shear bands. The process has been found to result in good machinability of metallic glass such as $Zr_{60}Cu_{30}Ti_{10}$ [7]. The micro version of the process can be used to develop intricate complex profiles in wide range of materials at micro levels. Cheema et al. have demonstrated the use of the process to develop serpentine micro channels [8].

Figure 1.1 shows basic elements of an Ultrasonic Machining set up involving brazed and screwed tooling [9]. Variations on this basic configuration include Rotary Ultrasonic Machining (RUM), hybrid of USM combined with Electrical Discharge Machining (EDM) and Abrasive Flow Machining (AFM), Ultrasonic assisted conventional and non-conventional machining and non-machining applications like Ultrasonic polishing etc. The machines from USM range from table top sized units to large capacity production machine tools. However regardless of the physical size, all USM machine tools are equipped with common subsystems comprising of power supply unit, transducer unit, tool holder, tool and abrasives slurry circulation system.

USM has been used in its other variants and in conjunction with other machining processes, as illustrated:

- Rotary Ultrasonic Machining (RUM), invented in 1964 [10], is a hybrid machining process that combine material removal mechanism of diamond grinding and ultrasonic machining [11]. The setup is similar to stationary USM except for addition of 0.37 – 0.56 W rotary spindle motor capable of rotating at 5000 rpm and involves the use of rotating diamond plated tools on drilling, milling and threading operations [3,5].

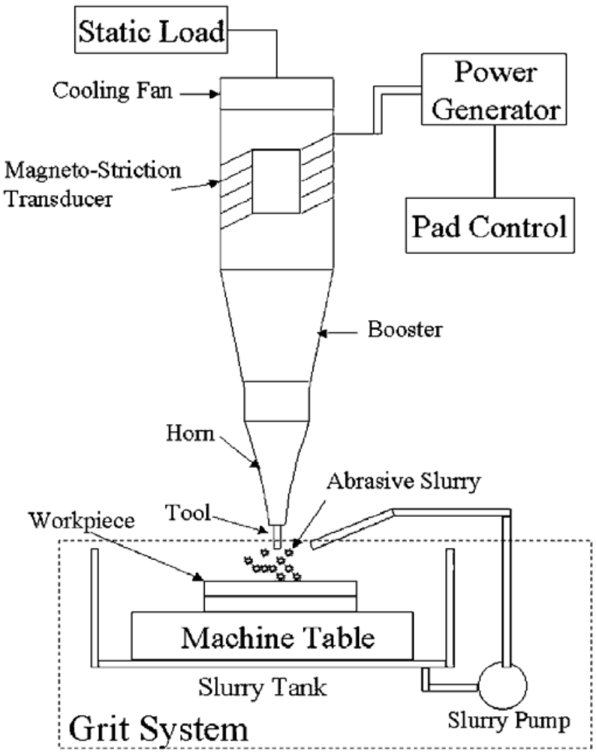

Figure 1.1 Basic elements of ultrasonic machining *[9]*

Churi et al. [12] demonstrated the feasibility of RUM for drilling holes in titanium alloys and concluded that the tool wear, cutting force and surface roughness were significantly better than diamond grinding. Extensive studies on machining of Titanium with RUM and the effect of machining variables, tool variables have been reported by Churi et al. [12,13]. Komaraiah and Reddy [14] and Komaraiah et al. [15] proposed that machining performance of USM in rotary mode is found to be much better than conventional mode.

- Hybrid of USM combined with Electrical Discharge Machining (EDM) and Abrasive Flow Machining (AFM) and Ultrasonic Assisted conventional and non-conventional machining is often used these days. USM assisted turning has been claimed to improve surface quality of titanium alloy with increase in vibration frequency and amplitude. Reduced machining time, workpiece residual stresses and strain hardening and improvement in the surface quality and tool life as compared to conventional turning have been linked with ultrasonic assistance [16,17]. Assisted ultrasonic machining has been established as an efficient technique to improve the machinability of many aeronautic materials such as aluminum or Inconel 738 [18,19]. Problem of hole oversize, drill skidding, surface roughness and circularity have been found to improve considerably in nickel and titanium based super alloys like Inconel 718 with ultrasonic assisted drilling as shown in Fig 1.2 [19]. EDM, though in itself, is very effective in machining all kind of deep, small, inclined and blind holes, however machining small and deep holes in titanium is a problem with EDM because of difficulty in eliminating debris and unsteadiness of machining status [20].

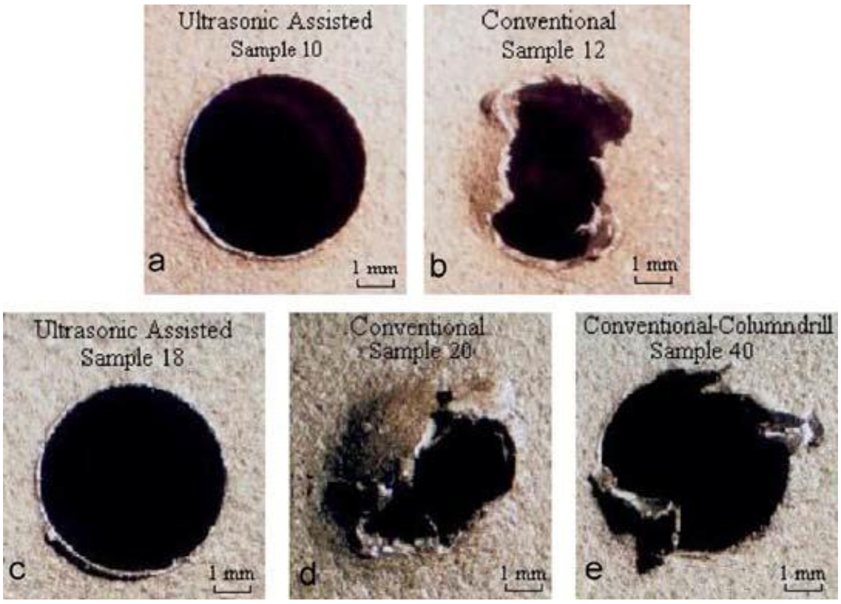

Figure 1.2 Comparison of (a) burr type's samples at drill exit and (b) drill skidding samples at drill entrance in conventional and ultrasonic assisted drilling of Inconel 738 *[19]*

A combination of ultrasonic vibration into deep-hole EDM can improve the machining quality and efficiency [21]. The liquid flow behavior improves substantially by ultrasonic vibrations in EDM and thus avoid the erosion product sedimentation and hence improving effective pulse discharge ratio, machining efficiency and stability. Additionally, combination of a rotating single notch electrode EDM together with ultrasonic vibration EDM eases machining deep and small hole in titanium alloys [20]. MRR while machining titanium alloys with combination EDM/USM process and distilled water as dielectric fluid is higher than conventional EDM process and with a thinner recast layer [22]. Similar results with regard to better material removal rate, low relative electrode wear rate at high peak currents and lower surface roughness have been reported by Chen and Lin [23] with combined EDM and USM process on machining of Al-Zn-Mg alloy with addition of TiC particles in dielectric. The problem of low MRR of EDM in gas has been solved by applying ultrasonic actuation on work piece [24]. Ultrasonic assisted drilling, wherein high frequency (1-200kHz) and low peak to peak magnitude (2-26μm) in the feed direction to the tool or work piece is added, is reported to reduce burr size in drilling by reducing thrust forces and affecting chip formation [25]. Pujana et al. have reported a reduction in cutting force in ultrasonic assisted drilling of Ti-6Al-4V alloy, though with a corresponding increase in tool temperature [26]. Chemical assisted USM has been used to overcome the problem of low MRR and surface quality in machining of glass by addition of Hydrofluoric acid to the abrasive slurry. Reaction of HF with glass causes a weakening of bonding forces on surface and MRR has been found to increase by 200% [27]. Ultrasonic assisted grinding has been shown to reduce the grinding forces significantly and is an efficient method for machining of hard and brittle materials like monocrystal silicon [28]. Application of ultrasonic vibrations have successfully resulted in drilling of micro-holes using Electrochemical machining with cylindrical tool due to improved electrolyte diffusion and that too at a higher machining rate [29]. Ultrasonic vibration assistance led to availability of higher time for discharge activities due to formation of thinner gas film at tool-work interface in Electrochemical Discharge Machining (ECDM) resulting an increased rate of machining [30].

- Non machining ultrasonic applications like cleaning, plastic/metal welding, chemical processing, coating and metal forming

1.3 ELEMENTS OF ULTRASONIC MACHINE TOOL

The basic elements of an ultrasonic machine tool are:

1.3.1 Ultrasonic Power Supply (USM Generator)

The power supply for USM is high power sine-wave generator that offers the user control over both the frequency and power of the generated signal [3]. Reliability, Efficiency and design simplicity are some of the major requirements of USM generator [31]. It converts low-frequency (60 Hz) electrical power to high-frequency (approximately 20 kHz) [32]. This electrical signal is supplied to the transducer for conversion in to mechanical motion [3] [5].

1.3.2 Ultrasonic Transducer

USM transducer converts electrical energy into mechanical vibrations [3,5,33]. The transducer is driven by a signal generator followed by power amplifier. The tool and horn are tuned mechanically and are set by adjusting their dimensions as per the requirements to obtain resonance in a conventional generator system [33]. However in recent years resonance following generators have been developed which are capable of adjusting the output high frequency automatically to match the exact resonance with the horn/tool assembly [34]. These generators are accomplished to accommodate even small error in set up and tool wear, leading to minimum acoustic energy loss and very small heat generation [35].

Two types of transducers often used in USM are Piezoelectric and Magnetostrictive. Mechanical motion in piezoelectric transducers is generated by virtue of the piezoelectric effect exhibited by certain materials such as quartz, lead zirconate titanate etc. due to which they generate an electric potential in response to an applied mechanical stress [36]. Piezoelectric transducers exhibit particularly high electromechanical conversion efficiency (up to 96%) [3,5] and eliminate the need for the water-cooling of the transducer [3,32]. These transducers are available with power capabilities up to 900W. Magnetostrictive transducers on the other hand are constructed from a laminated stack of nickel or nickel alloy sheets that, when influenced by strong magnetic field, have a change in their length. Magnetostrictive transducers offer higher power capacities but low electromechanical conversion efficiency (20 - 35%) [32]. These transducers also require water cooling. Magnetostrictive transducers are most popular and robust amongst all. Coefficient of magnetostrictor elongation ϵ_m is given by:

$$\varepsilon_m = \frac{\Delta l}{l} \qquad \textit{Eq. 1.1}$$

where Δl is incremental change in length of core of magnetostrictor while l is the original length. Higher value of magnetostrictive elongation makes the material suitable for use as magnetostrictor. Alfer (13% Aluminium and 87% ferrous), Hypernik (50% Ni and 50% Fe) and Permalloy (40% Ni and 60% Fe) are some of the common magnetostrictive materials and possess a coefficient of magnetostricive elongation of the order of 40, 25 and 25 respectively [1].

1.3.3 Mechanical Amplifier

The elongation obtained at the magnetostrictor is usually too small for any practical machining applications and hence has to be amplified. The vibration amplitude is further amplified by using an amplifier, referred to as acoustic horn. The horn or concentrator is a wave-guide, which amplifies and concentrates the vibration to the tool tip from the transducer [37]. Horn or tool holder is attached to the transducer through a large, loose-fitting screw. Half hard copper washers are inserted between the transducer and tool holder to dampen and provide cushion to the interface and at the same time reducing the chances of unwanted ultrasonic welding [3]. High mechanical quality factor (measure of transformation of electrical energy into mechanical energy in transducer), high fatigue resistance and a proper attachment to machine to avoid damping and propagation of vibrations, are some of the pre-requisites for an acoustical system (shown in Figure 1.3) to transfer maximum energy to the tool in USM [38]**.** To obtain the highest amplitude of vibration (resonance) concentrator is made in multiples of one-half the wavelength of sound in the respective horn material. Final amplitude is also controlled by the shape of the acoustic horn which is generally manufactures in cylindrical, stepped, exponential, conical and hyperbolic cosine form [39].

Whereas cylindrical horns are non-amplifying, depending upon the requirement, amplitude can be increased by employing one or more type of remaining acoustic horns [1]. Figure 1.4 shows some of the types of tool horns used with conventional ultrasonic machining [40]. Amplifying tool holders are designed to increase the amplitude of the tool stroke by as much as 600% [32]. Figure1.4 shows amplification using two-step acoustic horn. Horn has to be tuned to within few kc/s of the requisite frequency for efficient performance and being a half wave resonator, the ends of the horn move in opposite direction causing immense stresses at nodal plane [31]. Thus materials which possess good acoustic properties and are highly resistant to fatigue cracking, like monel, titanium, stainless steel are used to construct tool holders [32].

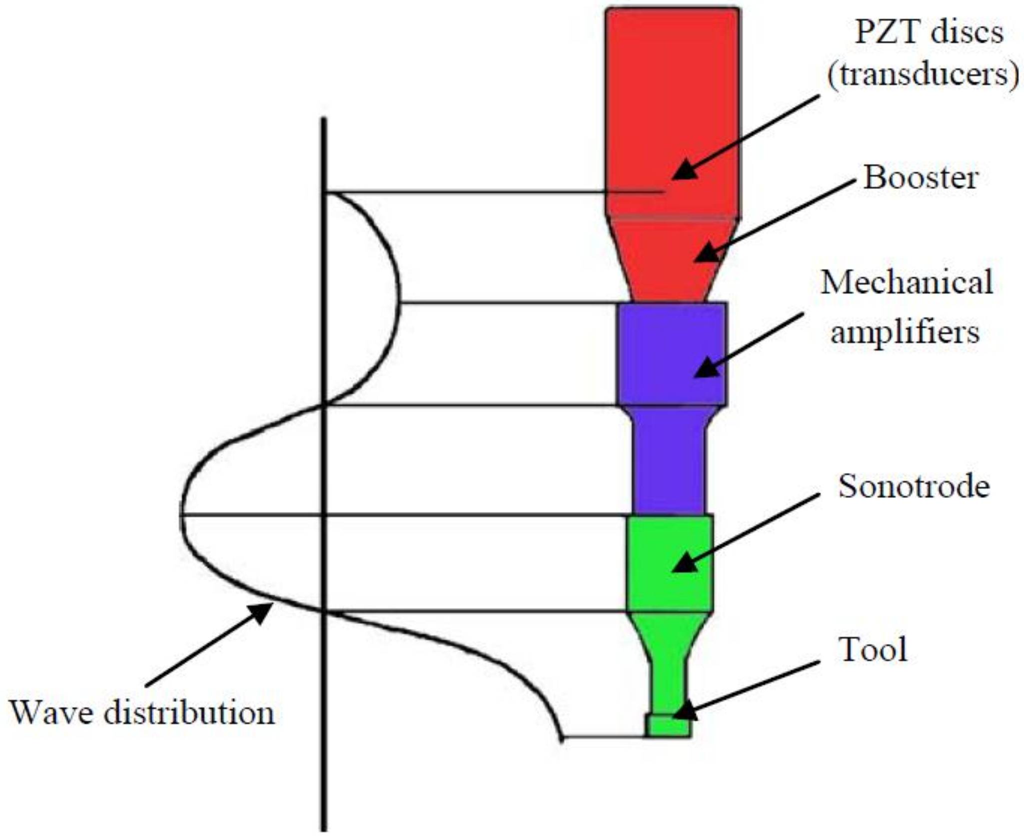

Figure 1.3 Longitudinal wave in acoustic system *[38]*

Tool can be attached to the horn by either soldering or brazing while screw/taper fitting is also very commonly used for attaching the tool to the horn [5,41]. The actual tool configuration can also be machined at the end of the horn [3,5,42]. To facilitate of quick and easy tool changing, threaded joints are also conventionally used.

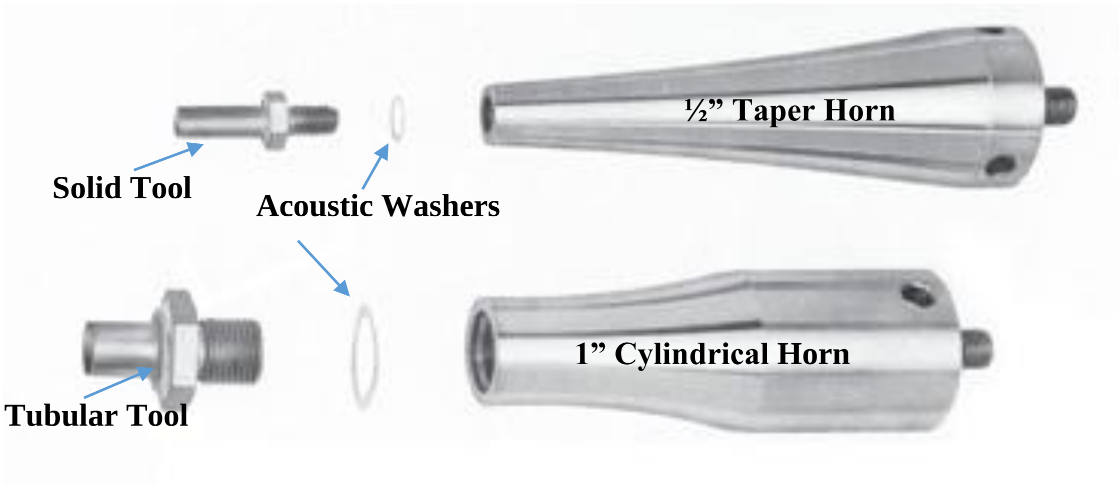

Figure 1.4 Amplifying tool holders, and mechanically attached tools for USM *[40]*

1.3.4 Tool and Abrasives

Tungsten carbide, silver steel, and monel are some of the commonly used tool materials [5]. Polycrystalline diamond (PCD) has recently been used for the machining of very hard work piece material. Use of relatively ductile materials such as stainless steel, brass and mild steel for construction of tools can minimize the tool wear [3,5]. Depending upon the type of abrasive material used and the properties of the work piece material, work piece/tool wear ratio can range from 1:1 to 100:1 [3]. The tool is normally held against the work piece by a static load exerted via a counter weight/static weight, spring, pneumatic/hydraulic or solenoid feed system [15,43]. During machining the system should maintain a uniform working force and should be sufficiently sensitive to overcome the resistance due to the cutting action to exhibit optimum results [44]. Area of the tool tip has influence on penetration rate and a smaller contact area facilitates improved flow of abrasives under tool and thus causes improved rate of machining .Ideally this area should not be more than 10-15percent of the smallest section of tool horn [31]. Hardness, usable life, cost and particle size form the criteria for selection of abrasives. Boron carbide, Silicon Carbide and Alumina are the commonly used abrasives in order of hardness. Though costly, Boron Carbide has extended usable life of almost 200 machine-operating hours and creates high removal rates. The size of abrasive particles influences the material removal rates and surface finish. With USM the abrasive grit size generally ranges from 240 – 800 [3]. The transport/carrying medium of the abrasive particles should have low viscosity alongwith a density approaching that of the abrasive. Among other attributes, good wetting properties, high thermal conductivity and specific heat for ensuring efficient cooling make a good transport medium and water meets most of these requirements [45]. The abrasive material is mixed with water to form the slurry. 50% by weight constitute the most common abrasive concentration in the mixture which, though, can vary from 30–60%. [3]; Thinner mixtures are used to promote efficient flow which are required especially when drilling deep holes or forming complex cavities.

1.4 USM PROCESS PARAMETERS

USM process variables affecting material removal rate, accuracy, and surface finish can be categorized into variables related to machine, tool, abrasives and workpiece. The categorization of these parameters is shown in Figure 1.5.

Among the machine relates parameters, amplitude (ξ) of the tool motion affects the machining rate and determines the maximum size of the abrasive particles that can be used. Material removal is proportional to square of amplitude at constant frequency and static load [3]. Ideally the amplitude should be equal to the mean diameter of the abrasive grit used in order to optimize cutting rate [34,46]. MRR has also been proposed to be proportional to ξ [47]. Frequency during machining has to be in resonance with acoustic system to have maximum amplitude at tool tip and thus to get optimum utilization of acoustic system [31]. Several hypothesis have been proposed about effect of frequency on machining response. A linear relationship was predicted by Shaw [48] and Goetze [47] while Neppiras and Foskett [49] put forth a non-linear relationship with rate of machining.

Typical horn design of USM includes cylindrical, stepped, conical and exponential types. Dam et al. [50] proposed that a horn can be designed which converts the longitudinal ultrasonic action into a mixed lateral and longitudinal vibration mode which aids contouring work. As stated in previous sections, horn mechanically modifies the vibratory energy to attain requisite force-amplitude ratio. Accordingly it could be of low gain or high gain type. The former generates low amplitude with higher forcibility, while the later has a high amplitude and rather lower force capability [31].

Machining rate and surface finish are also affected by applied static load which tends to increase the material removal rate upto a maximum value and then any further increase in static load starts decreasing the machining rate. The point of maxima for machining rate shifts with change in amplitude and frontal area of the tool. The increased static load can cause crushing of abrasive particles as well and thus may improve surface finish. Abrasive particle Size strongly influences material removal rate. Material removal rate increases proportionally with abrasive size. However a maximum material removal rate stage is achieved when the size of particle becomes comparable with tool amplitude [3].

1.5 MATERIAL REMOVAL MECHANISM IN USM

Material removal process in USM can be considered as similar to that during grinding or as in single tool cutting since machining takes place by an individual tool or abrasive particle displacing and fracturing the work surface.

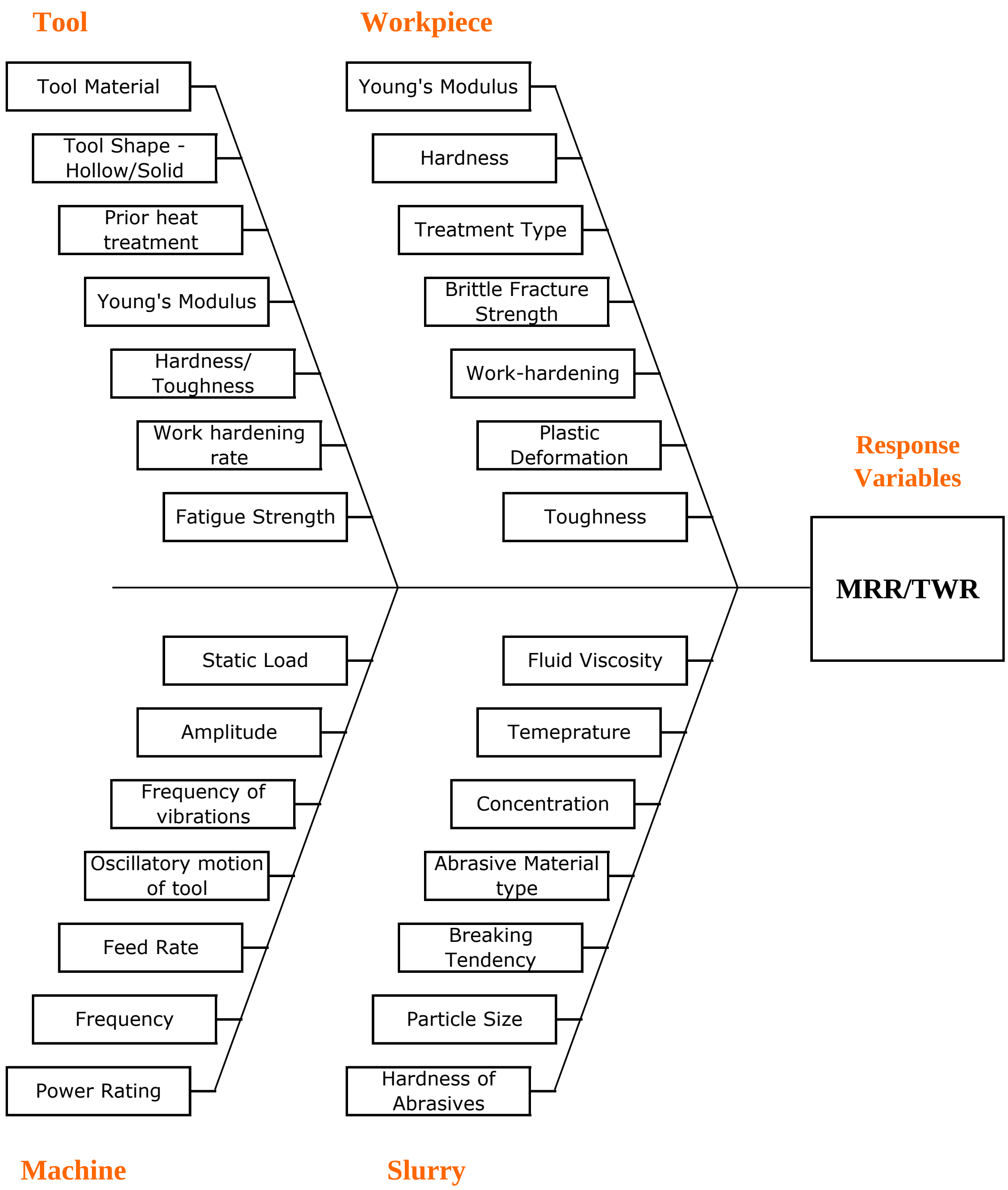

Figure 1.5 USM Process Parameters related to Machine, Workpiece, Tool and Abrasive Slurry

The workpiece material is speared off in the form of several minute particles as a resultant of the impact of abrasive grains energized by the tool tip leading to brittle fracture in materials like glass and ceramics [51]. The machining process can thus be summarized as a sequence of first indentation, then initiation and propagation of crack and subsequently chipping off from the work surface.

USM may be classified as a three-body abrasive wear from the tribological point of view [52]. The material removal in USM takes place mainly due to direct hammering and impact action of the abrasive particles at the surface of the workpiece [37,48,53-54]. Soundararajan and Radhakrishnan [55] found that direct hammering of the abrasive particles by the tool at the workpiece surface results in material removal and particle crushing and may contribute up to 80 % of the stock removal in materials classified as brittle solids such as glass. El-Hofy [1] has identified material removal as a summation of mechanical abrasion by direct localized hammering of abrasive grains on work surface, microchipping by free impact of particles and cavitation erosion due to slurry stream. However soft and elastic materials such as mild steel undergo considerable plastic deformation prior to fracture under the impact of grains. Agarwal [51] has proposed that material removal is attributed primarily to the micro-brittle fracture on the surface of the workpiece with formation of median and radial cracks. Initiation and propagation of median, radial and lateral cracks cause chipping of the brittle material and cause the material removal process in machining of such materials as glass. Wang and Rajurkar [56] proposed that dynamic impact of both the grits and the tool head causes deterioration and crack development in the thin layer just below the work surface under the grits and the impact eventually dislodges the material from the work. Cavitation effects from the abrasive slurry [45,55,57] and chemical action [45] associated with the fluid employed have been reported as minor material removal mechanisms. Fig.1.6 shows material removal mechanism in USM [1].

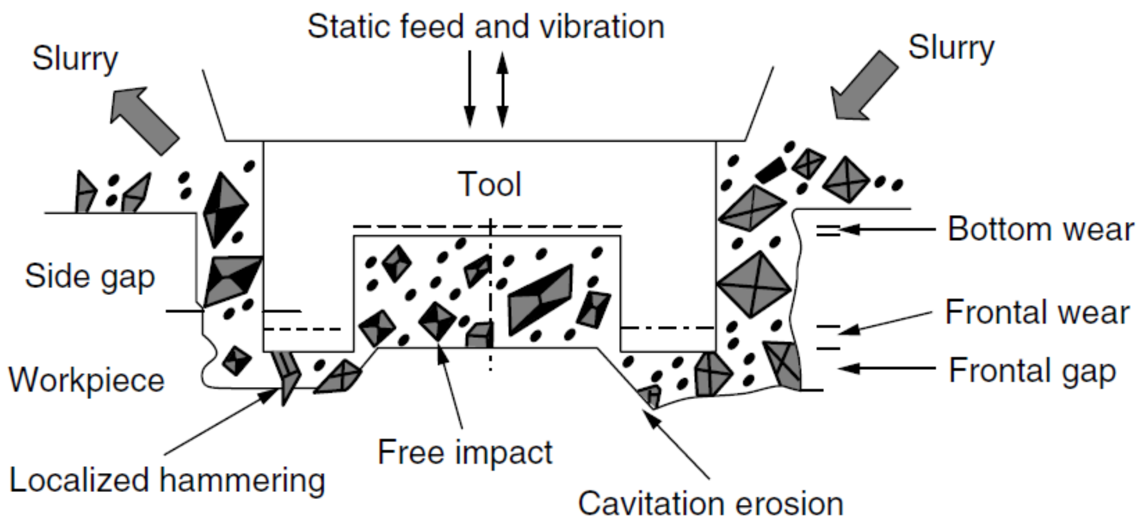

***Figure 1.6 Material removal Mechanism in USM** [1]*

Because of the inherent nature of the process, the materials are neither altered chemically nor are any metallurgical changes involved. The process is suitable for machining all materials harder than HRC 40 irrespective of their electrical conductivity [17,34,46].

1.6 TITANIUM AND ITS ALLOYS

Titanium is the fourth most abundant structural metal in the earth's crust after aluminium, iron and magnesium [11]. Titanium has been recognized as an element (Symbol Ti; atomic number 22; and atomic weight 47.9) for at least 200 years. Despite of being a difficult to machine material titanium and its alloys find wide applications in aerospace, chemical, automotive, petroleum, medical and sporting goods industry [11,58]. Commercially pure titanium alloys (ASTM Grades 1–4, 7, 11) are used mainly for their corrosion resistance properties in applications requiring adequate strength while high-strength alloyed forms are sub graded into three main groups: α – alloys, β- alloys and αβ – alloys and are used mostly for their superior strength-to-weight ratios and good corrosion resistance for applications in aerospace, automotive, and biomedical sector [59]. The most popular of these, used in aircraft construction for parts under low thermal stress, is Ti-6Al-4V that belongs to αβ-alloys [60]. It is the most common of all the Ti alloys and accounts for more than 50% of the titanium alloys usage [59]. Although the three general alloy types require specific and different mill processing methodologies, each offers a unique combination of properties, which may be advantageous for a given application. Among the pure Titanium, Grade 2 and 4 are the most widely used forms. Both these forms possess excellent corrosion resistance. While Grade 2 is used in applications such as heat exchangers, Grade 4 that possesses better mechanical properties of the two, is extensively used in biomedical applications [59]. The extensive use of Titanium and its alloys in aerospace is due to their excellent combination of high strength-to-weight ratio the is sustained even at elevated temperature, their superior fracture resistant characteristics, and exceptional resistance to corrosion derived from protective oxide film [61]. They are also being used increasingly (or being considered for use) in other industrial and commercial applications, such as petroleum refining, chemical processing, surgical implantation, pulp and paper, pollution control, nuclear waste storage, food processing, electrochemical (including cathodic protection and extractive metallurgy) and marine applications [62]. Today titanium alloys are commonly and readily available engineering metals that compete directly with stainless steel and several specialty steels, copper alloys, nickel based alloys and composites.

However, despite of such vast areas of applications, the titanium and its alloys are still considered a special group of elements requiring considerable attention in machining and are labeled as difficult to machine materials. Several researchers have cited several reasons for inherent poor machinability of titanium. The reasons and the principal problems associated therein are as discussed below:

i) Titanium is chemically very reactive and therefore has a tendency to weld to the cutting tool during machining and thus leads to premature tool failure [58,62]. Titanium and its alloys react chemically with almost all tool materials available at cutting temperatures in excess of 500°C and there is a tendency for chips to pressure weld to cutting tools [62].

ii) The poor thermal conductivity of titanium is the biggest of the concerns. Due to that the workpiece is unable to transfer out the heat generated in machining and thus the heat tends to concentrate at the cutting edge causing the edge temperature to reach 1000°C [63] and thereby result in rapid tool wear. A large proportion of the heat, about 80%, generated when machining titanium alloy Ti-6Al-4V is conducted into the tool because it cannot be removed with the fast flowing chip or bed into the workpiece due to low thermal conductivity of titanium alloys which is about 1/6th of steel [64-65]. Heat affected zone in machining of titanium is much smaller and much closer to cutting edge and alongwith steep temperature gradients [61].

iii) High strength and hardness retained at elevated temperatures further impairs machinability of titanium as there is more force and stress on cutting edge [63]. Coupled with small chip-tool contact area, this inherent property of titanium results in much higher mechanical stresses in the immediate vicinity of cutting edge [64,66]. Konig [64] has reported higher stresses on tool when machining Ti-6Al-4V than when machining Nimonic 105 and three to four times those observed when machining Ck 53N.

iv) Low modulus of elasticity of titanium poses another major problem, called Chatter, when machining titanium alloys, especially for finish machining. Titanium deflects nearly twice as much as carbon steel when subjected to cutting pressures. The greater springback behind the cutting edge results in premature flank wear, vibration and higher cutting temperatures [66]. The appearance of chatter may also be partly ascribed high dynamic cutting forces in machining of titanium.

v) Formation of serrated chips due to localization of shear strains in a narrow band and thus fluctuations in cutting forces, especially in case of α-β alloys like Ti-6Al-4V, combined with vibrational force and high temperatures exert micro fatigue loading on cutting tool which is believed to be partially responsible for severe flank wear [67]. Adiabatic shear localization and thermally driven phase transformations at high speeds cause chip segmentation in dual phase titanium alloys [68].

One of the ways to minimize these problems is by using proper cutting tools having qualities like high hot hardness, good thermal conductivity, good chemical inertness, toughness and fatigue resistance to withstand the chip segmentation process and high compressive, tensile and shear strength [61]. Other way around, by designing special tools or using non-conventional cutting methods can also offer solution to the above stated problems [61]. Commercially these alloys are machined by non-conventional electric discharge machining (EDM), which gives good material removal rate however accuracy and surface finish are some problematic area [69-70].

The combined process of EDM with USM improved the machining efficiency and accuracy [22]. The problem of length of unsupported section of drill has been solved easily using USM. Here the portion of drill is no longer and still allows the chips to flow unhampered out of the hole [71-72]. This permits application of maximum cutting pressure, as well as rapid drill removal to clear chips and drill re-arrangement without breakage. Extensive experimentation on TITAN 15 and TITAN 31 as work material with different slurries have been performed on USM by Singh and Khamba [73].

1.7 CRYOGENIC TREATMENT AND ITS EFFECT

Cryogenic treatment is an inexpensive, one time, permanent treatment affecting the entire section of component unlike coatings. NASA engineers first noticed the effects of cold temperatures on materials. They discovered that many of the metal parts in the aircraft, returned from the cold vacuum of space, became stronger than they were before flight. Since then sub-zero treatment (-80° C) has been used for many years, but with inconsistent results. Many of the inconsistencies were reduced by longer soaking periods and with deep cryogenic treatment (-190° C) [74].

Cryogenic treatment is an add on process over conventional heat treatment wherein samples are cooled down to prescribed cryogenic temperature level at a slow rate, maintained at this temperature for a long time and then brought back to room temperature [75]. The process uses sub-zero temperatures down to –300ºF to alter the micro-structure of the material. Cryogenic treatment stimulates additional transformations in metals and ultimately improves the performance of the metal. In tool steels cryogenic treatment is known to convert retained austenite into martensite. Cryogenic treatment is an extension of the heat-treating process that further improve material properties by relieving residual stresses, promoting a more uniform micro-structure and precipitating carbides in steels for increased resistance to wear. Appropriate heat treatment can transform 85-90% of the austenite into martensite while cryogenic treatment can convert the additional 10-15% of retained austenite into martensite to improve the mechanical properties of the materials. An important aspect of cryogenic treatment is that it exhibits volumetric effect on the material. That means changes are witnessed in the whole volume of the material which remain unaltered after successive re-grindings. CT was thus found to be superior to TiN coatings in tool and die steels [75].

Depending upon the lowest temperature to which the material is carried, cryogenic treatment is classified as Shallow Cryogenic Treatment (SCT) or Deep Cryogenic Treatment (DCT). The lowest temperature in the former is 193K which is near to temperature of dry ice while for the later it is 77K, that is at the liquefying temperature of nitrogen. The ultra low temperatures in deep cryogenic treatment are attained using well insulated computer controlled chambers and with the help of liquid nitrogen. The efficacy of cryogenic treatment is also affected by the type of treatment cycle adopted. Apart from the lowest temperature attained in the cycle, cooling rate that is the rate at which drop in temperature is attained and period of soaking that is the time for which material is kept at the low temperature significantly determines the effectiveness of cryogenic treatment. Rate of re-heating to bring the work piece back to room temperature can also have effect on the properties attained post cryogenic treatment. Accordingly the selection of an appropriate cycle for carrying out cryogenic treatment is also important. Furthermore, Cryo-processing is not a substitute for good heat treating, rather it is an add-on or a supplemental process to conventional heat treatment to be done at the end of heat treatment and prior to tempering. Presence of extreme residual stresses after CT deprives material of favourable fatigue properties and leads to development of cracks which necessitates tempering for SCT as well as DCT samples [76].Some studies have also advocated the execution of cryogenic treatment after tempering in the conventional heat treatment cycle and then followed up by soft tempering for stress relieving. Tempering tenmperature post cryogenic treatment has been reported as a higly significant parameters affecting sample hardness [77-78]. Ray and Das [79] proposed that cryotreatment is most effective when carried out after conventional hardening and prior to tempering though the authors recommended some stress relieving for tools having higher cracking sensitivity. Some of the common cryo-processing cycles used in the reported studies are shown in Fig1.7 [80] and Fig 1.8 [81].

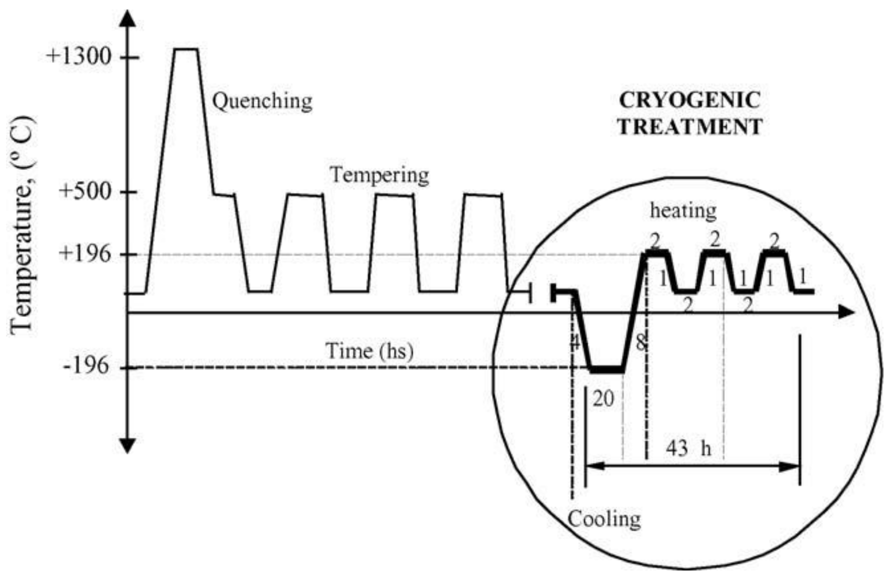

***Figure 1.7 Cryogenic Treatment Cycle involving triple tempering on either side of Cryogenic Treatment** [80]*

The improvement in mechanical properties of Tool steels post cryogenic treatment have been attributed to transformation of retained austenite into martensite and precipitation of smaller secondary carbides in the matrix [82-86].

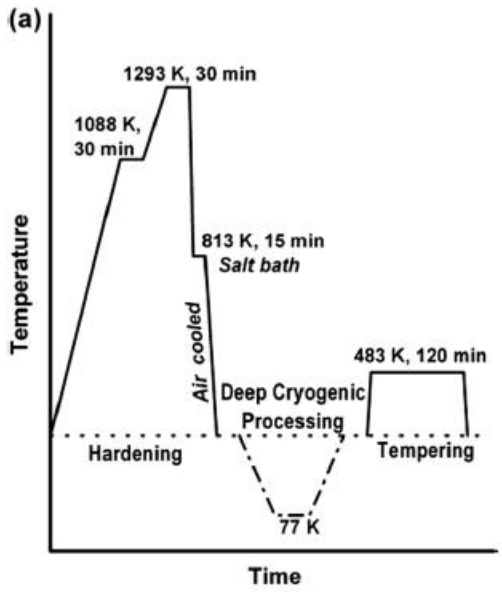

***Figure 1.8 Cryogenic treatment carried out as intermediate step between hardening and tempering** [81]*

Though several published studies have advocated the improvement in wear resistance of tool steels post cryogenic treatment [80-81, 86-91], effect on toughness of the materials is still not very clear as varied findings have been reported by several authors. Das and Ray [89] reported a marginal reduction in fracture toughness of cryogenic treatment of D2 steel, Molinari et al. [92] found no change in impact toughness when cryogenic treatment was carried out after tempering. However Prieto et al. [93] have reported an improvement in impact toughness of SS420. Podgornik et al. [94] found that fracture toughness improved in low carbon cold worked steel after cryogenic treatment due to formation of martensite like fine needles alongwith deformation of primary martensite. The fracture toughness, though, was found to reduce for higher carbon and vanadium content cold worked steel due to presence of stable carbides which probably got adversely affected after cryogenic temperature. A little increase in micro-hardness of Ni-Ti endodontic instruments was reported by Kim et al. [95] which was attributed to may have been caused by strain, resulting from deposition of nitrogen in interstitial spaces, within the atomic lattice. An optimized cryosoaking period of 16 hours resulted in 18.5% decrease in wear rate in SAE8620 Gear Steel due to presence of finer needles of tempered martensite which got coarsened beyond this optimized soaking period [77].

CT has also been applied to non-ferrous materials with some success. Improvement in physical and mechanical properties post-cryogenic treatment have been attributed to changes in microstructure for materials such as aluminium, copper and magnesium.

Significant improvement in static mechanical properties like tensile strength and hardness was found for AZ31 magnesium alloy [96]. Improved tensile and yield strength was is reported for extruded Mg-Gd-Y alloy coupled with significant microstructural changes [97]. CT followed by tempering reduced the electrical resistivity of GRCop84 copper alloy by reducing the softening effect caused by thermal cycling [98]. Some studies have also been attempted on effect of CT on titanium and its alloys. Kim et al. [95] recorded marginal improvement in micro-hardness of cryogenic treated nickel-titanium endodontic instruments, although any change in crystalline phase composition was not detected. Kumar et al. [99] reported improved MRR, microhardness and surface roughness of Ti-5Al-2.5Sn in electric discharge machining. The improvement in MRR and SR was attributed respectively to improved conductivity and grain refinement. Vinothkumar et al. [100] found longer soaking periods associated with reduced vicker hardness for shape memory nickel titanium alloy. Cryogenic treatment prior to ageing at 650°C was found to improve the plasticity of Ti-6Al-4V alloy by 22.7% though with minor reduction in strength of the alloy without any significant change in microhardness [101]. The microstructure of cryogenic treated material revealed transformation of metastable β phase into stable β and α phase. Vickers Hardness was found to increase with reduction in temperature of cryogenic treatment and with longer soaking periods in Ti-6Al-4V. Improved wear resistance of alloy post cryogenic treatment exhibited smoother worn surfaces and shallower ploughed regions due to grain refinement and β-phase reduction [102]. Improvement in machining characteristics of Ti6246 while drilling on EDM was recorded for longer duration of machining times post deep cryogenic treatment of the work material. The improvements were attributed to improved conductivity and reduced thickness of TiC layer on machined surface [103].

1.8 OBJECTIVES AND ISSUES OF THE PRESENT STUDY

The study was aimed to carry out research on ultrasonic machining of titanium alloy (as work material) using different tool materials and abrasive slurries to know their impact on material removal rate (MRR), tool wear rate (TWR) and surface roughness to model these characteristics for their application in manufacturing industry. The following issues have been taken up during this research work.

1. To investigate the effect of various tool materials like; Stainless Steel, High Carbon Steel, and Titanium in ultrasonic machining using titanium and its alloys as work material

on the following machining properties like Material removal rate (MRR), Tool wear rate (TWR), Surface roughness, Dimensional Accuracy and Tolerance grades.

2. To investigate the effect of various abrasive slurries like Alumina, Silicon carbide and Boron Carbide and combination of different slurries using titanium and its alloys as work material on machining properties as above.

3. To investigate the effect of cryogenic treatment (plain, shallow and deep) including mechanist aspects on tool and work piece for machining of titanium and its alloys as work piece material in ultrasonic machining process.

4. All the responses (TWR, MRR and SR) would be optimized together using multi-response optimization methodology. Based upon statistical analysis, the results will be modeled to develop an empirical relationship.

1.9 SCOPE OF THE WORK

Commercially available Titanium alloy Ti-6Al-4V (Grade 5) was chosen as work material for the study. The alloy belongs to family of α+β titanium alloys and exhibits superior comprehensive performances due to its unique physical and mechanical properties such as low thermal conductivity, low modulus of elasticity, and high corrosion resistance. The alloy is also characterized with its high strength at elevated temperatures and strong chemical affinity. Because of its unique properties Ti-6Al-4V remains the most widely applied among all the titanium alloys and finds wide applications in aerospace industry, biomedical & surgical implantations, automobile and power generation. The alloy is also extensively used in construction as well as petroleum industries. However it still remains a difficult to machine material due to these very unique properties. Sun and Guo [104] summarized serrated chips, elevated cutting temperatures and tool stresses, poor tool life and uncertainity of surface integrity as the major characteristics of titanium machining. So accordingly this material was selected to explore its machinability with USM. Three different materials, viz High Carbon Steel (HCS), Stainless Steel (SS) and Titanium (Ti), were chosen for making tools for the study. The selection of tool materials was governed by several factors, those including the influence of previous works reported on similar studies and the objectives of exploring a wider range of mechanical properties with regard to hardness, ductility and toughness. Abrasives of mesh size ranging from 220-800 are generally recommended for use in

USM. Accordingly, the abrasive slurries in the mesh size of 220, 400 and 500 were chosen in the present study for three different abrasives viz Aluminium Oxide (Al_2O_3), Silicon Carbide (SiC) and Boron Carbide (B_4C). Additionally to explore the effect of mixing of these slurries, three more slurries of each of the three mesh size were prepared by mixing Al_2O_3 with SiC, SiC with B_4C and B_4C with Al_2O_3 in identical grit size. The 500W USM machine tool supplied by sonic mill is provided with manual knob to adjust power rating. Power rating in the present study was varied between 20% to 80% of the rated power i.e between 100W to 400W. Effect of Shallow as well as Deep Cryogenic Treatment was explored on tool as well as work material. Five response variables in form of Material removal Rate (MRR), Tool Wear Rate (TWR), Surface Roughness (SR), Dimensional Accuracy and Tolerance Grades have been established. The results obtained have been optimized using Grey relational Analysis and Analytical Hierarchical Process and have been modeled using Artificial Neural Network approach.

1.10 OVERALL METHODOLOGY OF THE STUDY

The overall research work was divided into following phases:

(i) Detailed literature survey

(ii) Pilot experimentation

(iii) Experimental Design

(iv) Analysis of Results

(v) Empirical Modeling to develop a generalized mathematical equation for MRR, TWR and SR.

(vi) Multi-response optimization of process parameters

Reported literature on ultrasonic machining and its constituent aspects has been extensively reviewed to understand the process, constituent process parameters and their effect on response variables such as MRR, TWR, SR etc for titanium as well as several other materials. The literature survey was focused on the various aspects of ultrasonic machining covering economic and technical viability as well as other aspects in the context of formulated problem such as cryogenic treatment, optimization methodologies and modelling techniques.

Material and Methods were finalized while designing the plan of study. Pilot experimentation was carried out for preliminary study of USM on titanium alloys to build familiarization with the equipment and to understand the machining behavior. The various machining conditions, their ranges and levels were selected from the outcomes of the pilot study. Cryogenic treatment of two degrees viz shallow cryogenic treatment and deep cryogenic treatment was performed on work material as well as tool materials.

Final experimentation was carried out as per the layout generated using Taguchi's Design of Experiments. L_{18} OA was used to design the experiments for analyzing six process parameters on response variables under controlled environmental conditions. Measurements were made to evaluate the values of MRR, TWR, SR and HOS.

Results obtained were analyzed using characterization techniques such as SEM, established theories and available literature for establishing the correlation between outputs and process parameters. Artificial Neural Network approach was used to model the results and relations for various response variables were formulated. All the four responses have been optimized together using Analytical Hierarchical Process for multiobjective optimization.

1.11 ORGANIZATION OF THESIS

Chapter – I Introduction

First chapter of the thesis has focused on development and description of non-traditional processes in general and ultrasonic machining in particular highlighting its constituent components, working principle, constructional features and mechanism of material removal involved. The chapter has also been aimed at briefly describing all the aspects of the thesis such as machining issues in titanium and factors governing selection of a process for the same, cryogenic treatment methodologies and effects.

Chapter – II Literature Review

This chapter presents an extensive description of the available literature in the field of ultrasonic machining in general and that of Titanium, in particular. While reporting the literature reviewed focus has been maintained on putting forward the effect of process parameters on response variables, experimentation details with regard to selection of variables and optimization and modelling techniques adopted by the various researchers.

Further this chapter also presents a review on effect of cryogenic treatment on different materials, including titanium and its alloys, from the cited research work.

Chapter – III Design of Study

This chapter focuses on presenting the findings of Pilot Study and steps involved in selection of Taguchi's OA for final experimentation using Design of Experiments. The selection of process parameters for the study, detailed methodology of the execution in DOE has been presented with the aid of flow charts, wherever required.

Chapter – IV Experimentation, Results and Discussion

This chapter presents the results of response variables viz MRR, TWR, SR, HOS and TG from the outcomes of final experimentation conducted as per Taguchi's L_{18} OA. The results obtained have been discussed and explained using requisite variation plots and appropriate theories supported by SEM and optical micrographs.

Chapter – V Modelling of Results

Intricacies of Artificial Neural Networks, their structure, architecture and controllable parameters have been elaborated and presented in this chapter. The four responses have been modeled using ANN with appropriate network architecture. The correlation coefficient and deviation of ANN predicted results from the experimental results has been shown using appropriate graphs.

Chapter – VI Optimization of responses

Use of Analytical Hierarchical process for optimization has been discussed in this chapter. Weights were generated, firstly for the four responses and subsequently for the experimental outputs of all the responses as per the underlying theories of AHP. Finally the four objectives have been optimized collectively using the process.

Chapter – VII Conclusions and Future Scope of Work

This chapter presents the summary of entire presented work in form of conclusions and also provides necessary recommendations for extending the work for further explorations. This chapter is then followed by the list of cited references.

CHAPTER – 2

LITERATURE REVIEW

Ultrasonic Machining is the solution to the expanding need for machining non-conductive, hard and brittle materials such as single crystals, glasses and polycrystalline ceramics. A lot of work has been reported for USM of such materials however very few people have worked on ultrasonic machining of tough materials like Titanium alloys. Researchers are actively engaged in experimentation related to USM process for improving material removal rate (MRR), tool wear rate (TWR), process improvement and surface quality work for various types of hard and tough metals and their alloys. Relevant literature pertaining to USM and the machining characteristics of titanium and titanium alloys by using USM and cryogenic treatment of tool materials has been reviewed as given below. The reviewed literature has been classified under four sub-sections. Literature related to machining of Titanium and the problems and challenges associated with the same has been placed in first section; Literature related to Ultrasonic Machining and its variants for machining of Titanium has been placed in second section while reviewed articles related to ultrasonic machining of materials other than titanium have been grouped in the third section. Relevant reviewed literature pertaining to cryogenic treatment has been placed in the last subsection. Thus the four sub-sections constituted for grouping of the articles are as follows:

- Machining of Titanium and Challenges
- Ultrasonic Machining and its variants for machining of Titanium
- Ultrasonic Machining of other materials
- Cryogenic Treatment

2.1 MACHINING OF TITANIUM AND CHALLENGES

Ezugwu and Wang (1997) in their review on machinability of titanium alloys recommended some special machining techniques such as use of ledge and rotary tools and other non-conventional machining methods for titanium as alternative to traditional methods for better metal removal rate. Traditionally, these alloys have been termed as difficult to cut materials due to high cutting temperature resulting because of poor thermal conductivity of metal among other factors like short chip-tool contact length and thin secondary zone. Also the cutting tool materials undergo severe thermal and mechanical loads during machining of titanium due to high temperatures near the cutting edge thus greatly influencing wear rate and tool life. Additional problems of strong chemical reactivity, chatter and much higher mechanical stresses in the immediate vicinity of cutting edge make it furthermore difficult to machine titanium alloys with conventional machining methods. It was also mentioned that a great care needs to be exercised to maintain the surface integrity to prevent mechanical failure. [61]

Wansheng et al. (2002) studied the effect of Ultrasonic vibrations in Electric Discharge Machining of small and deep holes. EDM though quite suitable for machining titanium, is not ideal for small and deep holes in these alloys. A machining taper occurs in deep and small holes machined by EDM because the evacuation of debris becomes difficult with an increase in depth/diameter ratio and if the working fluid is not renewed duly, the metallic debris accumulates easily and thus resulting into arc discharge and causing the wall of hole to be taper. Introduction of ultrasonic vibration along the tool axis is proposed as an efficient means to improve liquid status in hole. It was concluded that bringing ultrasonic vibrations into micro-hole EDM improves the liquid flow behavior substantially and thus avoids the erosuion products sediment and thus improves machining efficiency, stability and quality. [20]

Rahman et al. (2003) reviewed the machinability of titanium with conventional and advanced cutting tool materials. The review revealed that titanium and its alloys are hard to cut materials largely because of their low thermal conductivity and high chemical reactivity. The study also revealed in case of advanced tool materials like CBN and PCD, the high chemical reactivity of titanium with the binder materials in tool causes a lot of tool wear which is not the case with BCBN tool free from binders and thus gives better results with regard to tool wear. [58]

Che-Haron and Jawaid (2005) explored the machining of titanium alloy Ti-6Al-4V using uncoated carbide tools to determine the surface integrity of the machined workpiece. Poor machinability caused surface damage of the alloy and alongwith indication of microstructure altercations, plastic deformation and formation of hard white layer at the machined surface especially towards the later stages of machining with tool wearing out. Hardness at top layer of machined surface was found to be higher compared to average hardness of workpiece due to work-hardening. [105]

Zhang et al. (2008) presented a review on Mechanical Drilling Processes for Titanium alloys and discussed the important aspects in titanium drilling. The paper extensively covered the work done by various authors on titanium with twist drilling, vibration assisted drilling and USM and RUM etc. The authors found that twist drilling, though predominantly the most extensively used process for drilling on titanium alloys in aircraft industry, suffers from higher manufacturing cost owing to poor tool life and large cycle time. The authors found that not much work has been reported about manufacturing applications of USM for drilling titanium due to possibilities like difficulty in slurry circulation for horizontally oriented holes and lack of portability which is so important for aircraft manufacturing. [106]

Arrazola et al. (2009) compared the machinability studies of Ti555.3 with Ti6Al4V for aeronautical applications and found that diffusion process cause formation of a layer of adhered material on rake face of the tool while machining both the materials. The layer was found to caused by Ti and TiC which suggests diffusion of carbon from cutting tool inserts to workpiece. Cutting forces were found to be higher with the former as compared to Ti6Al4V. [107]

Crawforth et al. (2012) carried out precision turning trials on titanium alloy Timetal 834 (Ti-834) by varying cutting speeds in the range of 50 to 120m/min. Severe plastic deformation comprising of slip and twinning was observed at greater depths. These sites may act as nucleus for crack intitiation during cyclic loading and hence are referred to as damade during critical service applications. The average depth and frequency of appearance of twins increases with increase in cutting speed. Increased strain rate corresponding to higher surface speed caused increased sub surface damage, while formation of unstable built-up edge ahead of tool caused damage at lower cutting speeds. Optimum speed of 70m/min was found to be associated with minimum damage. [108]

Khanna and Davim (2015) investigated the effect of machining control factors such as cutting speed and feed rate to ascertain the machinability of different titanium alloys measured in terms of cutting and feed force and tool temperature using Taguchi’s Design of Experiments. Poor heat conductivity, high chemical reactivity and low modulus of elasticity were listed as factors causing high tool wear and lower production rates due to thus necessitated use of lower machining speeds. It was inferred that the optimum selection of the chemical composition is required to ascertain the affable evolution of microstructure for maximum machinability which was found to be with Ti-6Al-4V among the selected variants for the study due to lower content of β phase stabilizers. [109]

Gupta and Laubscher (2016) have presented an elaborative review on sustainable machining of titanium and its alloys and have concluded that economically viable and quality in machining of titanium and its alloys is feasible by use of optimized machining conditions, suitable cutting tool materials and their geometries with appropriate lubrication strategies even though there are inherent difficulties attached with machining of these alloys. The authors have proposed use of certain coated tool materials to minimize the wear, MQL and cryogenic cooling based lubrication methods, assisted machining methods comprising of Laser and Ultrasonic vibration assistance and combination of these strategies as some of the viable solutions for further improving the machinability of the alloys. [59]

Thus it can be inferred from the published literature that despite of extensive use of titanium and its alloys for specialized applications in the sectors associated with aerospace, medical and general industry due to their superior mechanical and physical properties such as strength-to-weight ratio and corrosion resistance, the machining of these alloys still remains a challenge. Literature shows extensive work has been done, and still being done, on identification of advanced cutting tools such as PCD and CBN. Coated tools having coatings such as those of TiAlN, TiN, Al_2O_3, and AlCrN have shown good results to reduce the tool wear. The strong chemical reactivity of Ti alloys demands careful selection of any tool material. Use of advance manufacturing strategies such as MQL and cryogenic machining has also been explored and results have been displayed with their own merits and de-merits. Some researchers have explored the possibility of ultrasonic and laser assistance in conventional machining, such as turning operations, and non-conventional machining such as electric discharge machining with reasonable success. Some studies have also been reported on use of different variants of ultrasonic machining such as stationary and rotary USM for machining of titanium and is particularly useful for micromachining of these alloys.

2.2 ULTRASONIC MACHINING AND ITS VARIANTS FOR MACHINING TITANIUM

Despite of the great advancements in cutting tools' development like coated carbide, ceramics, CBN and polycrystalline diamond, none have had successful implementation in machining of titanium with conventional machining methods [110]. Though straight tungsten carbide cutting tools have proven their superiority in almost all machining processes of titanium alloys but still there is a great scope for improvement in machining efficiency [110]. Resultant work hardening after conventional drilling makes it difficult to re-establish the cut, so the conventional drilling is unable to provide good machining characteristics [111]. Non traditional methods like EDM and LBM have been applied to machining of titanium but even they have showed limitations with regard to accuracy and surface finish [69-70, 112]. Problem of debris elimination and unstability of machining status is encountered during drilling of deep and small holes in titanium alloys using EDM [20]. Presence of thinner zone affected by machining and efficient and generous flow of abrasive slurry resulting in better heat dissipation, as required for low thermal conductivity titanium, makes USM a suitable candidate for machining titanium [113]. Also the depth of cut can be maintained due to rigidity of tool fixed in tool holder, and chemically active medium can be used to transfer heat efficiently and reduce cutting forces between the tool and work piece. Loss of fatigue strength and hence surface integrity is another important issue in machining of Ti. In USM, favourable compressive surface stresses caused by repeated impacts of abrasive grains improve the fatigue life and surface integrity of Ti components [114]. Singh [115] has also reported that no major fatigue problems were encountered during machining of Ti with HSS, WC and SS tool in USM. Application of USM for Ti and its alloys have been proposed by a few researchers. Singh [115], Singh and Khamba [33,41,71-72,116-119], Kumar and Khamba [120] and Kumar et al. [110,121] have explored the USM of Ti in recent years. The detailed review of the work done on Titanium with Ultrasonic Machining in its different variants is presented as follows:

Churi et al. (2005) investigated the feasibility of machining titanium alloys with rotary ultrasonic machining and compared the results of machining responses with those of diamond grinding. The process was found to be capable of drilling holes in titanium alloy Ti-6Al-4V and a significant reduction in tool wear rate, cutting forces and surface roughness was reported compared to conventional diamond drilling. [12]

Singh and Khamba (2006) presented a review on ultrasonic machining of titanium and its alloys and concluded that it is possible to drill holes ultrasonically in titanium without causing excessive surface integrity damage and without causing deformation of workpiece microstructure. The study revealed the effect of design of parameters like power supply, static load. Abrasive slurry, amplitude and tool horn design on MRR, TWR and surface finish. [4]

Churi et al. (2007) investigated Rotary Ultrasonic Machining of titanium alloys. Four tools with different specifications (diamond grit size, diamond concentration and metal bond type) were used to drill holes in titanium alloy work pieces and their cutting force, surface roughness on machined area and tool wear rate were compared. It was concluded that cutting force was reduced significantly as the diamond concentration increased from 80 to 100, while with a change of grit size from #60/80 to 80/100 the cutting force was reduced to 50%. Surface roughness also decreased significantly as the grit size changed from #60/80 to 80/100, however surface roughness was directly proportional to diamond concentration. Tool wear rate increased slightly with a change in mesh size from #60/80 to 80/100. Tool wear also increased slightly with an increase in diamond concentration. [11]

Singh and Khamba (2007) conducted experiments in two setups in in their investigation on ultrasonic machining of titanium and its alloys to determine the effect on Ti 15 and Ti 31 work piece of H.S.S tool using slurry of 320 grit size with 25% concentration in distilled water and slurry of 100 grit size on 500 W USM at 30, 60 and 90% power rating and concluded that MRR and TWR reduced with an increase in grit size, though surface finish increased with increase in grit size because of fineness of abrasive particles. Tool wear and MRR patterns with power rating were also presented in the study. The study indicated that higher hardness of work piece is not the criteria for higher material removal rate in Titanium alloys rather it is combination effect of material composition relative of tool resulting in work hardening of work piece or tool. [116]

Singh and Khamba (2007) studied the relationship between MRR and controlling machining parameters and proposed a model to predict MRR in stationary USM based upon the macro modelling approach. Based upon Signal-to-noise ratio as a function of different input parameters and F-test values, it was deduced that the best settings of USM for the MRR were obtained using an SS tool at 90 percent power rating with boron carbide slurry and the result agreed with experimental observations made by other means. For TWR the optimized results were obtained with an SS tool at a 90 percent power rating and a grit size of 500. [117]

Dvivedi and Kumar (2007) performed drilling on pure titanium and Ti-6Al-4V to investigate the effect of process parameters on surface roughness using Taguchi's design of experiments. USM was proposed as an effective way to obtain good surface quality on titanium and its alloys. Concentration of abrasive slurry and abrasive grit size were found to be the most significant parameters affecting surface roughness in the study. Higher concentrations and coarser abrasives were found to be associated with poor surface finish on the work surface. [122]

Singh and Khamba (2008) in their experimental research on production of 5mm diameter holes in pure titanium (TITAN 15 ASTM Gr 2) and titanium alloy (TITAN 31 ASTM Gr5) with three slurries comprising of silicon carbide, boron carbide and alumina and using tools of stainless steel, titanium and High Speed Steel under six different setups observed that MRR of TITAN 15 is overall lower than TWR while using SS tool with Alumina slurry. However in machining of TITAN 31 with SS tool the MRR and TWR were different due to strain hardening of work piece/ tool material at specific ultrasonic power based upon its mechanical/chemical composition. For machining of TITAN 31 with SS tool the best parameter setting was observed at 300 W with Boron Carbide slurry. [118]

Kumar and Khamba (2008) reported the optimization of process parameters on machining characteristics viz Tool Wear Rate and Surface Roughness on titanium (ASTM Grade I) work piece taking tools of HCS, HSS, cemented Carbide, titanium and titanium alloy with three types of abrasive slurries i.e. SiC, alumina and boron carbide of grit size 220, 300 and 500 using Taguchi Method. It was found that TWR was minimum with titanium alloy tool followed by titanium and HSS tool while cementite carbide exhibited maximum TWR. Higher power rating and higher grit size had an adverse effect on TWR as it became more. The optimum process conditions for TWR and Surface Roughness was found to be with 500 grit size alumina slurry and 100 W power and with Titanium alloy as tool material. [120]

Kumar et al. (2008) in their investigation conducted experiments to assess the effect of tool material, grit size of slurry and power rating of USM on machining characteristics of titanium (ASTM Grade I) using ultrasonic machining and concluded that titanium is fairly machinable with USM. The experiments concluded that High Carbon Steel as tool material resulted in better machining performance as compared to titanium in terms of MRR due to higher hardness of HCS. The MRR and TWR were found to be more with coarseness of grain size of abrasive slurry because of more energy input by coarser grains on impact with tool and work piece. Best results for MRR were obtained at 220 grit size of alumina slurry at 400 W with High Carbon steel tool while the best results for TWR were obtained at grit size 500 at 200 W with titanium alloy as tool material. [110]

Kumar et al. (2009) used dimensional analysis and Buckingham's pie theorem to develop micro-model for tool wear rate from the results obtained in ultrasonic machining of titanium by applying Taguchi design. Dependence of tool wear rate on Ultrasonic power, elastic modulus of tool, grit size and slurry hardness was considered to develop a relation of these variable with TWR. Whereas a 3rd degree polynomial equation has been reported for Boron Carbide and Silicon carbide slurry, a fifth degree polynomial equation with elastic modulus was recorded for alumina slurry at 400W power and 220 grit size. [121]

Pujana et al. (2009) performed ultrasonic vibration assisted drilling on Ti-6Al-4V alloy. The use of ultrasonic assistance was found to significantly reduce the feed force and resulted in increased process temperatures in comparison to conventional drilling process and the magnitude of these improvements was found to increase with amplitude of assisted vibration. However the vibration assistance seemingly did not have any effect of chip geometry. [26]

Dhuria et al. (2011) have presented a review of ultrasonic machining of titanium and its alloys with specific focus on fundamental principles of USM and work done with regard to investigation of operating parameters on machining response such as MRR, TWR and surface finish with titanium as work material. The authors have concluded that Ti can be machined by USM and has a specific advantage over EDM with regard to surface finish requirements. It was also concluded that selection of operating parameter levels is critical in order to achieve acceptable productivity and combined effect of material composition (hardness of work piece) relative to the tool and work piece determines the MRR. The authors found from their review that MRR and TWR vary, among other things, with static load, work material, tool material, tool size, type of abrasive and its grain size, machining time and depth of hole drilled. [123]

Kumar (2013) has presented an extensive review on ultrasonic machining and concluded that the process has enormous potential to establish economical viable machining solutions for relatively tough metals such as alloys of titanium and nickel. Propagation and intersection of cracks induced by indentation of abrasive grains on work surface cause material removal in the process. The material removal mechanism is composed of mixture mode of brittle fracture and plastic deformation during machining of tough materials such as titanium alloys. Change in tool shape at the frontal surface and increase in microhardness of the machined surface especially during machining of tough materials are some of the several findings of the extensive review. [124]

Patil et al. (**2013**) found that ultrasonic assistance resulted in considerable reduction in the stresses on tool during approach, contact and unloading. However the magnitude of reduction decreased with increase in cutting speed, thus making the use suitable for low speed machining. Cutting temperatures and surface roughness was also found to improve in assisted machining compared to conventional turning. The significance of effect on cutting temperature was also reduced with increase in cutting speed. The matte surface resulted in ultrasonic assisted turning had lesser value of average surface roughness as compared to glossy surface generated in conventional turning. [125]

Muhammad et al. (2014) presented a novel hybrid machining process using ultrasonic assistance in hot turning. Presence of high temperature in hot machining reduces the shear strength and rate of strain-hardening especially in high-strength materials due to thermal softening. Ultrasonic Vibration assistance further cause reduction in cutting forces. The results when compared with conventional turning brought a significant reduction in cutting forces in the novel hybrid process with improvement in surface roughness. [126]

Roy and Silverschmidt (2014) have presented a couple of case studies on application of hybrid technology to turning of Titanium alloys. Their experimentation involved comparison of conventional turning, ultrasonic vibration assisted turning and application of ultrasonic vibration assistance to hot turning. The results displayed improvement in surface topography and reduction in cutting forces in the presence of vibration assistance.

The authors have recommended the use of specially designed advance cutting tools with regard to geometry and coatings for applications related to vibration assisted machining. [127]

Kumar (2014) investigated the effect of USM parameters on surface quality and micro-hardness of the machined region in ASTM Grade – I pure titanium and proposed that the mode of material removal in USM is a function of rate of energy input. Plastic Deformation was observed at lower rates of energy input while brittle fracture was noticed at severe rates of energy input. It was found that lower values of power coupled with fine abrasives and a tough and ductile tool material resulted in finer surface after machining. The micro hardness gain was found to be linked to rate of machining. Lower rates of machining were observed to create more gain in micro-hardness. [128]

The published articles suggest that the ultrasonic machining alongwith its other variant RUM is capable of machining the difficult to machine group of materials comprising of titanium and its alloys with some merits and demerits. Low MRR and relatively higher TWR is an issue that remains to be solved with the use of USM for machining of these alloys even though the process is capable of generating very good surface finish. Use of finer grits can further improve the surface quality and reduce the tool wear but also results in reduced machining rates. So the process needs to be optimized with a focus on minimizing the tool wear and maximizing the machining rates.

2.3 ULTRASONIC MACHINING OF OTHER MATERIALS

Adithan and Venkatesh (1976) studied the effect of USM parameters in production accuracy which was measured in terms of hole oversize and form accuracy measured by out of roundness and conicity of the drilled hole. Glass was the work material and mild steel tool was used alongwith boron carbide abrasives of #280 size. Abrasive grit was found to be the most influential parameter in determining the machining accuracy, and hence oversize, while static load and amplitude of vibration were found to be relatively less significant in establishing dimensional accuracy. Finer grit size resulted in minimum oversize which was also found to be reduced with increased machining time and static load due to wear and crushing of abrasives, respectively. Hole oversize was found to be higher at entry as compared to exit due to continuous wear of progressive tool and maximum effect of transverse vibrations at the start of cut, thus resulting in taper of the hole. [129]

Komaraiah et al. (1988) investigated surface roughness and accuracy of machining in four different brittle materials using USM with various tools. Machining rates were found to be related with ratio of hardness to modulus of elasticity (H/E). A higher H/E ratio means a reduction in resistance towards crack propagation in such materials which increased rates of machining which was also associated with increased surface roughness. Abrasive grain size was found to affect the surface finish and accuracy significantly and a finer grains was found to improve the two variables**.** Higher static load was also found to be associated with better accuracy owing to suppression of lateral vibrations of tool as well as crushing of abrasive particles. A higher hardness to modulus of elasticity ratio (H/E) was found to be associated with more out of roundness of the drilled holes due to reduced resistance to propagation of radial cracks. [15]

Koamaraiah and Reddy (1993) investigated the effect of work material properties such as hardness and toughness on machining rates in stationary and rotary USM. Five different brittle materials such glass, porcelain, ferrite, alumina and tungsten carbide were selected for investigation. Measurements of cracks caused by indentation were used to establish fracture toughness values. It was found that fracture toughness is an important parameter in establishing material removal rates in brittle material and the same should be incorporated in various models. MRR was found to decrease with increase in workpiece hardness and toughness for both variants of USM. [14]

Guzzo et al. (2004) investigated the ultrasonic abrasion of different work piece materials like alumina, zirconia, quartz, glass, ferrite and LiF with a rectangular shaped tool and Silicon Carbide slurry at a stationary USM and concluded through SEM micrographs that brittle micro cracking was the primary mechanism involved with material removal in case of hard and brittle materials. In case of LiF single crystal, brittle cleavage is the major mechanism contributing to improve the surface quality. The experimental results concluded that rate of material removal abruptly decreased with machining depth for work piece materials in which hardness is of same order of magnitude than the hardness of abrasive grits used (SiC) as was in case of Alumina, Zirconia and quartz. However in glass, ferrite and LiF material removal rate was independent of depth of machining. [52]

Jadoun et al. (2006) conducted ultrasonic machining studies on three different types of alumina based ceramic composites with different composition of constituent materials using tools of high carbon steel, high speed steel and tungsten carbide. The cutting ratio which was defined as ratio of rate of material removal from workpiece and tool was found to decrease with increase in alumina content of the composite material while tungsten carbide tool resulted in best cutting ratio among the three tool materials owing to minimum tool wear rate of this material. Rate of material removal though was highest with HSS but it also lead to high tool wear. Cutting rate was highest with finer grit size abrasives while cutting ratio increased linearly with USM power. [131]

Jadoun et al. (2006) studied the effect of process parameters on TWR of ultrasonic drilling on alumina based engineering ceramics with silicon carbide abrasives and concluded that tool material, abrasive grit size, power rating and slurry concentration significantly affect Tool wear Rate using Taguchi's L_{27} OA. Tungsten carbide tool with a power rating of 200W and a grit size of 500 gave the optimum results for Tool Wear Rate. [132]

Kumar and Khamba (2009) studied the effectiveness of use of USM for machining Stellite 6 cobalt alloy using Taguchi's design of experimentation. Power rating of the machine tool was found to be the most significant and contributing parameter followed by abrasive grit size and tool material while abrasive type and slurry concentration were found to be less significant parameters for establishing MRR and TWR. Taguchi's methodology was used to optimize the process simultaneously for the two conflicting response variables. [133]

Jadoun et al. (2009) presented the effect of USM parameters such as tool material, power rating, grit size and slurry concentration alongwith workpiece material on production accuracy during ultrasonic drilling of alumina based ceramics. Dimensional accuracy which was measure in terms of hole oversize and form accuracy was found to be affected due to influx of abrasive particles causing enlargement of the hole compared to tool diameter. Abrasive grit size was found to be the most significant parameter affecting hole oversize and form accuracy and bigger grit size resulted in poor accuracy due to correspondingly larger influx gap. Tool material was a significant parameter affecting form accuracy which was found to be the best with tungsten carbide tool. HCS tool resulted in maximum form inaccuracy. [134]

Lalchhuanvela et al. (2012) performed ultrasonic drilling to machine hexagonal shaped holes in high alumina ceramic workpiece material. Effect of process parameters was studied and RSM based models for MRR and SR were proposed. Higher concentration of slurry, coarser abrasives and high USM power were associated with higher MRR whereas on contrary surface finish was improved with finer abrasives and lower values of power. Due to conflicting nature of the response variables, the results were therefore modeled using multi-objective optimization. [135]

Lalchhuanvela et al. (2013) studied the influence of USM process parameters on profile accuracy of the machined holes in alumina ceramics. Measurements were made for angular deviations at corner angles and dimensional deviations across corners and flats in US generated hexagonal profiled holes. Abrasive grit size was found to have significant effect of profile accuracy and the effect of the grit size was found to be more dominant on dimensional deviation across corners and less across flats. However there was not any significant angular deviation across corners with different abrasive grit sizes. Finer abrasives resulted in better profile accuracy. Long duration machining and higher slurry concentrations adversely affected profile accuracy due to higher interaction of abrasives on lateral surfaces. USM power was not found to have significant effect on the accuracy while either extremes of feed rates resulted in poor accuracy and only moderate values were recommended for the same. [136]

Bhosle et al. (**2014**) proposed that amplitude is a significant parameter affecting response variables like MRR, TWR and surface roughness while machining of alumina zirconia ceramic composites. An increase in amplitude was found to enhance the tool wear rate and surface roughness due to higher energy corresponsding to increased intensity of vibrations. Though MRR was found to be reduced with increased amplitude from 70% to 100% and the reduction was attributed to formation of work hardened layer due to large plastic deformation. Slurry concentration and slurry type were also found to be significant paramteres affecting the response variable. [137]

Kataria et al. (2015) presented the effect of USM parameters related to machine, tool and workpiece on the hole quality in drilling on WC-Co composites. Dimensional accuracy was largely affected by size of abrasive particles in the slurry with coarser particles causing higher oversize. Moderate values of USM were associated with minimum oversize with higher values causing lateral vibrations and lower values causing increased machining time resulted in poor accuracy. Higher cobalt content in workpiece improved dimensional accuracy due to increased fracture toughness, thus reducing lateral machining. Similar trend was also observed for profile accuracy with abrasive grit size and cobalt content of the work material. [138]

Cheema et al. (2016) have developed a three dimensional mathematical model for tool wear by quantifying the 2-D linear wear. The tool wear model has been developed for longitudinal, lateral and edge rounding wear and was verified by experimentation on ultrasonic machining of glass using tungsten carbide tool. The depth, taper and rounding of corners of the machined microchannels were governed by longitudinal, lateral and edge rounding wear respectively. Higher power rating and higher slurry concentration were associated with increased tool wear owing to increased impact energy and increased interaction of tool with abrasive respectively. The form accuracy was maximum with moderate size of abrasive, with either extreme causing poor accuracy due to accumulation of finer particles and large indentations by bigger particles. [130]

Kataria et al. (2016) carried out their studies on ultrasonic machining of WC-Co composites and studied the effect of parameters such as amount of cobalt content in the composite, thickness of the workpiece, tool profile and material, grit size and USM power on machining response of MRR and TWR using Taguchi's L_{36} OA and optimized the results using GRA. Increased cobalt content and workpiece thickness were associated with reduction in MRR owing to improved fracture toughness and difficulty in propagation of abrasive particle respectively for the two parameters. Hollow tools due to their improved inertia cause effective distribution of slurry particles and possess lesser surface area and hence resulted in improved rates of machining. Tools of higher hardness were found to cause deeper indentations and thus improved machining rates. Higher power and coarser grains also resulted in improved rate of machining. [139]

The reviewed literature on USM of different materials suggest that the tool material and workpiece material properties significantly determine the machining performance in USM. Hardness to modulus of elasticity ratio, fracture toughness and plasticity determine the extent of plastic deformation and fracture behavior in machining with USM and thus determine material removal and tool wear rates. Abrasive grit size, slurry concentration and hardness of abrasive particles alongwith USM power rating are some of the controllable parameters that establish the machining performance with USM. Use of solid and hollow tools also have their own merits and demerits and hence the selection for the same has to be made based on nature of application.

2.4 CRYOGENIC TREATMENT

Barron (1974) proposed that besides the transformation of the retained austenite into martensite, the improvement in wear resistance of tools was also caused by presence of hard and small carbide particles well distributed among the larger carbide particles within the martensite that resulted due to cryogenic treatment. Before the cryogenic treatment the microstructure showed relatively large carbides of the order of 20 µm dispersed in the matrix, however, after the cryogenic treatment, carbide particles as small as 5 µm were found. The carbide refinement could in such a way have also contributed to the improvement of the wear resistance which was evident from the experiments that the tool steels submitted to cryogenic treatment showed improved performance during machining. [82]

Marquardt et al. (2000) collected, compiled and correlated property information for materials used in cryogenics and found thermal conductivity, thermal expansion and specific heat of various materials including Ti-6Al-4V alloy across four temperature scale ranges i.e. less than 4K, 4 K to 77 K, 77 K – 300 K and 300 K to melting point. [140]

Hong and Ding (2001) applied the cryogenics to conventionally machine Ti-6Al4V alloys. The study was carried out to evaluate cutting temperatures in these difficult to machine alloys under different set of cooling conditions. A jet of liquid Nitrogen (LN2) was used to provide the cooling at cutting interface and results of various cooling approaches were found. The study concluded that applying LN2 in close proximity to the tool cutting edge can significantly reduce the tool temperature. It was also found out that with cryogenic cooling, titanium’s diffusivity to tool materials, a characteristic responsible for most tool wear in Ti6-4 machining, becomes negligible. [67]

Sekhar Babu et al. (2005) studied the effect of cryogenic treatment on wear resistance of M1 (Molybdenum High Speed Steel), EN 19 (chromium molybdenum constructional steel) and H 13 (chromium/molybdenum hot die steel) tool steels. The samples were first heat treated and re-tempered after cryogenic treatment which was carried out at 0°C, -20°C, -40°C, -80°C and -190°C. The results were highly significant as improvement in wear resistance under deep cryogenic treatment ranged from 315% in EN 19 to 382% in M1 samples. [74]

Silva et al. (2006) carried out experiments after deep cryo-treatment of M2 high speed steel Lathe tool, twist drill and milling cutter tools to verify the effect of cryogenic treatment. It was found that the retained austenite after treatment was near 0%. The

Laboratory tests on lathe tools didn't indicate any effect on hardness of treated tools under X-ray diffractometer and it was found to be same as that of untreated tools, while on rapid facing tests it was discovered that cryogenically treated tools presented longer tool lives at different spindle speeds and feed rates. The laboratory tests on twist drills also indicated higher tool life of cryogenically treated tools. However shop floor tests on coated HSS milling cutters showed adverse effects of cryogenic treatment on tool life when shaping the teeth of gear rings. [80]

Das et al. (2007) investigated the effect of cryogenic treatment on D2 tool steel when carried out in between conventional heat treatment and tempering. Holding period of 36 and 84 hours was explored for the effect on hardness and wear resistance of the steel. It was found that cryogenic treatments leads to formation and increase in volume of refined secondary carbides and cause their uniform distribution. he results showed a marginal increase of 5% in hardness of cryogenic treated specimens compared to conventionally heat treated specimens which was attributed to conversion of retained austenite to martensite. Further, the duration of soaking period did not appear to have any effect of hardness. At lower loads, there was immense improvement in wear resistance of cryogenic treated samples. However the magnitude of improvement was reduced at higher loads which could have been due to stress induced transformation of retained austenite in conventionally treated specimens into martensite that reduced the gap of difference in wear resistance of two categories of the samples. [81]

Dhokey and Nirbhavne (2009) investigated the effect of multiple tempering post cryogenic treatment on material properties in D3 tool steel. Five categories of samples were prepared that included conventional heat treated, cryogenically treated and cryogenically treated with varied number of tempering ranging from 1 to 3 at 150^{0}C. Tool steel exhibited coarsening of carbides post multiple tempering which could have been due to Oswald ripening. The samples with single tempering exhibited best wear resistance which was more than conventional treated as well as only cryogenic treated. However with increase in number of tempering to 2 and then to 3, the wear resistance actually dropped down which attributed to coarsening of carbides. [141]

Akhbarizadeh et al. (2009) studied the effect of deep (-185°C) and shallow (-63°C) cryogenic treatment (including cryogenic temperature, cryogenic time and stabilization) on wear behavior of D6 tool steel by performing wear tests using a pin-on-disk wear tester. The findings revealed that cryogenic treatment decreased the retained austenite and hence improved the wear resistance and hardness. The improvement was significant in DCT due to more homogenized carbide distribution, the retained austenite elimination and higher chromium carbide percentage in comparison with SCT. [142]

Gill et al. (2009) discussed the wear behavior of cryogenically treated tungsten carbide inserts under dry and wet conditions and concluded that performance of cryogenically treated carbide inserts depends a lot on cutting conditions. The fact that tungsten carbide inserts retained superior properties induced by cryogenic temperature for a relatively longer time during wet machining was attributed to the application of coolant which reduces tool-work-piece interface temperature. In USM the slurry continuously flows between tool-work-piece and thus the cryo-treatment may be able to provide the retained properties for a longer duration of time. [143]

Amini et al. (2012) proposed that there is an optimum duration of holding time for cryogenic treatment that correspond to most homogeneous distribution of carbides and having a higher holding period than this optimum values doesn't contribute to any further improvement in the desired properties such as microhardness, carbide distribution and particle size among others. The study was carried out on 1.2080 steel by varying the holding time duration from 24 hours to 120 hours. Carbide percentage was found to increase upto 36hours of holding time and same was the case with microhardness. Formation of bigger carbides beyond this time prohibited the further formation of fine carbides. [91]

Senthilkumar and Rajendran (2012) presented the effect of four parameters viz hardening temperature, soaking period, tempering temperature and duration, through Taguchi's L27 OA on wear loss of 4140 steel. The results were optimized for minimum wear loss. Among the four factors, hardening temperature was the most significant followed by tempering temperature though some factor interactions were more significant than this tempering temperature. Too high temperature tempering caused formation of cementite and coarser alloy carbides whereas tempering at 200° resulted in formation of transition carbides that improved wear resistance of the steel. [90]

Gu et al. (2013) investigated the effect of cryogenic treatment on tensile behavior and microstructure of Ti-6Al-4V alloy. Work-pieces were divided into nine groups to study the effect of different combinations of treatments involving cryogenic with and without aging. Cryogenic treatment alone caused slight reduction in strength but increase in elongation. Cryogenic treatment prior to aging at 650°C caused maximum improvement in plasticity of the alloy though alongwith reduction in strength. There was not any appreciable effect on microhardness. Transformation of metastable β phase into stable β and α phase was noticed post cryogenic treatment. Aging after cryogenic treatment caused increase in dislocation densities and formation of twins. [101]

Prieto et al. (2014) investigated the effect of cryogenic treatment on impact toughness and hardness and analyzed microstructural changes in martensitic AISI 420 stainless steel. Microstructure evaluation showed precipitation of small carbides due to increased strain state and their homogeneous size distribution post cryogenic treatment that caused improvement in mechanical properties such as hardness and impact toughness. Stabilization and longer soaking were not found to be of significance because of very little retained austenite presence. [93]

Gu et al. (2014) investigated the effect of cryogenic temperature and soaking period on wear resistance of Ti-6Al-4V alloy used for biomedical applications. Vicker hardness of the alloy was found to increase slightly with lower temperature of cryogenic treatment and prominently with the duration of holding time due to resultant increase in dislocation densities and twins. There was not any phase transformation after the cryogenic treatment. However refinement of grains and reduced β phase was detected and caused improved wear resistance of the alloy which was evident from the smooth and shallow plowing in the worn surface. [102]

Vinothkumar et al. (2015) carried out investigation of effect of dry cryogenic treatment (CT) temperature and soaking period on Vickers hardness and wear resistance of nickel‑titanium (NiTi) martensitic shape memory alloy. The comparisons were made for different degrees of cryogenic treatment at -185°C and -80°C at soaking periods of 24 hr and 6hr each. The results shows that here was a significant drop in wear resistance and hardness of the shape memory alloys post dry cryogenic treatment carried out at -185°C for 24 hrs soaking period. [100]

Akincioglu et al. (2015) have presented a detailed review on cryogenic treatment of cutting tools highlighting the various aspects of treatment process such as rate of cooling, soaking period, soaking temperature and post treatment tempering and their effect on material properties. The review highlights that the treatment can be effectively used for reducing machining costs associated with tool wear and can be applied to a variety of tool material ranging from tool steels, carbides and coated tools. The review also recommends use of optimum cycle with regard to soaking temperature, cooling rate and holding time for extracting maximum advantage from the process. Tool wear resistance arising out of cryogenic treatment has been attributed to improved mechanical properties and the improvement is volumetric that is homogeneously throughout the material unlike coatings. Homogenization of carbide distribution and transformation of retained austenite has been reported as the driving forces for improvement in mechanical properties of tool steels. In carbides improved thermal conductivity of tools due to higher particle size and reformed particle boundaries of cementite carbides caused lesser tool wear post cryogenic treatment. Additionally crystal structure changes have also been reported in the binder phases as responsible for improvement in wear behavior of tungsten carbide tools. [144]

Kumar et al. (2016) investigated the effect of shallow and deep cryogenic treatment on machining performance of Ti-6Al-2.5Sn in electric discharge machining. Cryogenic treatment was found to exhibit a considerable improvement in response variables of MRR, TWR, SR and microhardness as compared to machining of untreated samples. The increase in MRR was attributed to improved conductivity and hence rate of heat absorption and dissipation while reduction in tool wear rate was attributed to restricted penetration of carbon at electrode surface due to modification in microstructure post cryogenic treatment. Surface roughness was also found to be reduced owing to smaller crater formation due to faster heat dissipation in the cryogenic treated workpiece because of it improved thermal conductivity. [99]

Ray and Das (2016) have reviewed state of cryogenic treatment in tool steels and the corresponding effect on mechanical properties such as wear resistance and microstructural modifications including the effect of retained austenite and secondary carbides. Lowest temperature of cryoprocessing was recommended to be close to 77K with cooling and heating rates as the fastest possible without causing cracking of the material. The authors found that improvement in wear resistance is of higher magnitudes when mode and mechanism of wear is different in conventional and cryo treated samples which otherwise is only a few times better under similar mode and mechanism of wear.

The treatment significantly influences the precipitation of secondary carbides without altering the nature of carbides. Precipitation of carbides was found to be governed by two hypotheses, first based on enhanced diffusion of carbon atoms due to defects and crystal imperfections and second on formation of atomic clusters due to plastic deformation of martensite which then act as nucleating sites for carbide precipitation. [79]

Cryogenic treatment has been used extensively especially for improving the wear resistance in tool steels. However the degree of improvement varies across materials. The primary reason for improvement in steels has been conversion of retained austenite to martensite and refinement of carbides. The efficacy of the treatment depends on, among other things, the treatment cycle which has attributes such as holding time and cooling rates as well as the positioning of the cryogenic treatment in the entire heat treatment cycle with different degrees of results having been reported by carrying out the treatment before and after tempering. Though significant improvements in wear resistance and marginal improvements in hardness have been almost uniformly reported by many researchers, effect on fracture toughness has still not been fully understood. Further, the effect of cryogenic treatment in non-ferrous materials is still not completely established and varied degrees of reporting has been made on materials such as Titanium and aluminium alloys.

2.5 SUMMARY AND GAPS IN LITERATURE REVIEW

From the literature reviewed, it can be inferred that the excellent combination of high specific strength and corrosion resistance makes titanium an excellent choice for applications such as those in aerospace industry, surgical implants, nuclear and marine applications among several others. Despite of the great advancements in cutting tools' technology like coated carbide, ceramics, CBN and polycrystalline diamond, none have had successful implementation in machining of titanium covering all the desirable aspects with conventional machining methods and the machining of titanium is still considered to be a challenging issue owing to several inherent properties of titanium and its alloys. Problem of machining efficiency with straight tungsten carbide cutting tools, work hardening in conventional drilling are some of the issues in even best of the methods whereas problem of debris elimination is encountered during drilling of deep and small holes in titanium alloys using EDM. Presence of thinner zone affected by machining and efficient and generous flow of abrasive slurry resulting in better heat dissipation, as required for low thermal conductivity titanium, makes USM a suitable method for machining titanium. A few researchers have presented their work on Ultrasonic machining of titanium in past and results have been modeled for different tool materials, slurry types, grit size and power ratings for different grades of Titanium. However no work hitherto has been reported about impact of cryogenic treatment of titanium and tool materials on ultrasonic machining. Cryogenic treatment, as suggested by several researchers, has been found to improve wear behavior and machining characteristics of certain materials under conventional machining. Effect of the same at different temperatures ranging from without cryogenic treatment to shallow and deep cryo-treatment can be studied to know the impact on parameters like TWR, MRR and Surface Roughness in ultrasonic machining of titanium. Hitherto very little work has been reported on dimensional accuracy and tolerances in ultrasonic machining of titanium. Phenomenon of dish formation in the tool has been reported by some researchers due to plastic deformation at the centre of tool face. This will have some impact on dimensional accuracy of the hole. Variation in the size of abrasive grains will determine the tolerance for the diameters of the drilled holes in USM. All the work that has been done on ultrasonic machining involves slurries of Boron Carbide, Alumina or Silicon Carbide. Mixing of certain additives and chemicals or blending of different slurries may have different effect on material removal and other related parameters but very scarce work has been reported in ultrasonic machining of titanium. The same may be explored to see if any improvements can be attained. Accordingly in the light of the above, the current study was envisaged to undertake following objectives:

1. To investigate the effect of different tool materials in ultrasonic machining using titanium and its alloys as work material on the machining variables such as Material removal rate (MRR), Tool wear rate (TWR), Surface roughness, Dimensional Accuracy and Tolerance grades.

2. To investigate the effect of different abrasive slurries and combination thereof using titanium and its alloys as work material on machining properties as above.

3. To investigate the effect of cryogenic treatment (plain, shallow and deep) including mechanist aspects on tool and work piece for machining of titanium and its alloys as work piece material in ultrasonic machining process.

4. Simultaneous optimization of responses such as TWR, MRR and SR using multi-response optimization methodology. Based upon statistical analysis, the results will be modeled to develop an empirical relationship.

CHAPTER - 3

DESIGN OF STUDY

Ultrasonic machining originated out of the need to carry out machining operations on hard and brittle and difficult to machine materials such as ceramics, glass, tungsten carbide and titanium. Selection of machine and tool is first important step in executing a manufacturing process. Further, the performance of machining, which could be measured in terms of response variables such as rate of machining, tool wear rate, quality of surface generated and dimensional accuracy depends on setting of process parameters, also referred to as control variables. Selection of appropriate process parameters and their various levels play a major role in establishing the value of response variables. Levels here refer to the various values that a control variable attains during experimentation. Each process parameter can be varied across a range of values that usually is determined by the machine capability, if it is a machine related parameter. For different work and tool materials, the selection of levels depends upon the constraints associated with materials. An exhaustive experimentation will be the one that involves exploration of maximum number of process parameters and their levels varied over a reasonably wide range with each experiment corresponding to certain specific value of level of each controlled factor. However given the time and economic constraints, it is generally very difficult to explore that many number of factors as this would require carrying out a large number of experiments. Therefore, the selection of adequate number of factors, and their levels, to improve machining performance is a challenging task for researchers. This requires a meticulous planning in designing the study to obtain desirable accuracy in the outcomes.

Accordingly, with a focus on the above stated points, a two-phase experimentation was planned for the present study. A preliminary pilot experimentation wherein various input factors were varied at several levels using one factor at a time (OFAT) approach. In OFAT approach, only one factor is varied at different levels and the variation in response is attributed to that factor as all other parameters are kept constant. However when a number of factors are involved and when there is inter-dependency of some factors, one factor at a time approach is neither economical nor conclusive. Factorial experimental designs, suggested by Sir Ronald A. Fisher in the decade of 1920s has since gained prominence among researchers. Use of factorial designs has got several merits over conventional OFAT approach. In contrast to large number of experiments required to be performed with OFAT approach, fewer experiments are required for almost similar precision in the estimation of effects using factorial designs. OFAT approach misses out on evaluation of combined effect of different parameters and interaction among them and instead is focused only on each individual parameter. With the inherent methodology involved, OFAT approach can, at times, even miss out on determining optimal setting of control variables. Thus, a very useful approach, referred to as Design of Experiments (DOE) is extensively being preferred over OFAT approach. There are several methods and types of DOE approach available which is a powerful statistical tool to simplify, without significant loss of accuracy and precision, the experimentation when effect of multiple control variables is to be explored simultaneously. Fisher established the elementary principles of DOE using Analysis of Variance (ANOVA) for analyzing the associated data. Several DOE techniques such as orthogonal arrays (OA's), response surface methodology (RSM), full factorial and fractional factorial designs are popular amongst researchers. Orthogonal arrays are employed in Taguchi's approach to vary and explore the effect of different levels of process parameters on one or more response variables.

The DOE process is sectioned into three major phases viz planning phase, conducting phase and analysis phase [145]. Dr. Genechi Taguchi carried out enormous research with DOE in late 1940s in Japan and the standardized version of Taguchi's DOE, popularly known as Taguchi method or Taguchi approach was introduced in early 1980s. The much sought after need of economically viable approach of problem solving and process design optimization has been facilitated by the use of DOE. The detailed use of Taguchi's methods is illustrated in section 3.3.

3.1 PILOT EXPERIMENTATION

To meet the proposed objectives, the entire study was accomplished in two phases. The first phase comprised of pilot experimentation wherein one factor at a time approach was used to study the effect of various process parameters. The approach involves change of only one factor across different levels when all the remaining factors are kept constant. Pilot experimentation is an important stage in scientific study as it enables the researcher to identify the critical to process parameters as well as the range and the levels that need exploration. At the same time it lends hands-on familiarization with the equipment, material and process involved. Parameters such as power rating, abrasive grit size and slurry type were selected for examination during the pilot stage. The complete sequence of events for experimentation is shown in Figure 3.1.

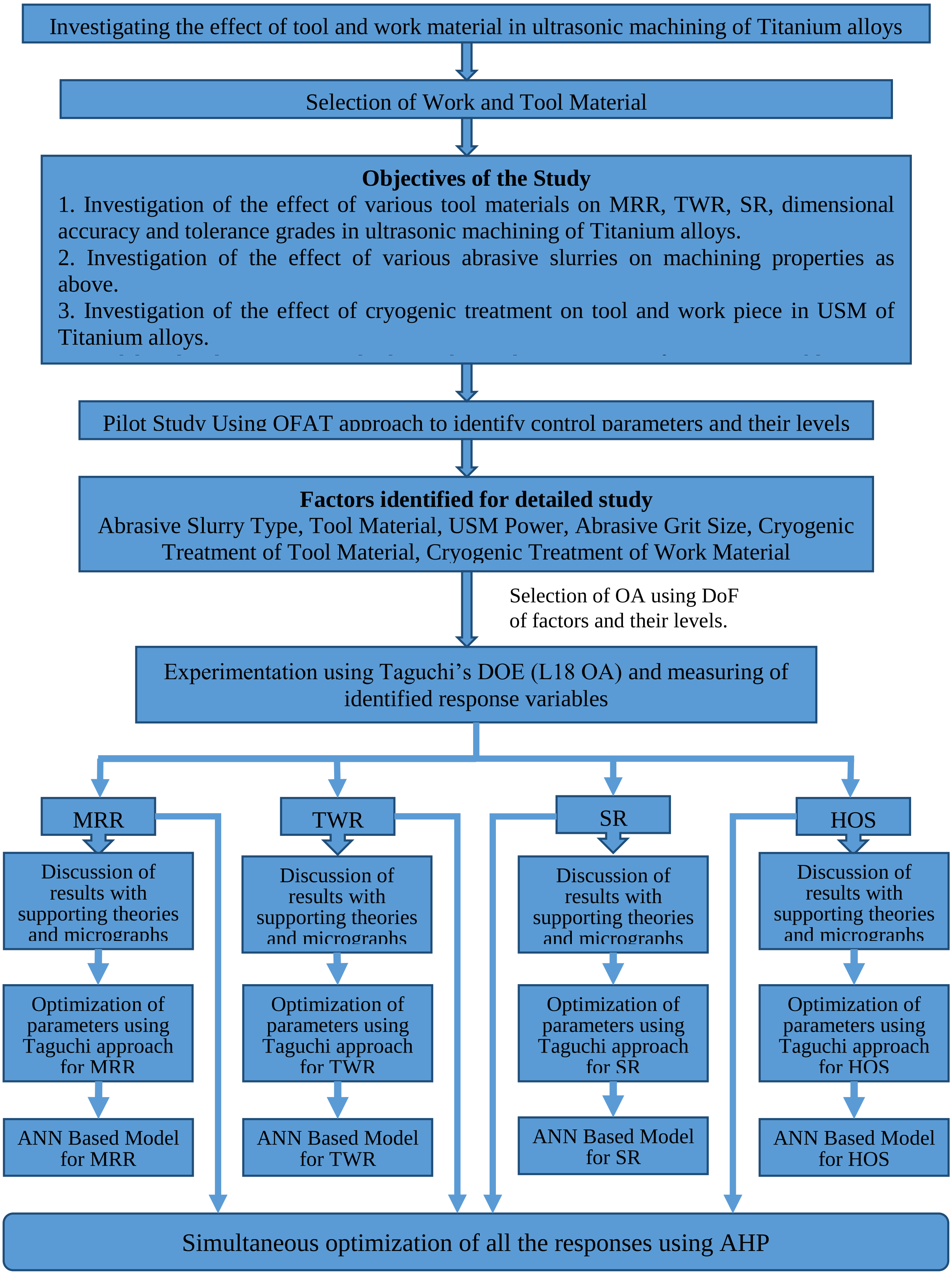

Figure 3.1 Experimental Layout

The experiments were performed on Ultrasonic drilling machine AP-500 supplied by Sonic Mill, USA available at Thapar University, Patiala. A typical ultrasonic machining set up is shown in Fig 3.2. The sinker ultrasonic machine tool supplied by Sonic Mill, USA (Model No. AP 500) was used for experimentation work. The USM setup, shown in Figure 3.2, consists of an ultrasonic spindle kit comprising of a power supply system and an ultrasonic spindle mounted system having a cylindrical horn of φ25.4 mm, a constant pressure feed system and an abrasive slurry pump.

The machining set up has variety of applications and is capable of, among other things, drilling small, single as well as multiple, holes and machining features into various substrates and machining round discs used for manufacturing of power diodes [40]. The different constituent parts of the USM machine tool used for present investigation are elaborated briefly as under [40]:

The z-axis assembly of the machine tool (Figure 3.2) has a machined aluminum tool carrier which rides on roller bearings that run smoothly two hardened and ground steel shafts. The bearing-shaft unit ensures repeatable tool placement on the workpiece. These are protected from abrasion through use of rubber boots. The assembly is equipped with a depth gauge to control cut with an accuracy up to .01mm. The dial movement aids visual indication of machining process. A complete slurry recirculating system is also included with the machine.

The power supply unit of the machine converts line voltage into 20kHz at maximum power of 500W. A built-in overload protector prevents the machine during the period of higher power supply than normal.

The transducer part or the converter of the machine tool (Figure 3.2) is a piezo-electric wafer that converts electrical impulses of the power supply into mechanical motion. Unlike ferrite or iron core-type converters, this wafer will last almost indefinitely unless abused. Unlike ferrite converters, this does not require a fan or water and is totally enclosed to ensure protection from any external damage including that caused by abrasives.

Amplitude couplings (Figure 3.2) can be customized to increase the flexibility of machine by varying the amplitude from half to 21/2 times normal motion, thus can provide optimum cutting ratio.

The machine tool is equipped with replaceable titanium horns which often are the most economical tooling and are thread fastened to the machine unit. The experiments in the present study were performed with standard 25.4mm (1-inch) tool horn.

Ti-6Al-4V (Titanium Grade V) was used as work material for preliminary pilot study while stainless steel and high carbon steel were used as tool materials. Effect of power rating and abrasive grit size alongwith tool material was explored on the three response variables namely MRR, TWR and SR. USM power was varied from 20% to 80% of the maximum rated value of 500W while abrasive grit size of #220, #320, #400 and #500 of aluminium oxide and silicon carbide was chosen for pilot study. MRR and TWR were measured in terms of volumetric reduction in workpiece and tool, respectively, per unit time (mm^3/min) after machining with USM while average value R_a for surface roughness was measured using Mitutoyo surface roughness tester. Silicon Carbide slurry with a concentration of 20% by weight of abrasive particles in abrasive-water mixture at a near constant flow rate of 8l was used during the experimentation alongwith other machine related parameters.

3.1.1 Results of Pilot Experimentation

Pilot experimentation was performed in four rounds. For these preliminary rounds, untreated tool and untreated work material were used for machining. First and second round were aimed at exploring the effect of Power Rating using HCS and SS tool, respectively, on MRR, TWR and Surface Roughness in ultrasonic machining of Ti-6Al-4V.

Table 3.1 Findings of Round 1 and 2 of Pilot Experimentation

Fixed Parameters ⟶	**Slurry Type: SiC #400 Tool – HCS Slurry Concentration: 20% Flow Rate : 8l/min**			**Slurry Type: SiC #400 Tool – SS Slurry Concentration: 20% Flow Rate : 8l/min**		
USM Power	MRR (mm^3/min)	TWR (mm^3/min)	SR (micron)	MRR (mm^3/min)	TWR (mm^3/min)	SR (micron)
100	0.188	0.228	1.04	0.215	0.204	1.06
150	0.180	0.245	1.10	0.224	0.238	1.11
250	0.278	0.304	1.29	0.311	0.275	1.25
350	0.323	0.371	1.34	0.365	0.384	1.33
400	0.405	0.44	1.39	0.44	0.464	1.36

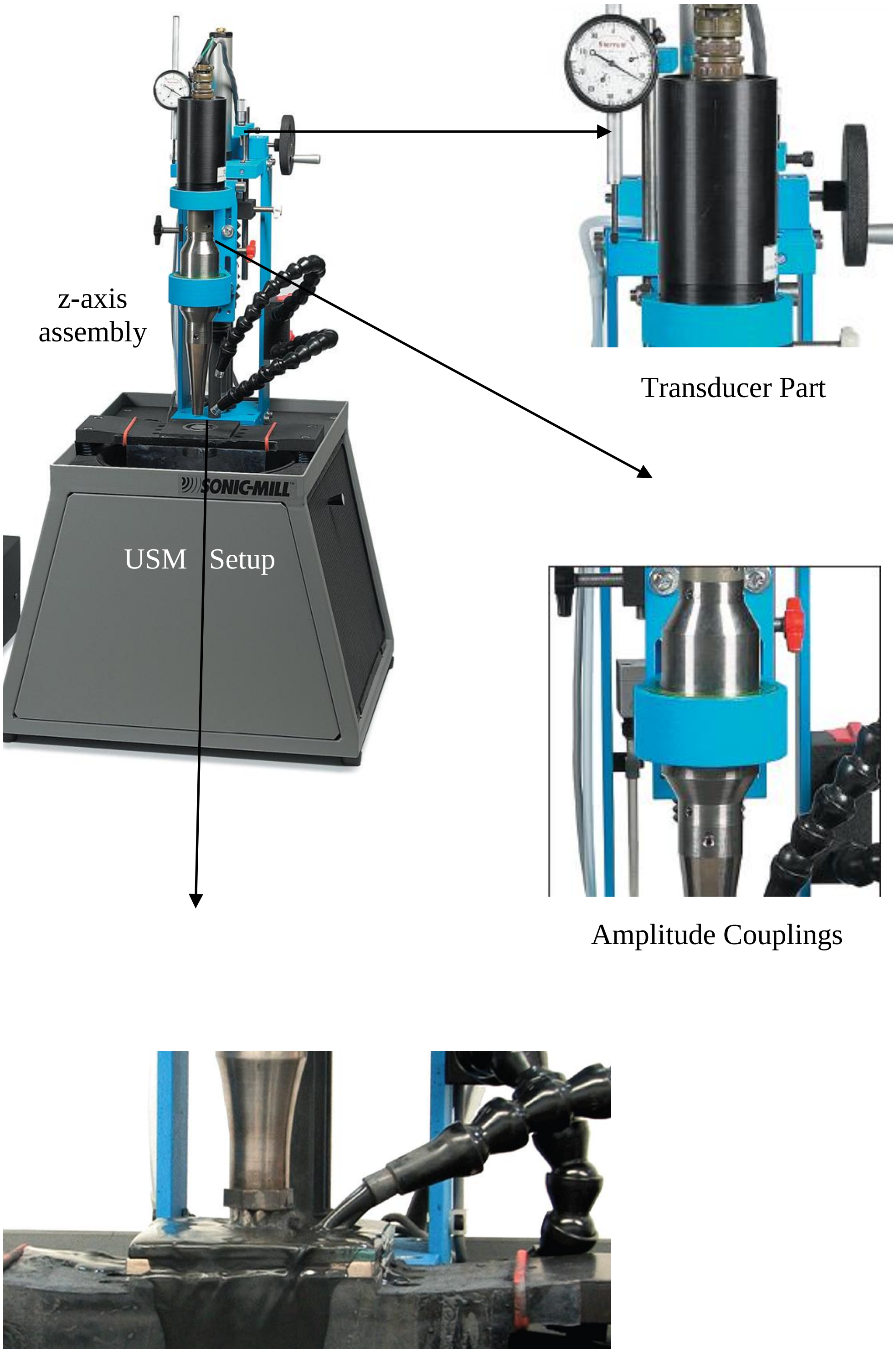

Figure 3.2USM Set up *[40]*

Similarly, 3rd and 4th round were carried out to explore the effect of abrasive slurry grit size using HCS and SS tool respectively. USM power was changed from 250W to 350 W while shifting to 4th round of preliminary study. The results of pilot experimentation have been presented in Table 3.1 and 3.2.

Table 3.2Findings of Round 3 and 4 of Pilot Experimentation

Fixed Parameters →	**Slurry Type: SiC Tool – HCS Slurry Concentration: 20% Flow Rate : 8l/min USM Power: 250W**			**Slurry Type: SiC Tool – SS Slurry Concentration: 20% Flow Rate : 8l/min Power: 350W**		
Slurry grit size	MRR (mm^3/min)	TWR (mm^3/min)	SR (micron)	MRR (mm^3/min)	TWR (mm^3/min)	SR (micron)
#220	0.325	0.38	1.56	0.431	0.472	1.60
#320	0.302	0.355	1.38	0.385	0.415	1.45
#400	0.278	0.304	1.29	0.365	0.384	1.33
#500	0.195	0.274	0.90	0.306	0.318	0.98

Exploration of effect of parameters on MRR

Figure 3.3 presents the effect of USM power on MRR. The USM power was varied from 100W to 450W. Machining efficiency gets very low at less than 100W, therefore lower values were not used for exploration. It was also observed that at very high power rating of 450W, machining status became highly unstable and a cylindrical whirl of slurry was created around the tool pin due to higher intensity in lateral vibrations. Impact of energized abrasive slurry even led to erosion from the face of tool shoulder. Therefore the use of 450W power was discontinued after some time and observations were recorded for variation of power between 100-400W. The variation in the graph indicates that an increase in USM power results in increase in MRR except at very low values when there was not any appreciable change in MRR. The increment, though, occurs with different slope indicating that the MRR does not increase uniformly across power incremental values.

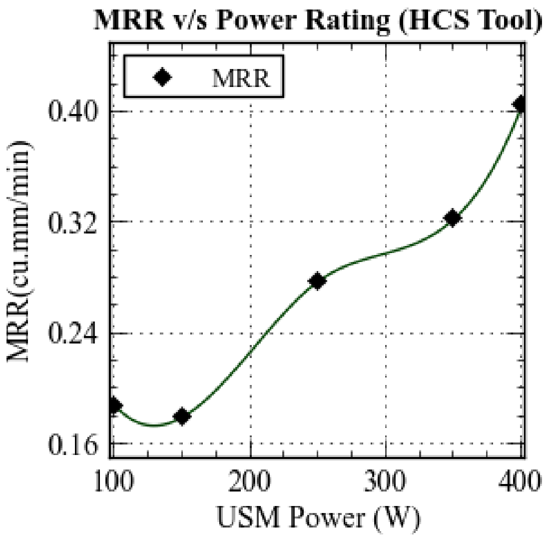

Figure 3.3Variation of MRR with Power (SiC slurry, #400 grit size, HCS Tool)

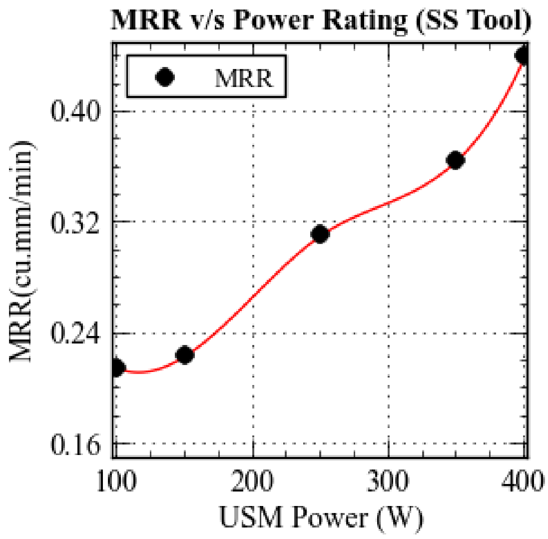

Figure 3.4 Variation of MRR with Power (SiC slurry, #400 grit size, SS Tool)

Variation in MRR using SS tool for machining is shown in Figure 3.4 that also indicates almost linear increase in MRR with USM power. The increment in this case is not as steep as was with HCS tool across certain regions. However, variation pattern was found to be more linear with SS tool. A comparison of the two plots indicate relatively higher values of MRR for SS tool. It is worth mentioning here that discrete individual readings of the pilot experimental outcome have been joined with a curve to indicate a trend. These however may or may not reflect the true relationship that exist between response at various parametric settings.

To determine the effect of abrasive grit size, four sizes of abrasives of silicon carbide were used for pilot experimentation. To compensate for inevitable variations in the volume of circulating slurry and fluctuations in slurry flow in the working gap between tool-workpiece, a large volume of all the slurries was prepared by keeping a fixed ratio of 1:4 by weight for abrasive and water respectively. The variation recorded in MRR for these slurries is shown in Figure 3.5 and 3.6. It can be seen from the Figure 3.5 that MRR varies inversely with grain fine-ness number. Coarser abrasive grits of #220 were associated with higher MRR while finer abrasive particles of # 500 recorded lower MRR due to difference in momentum associated with the particles. Coarser particles strike the work piece with higher impact energy and hence cause ploughing of bigger craters at work surface as compared to finer particles. The reduction in MRR was more dominant as grit size reduced from #400 to #500.

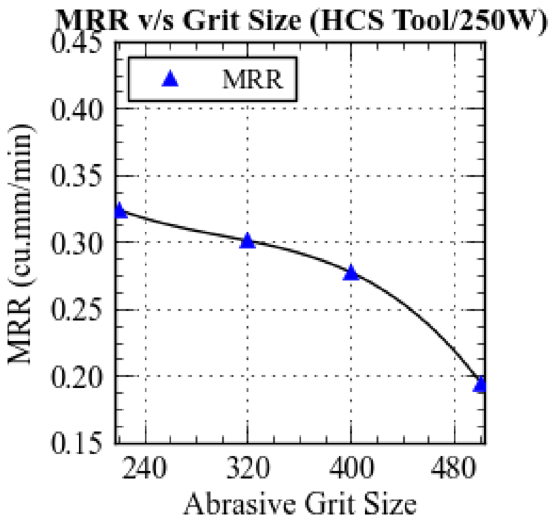

Figure 3.5 Variation of MRR with grit size (SiC abrasive slurry, HCS Tool, 250W power)

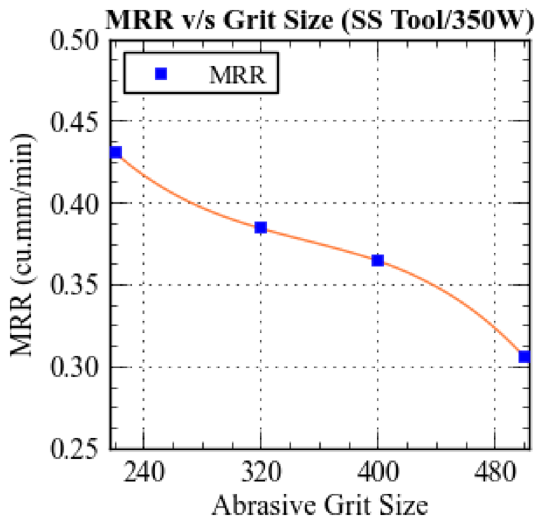

Figure 3.6 Variation of MRR with grit size (SiC abrasive slurry, SS Tool, 350W power)

Figure 3.6 shows effect of abrasive grit size with the use of SS tool at 350W power. This also indicates that MRR reduces with finer grains and increases with increase in particles size of abrasives.

Exploration of effect of parameters on TWR

A higher MRR is necessary for maintaining adequate rates of production for any manufacturing scenario. However minimizing the tool wear is also a very important criterion since a worn tool incurs cost of replacement as well as cost of lost time during changeover. Therefore for any manufacturing situation it is of ample importance to reduce the tool wear rate. Pilot study conducted herein also aimed at exploration of effect of change of parameters on TWR by one factor at a time approach.

Figure 3.7 to 3.10 represent the effect of process parameters on TWR.

Figure 3.7 shows the effect of USM power on TWR when machining was carried out using HCS tool and SiC abrasive slurry of #400 grit size. Tool Wear increases almost linearly with increase in power rating. The wear at tool surface is caused by the energized abrasives under the ultrasonic vibrations. Higher power rating leads to transfer of more energy to abrasives causing higher tool wear.

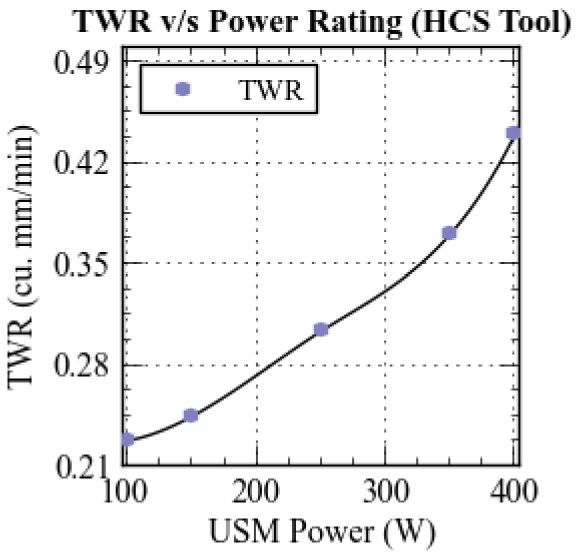

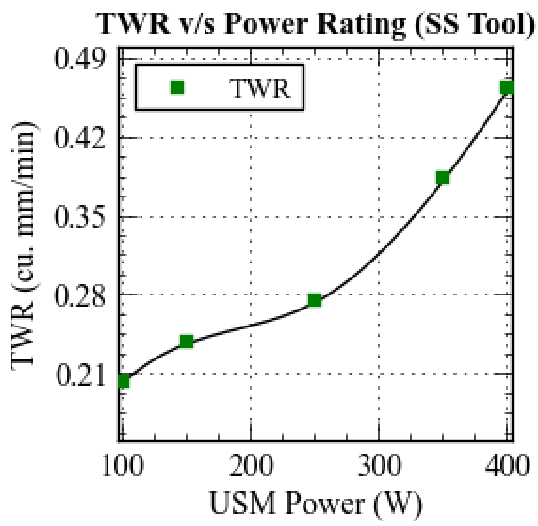

Figure 3.7 Variation in TWR with USM Power (SiC slurry, #400 grit size, HCS Tool)

Figure 3.8 Variation in TWR with USM Power (SiC slurry, #400 grit size, SS Tool)

Fig 3.8 shows variation in TWR with the use of SS tool alongwith SiC slurry of #400 grit size. The pattern of variation is similar to what was observed with HCS tool though the increment in tool wear values was not as linear as was with HCS tool.

Figure 3.9 shows variation of TWR with abrasive grit size using HCS tool at 250W power. Coarser particles lead to higher transfer of energy to the tool owing to larger associated momentum and hence cause more erosion at the tool surface compared to finer particles. It +can also be seen that points of peak MRR also correspond to high TWR.

Figure 3.10 shows variation of TWR with abrasive grit size using SS tool at 350W power. The trend of reduced TWR with finer particles can be seen in this case too though the reange of tool wear was very narrow as compared to that was achieved with HCS tool.

Exploration of effect of parameters on SR

Surface roughness is measure of irregularities in the form of peaks and valleys on the work surface caused due to impact of abrasive particles under the effect of ultrasonic vibrations transferred through tool. Figure 3.11 to 3.14 show the effect of various process parameters on surface roughness during the pilot study.

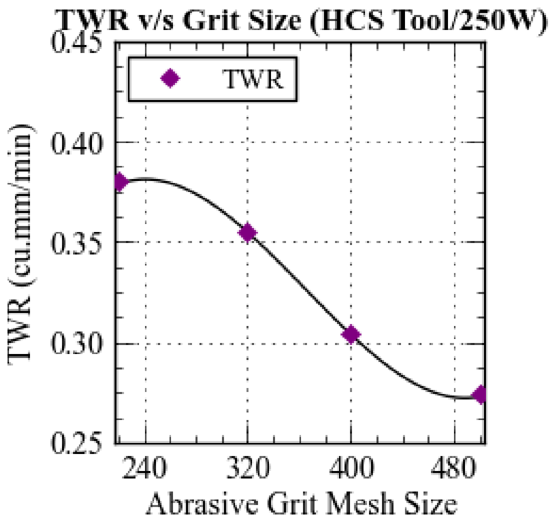

Figure 3.9 Variation of TWR with grit size (SiC abrasive slurry, HCS Tool, 250W power)

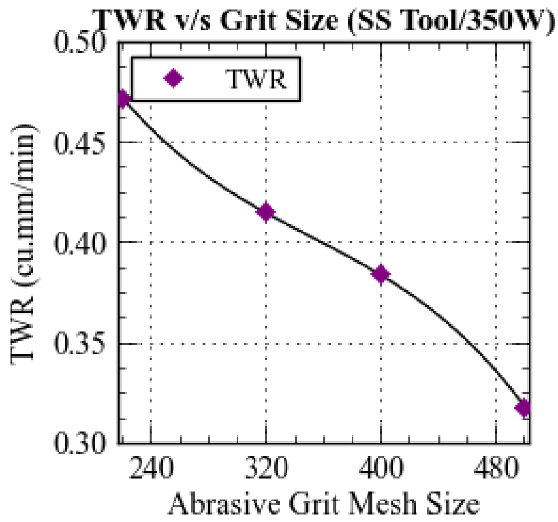

Figure 3.10 Variation of TWR with grit size (SiC abrasive slurry, SS Tool, 350W power)

Figure 3.11 shows the effect of power rating on surface roughness obtained in ultrasonic machining of Ti when power was varied from 100W to 450W using HCS tool and SiC slurry of #400 grit size. Surface roughness is caused by irregularities at the surface due to machining caused by ploughing of work material by the abrasive particles. Higher USM power caused deeper impacts on work surface causing higher values of roughness. Surface roughness thus reduces with lower values of USM power.

Figure 3.12 shows variation of surface roughness with USM power using SS tool with SiC slurry of #400 grit size. Almost similar trend of variation has been observed with this set of experiments as was with HCS tool and higher power ratings were found to cause higher surface roughness.

Experiments were also carried out to determine variation of surface roughness with abrasive grit size. Figure 3.13 shows that surface roughness of the machined region decreases remarkably as the abrasive grit size reduced. Finer particles caused small craters on work surface and resulted in smoother surface compared to coarser abrasive particles. Accordingly, the use of #220 abrasive particles was associated with higher surface roughness as compared to finer particles of #400 and #500 when machining was carried out using HCS tool with SiC slurry at 250W power.

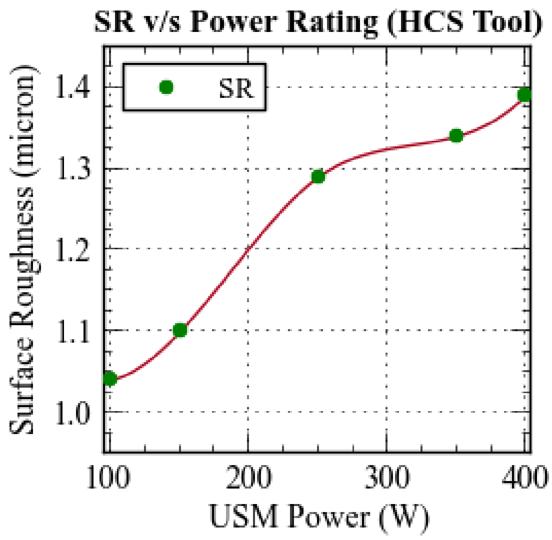

Figure 3.11 Variation of SR with Power (SiC slurry, #400 grit size, HCS Tool)

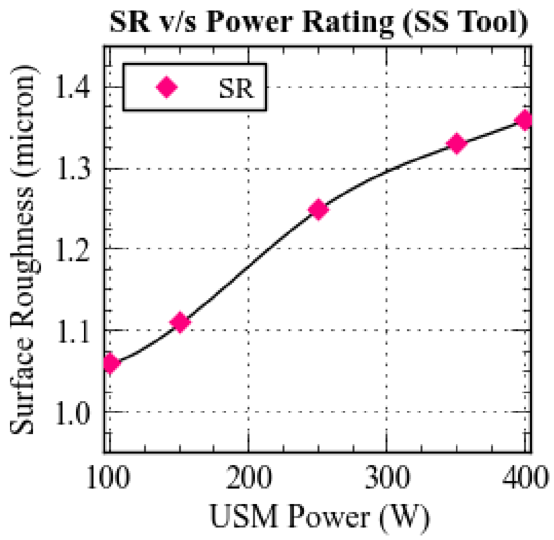

Figure 3.12 Variation of SR with Power (SiC slurry, #400 grit size, SS Tool)

Similar trend of variation in surface roughness with abrasive particle size was also observed with the use of SS tool at 350 W. A sharp improvement was recorded in surface finish when abrasive grit size was changed from #400 to #500 as shown in Figure 3.14.

It is evident from the outcomes of pilot experimentation that there is significant change in response variables of MRR, TWR and SR with variation in controlled parameters like power rating and slurry grit size. Further it can also be seen that zones of desirable high MRR also get overlapped with zones of high tool wear rate and high surface roughness, thus making it all the more critical to control the parameters for an optimized output. Higher power and coarser abrasives impart higher momentum at work surface and hence cause higher MRR but at the same time lead to formation of deeper craters, causing poor surface finish.

3.2 TAGUCHI METHOD AND STEPS IN IMPLEMENTATION

A robust parameter design for product as well as process design with major focus on minimization of variation and sensitivity towards noise was propounded by Dr. Genichi Taguchi as stated in previous section. Taguchi's approach for DOE offers a powerful and highly efficient method of designing for consistent and optimum performance under a variety of conditions [145-146].

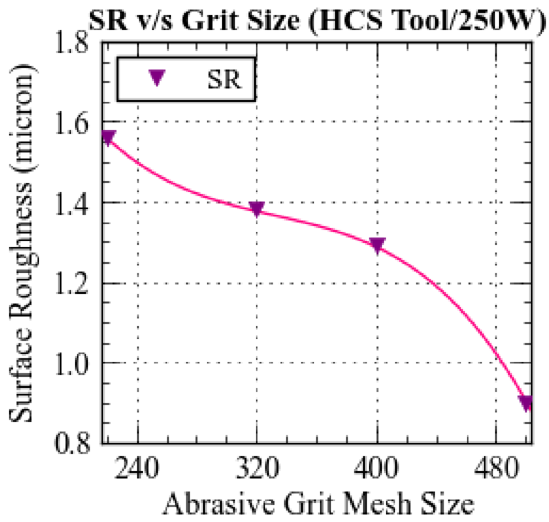

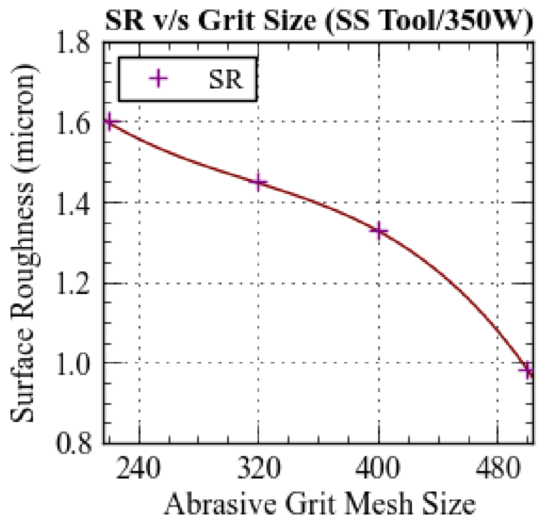

Figure 3.13 Variation of SR with grit size (SiC abrasive slurry, HCS Tool, 250W power)

Figure 3.14 Variation of SR with grit size (SiC abrasive slurry, SS Tool, 350W power)

The focus in Taguchi’s approach has been that of achieving the target with minimum variability instead of the traditional definition of quality that emphasizes on achieving conformance to specification [147]. In contrast to OFAT, the Taguchi’s method involves experimentation by statistical design techniques and use of orthogonal arrays to vary several factors simultaneously and has been used extensively by researchers to solve diverse design and manufacturing problems [99,109-110,117,132-133,148,149]. There are two types of factors that characterize the process in Taguchi’s technique and classified as controllable or design factors and uncontrollable or noise factors. While the former are adjusted on the machine, the latter are the source of variation in the process associated with the operational environment. The noise here refers to variation caused due to operating conditions or due to manufacturing imperfection.

The controllable factors on the other hand are classified into those affecting average levels of response variable, variability in the response and those controlling economic requirements. Accordingly they are referred to as target control factors (TCF), variability control factors (VCF) and cost factors. A perfect Taguchi design aims at minimizing the variability by controlling VCF without affecting performance by adjusting target control factors. Figure 3.15 shows these factors encountered in Taguchi Design. The various stages in creating a complete and effective design of experiments as suggested by Taguchi are shown in Figure 3.16. Working on the methodology given in Figure 3.16, the steps were implemented for the present study:

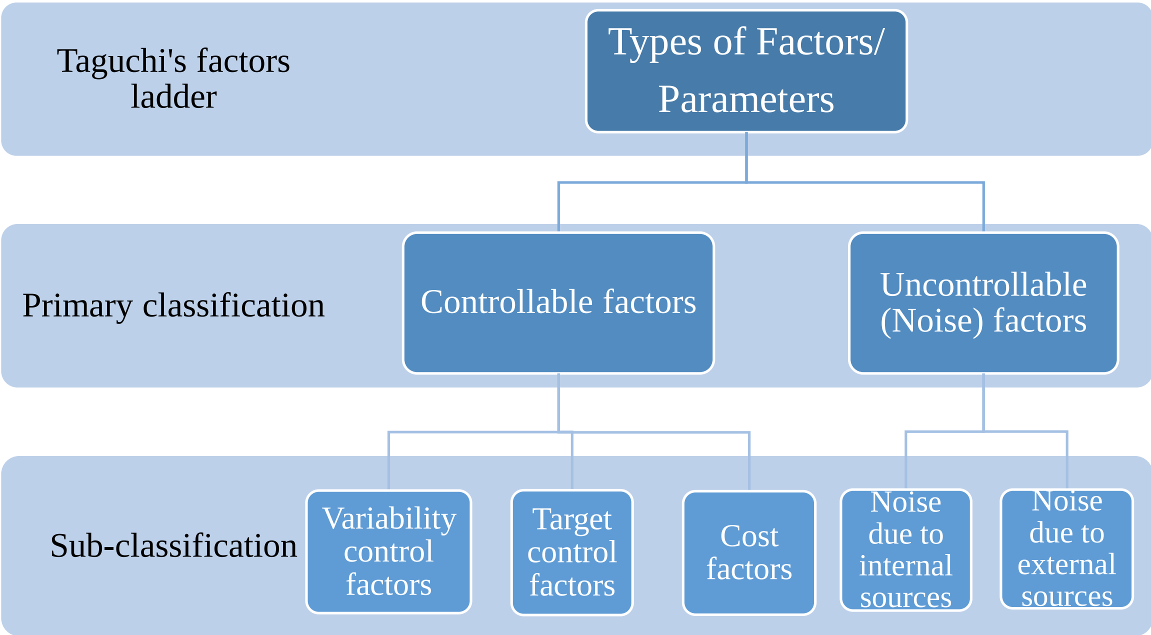

Figure 3.15 Taguchi's Factor Ladder

3.2.1 Statement of intent of study

A clear and precise statement, if developed, gives an insight into the proposed work and facilitates the experimentation by proper visualization of goal through this statement. Accordingly, the objective of the present study is to investigate the effect of cryo treated tool and work material in ultrasonic machining of Titanium Alloys.

3.2.2 Objectives

Once the problem has been stated now the detailed objectives to accomplish the goal of solving the problem need to be listed. At first the quality characteristics and measurement systems need to be identified. Material Removal Rate (MRR), Tool Wear Rate (TWR), Surface Roughness (SR), Dimensional Accuracy and Tolerance Grades were identified as performance characteristics (responses) in the present study. Subsequently all the factors that may affect the performance variables were identified using Cause and Effect diagram. Based on pilot study and available literature, the factors selected for analysis in the study were identified and their range of variation was determined. Accordingly in the present study, USM Power Rating, Abrasive Grit Size, Abrasive type, Tool Type and type of cryogenic treatment given to tool and work piece were selected as the process parameters whose influence on the response variable was to be determined. A detailed account of process of selection of factors has been given in Section 3.4. After finalizing the factors to be explored, the range and the levels were decided by performing pilot experimentation using OFAT approach.

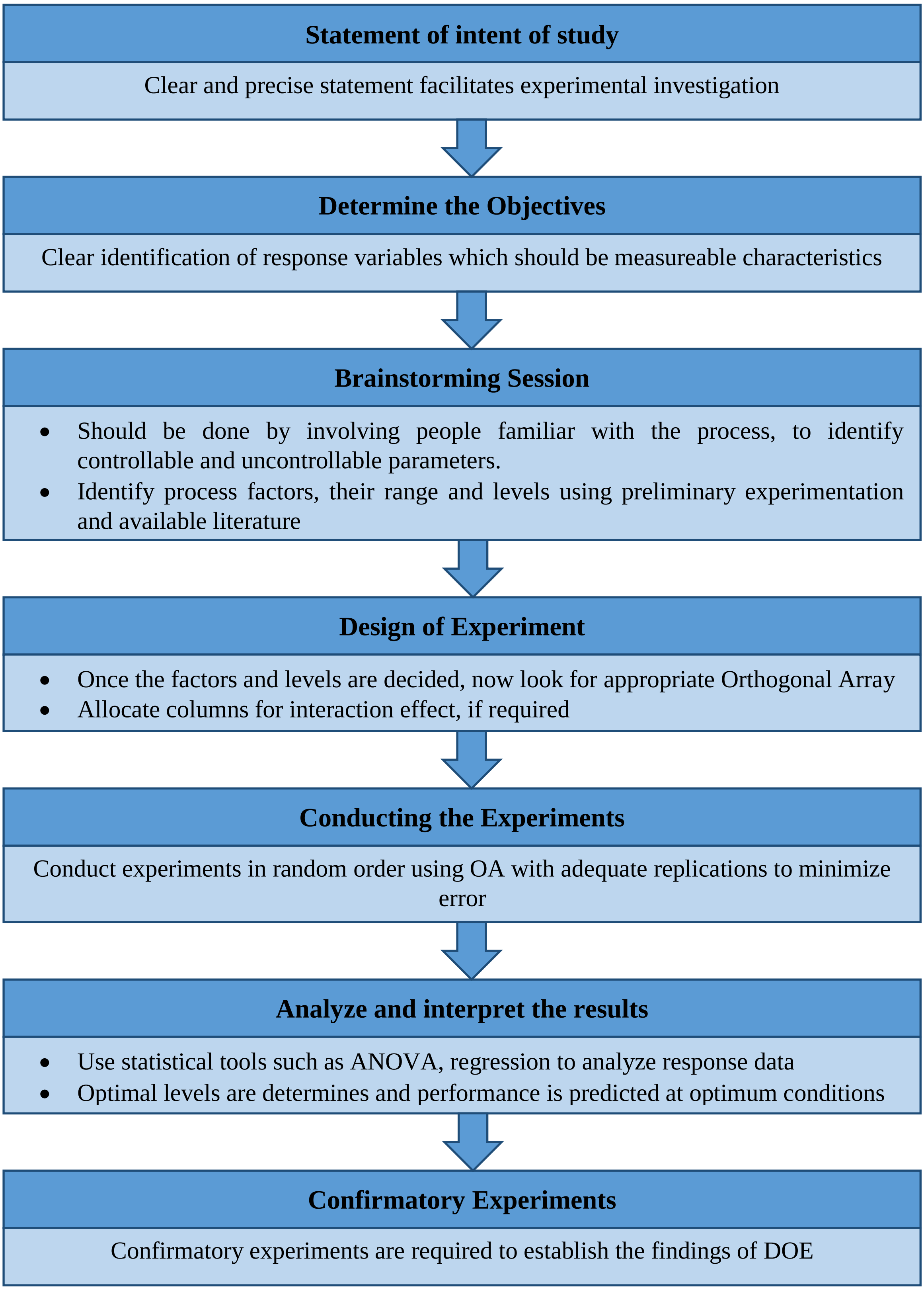

Figure 3.16 Stages in Design of Experiment process

3.2.3 Selection of Orthogonal Array

Robust Design of Taguchi Methodology is attributed to utilization of a mathematical tool called as Orthogonal Arrays. Use of these arrays considerable reduces the number of experimental trials required to establish the effect of process parameters on response variables especially when a large number of factors and their levels are involved that make full factorial experimentation infeasible and un-economical. The earliest usage of orthogonal arrays, a mathematical approach, dates back to 1897 and is credited to French mathematician Jacques Hadmard. Plackett and Burman, British statisticians further explored the use of these arrays in the post world war II era [150-151].

Orthogonal arrays may be termed as 'fractional factorial designs' that consist of symmetrical subsets of all the possible combinations of various levels of input process parameters corresponding to full factorial designs. Selection of an appropriate OA is of immense importance for success of experimental investigation and the selection process is governed by several criterion, the prominent among them being the number of factors and their levels to be explored and the possible interactions among the various factors that need to be incorporated in the design of experimentation. Subsequently those values which indicate a major shift in the value of response variable are selected for inclusion into design of experiment. Available literature on the related studies can also aid in determining levels of factors for DOE. Second aspect in designing the experimentation is determining the interaction effect. A number of two level interactions are possible in a given situation. Selection of appropriate interactions generally depends upon the previous experience of the researcher and is also influenced by the available literature and data on the similar studies conducted in the past. A hit and trial approach may also be used to identify the appropriate interactions affecting the response variable in a given experimental design.

Once the factors, their levels and the interactions to be explored are established, the next step is to identify and select appropriate OA for designing the study. Several standard arrays are available such as L_8, L_{12}, L_{16}, L_{32} for two-level factors while for L_9, L_{27} may be used for 3 level factors. Several options of arrays are also available when there are multiple factors with different number of levels for example one factor with 2 level and some factors with 3 level then L_{18} can be used. The final selection however is governed by quantification of degrees of freedom (DOF) in a given study. In statistical terms, DOF is associated with estimation of information from the data and determines the minimum number of treatment conditions. The total degrees of freedom for a given array are determined by summation of DOF of each individual factor and of interactions being studied. While the DOF of each factor may be obtained by subtracting one from number of levels of the factor, DOF of a 2-factor interaction is obtained by multiplying the DOF of individual factors involved in the interaction. Approximation of total DF involved in a study resolves the minimum number of experiments required to be conducted to adequately investigate the factors involved. DOF of OA is equal to one less than the number of experiments involved in an array. Several solutions may be possible with regard to selection of array based on DOF. The final selection is then attempted with an array that has more suitability from economical and accuracy point of view [150]. The array which leads to minimum error in results and minimum cost of experimentation could then be selected for designing the experimentation. A control log table is prepared by assigning the level of each factor corresponding to all the experiments in the OA. Each row of the matrix table thus formed contains the factor-level setting corresponding to each experiment of the OA and is thus called a run or treatment of experiment. The experiments are conducted in random order, not following any sequence, and repetitions are performed to eliminate the error.

3.2.4 Analysis and Interpretation of Results

The results obtained from experimentation conducted based on Design of Experiments need to be analyzed and interpreted so as to improve the quality characteristics and establish the relative importance of each factor on the process performance. Analysis of Variance (ANOVA) is an important statistical tool extensively used to determine total variability of the observed outcomes which is the summation of variance due to various input parameters under control and experimental error. The ANOVA also leads to identification of significant and non-significant parameters of the study and percentage contribution of each of them on the response variable value. Performing the F-test establishes the extent of significance of each parameter which is determined by comparing the F-value corresponding to each parameter with tabulated F-value at some confidence interval corresponding to the requisite degree of freedom.

3.2.5 Signal to Noise Ratio

An important aspect of Taguchi's philosophy is signal to noise (S/N) ratio. Quality characteristic during experimentation under different values of controlled factors is bound to vary and the variation that is attributed to change in a factor value is referred to as signal and represents a desirable part. However at the same time there could be influence of some uncontrolled parameters on quality characteristics which were actually not part of the factors being explored. This effect due to external factors in response characteristic is referred to as noise and therefore represents undesirable value. S/N ratio, thus is actually a measure of sensitivity of quality characteristic, under investigation in controlled conditions, to uncontrollable external influencing (noise) factors and hence represents extent of variation in measured performance characteristic. Accordingly, a higher value of S/N ratio represents more controlled experimentation wherein signal value is much higher than undesirable noise value. Highest S/N ratio thus yields optimum quality at minimal variance [152]. Depending upon the type of response, a performance characteristic can be categorized into higher-the-better, lower-the-better and nominal-the-best like the case of volume of production, cost of manufacturing and dimensional accuracy respectively in reference to a manufacturing industry scenario. Appropriate selection of S/N ratio for each of the three situations is mandatory for accurate solution of optimization of response variables. Calculation of S/N ratio for the stated three types of situations may be described as follows:

$$\text{Higher-the-better S/N ratio, } \eta = -10\log_{10}\frac{1}{n}\sum_{i=1}^{n}\frac{1}{y_{ij}^{2}} \qquad \textit{Eq. 3.1}$$

$$\text{Lower-the-better S/N ration, } \eta = -10\log_{10}\frac{1}{n}\sum_{i=1}^{n}y_{ij}^{2} \qquad \textit{Eq. 3.2}$$

$$\text{Nominal-the-best S/N ratio, } \eta = 10\log_{10}\left[\frac{\bar{y}^{2}}{s^{2}}\right] \qquad \textit{Eq. 3.3}$$

where y_{ij} is the ith experiment at jth test and no. of trials in each experiment have been represented by n while $\bar{y}$ is mean of samples when s is sample size.

S/N ratio is measured in decibel (dB) units and is represented by η.

Among the four responses measured in the presented study MRR is listed as a higher-the-better characteristic while TWR, SR and dimensional accuracy measured in terms of hole oversize have been categorized as lower-the-better type characteristic.

3.2.6 Confirmatory Experiment

The final phase of DOE process consists of conducting the confirmatory experiment for validation of conclusions drawn from the analysis of the study. A confirmatory test is performed by conducting the experiment at as specific combination of factors and their levels as recommended by fulfilment of the objective of the study. For example if the objective is to maximize the MRR, then confirmatory experiment is carried out at that combination of process parameters which lead to maximum MRR as per DOE and then validation is made from the outcome of the confirmatory test.

3.3 SELECTION OF INPUT PROCESS PARAMETERS FOR FINAL DESIGN OF EXPERIMENTATION

From the analysis of pilot experimentation presented in Section 3.2, it is evident that a lower value of power rating resulted in better performance with regard to tool erosion which was minimum at lower values. Surface roughness values were also found to be desirable at lower value of power ratings and with the use of finer abrasive particles. Accordingly, 100W power and #500 abrasives resulted in desired values of outcomes for TWR and SR among the chosen levels of parameters for pilot study. However this also meant a compromise on machining rates as these machine/abrasive settings were found to be associated with lowest rates of material removal from work surface. So lower values of USM power and abrasive particle size are desirable from TWR and SR viewpoint but not from MRR view point. Similarly, higher power values of USM power ranging towards 400W and coarser abrasive particles of #220 mesh size resulted in much improved rates of machining but also caused poor surface texture and were associated with increased cost of tooling due to frequent wear and changeover. So for combined optimization of all the parameters, the power rating was varied across three levels from ranging from either extremes of 100W to 400W and 250W being the intermediate value and similarly for abrasive grit size #400 was chosen as the intermediate abrasive particle size among the extremes of #220 and #500. During pilot experimentation only Silicon Carbide slurry was used for experimentation and all the trials were conducted using this slurry only. However, two additional slurries in form of Aluminium Oxide and Boron Carbide were also selected each in grit size of #220, #400 and #500 for final experimentation thus giving rise to nine such abrasive slurries. The idea of using different types of slurry emanated from difference in knoop hardness and thus the cutting ability of these slurries. The published related literature on USM of titanium also indicates use of these three types of slurries [110,116-117,122,133,139]. Since coarser and finer grains impacted differently on work material and accordingly different mesh sizes were chosen to explore their effect. However, hitherto very little work has been reported on use of mixture of two different types of slurries and accordingly the present study was also focused at exploring the effect of hybridizing the slurries by creating mixtures of identical grain size in equal proportions to determine their effect on machining variables. This has also got economic aspect associated with it considering the large difference in cost associated with boron carbide and other two slurries.

Pilot study indicated a significant difference in the output response variables when using tools of two different materials. High carbon steel and stainless steel were used as tool materials in pilot study. The selection of tool materials was governed by the objective of exploring a wider range of mechanical properties with regard to hardness, ductility and toughness and accordingly a third a tool material of titanium was also selected for the study owing to its altogether different mechanical properties compared to the two ferrous based tool materials. The available literature on similar studies also indicates use of tool steels, carbides, stainless steel and titanium as tool materials [110,116,117,122]. Thus tools made of HCS, SS and Ti were selected with a focus on exploring their effect on response variables. The study was aimed at investigation of cryogenic treatment on tool and work material in ultrasonic machining of titanium alloys. Therefore, to make the comparison, tools and work material were grouped into three categories comprising of untreated (UT) set wherein no cryogenic treatment was involved, shallow cryogenic treatment (SCT) wherein the material was soaked at a temperature of -80^{0}C and deep cryogenic treatment (DCT) carried out at a soaking temperature of -196^{0}C.

In the light of above discussion, following selection was made for parameters and their levels:

Abrasive Type: Aluminium Oxide (Al_2O_3) , Silicon Carbide (SiC), Boron Carbide (B_4C), Mixture of Aluminium Oxide and Silicon Carbide in equal proportion (Al_2O_3 + SiC) , Mixture of Silicon Carbide and Boron Carbide in equal proportion (SiC + B_4C) and Mixture of Aluminium Oxide and Boron Carbide in equal proportion (Al_2O_3 + B_4C)

Tool Material: High Carbon Steel (HCS), Stainless Steel (SS), Titanium (Ti)

Power Rating of USM: 20% of rated power (100W), 50% of rated power (250W) and 80% of rated power (400W)

Abrasive Grit Size: mesh size #220, #400, #500

Type of cryogenic treatment given to tool: Untreated (UT), Shallow Cryogenic Treated (SCT), Deep Cryogenic Treated (DCT)

Type of cryogenic treatment given to workpiece: Untreated (UT), Shallow Cryogenic Treated (SCT), Deep Cryogenic Treated (DCT)

So it is evident that one factor i.e. abrasive slurry type was varied over six levels while all the other 5 factors were varied over 3 levels each. Whereas power rating and grit size are numerical factors, the remaining four are categorical factors and thus can take only the discrete values as specified in the table.

The factors, levels and coding of the selection is given in Table 3.3.

Now if we plan to carry out experimentation using one factor at a time approach for exploring the effect of parameters at the levels as specified, it will require ($6 * 3^5 = 1458$) number of runs for completing task, thus making it very time consuming as well as expensive. To overcome this issue, Taguchi's method for Design of Experimentation was adopted.

Table 3.3 Factors and their levels under study

Factor	Factor Code	Level 1	Level 2	Level 3	Level 4	Level 5	Level 6
Slurry Type	**A**	Al_2O_3	SiC	B_4C	Al_2O_3 + SiC	SiC + B_4C	Al_2O_3 + B_4C
Tool Material	**B**	HCS	SS	Ti	--	--	--
Power Rating	**C**	100W	250W	400W	--	--	--
Abrasive Grit Size	**D**	#220	#400	#500	--	--	--
Treatment to Tool	**E**	UT	SCT	DCT	--	--	--
Treatment to W/piece	**F**	UT	SCT	DCT	--	--	--

3.4 SELECTION OF ORTHOGONAL ARRAY

In the current study a total of six factors have been selected for exploration as shown in Table 3.3. Except one factor, all other are varied over 3 levels each and the single factor has been varied over six levels each. Degree of freedom corresponding to each factor is one less than no. of levels. Thus a total of 15 degree of freedom are there for the current plan of experimentation. For selecting an appropriate OA, degree of freedom of the array should be more than or equal to DOF of the experimentation plan. One of the most suitable outcome here becomes L_{18} orthogonal array since it has adequate number of degrees freedom as well as can adequately accommodate the mixed nature of levels of factors. The said OA can accommodate, alongwith one factor at six levels, upto 6 factors at 3 levels each. Factor with six level has been accommodated in first column and other factors have been assigned to column 2-6. The selected array is shown in Table 3.4 where numbers 1,2,3…6 correspond to levels of process factors A to F.

Table 3.4 Standard Mix Type of L_{18} orthogonal array

	Factors and their Levels					
Exp. No.	**A**	**B**	**C**	**D**	**E**	**F**
1	1	1	1	1	1	1
2	1	2	2	2	2	2
3	1	3	3	3	3	3
4	2	1	1	2	2	3
5	2	2	2	3	3	1
6	2	3	3	1	1	2
7	3	1	2	1	3	2
8	3	2	3	2	1	3
9	3	3	1	3	2	1
10	4	1	3	3	2	2
11	4	2	1	1	3	3
12	4	3	2	2	1	1
13	5	1	2	3	1	3
14	5	2	3	1	2	1
15	5	3	1	2	3	2
16	6	1	3	2	3	1
17	6	2	1	3	1	2
18	6	3	2	1	2	3

Each row of the OA table gives the plan for conducting the experimentation and thus the eighteen rows provide the parametric setting for conducting the requisite 18 number of experiments which should be performed in an entirely random order with a minimum of two repetitions to counter the effect of uncontrollable factors, if any. At the end of every experiment, measurements are made to evaluate the response parameters which in this case are MRR, TWR, SR and HOS (Hole oversize). Subsequently tolerance grades are also established on the basis of dimensional accuracy measured in terms of hole oversize.

Table 3.5 shows the various response variables measured in the present study and their measuring characteristic as per the explanation cited in Section 3.3.5

Table 3.5 Investigated response variables

S. No.	**Response Parameter**	**Measuring Units**	**Response Characteristic Type**
1	Material Removal Rate	mm^3/min	Higher-the-better
2	Tool Wear Rate	mm^3/min	Lower--the-better
3	Surface Roughness	microns (R_a)	Lower--the-better
4	Hole-oversize	mm	Lower--the-better
5	Tolerance Grades	Grade No.	Lower-the-better

CHAPTER - 4

EXPERIMENTATION, RESULTS AND DISCUSSION

4.1 MACHINE TOOL, MATERIAL AND MEASUREMENT

4.1.1 Machine Tool

The sinker ultrasonic machine tool supplied by Sonic Mill, USA (Model No. AP 500), shown in Figure 4.1, was used for experimentation work. The USM setup comprised of three major units: The main machining unit that houses z-axis moving assembly comprising of converter, coupler and acoustic horn (Figure 4.1b) alongwith constant pressure feed system; power supply unit to convert conventionally available power into 20 kHz electrical energy; and the slurry pump unit installed in tank for circulation of abrasive slurry. The details of the equipment have already been furnished in Section 3.1.1 and figure 3.2 shows the main components of the z-axis assembly unit of the USM setup used for the study. The machine feed rate or the descending rate of the head assembly is adjusted through the vertical round cylinders controlled by the levers provided at their bottom (Figure 4.1c). The cylinder nearer to front of machine caters to descending rate while the rear one controls the feed rate. Too fast feed results in trapping of slurry particles between tool and workpiece and hampers machining rate. Constant feed rate was adjusted to ensure continuous long duration machining. Abrasive concentration of 20% by weight in the mixture of abrasive particles and water and slurry flow rate of 8l/min were maintained constant during experimentation.

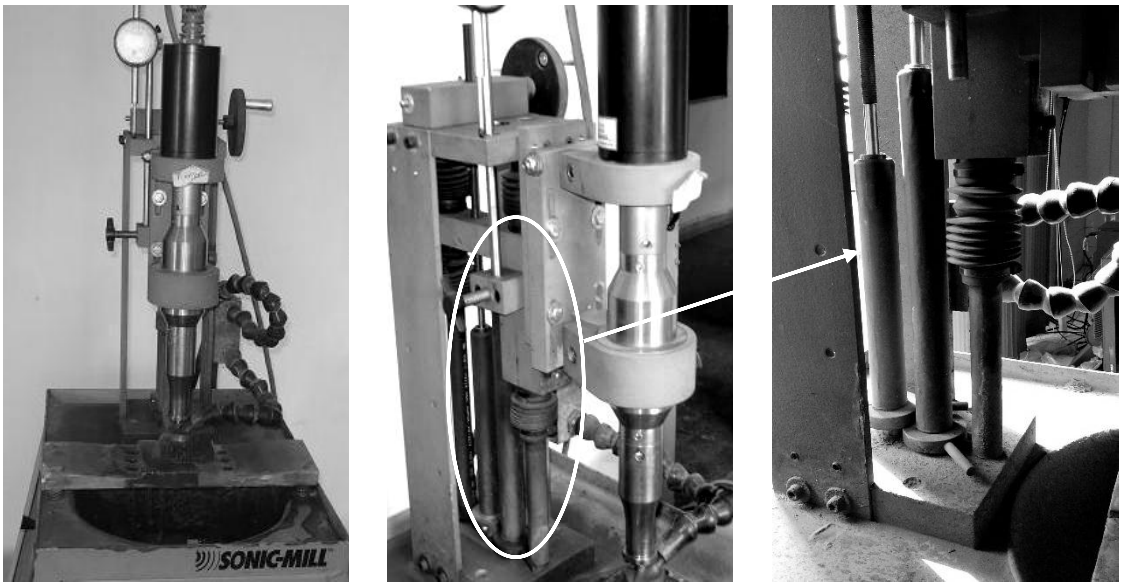

(a) (b) (c)

Figure 4.1 USM Set-up used for the present study

4.1.2 Work and Tool Material

Ti Grade 5 (Ti-6Al-4V) was selected as work material for the study. A round bar of 50mm was taken and samples of 8mm thickness were cut from the bar for the presented work. The composition and properties of the work material are listed in Table 4.1.

Table 4.1Work material composition

	Chemical Composition (%)							Mechanical Properties		
	O	N	C	Fe	Al	V	Ti	Hardness	Density	UTS
Ti Gr. 5	0.15	0.05	.07	.25	5.95	4.1	Bal.	323VHN	4.43g/cc	895MPa

Three different materials viz High Carbon Steel (HCS), Stainless Steel (SS) and Titanium (Ti) were selected for making the tool. The composition of the tool materials is listed in Table 4.2. The tools were made as a single piece, machined from round bars of appropriate diameter, and were threaded into the USM 4horn. The tools were prepared in accordance with the guidelines of Sonic Mill and were made to keep their weight as close to 50gm as possible.

Table 4.2 Tool Materials Composition

Material	**Chemical Composition (%)**									
	C	Si	Mn	P	Cr.	Mo	V	Fe	Ti	Hardness
Stainless Steel	0.17	0.6	0.7	0.05	13.1	--	--	Bal.	---	48 HRC
HCS	1.5	0.3	0.3	0.03	12.2	1.0	0.4	Bal.	---	61HRC
Ti									99.6	282VHN

Due to variation in density of tool material, the weight was maintained almost constant by altering the thickness of the shoulder part and maintaining the constant value for threaded part and protruding tool tip. The tool shape and drawing is represented in Figure 4.2.The weight of the tool was controlled by altering the dimension specified by '*m*' in the diagram. Three sets of multiple tools of each of the three material were prepared. One set each for Un-treated group of samples (UT), Shallow Cryogenic Treatment (SCT) and Deep Cryogenic Treatment (DCT). Multiple tools of each type were prepared to cover the risk of breakage or failure of tool during the experimentation. The tendency of dish formation of tools after experimentation necessitates that after each experiment the tools were subjected to facing on conventional lathe machine.

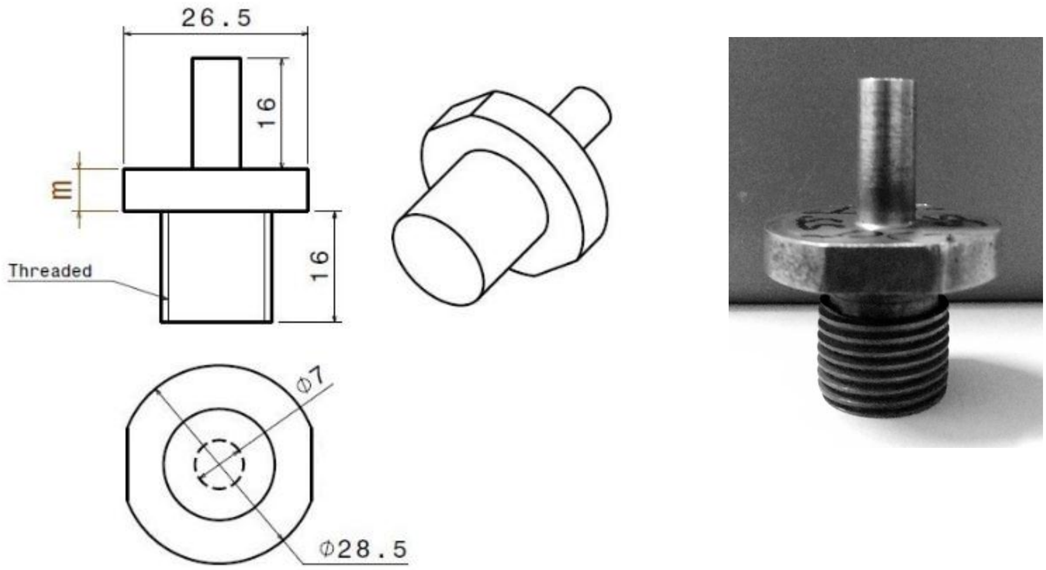

Figure 4.2 USM Tool Drawing

4.1.3 Cryogenic Treatment

Hardened and tempered tools of High Carbon Steel (HCS) and Stainless Steel (SS) along-with Ti tools made from the rolled bar of Titanium were subjected to cryogenic treatment as per the treatment cycle shown in Figure 4.3 for Shallow Cryogenic Treatment (SCT) and Deep Cryogenic Treatment (DCT), at temperatures of -80°C and -196°C respectively. Low temperature double tempering was carried out after both types of cryogenic treatments to remove the stresses induced, if any. Same process was used for cryogenic treatment of workpiece.

4.1.4 Abrasive Slurry

Aluminium oxide, silicon carbide, boron carbide were selected as abrasives for preparing one slurry each in mesh size of #220, #400 and #500 thus giving rise to nine such abrasive slurries. In addition to these, nine more slurries were prepared out of mixture of similar grit size of aluminium oxide and silicon carbide, aluminium oxide and boron carbide and silicon carbide and boron carbide. Thus in total there were 18 different types of slurries prepared for the study. The slurry concentration was fixed as 20% by weight with water as the dissolving media.

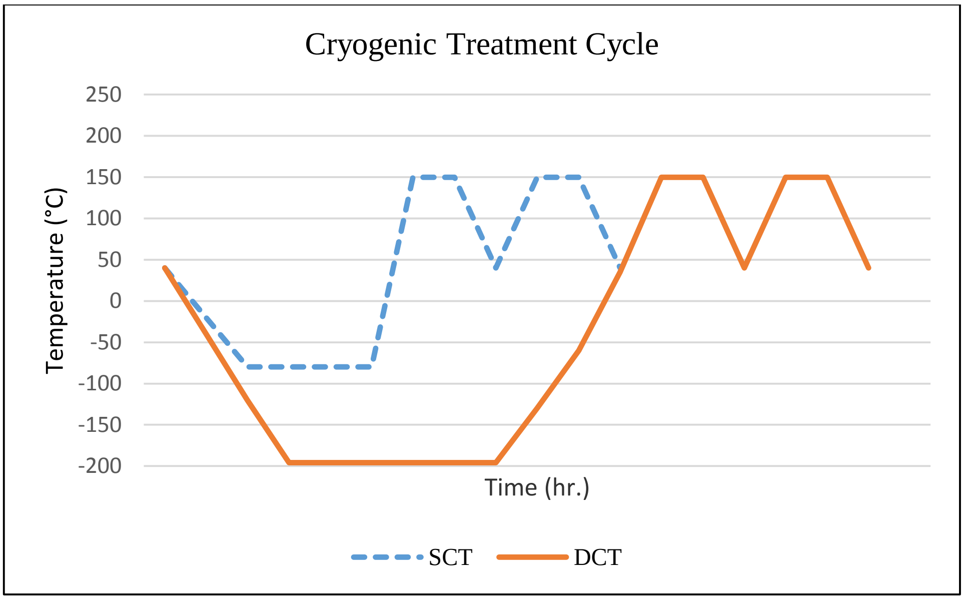

Figure 4.3 Cryogenic Treatment Cycle used for current study

4.1.5 Measurements

To determine MRR and TWR, the workpiece and the tool were weighed before and after each experiment to determine the rate of material removal on a digital electronic weighing balance having an accuracy of 0.1mg. Since the entire machining was carried out in flowing slurry, it was important to ensure that tool and work material were completely dry before weighing. The MRR and TWR were the determined using equations 4.1 and 4.2 respectively:

$$\mathrm{MRR} = \frac{M_{w1} - M_{w2}}{\rho_w \times t_m} \qquad \textit{Eq. 4.1}$$

where

MRR = Material Removal Rate in *mm³/min*

M_{w1} = Mass of work piece before machining (*g*)

M_{w2} = Mass of work piece after machining (*g*)

t_m = Machining time (*min*)

ρ_w = Density of work piece (*g/mm³*)

$$\mathrm{TWR} = \frac{M_{t1} - M_{t2}}{\rho_t \times t_m} \qquad \textit{Eq. 4.2}$$

where

TWR = Tool Wear Rate in *mm³/min*

M_{t1} = Mass of tool before machining (*g*)

M_{t2} = Mass of tool after machining (g)

t_m = Machining time (*min*)

ρ_t = Density of tool (*g/mm*^{3})

Surface roughness, average value R_a, was measured using Mitutoyo surface roughness tester (Model SJ-300). SR was measured on three separate locations in each machined zone resulted from 54 experimental runs. The three readings were averaged to establish the SR for that experiment.

Hole diameter at the entry was measured on three separate locations for each of the machined region using coordinate measurement machine (CMM). Dimensional accuracy was measured in terms of hole oversize (mm) which was calculated by subtracting tool diameter from the average diameter at hole entry (equation 4.3) as shown in Figure 4.4.

$$HOS = (\varphi_{hole} - \varphi_{tool})\ mm \qquad \textit{Eq. 4.3}$$

where $\varphi_{hole} = Hole\ diameter\ at\ entry\ (mm)$; $\varphi_{tool} = Tool\ tip\ diameter\ (mm)$

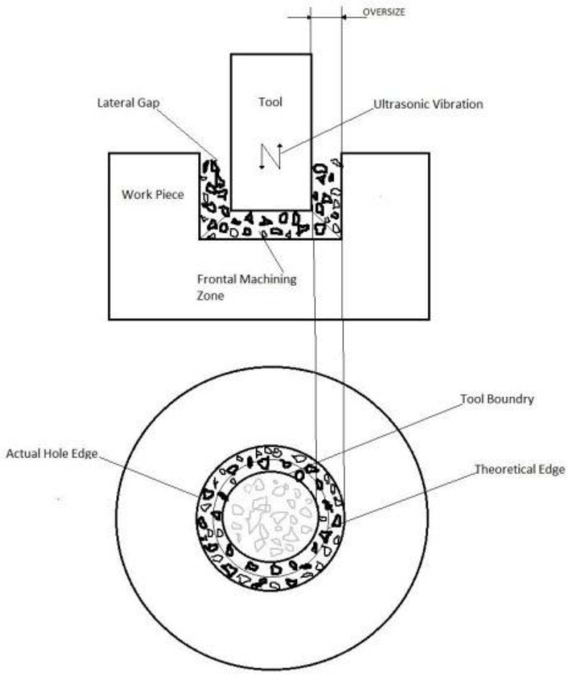

Figure 4.4 HOS and interaction of abrasive particles between tool and work-piece

The results of dimensional accuracy were used to determine the tolerance unit *n* which is required for establishing tolerance grades. Tolerance unit *n* actually derives from standard tolerance factor *i* (measured in micrometers) as defined in ISO standard UNI EN 20286 – 1 (1995) [153] and is given by Equation 4.4:

$$i = 0.45 \times D^{1/3} + 0.001 \times D \qquad \textit{Eq. 4.4}$$

'D' (in mm) in Equation 4.4 represents geometric mean of range of nominal size

For similar manufacturing processes, the relationship between magnitude of manufacturing error and the basic size approximates to a parabolic function forms the proposition for the empirically derived formula for *i*.

The values of standard tolerance are not determined individually for each nominal size but rather are for a range of nominal size. For the generic nominal dimension D_{JN} , when D_{JM} is the measured dimension, the value of tolerance unit n is calculated as follows in Equation 4.5:

$$n = \left[1000 \times \left(D_{JN} - D_{JM}\right)\right] / i \;\; = k/i \qquad \textit{Eq. 4.5}$$

where $k = \;\; 1000 * \left(D_{JN} - D_{JM}\right)$

4.2 EXPERIMENTATION

Experimentation for the present study was conducted using Taguchi's DOE methodology. As stated in previous chapter, selection of a particular orthogonal array is governed by the number of factors and their levels and number of interactions that are to be investigated [145,150]. The current study was aimed at finding the effect of abrasive slurry, tool material and cryogenic treatment of tool and workpiece on MRR and TWR in USM of Ti alloy Ti-6Al-4V. Accordingly all these parameters, varied at different levels, were chosen for conducting the experimentation. In addition to Slurry Type and Grit Size, Tool Material and type of Cryogenic Treatment given to tool and work-piece, another parameter Power Rating of USM was also included in the study thus making it a total of six process parameters. The 500W Sonic Mill USM was used across three power ratings of 20%, 50% and 80% thus accounting for 100W, 250W and 400W of power respectively. Other parameters such as slurry flow rate, feed rate, frequency and amplitude were not altered during the entire experimentation and were kept fixed according to machine guidelines. Based on the levels of the factors involved for study as shown in Table 3.1, Taguchi's L_{18} Orthogonal Array capable of handling, as required, one factor at 6 levels and 5 factors at 3 levels, was selected for Design of Experiments. The experiment pattern of L_{18} Array is shown in Table 4.3.

Table 4.3 Design of Experimentation based on Taguchi's L18 Orthogonal Array

Expt. No.	**Abrasive Slurry (A)**	**Tool Type (B)**	**Power Rating (C)**	**Grit Size (D)**	**Cryogenic Treatment of Tool (E)**	**Cryogenic Treatment of Work (F)**
1	Al_2O_3	HCS	20%	#220	UT	UT
2	Al_2O_3	SS	50%	#400	SCT	SCT
3	Al_2O_3	Ti	80%	#500	DCT	DCT
4	SiC	HCS	20%	#400	SCT	DCT
5	SiC	SS	50%	#500	DCT	UT
6	SiC	Ti	80%	#220	UT	SCT
7	B_4C	HCS	50%	#220	DCT	SCT
8	B_4C	SS	80%	#400	UT	DCT
9	B_4C	Ti	20%	#500	SCT	UT
10	Al_2O_3+ SiC	HCS	80%	#500	SCT	SCT
11	Al_2O_3+ SiC	SS	20%	#220	DCT	DCT
12	Al_2O_3+ SiC	Ti	50%	#400	UT	UT
13	SiC + B_4C	HCS	50%	#500	UT	DCT
14	SiC + B_4C	SS	80%	#220	SCT	UT
15	SiC + B_4C	Ti	20%	#400	DCT	SCT
16	Al_2O_3+ B_4C	HCS	80%	#400	DCT	UT
17	Al_2O_3+ B_4C	SS	20%	#500	UT	SCT
18	Al_2O_3+ B_4C	Ti	50%	#220	SCT	DCT

L_{18} orthogonal array possesses a special attribute that the two way interactions among the parameters are partially confounded with some columns. Therefore the effect on assessment of the main effects of the parameters gets minimized. Accordingly, even though it is not possible to estimate the effect of possible two factor interactions in this array, but the main effects of different process parameters can be estimated with sufficient accuracy [154].

Each experimental run was replicated twice and experiments were carried out in a random order. Each experimental run comprised of an ultrasonic drilling operation carried out for a duration of 70 minutes. The time duration was fixed so as to get an adequately detectable change in weight of tool and work-piece prior to and after the drilling operation.

The eighteen set of experiments, as per plan given in Table 4.3, were replicated three times thus resulted in performing of (18×3) 54 experimental runs. Multiple runs were performed on same work piece. A typical geometry of the workpiece after machining of several experimental runs is shown in Fig 4.5. Response variables of MRR, TWR, SR, HOS and TG were measured across all the runs and have been plotted in Tables 4.4-4.21.

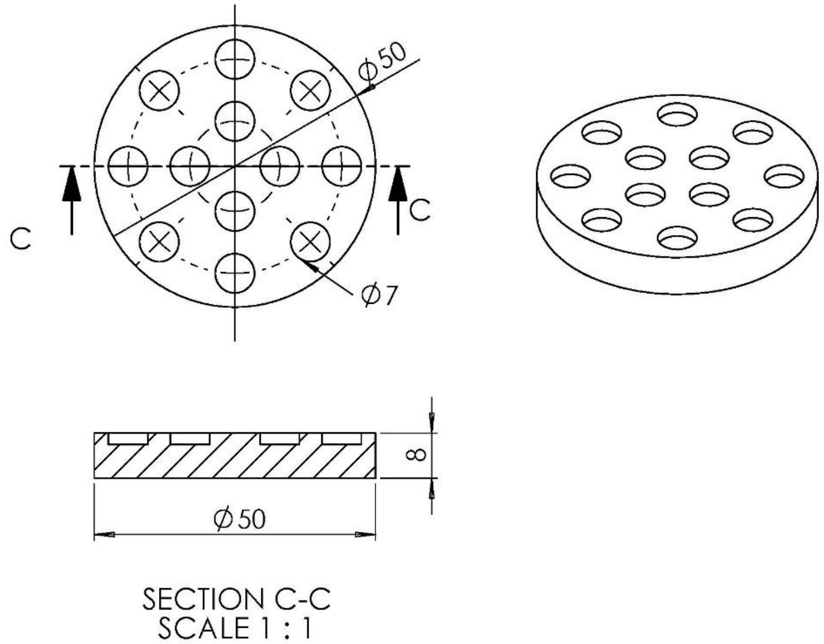

Figure 4.5 Workpiece Geometry

Table 4.4 shows control log for experiment no. 1 which was performed with aluminium oxide slurry, high carbon steel tool, 100W power, #220 grit size and with untreated tool and work material. Five response variables of MRR, TWR, SR, HOS and TG are listed in the table for the three runs of the experiment.

Table 4.4 Control Log and Observations for Experiment No. 1

Control Log					
Slurry Type	**Tool Type**	**Power Rating**	**Grit Size**	**Cryo Tool**	**Cryo Work**
Al_2O_3	HCS	20%	220	UT	UT
Observations					
Run No.	**MRR (mm^3/min)**	**TWR (mm^3/min)**	**SR (microns)**	**HOS (mm)**	**Tol. Grade**
1	0.1089	0.2045	1.18	0.275	IT 14
2	0.0854	0.212	1.19	0.31	IT 14
3	0.1268	0.2454	1.29	0.318	IT 14

Second experiment was performed using shallow cryogenic treated tool and work material at moderate USM power of 250 W and intermediate grit size of #400. Stainless steel and aluminium oxide were the tool and slurry material respectively for this experiment. Results obtained have been shown in Table 4.5.

Table 4.5 Control Log and Observations for Experiment No. 2

Control Log					
Slurry Type	**Tool Type**	**USM Power**	**Grit Size**	**Cryo Tool**	**Cryo Work**
Al_2O_3	SS	50%	400	SCT	SCT
Observations					
Run No.	**MRR (mm^3/min)**	**TWR (mm^3/min)**	**SR (microns)**	**HOS (mm)**	**Tol. Grade**
1	0.1285	0.1058	1.12	0.228	IT 14
2	0.1597	0.1354	1.09	0.194	IT 14
3	0.1387	0.098	0.97	0.221	IT 14

Titanium tool was used with aluminium oxide slurry of finest grit size of #500 at the highest selected USM power of 400W for third experiment. Tool as well as work material were subjected to deep cryogenic treatment. Observations of the response variables for

MRR, TWR, SR, HOS and Tolerance Grade for three repetitive runs of the experiment are shown in Table 4.6.

Table 4.6 Control Log and Observations for Experiment No. 3

Control Log					
Slurry Type	**Tool Type**	**Power Rating**	**Grit Size**	**Cryo Tool**	**Cryo Work**
Al_2O_3	Ti	80%	500	DCT	DCT
Observations					
Run No.	**MRR (mm^3/min)**	**TWR (mm^3/min)**	**SR (microns)**	**HOS (mm)**	**Tol. Grade**
1	0.1365	0.1473	0.6	0.134	IT 12
2	0.1423	0.1624	0.54	0.135	IT 12
3	0.1126	0.1123	0.51	0.121	IT 12

Table 4.7 shows the control log and observations corresponding to experiment no. 4 which was carried out with SiC slurry of #400 abrasive particle size at 100W of USM power using HCS tool material. The tool material was subjected to shallow cryogenic treatment while deep cryogenic treatment was given to work material.

Table 4.7 Control Log and Observations for Experiment No. 4

Control Log					
Slurry Type	**Tool Type**	**Power Rating**	**Grit Size**	**Cryo Tool**	**Cryo Work**
SiC	HCS	20%	400	SCT	DCT
Observations					
Run No.	**MRR (mm^3/min)**	**TWR (mm^3/min)**	**SR (microns)**	**HOS (mm)**	**Tol. Grade**
1	0.1834	0.2365	0.86	0.223	IT 14
2	0.1521	0.1775	0.97	0.196	IT 14
3	0.168	0.192	0.93	0.202	IT 14

Parametric setting for fifth experiment in the DOE was chosen as shown in Table 4.8. The machining was performed using stainless steel tool and SiC slurry of #500 grit size.

Whereas the tool material was subjected to deep cryogenic treatment, workpiece used was untreated. The results obtained for MRR, TWR, SR, HOS and Tolerance Grades during the three runs of the experiment are tabulated in the Table 4.8.

Table 4.8 Control Log and Observations for Experiment No. 5

Control Log					
Slurry Type	**Tool Type**	**Power Rating**	**Grit Size**	**Cryo Tool**	**Cryo Work**
SiC	SS	50%	500	DCT	UT
Observations					
Run No.	**MRR (mm^3/min)**	**TWR (mm^3/min)**	**SR (microns)**	**HOS (mm)**	**Tol. Grade**
1	0.186	0.1934	0.79	0.102	IT 12
2	0.1915	0.1678	0.87	0.12	IT 12
3	0.1687	0.1412	0.89	0.108	IT 12

Highest USM power of 400W and coarse SiC slurry of #220 was used for carrying out experiment no. 6. Whereas the tool material of Ti was not subjected to cryogenic treatment in this experiment, the work material was subjected to shallow cryogenic treatment. The control log and results of experiment are shown in Table 4.9.

Table 4.9 Control Log and Observations for Experiment No. 6

Control Log					
Slurry Type	**Tool Type**	**Power Rating**	**Grit Size**	**Cryo Tool**	**Cryo Work**
SiC	Ti	80%	220	UT	SCT
Observations					
Run No.	**MRR (mm^3/min)**	**TWR (mm^3/min)**	**SR (microns)**	**HOS (mm)**	**Tol. Grade**
1	0.3505	0.3343	1.44	0.299	IT 14
2	0.3143	0.3978	1.46	0.271	IT 14
3	0.2754	0.3548	1.33	0.297	IT 14

Very coarse Boron carbide abrasive slurry consisting of #220 size particles was used at 250W power to perform machining corresponding to experiment no. 7. Deep cryogenic treated HCS tool was used to machine shallow treated work material and the results obtained for response variables of MRR, TWR, SR, HOS and Tolerance Grade for three repetitive runs of the experiment are shown in Table 4.10.

Table 4.10 Control Log and Observations for Experiment No. 7

Control Log					
Slurry Type	**Tool Type**	**Power Rating**	**Grit Size**	**Cryo Tool**	**Cryo Work**
B_4C	HCS	50%	220	DCT	SCT
Observations					
Run No.	**MRR (mm^3/min)**	**TWR (mm^3/min)**	**SR (microns)**	**HOS (mm)**	**Tol. Grade**
1	0.3354	0.4465	1.46	0.292	IT 14
2	0.368	0.3654	1.55	0.316	IT 14
3	0.3745	0.4177	1.52	0.313	IT 14

Table 4.11 shows the results and control log corresponding to three repetitions of experiment no. 8. This experiment was performed with stainless steel tool using #400 size boron carbide abrasive slurry at 400 W power. Tool material was not subjected to cryogenic treatment while work material underwent deep cryogenic treatment.

Table 4.11 Control Log and Observations for Experiment No. 8

Control Log					
Slurry Type	**Tool Type**	**Power Rating**	**Grit Size**	**Cryo Tool**	**Cryo Work**
B_4C	SS	80%	400	UT	DCT
Observations					
Run No.	**MRR (mm^3/min)**	**TWR (mm^3/min)**	**SR (microns)**	**HOS (mm)**	**Tol. Grade**
1	0.5488	0.5872	1.3	0.262	IT 14
2	0.5945	0.6067	1.17	0.292	IT 14
3	0.5333	0.6578	1.28	0.265	IT 14

Ninth experiment of DOE was performed with shallow cryogenic treated titanium tool material using #500 particle size boron carbide abrasive slurry at 100W USM power. Table 4.12 shows the control log and observations for response variables of MRR, TWR, SR, HOS and Tolerance Grade for three repetitive runs of the experiment.

Table 4.12 Control Log and Observations for Experiment No. 9

Control Log					
Slurry Type	**Tool Type**	**Power Rating**	**Grit Size**	**Cryo Tool**	**Cryo Work**
B_4C	Ti	20%	500	SCT	UT
Observations					
Run No.	**MRR (mm^3/min)**	**TWR (mm^3/min)**	**SR (microns)**	**HOS (mm)**	**Tol. Grade**
1	0.124	0.1172	0.48	0.154	IT 13
2	0.1087	0.0987	0.46	0.16	IT 13
3	0.1426	0.1432	0.56	0.172	IT 13

Table 4.13 shows control log and results of three runs of experiment no. 10. This experiment was performed using a mixture of identical grit size slurry of aluminium oxide and silicon carbide of #500 grit size with HCS tool at 400W power. The tool as well as the work material were subjected to shallow cryogenic treatment.

Table 4.13 Control Log and Observations for Experiment No. 10

Control Log					
Slurry Type	**Tool Type**	**Power Rating**	**Grit Size**	**Cryo Tool**	**Cryo Work**
Al_2O_3+ SiC	HCS	80%	500	SCT	SCT
Observations					
Run No.	**MRR (mm^3/min)**	**TWR (mm^3/min)**	**SR (microns)**	**HOS (mm)**	**Tol. Grade**
1	0.2245	0.3005	1.05	0.199	IT 14
2	0.2335	0.2675	0.96	0.184	IT 14
3	0.1987	0.2345	0.93	0.205	IT 14

Identical grit size mixture of aluminium oxide and silicon carbide slurry but of #220 particle size was used with stainless steel tool to carry out experiment no. 11. The tool as well as work material were subjected to deep cryogenic treatment and the power was maintained at 100W during the experiment. The results obtained for the five response variables across three repetitions of the experiment and control log are given in Table 4.14.

Table 4.14 Control Log and Observations for Experiment No. 11

Control Log					
Slurry Type	**Tool Type**	**Power Rating**	**Grit Size**	**Cryo Tool**	**Cryo Work**
Al_2O_3+ SiC	SS	20%	220	DCT	DCT
Observations					
Run No.	**MRR (mm^3/min)**	**TWR (mm^3/min)**	**SR (microns)**	**HOS (mm)**	**Tol. Grade**
1	0.1782	0.1845	1.16	0.286	IT 14
2	0.1527	0.1143	1.13	0.26	IT 14
3	0.16	0.1378	1.04	0.258	IT 14

The control log for experiment no. 12 is given in Table 4.15 which was carried out with #400 size slurry of aluminium oxide and silicon carbide mixture at 250W USM power. The titanium tool as well as work material were not subjected to any type of cryogenic treatment. The response variables for the three runs of the experiment have been recorded in the Table 4.15.

Table 4.15 Control Log and Observations for Experiment No. 12

Control Log					
Slurry Type	**Tool Type**	**Power Rating**	**Grit Size**	**Cryo Tool**	**Cryo Work**
Al_2O_3+ SiC	Ti	50%	400	UT	UT
Observations					
Run No.	**MRR (mm^3/min)**	**TWR (mm^3/min)**	**SR (microns)**	**HOS (mm)**	**Tol. Grade**
1	0.1405	0.1112	0.95	0.157	IT 13
2	0.1687	0.1166	1.04	0.184	IT 13
3	0.1278	0.1345	1.07	0.187	IT 13

Mixture of Silicon Carbide and Boron Carbide abrasive slurry was created in three different grit sizes for execution of experiment no. 13 to experiment no. 15. HCS tool was used for experiment no. 13 at 250W power using untreated tool material and deep cryo treated work material as given in Table 4.16. #500 grit size mixture was used for experiment no. 13 and the response variables have been recorded in the table.

Table 4.16 Control Log and Observations for Experiment No. 13

Control Log					
Slurry Type	**Tool Type**	**Power Rating**	**Grit Size**	**Cryo Tool**	**Cryo Work**
SiC + B_4C	HCS	50%	500	UT	DCT
Observations					
Run No.	**MRR (mm^3/min)**	**TWR (mm^3/min)**	**SR (microns)**	**HOS (mm)**	**Tol. Grade**
1	0.2769	0.3974	0.76	0.151	IT 13
2	0.3168	0.35	0.82	0.175	IT 13
3	0.287	0.3323	0.85	0.148	IT 13

Stainless steel tool material alongwith 400W USM power and coarser abrasive particles of #220 were used for carrying out experiment no. 14. The control log for experimentation involving shallow cryo treated tool and untreated work material and results obtained for the five response variables are given in Table 4.17.

Table 4.17 Control Log and Observations for Experiment No. 14

Control Log					
Slurry Type	**Tool Type**	**Power Rating**	**Grit Size**	**Cryo Tool**	**Cryo Work**
SiC + B_4C	SS	80%	220	SCT	UT
Observations					
Run No.	**MRR (mm^3/min)**	**TWR (mm^3/min)**	**SR (microns)**	**HOS (mm)**	**Tol. Grade**
1	0.5551	0.5117	1.68	0.364	IT 15
2	0.4888	0.4954	1.59	0.341	IT 15
3	0.5234	0.5565	1.56	0.35	IT 15

Effect of deep cryogenic treatment on tool material and shallow cryogenic treatment on work material was explored in experiment no. 15 using titanium tool material at 100W power and with #400 grit size of abrasive slurry comprising of mixture of boron carbide and silicon carbide. The control log and observations for MRR, TWR, SR, HOS and Tolerance Grades for the three runs of the experiment are given in Table 4.18.

Table 4.18 Control Log and Observations for Experiment No. 15

Control Log					
Slurry Type	**Tool Type**	**Power Rating**	**Grit Size**	**Cryo Tool**	**Cryo Work**
SiC + B_4C	Ti	20%	400	DCT	SCT
Observations					
Run No.	**MRR (mm^3/min)**	**TWR (mm^3/min)**	**SR (microns)**	**HOS (mm)**	**Tol. Grade**
1	0.1354	0.0976	0.72	0.192	IT 13
2	0.0954	0.1605	0.78	0.174	IT 13
3	0.111	0.1258	0.69	0.168	IT 13

Table 4.19 shows control log and observations for the five response variables corresponding to experiment no. 16 which was carried out at 400W power using HCS tool and #400 grit size of abrasive slurry formed from mixture of aluminum oxide and boron carbide. Tool material was given deep cryogenic treatment while work material did not undergo any type of cryogenic treatment.

Table 4.19 Control Log and Observations for Experiment No. 16

Control Log					
Slurry Type	**Tool Type**	**Power Rating**	**Grit Size**	**Cryo Tool**	**Cryo Work**
Al_2O_3+ B_4C	HCS	80	400	DCT	UT
Observations					
Run No.	**MRR (mm^3/min)**	**TWR (mm^3/min)**	**SR (microns)**	**HOS (mm)**	**Tol. Grade**
1	0.3461	0.3768	1.23	0.254	IT 14
2	0.3905	0.3576	1.32	0.248	IT 14
3	0.3268	0.3154	1.35	0.269	IT 14

Mixture of fine grit size of #500 of aluminum oxide and boron carbide abrasives was used for experiment no. 17. Untreated stainless steel was tool material and the machining was carried out at 100W power when shallow cryogenic treatment was imparted to work material. Detailed control log and the results obtained for all the response variables of are given in Table 4.20.

Table 4.20 Control Log and Observations for Experiment No. 17

Control Log					
Slurry Type	**Tool Type**	**Power Rating**	**Grit Size**	**Cryo Tool**	**Cryo Work**
Al_2O_3+ B_4C	SS	20	500	UT	SCT
Observations					
Run No.	**MRR (mm^3/min)**	**TWR (mm^3/min)**	**SR (microns)**	**HOS (mm)**	**Tol. Grade**
1	0.1511	0.1932	0.68	0.196	IT 14
2	0.152	0.1345	0.7	0.182	IT 13
3	0.1854	0.1781	0.6	0.177	IT 13

Table 4.21 shows the control log for experiment no. 18. The results obtained for MRR, TWR, SR, HOS and Tolerance Grade corresponding to three replications of the experiment are shown in this table when experiment was carried out using shallow cryogenic treated titanium tool #220 grit size slurry of aluminium oxide and boron carbide mixture. USM power was maintained at 250W while deep cryogenic treated work material was used. The analysis of variance (ANOVA) was performed on measured values to determine total variability of the observed outcomes which is the summation of variance due to various input parameters under control and experimental error.

Table 4.21 Control Log and Observations for Experiment No. 18

Control Log					
Slurry Type	**Tool Type**	**Power Rating**	**Grit Size**	**Cryo Tool**	**Cryo Work**
Al_2O_3+ B_4C	Ti	50	220	SCT	DCT
Observations					
Run No.	**MRR (mm^3/min)**	**TWR (mm^3/min)**	**SR (microns)**	**HOS (mm)**	**Tol. Grade**
1	0.2595	0.2232	1.01	0.235	IT 14
2	0.2145	0.1782	1.12	0.237	IT 14
3	0.237	0.186	1.14	0.217	IT 14

The ANOVA also leads to identification of significant and non-significant parameters of the study. In the presented study, ANOVA was performed on raw as well as S/N data and significance of parameters was determined from F-value at 95% confidence level by comparison with tabulated F-value. The analysis of each of the response variables is presented in following sections.

4.3 MATERIAL REMOVAL RATE (MRR)

Material removal rate corresponding to three runs of each experiment was calculated using Equation 4.1. Figure 4.6 shows average value of MRR for each of the eighteen experiments.

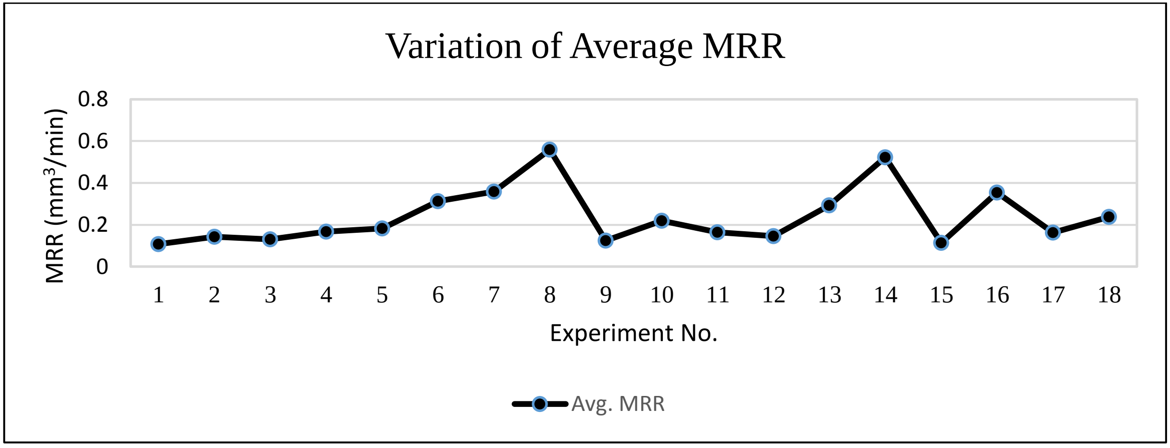

Figure 4.6 Average MRR across 18 sets of experiments

S/N ratio for material removal was calculated using Equation 3.1 since MRR is a *higher the better* quality characteristic. MINITAB 17 was used to calculate S/N ratios and perform ANOVA. Table 4.22 displays the ANOVA output for the corresponding S/N data.

Table 4.22 ANOVA Table for MRR (S/N ratios)

Analysis of Variance for SN ratios (MRR)

Source	DF	Seq SS	Adj SS	Adj MS	F	P
Slurry Type	5	109.842	109.842	21.9683	28.05	0.035*
Tool Type	2	41.197	41.197	20.5986	26.30	0.037*
Power Rating	2	155.945	155.945	77.9726	99.57	0.010*
Abrasive Grit Size	2	26.465	26.465	13.2324	16.90	0.056*
Cryogenic Treatment Tool	2	4.161	4.161	2.0807	2.66	0.273
Cryogenic Treatment Work	2	5.309	5.309	2.6545	3.39	0.228
Residual Error	2	1.566	1.566	0.7831		
Total	17	344.485				

DF:Degree of Freedom; Seq SS: Sequential Sum of Squares; Adj SS: Adjusted Mean Square Error

*Significant Prameters

The highest and lowest value of MRR detected from the total of 54 runs was 0.5845 mm^3/min and 0.0874mm^3/min. As is evident from the F-column of Table 4.22 and corresponding p-value, slurry type, tool type and power rating are the most significant parameters affecting MRR while grit size is slightly less significant. The variation of MRR data means and S/N ratios across different abrasive slurries is shown in Figure 4.7. Higher machining rates corresponding to boron carbide abrasive slurry are due to the highest knoop hardness associated with this abrasive slurry among the selected ones for the study which causes enhanced cutting ability of these particles leading to higher rates of work-piece removal.

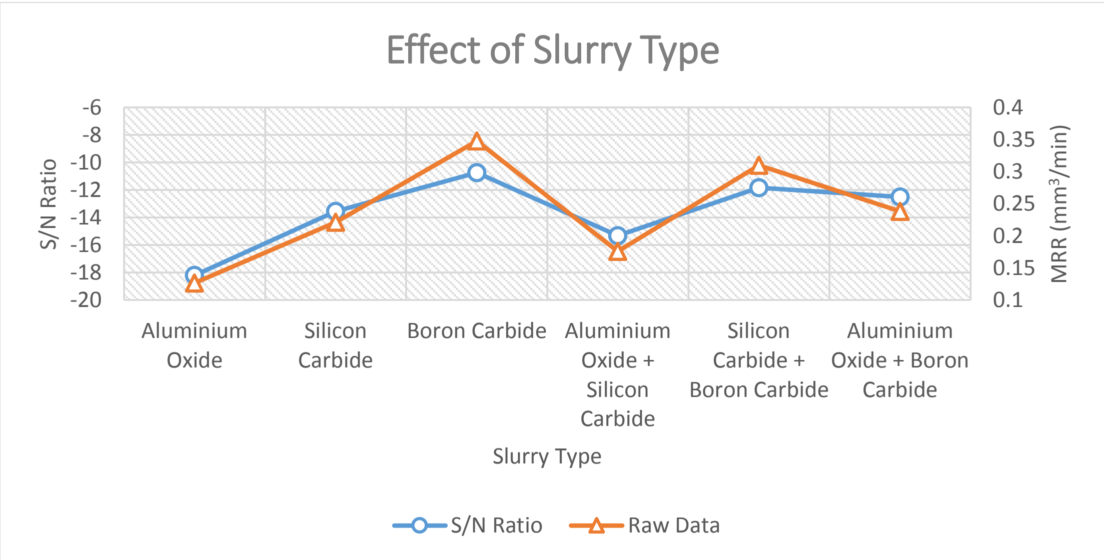

Figure 4.7 Variation of MRR with use of different abrasive slurries

In contrast, the aluminium oxide abrasives being the softest among the selected abrasives lead to lowest rates of machining. The mixture slurries have performed according to the relative cutting ability of the constituent slurries and there does not appear to be any adverse detrimental effect of mixing on the cutting ability of individual type of abrasive particles.

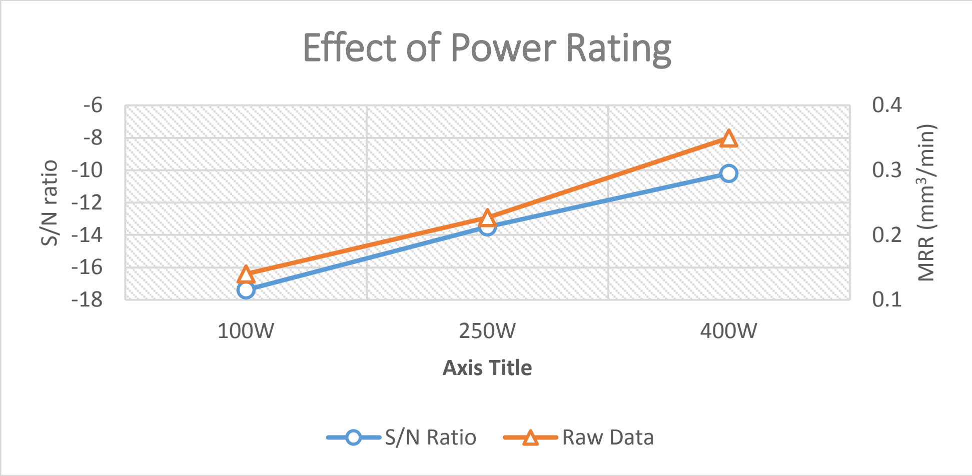

Figure 4.8 Variation of MRR with USM Power

The three pure slurries could be ranked in decreasing order of MRR from boron carbide to silicon carbide and then to aluminium oxide. Figure 4.8 and Figure 4.9 show the effect of power rating and tool type on MRR. USM power primarily accounts for mass of tool-horn combination that can be actually utilized for a given application and hence higher power ratings are associated with increased momentum transfer to workpiece [3,110,114,133,155] by the abrasive particles of the slurry impinging on the workpiece. MRR, therefore, was found to increase steadily with increase in percentage power rating of USM from 20% of the rated power (100W) to 80% (400W). Among the three tool materials used in the study, Stainless Steel tool resulted in maximum MRR while Titanium tool caused the lowest value of MRR when machining the alloy work-piece. HCS tool resulted in marginally lesser MRR compared to SS tool but resulted in significantly more MRR in comparison to Ti tool. MRR in USM is a function of relative tool-workpiece hardness and work-hardening ability. In some of the previously conducted studies of similar type, Kumar and others [110,114] have advocated a harder tool resulting in higher MRR, however Singh and Khamba [117] have found stainless steel as a better tool material for MRR due to superior tool-workpiece combination.

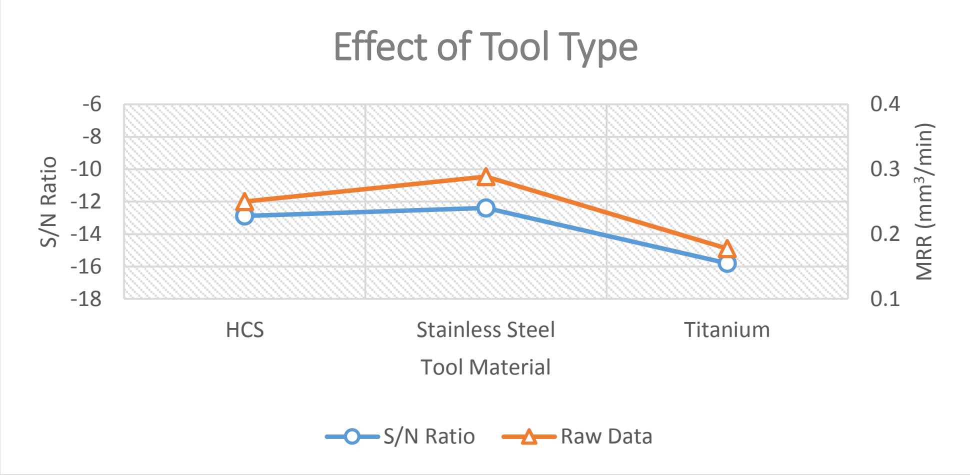

Figure 4.9 Effect of Tool Material on MRR

The use of stainless steel has also resulted in superior MRR in the present case as compared to a relatively harder HCS and softer Ti tool thus substantiating that it is not just the hardness of the tool but the relative tool-workpiece combination which determines the extent of strain hardening of work material resulting in plastic deformation of the material before fracture.

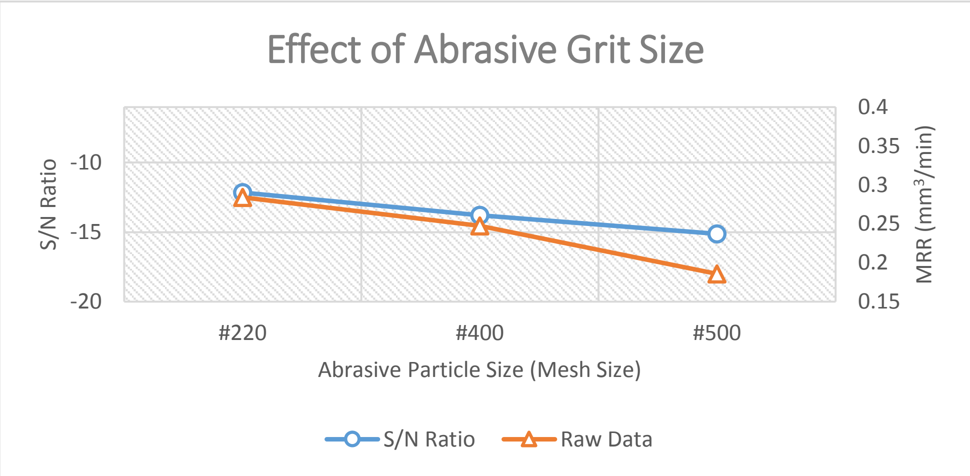

Figure 4.10 Variation of MRR with Abrasive Grit Size

Highest MRR was associated with the coarse abrasive slurry of particle grit size #220 among the three particle sizes explored in the study. Since the major mechanism of material removal in USM is that of hammering of abrasive grains, therefore coarser particles were associated with a larger hammering effect at localized regions under the tool causing higher impact energy owing to larger associated momentum and accordingly caused higher rates of material removal from the work surface. Figure 4.10 shows that MRR increases approximately linearly with increase in abrasive grit size from #500 to

#200. Deep cryogenic treatment of tool has been found to be associated with lower MRR while that for workpiece has been found to be associated with higher MRR as shown in Figure 4.11 and 4.12 respectively. However, this variation has been found to be statistically insignificant from the ANOVA Table 4.22, and might be attributed to some reduction in resistance to fracture for the alloy work-piece.

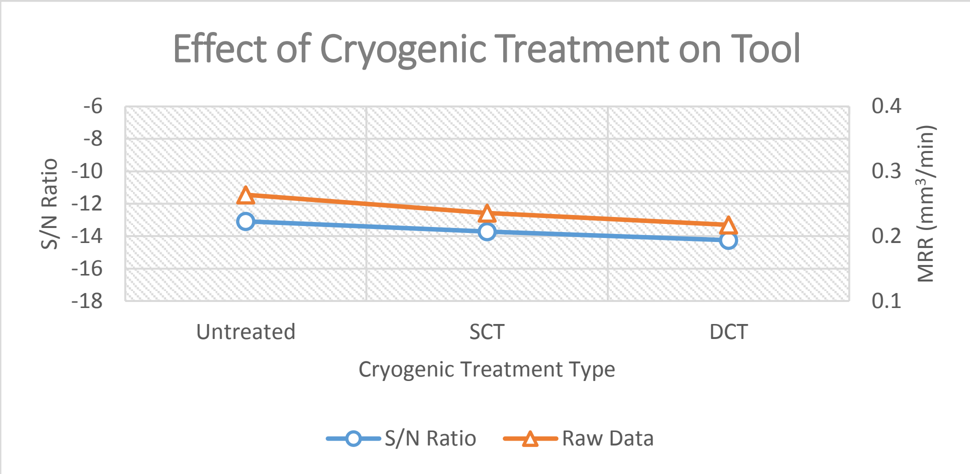

Figure 4.11 Effect of CT to Tool on MRR

From the findings of the current study it is apparent that the USM power rating is the most significant of all the parameters considered because it directly determines the extent of energy with which the abrasive particles strike the work-piece. A comparison with the reported studies of similar nature indicates some similarity with regard to pattern of variation across the various levels of parameters. Kumar and Khamba [114] also reported similar trend of variation across power rating, grit size and abrasive type for MRR. Singh and Khamba [117] have reported similar trend of variation across three different types of slurries while Titanium based tool material owing to its peculiar fracture toughness and work hardening characteristics resulted in lowest MRR among the chosen tool material in both the studies. Kataria et al. [139] have also reported a linear trend in variation of MRR with power rating and abrasive grit size with coarser abrasives and higher power rating resulting in higher MRR. However tool hardness was found to be directly affecting the material removal rate [139] whereas in present study and those conducted by Singh and Khamba [117] it is the relative combination of tool-workpiece that determines favourable extent of work hardening responsible for superior material removal rate. It has been found that a harder tool may not result in more MRR.

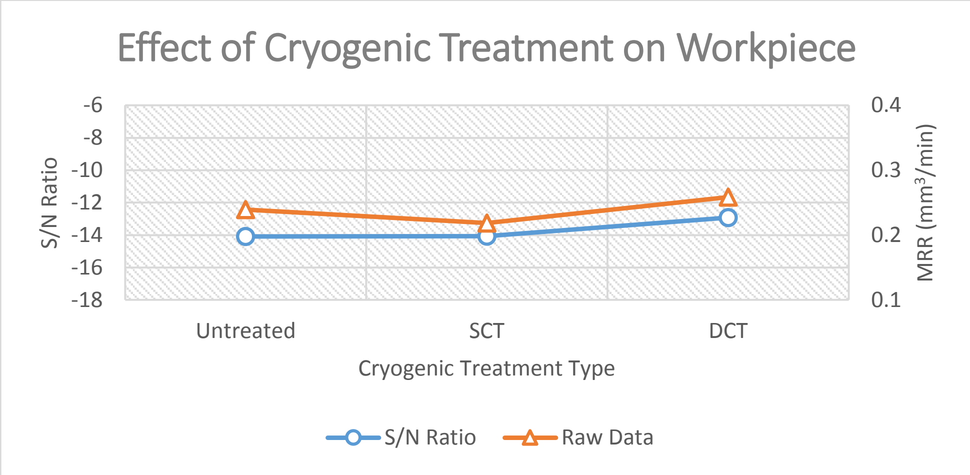

Figure 4.12 Effect of CT to work piece on MRR

From the analysis of the main effect plots for MRR, the parametric setting corresponding to the highest value of MRR is obtained at **$A_3B_2C_3D_1E_1F_3$** which corresponds to boron carbide slurry, stainless steel tool, 400W power rating, 220 grit size, untreated tool and deep cryo treated work-piece.

Titanium and its alloys owing to their superior fracture toughness undergo considerable plastic deformation prior to fracture in ultrasonic machining. Accordingly, material removal mechanism has been found to vary from being ductile to that of brittle mode during various experimental conditions under different values of control parameters while largely being a combination of the two modes. SEM micrographs of machined region indicate this variation. Figure 4.13 (a-b) show SEM micrographs of machined region corresponding to experiment no. 8 that was performed with Boron carbide slurry and stainless steel tool at a power rating of 400W.

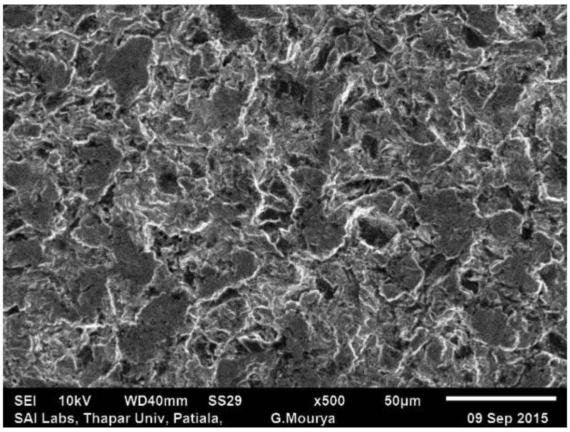

(a)

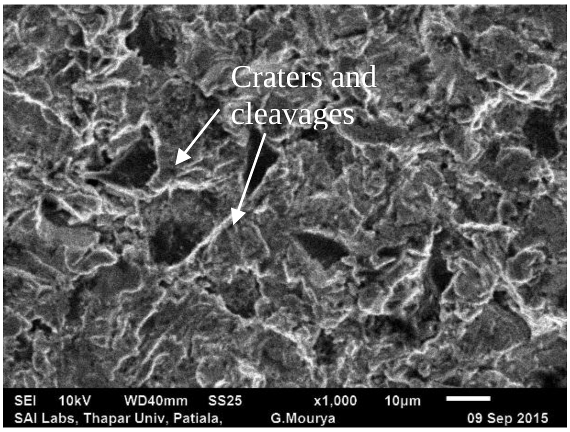

(b)

Figure 4.13 SEM Micrographs of Machined Region corresponding to Experiment No. 8 at magnification of a) 500X and b) 1000X

Impact of hard boron carbide abrasive particles striking with enormous momentum at the work surface cause shear and propagation of fracture into the work-surface. The fracture pattern is quite uniform across the workpiece and fracture boundaries indicate propagation of cracks into the surface causing cleavages indicating largely brittle mode of fracture with signs of plastic deformation

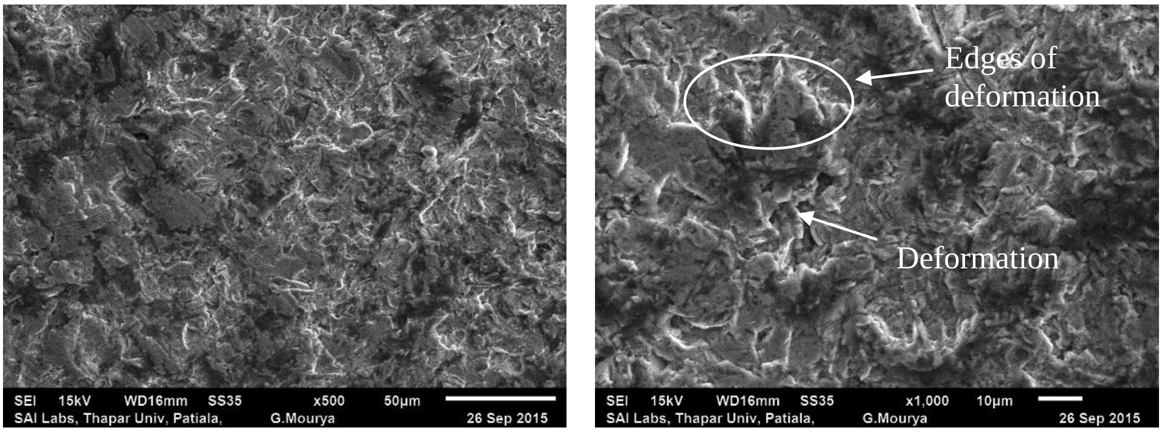

Figure 4.14 SEM Micrographs of Machined Region corresponding to Experiment No. 15 at magnification of a) 500X and b) 1000X

However as is evident from Figure 4.14 (a-b) and Figure 4.15 (a-b) corresponding to experiment no. 15 and experiment no. 1 respectively, there are dimples and depressions indicating large amount of plastic deformation with little indication of cracks. The fracture pattern thus indicates that of being predominantly of ductile mode.

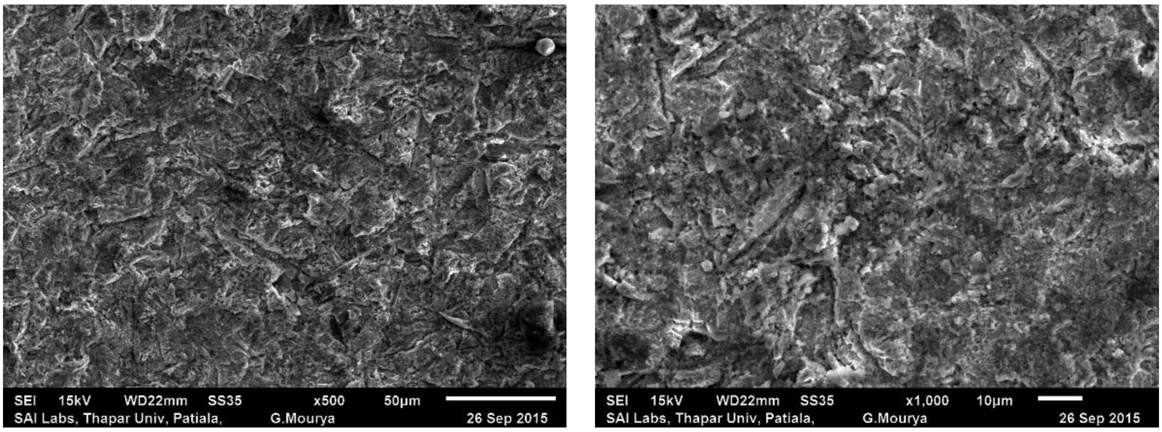

Figure 4.15 SEM Micrographs of Machined Region corresponding to Experiment No. 1 at magnification of a) 500X and b) 1000X

Under the low power of USM finer and not so strong abrasive grains repeatedly hammer the work surface causing enough of plastic deformation prior to fracture in micro shear planes similar to chipping of worksurface leading to failure mode similar to that in case of ductile fracture. Similar trend of extensive plastic deformation has also been observed in machined zone corresponding to experiment no. 9 wherein under the repeated impacts of very fine boron carbide particles at low momentum associated with 100W USM power, work material underwent strain hardening.

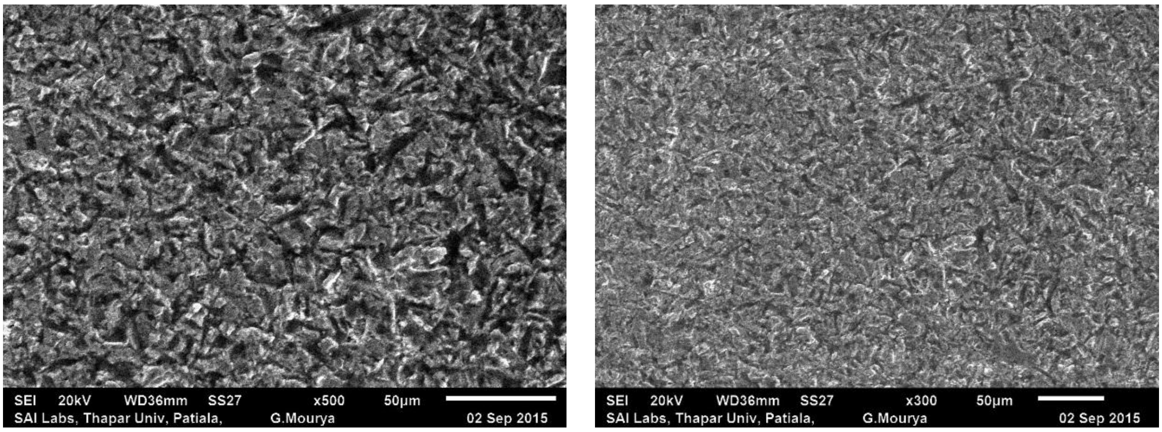

Figure 4.16 SEM Micrographs of Machined Region corresponding to Experiment No. 9 at magnification of a) 500X and b) 300X

Evidence of adequate plastic deformation is visible from the micrographs shown in Figure 4.16 (a-b). Cracks and depressions are sparingly distributed in machined zone indicating a combination of brittle and ductile fracture mode owing to mixture of aluminium oxide and boron carbide slurry with large difference in knoop hardness corresponding to experiment no. 16 as shown in Figure 4.17 (a-b).

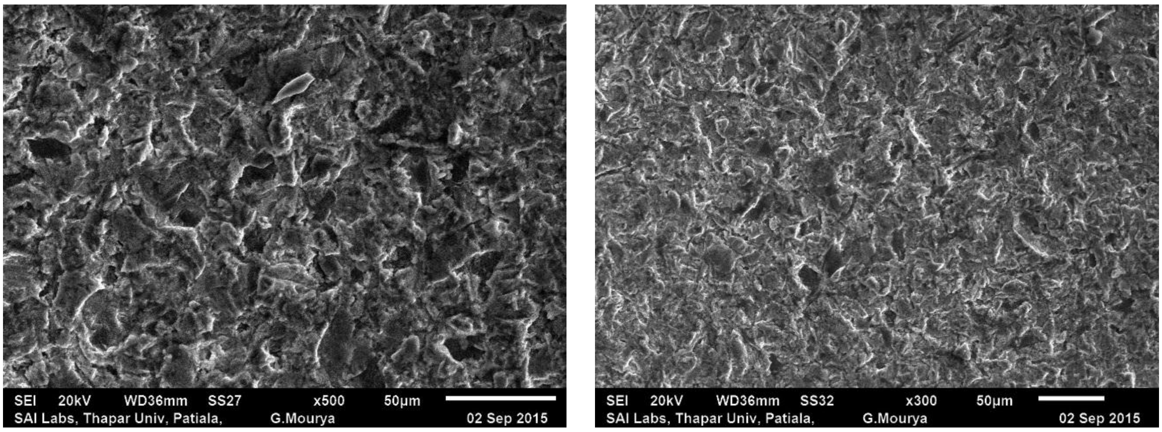

Figure 4.17 SEM Micrographs of Machined Region corresponding to Experiment No. 16 at magnification of a) 500X and b) 300X

Owing to finer particle sizes of relatively higher hardness being pushed hard into the workpiece by harder high carbon steel tool, a mixed fracture mode dominated by brittle fracture with fine cracks travelling beneath the surface were observed corresponding to experiment no. 13 as shown in Figure 4.18 (a-b).

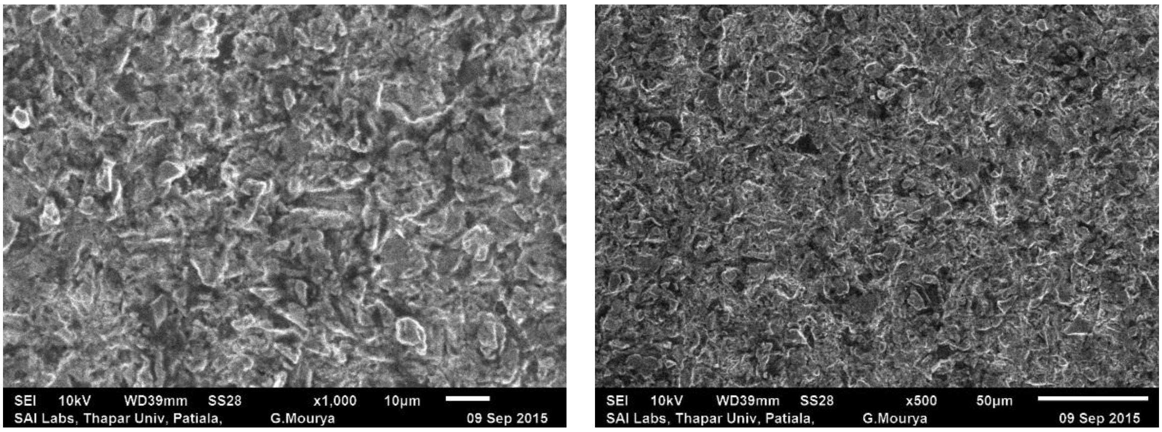

Figure 4.18 SEM Micrographs of Machined Region corresponding to Experiment No. 13 at magnification of a) 1000X and b) 500X

Big and deep craters with deep indents and cleavages are visible in the machined zone owing to strong and hard coarse abrasives hammered with large momentum into the workpiece corresponding to experiment no. 14 as shown in Figure 4.19 (a-b).

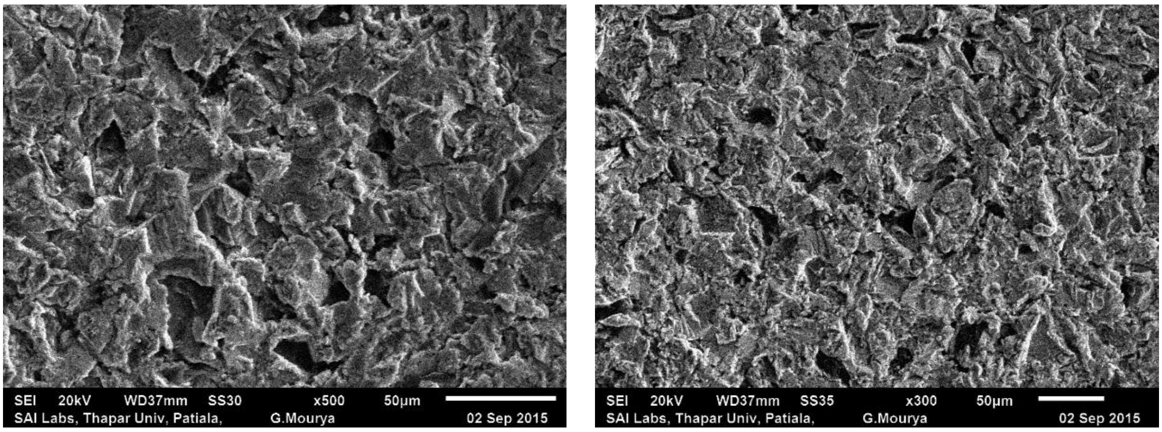

Figure 4.19 SEM Micrographs of Machined Region corresponding to Experiment No. 14 at magnification of a) 500X and b) 300X

4.4 TOOL WEAR RATE (TWR)

Tool wear rate was measured as volumetric loss of material from the frontal tool tip surface transferring energy to work surface through abrasive slurry media and was determined across the different runs of 18 experiments using Equation 4.2. Figure. 4.20 represents the variation of Average TWR across 18 experimental runs while table 4.23 displays ANOVA results for S/N data. S/N data was calculated using Equation 3.2 since

TWR is a *lower the better* characteristic. MINITAB 17 software was used to calculate S/N data and perform ANOVA on raw as well as S/N data.

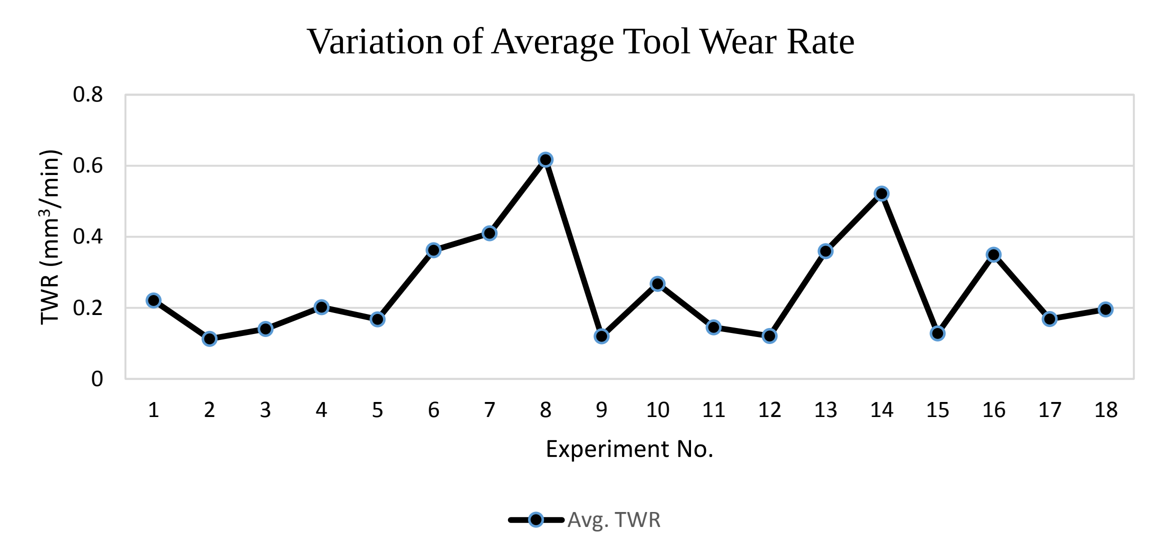

Figure 4.20 Variation of average TWR across 18 experimental runs

From the raw data of 54 experimental runs, it is evident that the variation of TWR was in the range of 0.096 – 0.646mm^3/min. It can be deduced from Table 4.23 that the slurry type, grit size, power rating and tool type are all highly significant parameters while cryogenic treatment of tool material is slightly less significant parameter to establish TWR.

Table 4.23 ANOVA Table for TWR (S/N ratios)

Analysis of Variance for SN ratios (TWR)

Source	DF	Seq SS	Adj SS	Adj MS	F	P
Slurry Type	5	91.797	91.797	18.3594	21.08	0.046*
Tool Type	2	77.088	77.088	38.5440	44.25	0.022*
Power Rating	2	132.377	132.38	66.1885	75.98	0.013*
Abrasive Grit Size	2	38.465	38.465	19.2325	22.08	0.043*
Cryogenic Treatment Tool	2	22.538	22.538	11.2691	12.94	0.072*
Cryogenic Treatment Work	2	3.249	3.249	1.6247	1.87	0.349
Residual Error	2	1.742	1.742	0.8711		
Total	17	367.257				

DF:Degree of Freedom; Seq SS: Sequential sum of square; Adj SS: Adjusted mean square error
*Significant Parameters

Higher USM power results in impacting of abrasive particles on the tool surface with higher momentum. Abrasive particles rebound from the work surface with higher intensity and cause erosion of tool surface [116,130], more so on periphery while exiting the machining zone, thus resulting in dish formation at the tool surface. Accordingly a nearly linear variation with power rating, as shown in Figure 4.21, indicates that higher power results in higher tool wear as was the case with MRR. The increase became even steeper as power increases from 250W to 400W indicating the increased influence of momentum at higher power.

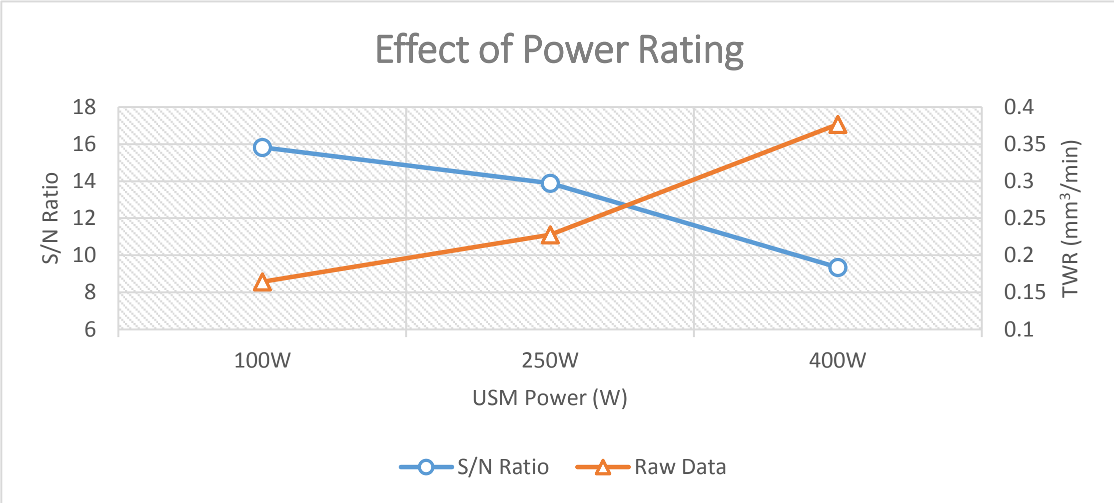

Figure 4.21 Variation of Tool Wear with Power

The tool material itself is a very important aspect for determining TWR as can be seen from Figure 4.22. Ti has a favourable characteristic with regard to relative tool-workpiece hardness which is an important consideration in determining the loss of material from either of the tool and work-piece.

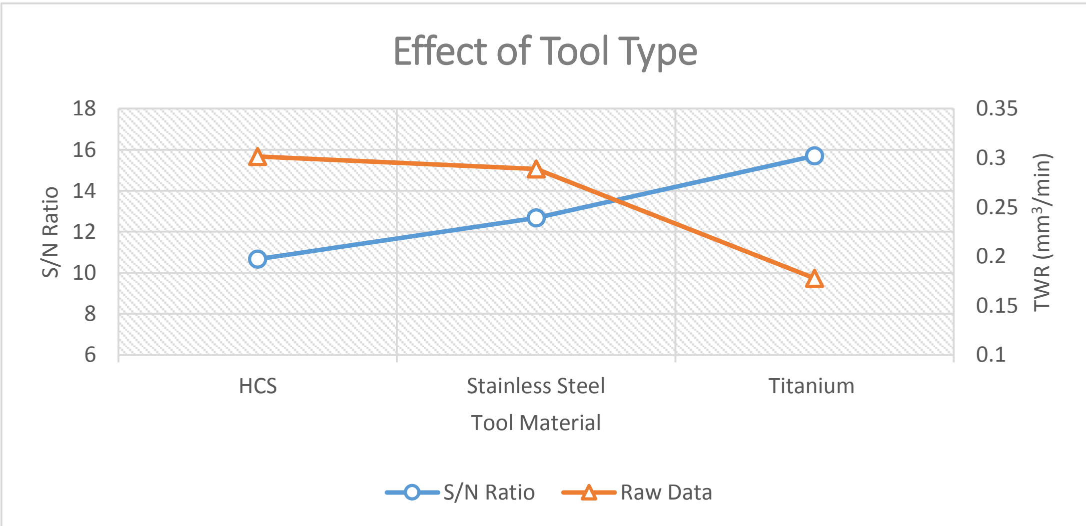

Figure 4.22 Effect of Tool Type on Tool Wear

In addition to this, superior work-hardening characteristics and better fracture toughness ensures that Ti undergo immense plastic deformation prior to failure, therefore Ti tool performed better among the three tool materials as far as TWR was concerned while HCS tool had maximum rate of wear.

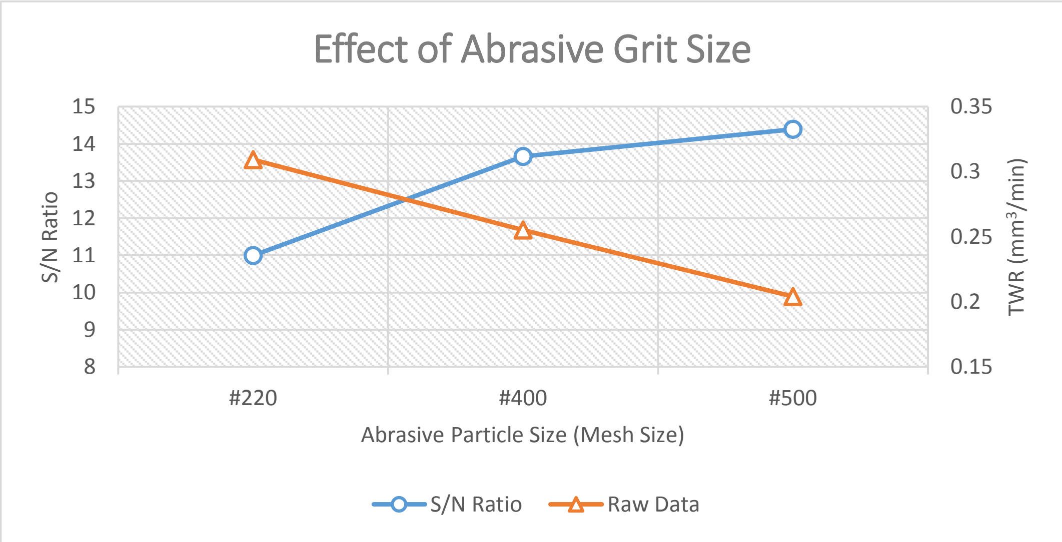

Figure 4.23 Effect of grit size on TWR

Among the abrasive slurries, higher cutting ability of boron carbide abrasives owing to its higher knoop hardness resulted in maximum tool wear while bigger particle size associated with #220 slurry led to more wear of tool as was the case with material removal from work piece due to higher associated impact energy. Figure 4.23 and 4.24 validates this pattern of effect of abrasive grit size and slurry respectively.

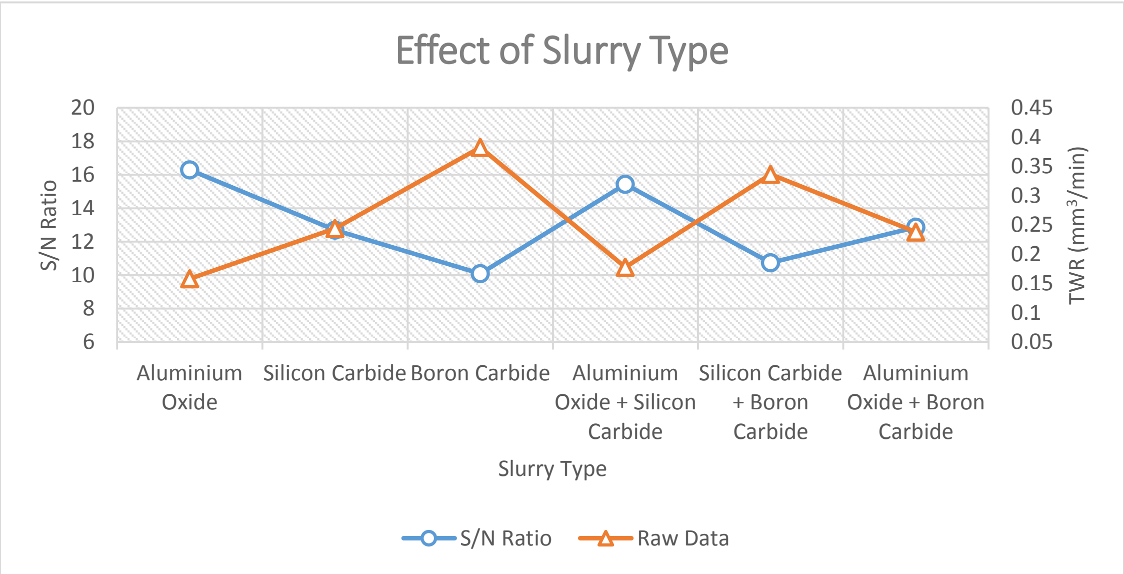

Figure 4.24 Variation of TWR with slurry type

In a similar study conducted on USM of pure titanium Kumar et al. [121], reported titanium alloy to be the best performing tool with regard to tool wear owing to its superior work hardening and fracture toughness properties and outperformed harder tools such as cemented carbide. Kataria et al. [139] have also reported similar trend of variation for abrasive grit size and power rating for establishing tool wear rate. Cryogenic treatment is known to improve the wear resistance in tool steels. Figure 4.25 show micrographs of tools and workpiece, respectively, post cryogenic treatment. The precipitation of fine secondary carbides (SC), appearing as small white dots, after cryogenic treatment alongwith distribution of primary carbides (PC), comprising of bigger white regions, in HCS tool causes improvement in wear resistance. Cryogenic treatment has resulted in refinement of grains in stainless steel as shown in Figure 4.25 (b). Gu et al. [101] found the reduction in β-phase particles in Titanium alloy after cryogenic treatment and attributed the same for improvement in plasticity. Consequently, cryogenic treatment has been associated with reduction in tool wear owing to these transformations in the materials. However, in USM fracture toughness is a more important property as it also affects the extent of work hardening. Effect of DCT has been found to be favourable for reducing tool wear rate as is indicated by S/N ratio plot shown in Figure 4.26, which means that DCT could have also marginally improved the fracture toughness of the steel based tool materials. However, the favourable characteristics of the extent of plastic deformation and work hardening with Ti tool on Ti-6Al-4V work-piece seems to have become the dominant property for reducing the tool wear in the present case.

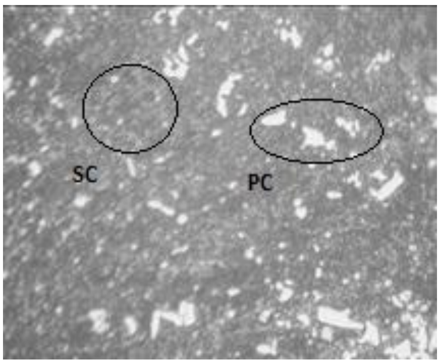

(a)

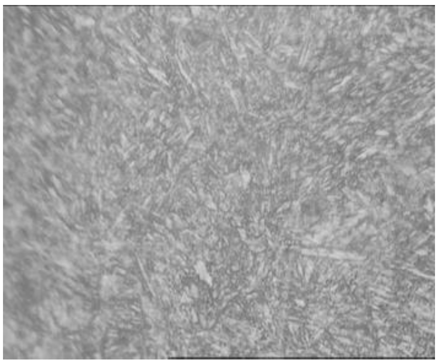
(b)

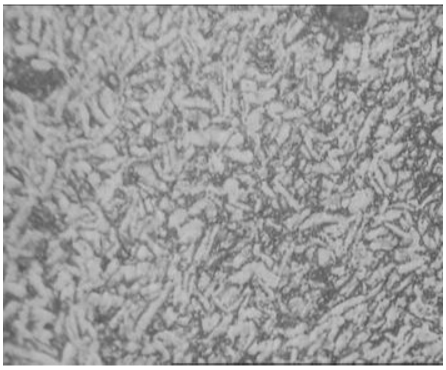

(c)

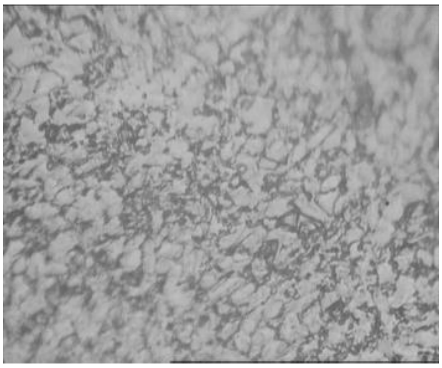

(d)

Figure 4.25 Optical micrographs at 400x of Materials post cryogenic treatment (a) HCS (b) SS (c) Titanium tool (d) Ti-6Al-4V workpiece

There are conflicting reports available in literature related to effect of cryogenic treatment on impact toughness of steels. While Das and Ray [89] reported a marginal decrease in fracture toughness of cryogenic treatment of D2 steel, Molinari et al. [92] found no change in impact toughness when cryogenic treatment was carried out after tempering as in this case. However Prieto et al. [93] has reported an improvement in impact toughness of SS420. So the results of present study indeed indicate that it is the relative tool-work-piece combination and extent of work-hardening which is a significant determinant of material removal from tool as well as work-piece. A favourable combination for MRR will be the one which will reduce the strain hardening of work material while a combination that results in extensive work hardening prior to fracture of tool will reduce the TWR.

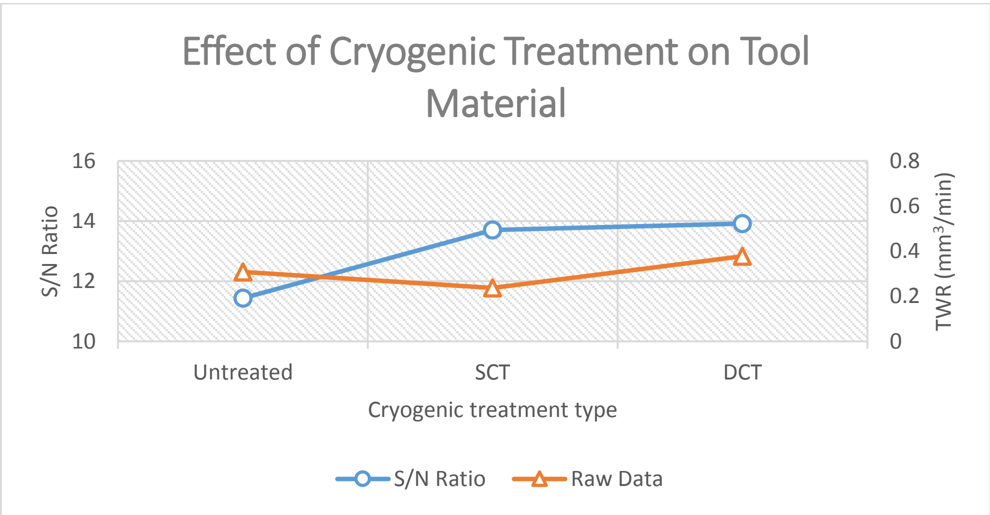

Figure 4.26 Variation of tool wear with CT

The most favourable setting for Tool Wear as determined from analysis of Main Effects plots (Figures 4.21-4.24, 4.26-4.27) from Taguchi Design of Experiments (S/N ratio analysis) is at **$A_1B_3C_1D_3E_3F_1$**. This is in accordance with fundamental principles of USM. In USM, the machine settings which contribute to higher MRR also cause higher TWR and vice versa [114,116]. The same is apparent from the peaks of variation plots.

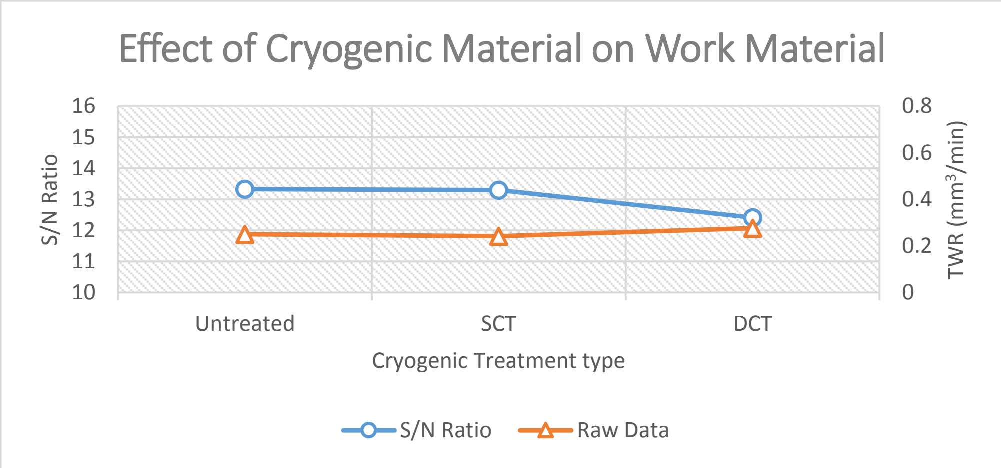

Figure 4.27 Effect of CT to workpiece on TWR

So lower values of power rating, finer grains and relatively softer abrasives are recommended for improving the TWR in USM. The confirmatory experiments conducted at best settings of MRR and Tool wear as per DOE, do establish the validity of the findings as the values for MRR and TWR have been found to be 0.6358mm^3/min and 0.0975mm^3/min respectively which are the highest and lowest values within the experimental space.

4.5 SURFACE ROUGHNESS (SR)

Surface roughness was measured in terms of arithmetic mean roughness, R_a, using Mitutoyo surface roughness tester with a sampling length of 2.5 mm. The average value of SR for each of the 18 experimental trials is represented in Figure 4.28.

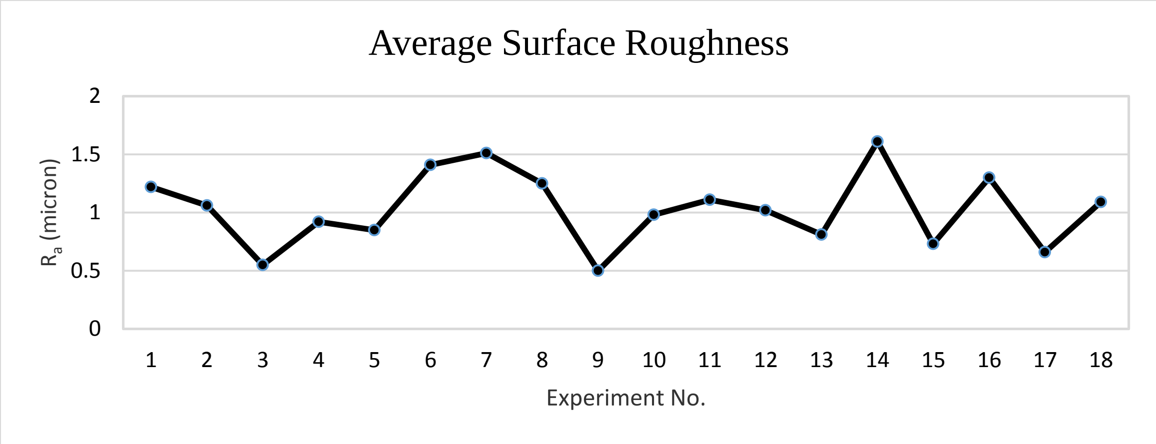

Figure 4.28 Average Surface Roughness Values

The main effects plot for S/N ratio and raw data are shown in Figure 4.29-4.33 and Figure 4.35. From the ANOVA table 4.24 and from main effects plots it is evident that Grit Size is the most important and the most influential parameter that determines the SR of machined area in ultrasonic machining. It can be deduced from table 4.24 that the percentage contribution of Grit Size towards determining SR is maximum at 62.46%. Bigger abrasive particle size associates with larger momentum transfer to the work piece and accordingly the crater size on the work piece is increased because of larger chunk of material removal thus hampering the surface finish.

Table 4.24 ANOVA Table for S/N Ratio for Surface Roughness

Analysis of Variance for SN ratios

Source	DF	Seq SS	Adj SS	Adj MS	F	P
Slurry Type	5	3.255	3.2553	0.6511	4.91	0.178††
Tool Type	2	21.224	21.2238	10.6119	80.06	0.012*
Power Rating	2	24.168	24.1680	12.0840	91.16	0.011*
Abrasive Grit Size	2	88.103	88.1025	44.0513	332.33	0.003**
Cryogenic Treatment Tool	2	1.396	1.3960	0.6980	5.27	0.160††
Cryogenic Treatment Work	2	2.646	2.6460	1.3230	9.98	0.091†
Residual Error	2	0.265	0.2651	0.1326		
Total	17	141.057				

** Highly Significant *Significant †Less Significant ††Not significant

According to Kumar [128], bigger particle size also results in increased friction between abrasive particle and work-piece due to lateral movement of the former under the vibrating tool which coupled with downward movement results in creation of irregular and rough surface. The dominating significance of abrasive grit size has also been reported by several researchers in the past [15, 52, 110].

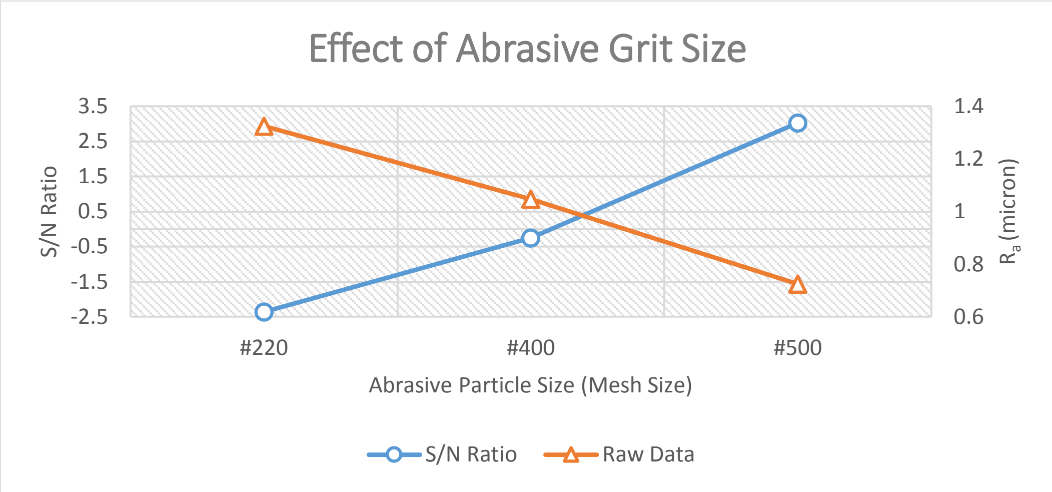

Figure 4.29 Variation of SR with Grit Size

However, power rating and tool type were also found to be significant parameters in establishing the surface finish in the present study and it can be deduced from Table 4.24 that the two account for 17.13% and 15.05% contribution, respectively, towards establishing the SR of the machined zone. USM power directly determines the momentum with which abrasive particles strike the work surface

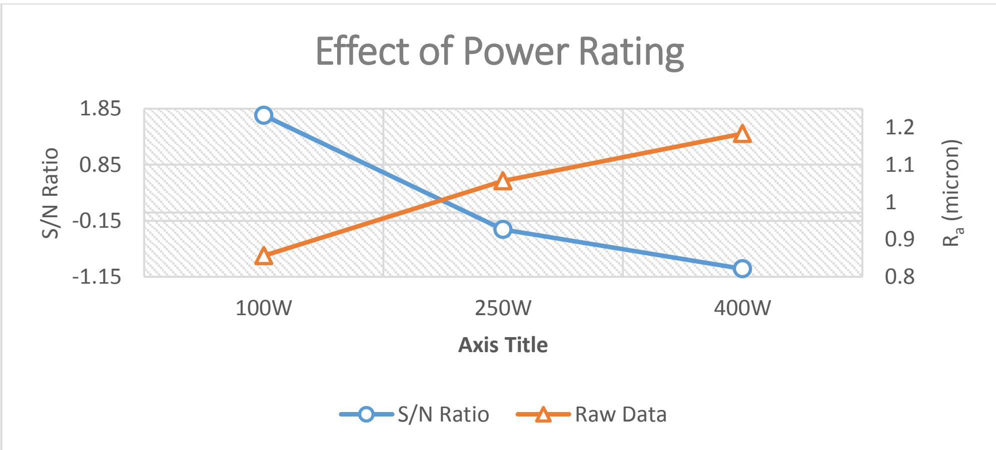

Figure 4.30 Effect of USM power on SR

A higher power results in higher momentum transfer to the abrasive particles causing them to strike the work surface with greater force. This results in deeper and wider craters and hence adversely affects the surface finish. Tool hardness also determines the energy of impact of abrasive particles to the work surface.

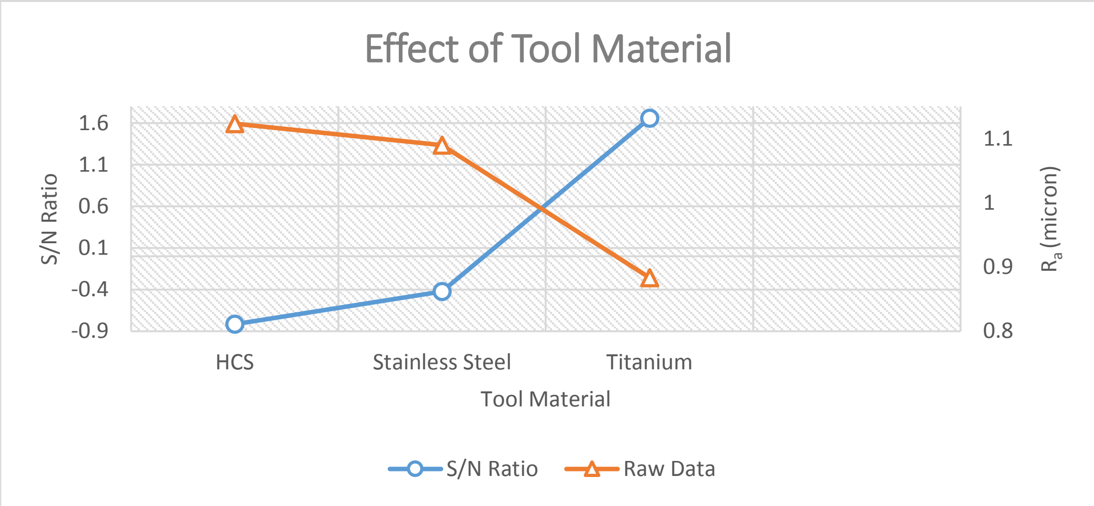

Figure 4.31 Variation of SR with tool material

The worst surface has been generated by high carbon steel tool because of its higher hardness whereas titanium being softest of the three tool materials resulted in best surface finish.

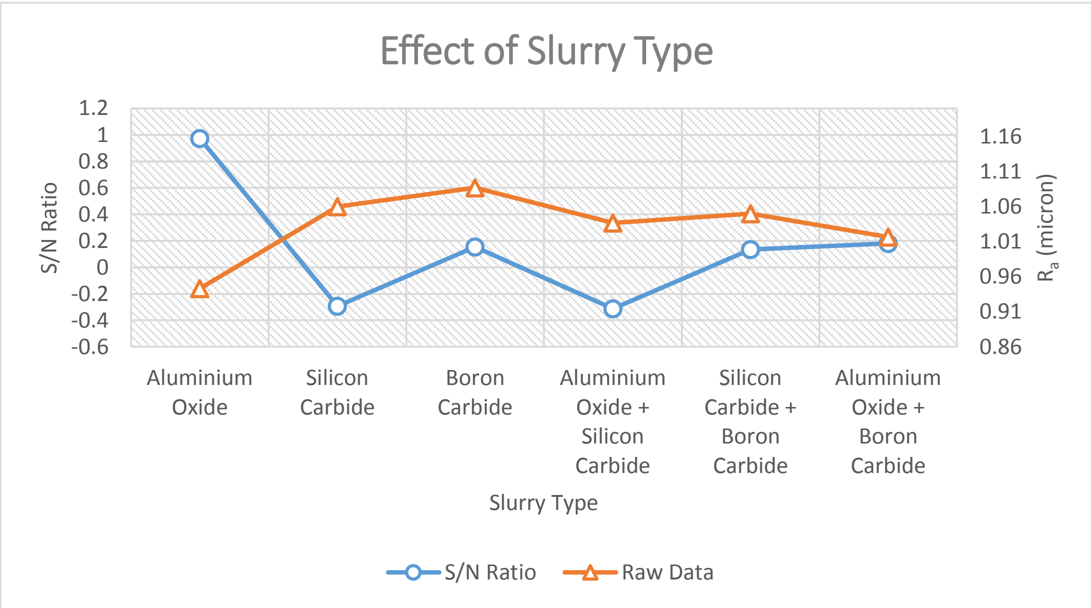

Figure 4.32 Effect of slurry type on SR

However, the surface finish of the tool is also responsible for quality of surface generated at the work-piece and that is precisely the reason why prior to start of every experiment facing operation was carried out on the tool surface to give identical finish to tool at start of each experiment. Apart from tool hardness, its toughness and resistance to fracture also affects surface integrity of tool during machining and hence quality of surface generated at work-piece.

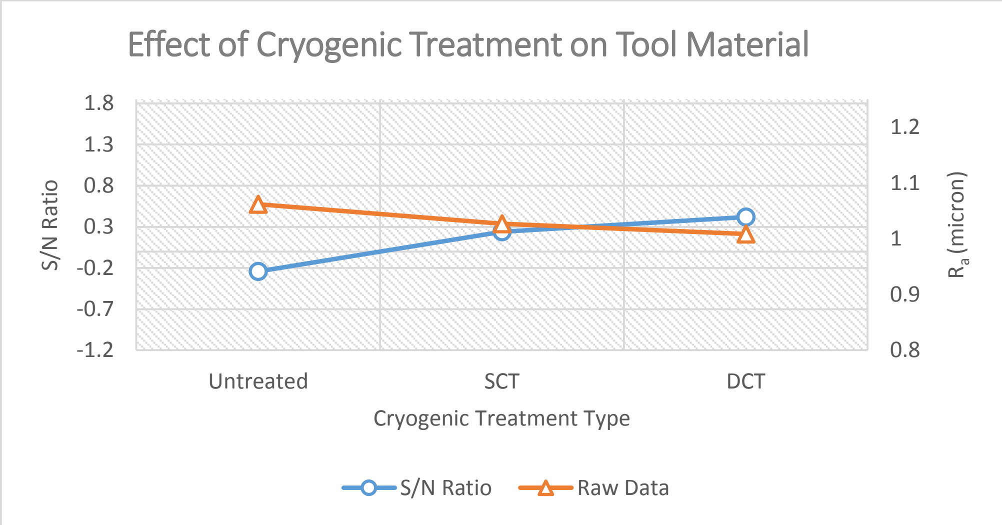

Figure 4.33 Effect of CT to tool on SR

Fracture at tool surface on titanium tool is hampered by its superior toughness which protects the surface from easy deterioration under the impact of abrasive grains and hence the Ti tool significantly outperformed the other two tool materials. Cryogenic treatment is known to improve the wear resistance in the steels largely due to conversion of retained austenite into martensite and precipitation of secondary carbides [80-81, 92].

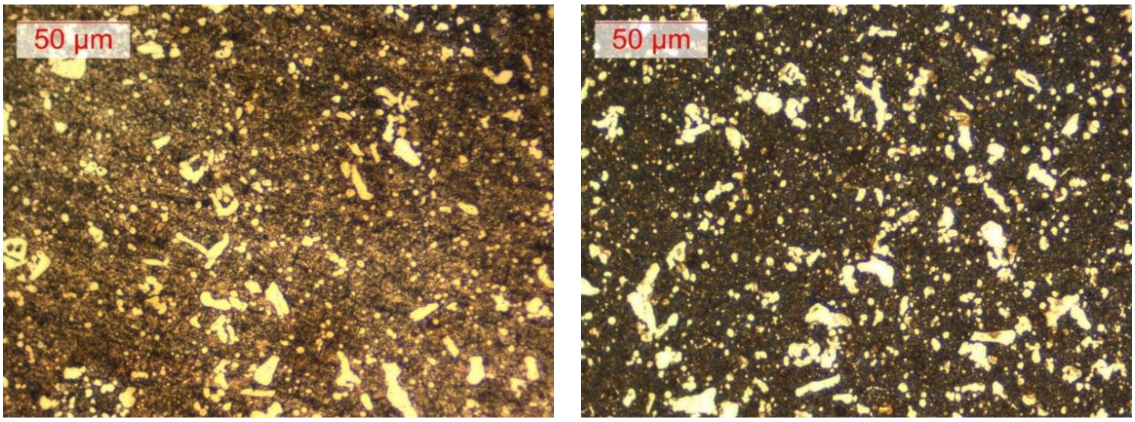

(a) (b)

Figure 4.34 Optical Micrograph of the HCS tool at 500X (a) Untreated (b) Deep cryogenic treated

Figure 4.34 shows precipitation of fine secondary carbides as effect of DCT on microstructure of HCS tool. DCT improves the wear resistance of the tool and therefore the DC treated tools were able to retain their shape and contributed towards improved surface finish. However the phenomenon of material removal from tool in USM is more complicated than just a sliding wear problem and also involves the effect of plastic deformation prior to fracture and strain hardening which probably was the reason behind the little significance of the parameter in this study. It can be observed from the main effects plot that there is marginal difference in surface finish between untreated samples and SCT samples while studying the effect of cryogenic treatment on work-material, however there is a markedly improved surface finish in DCT samples.

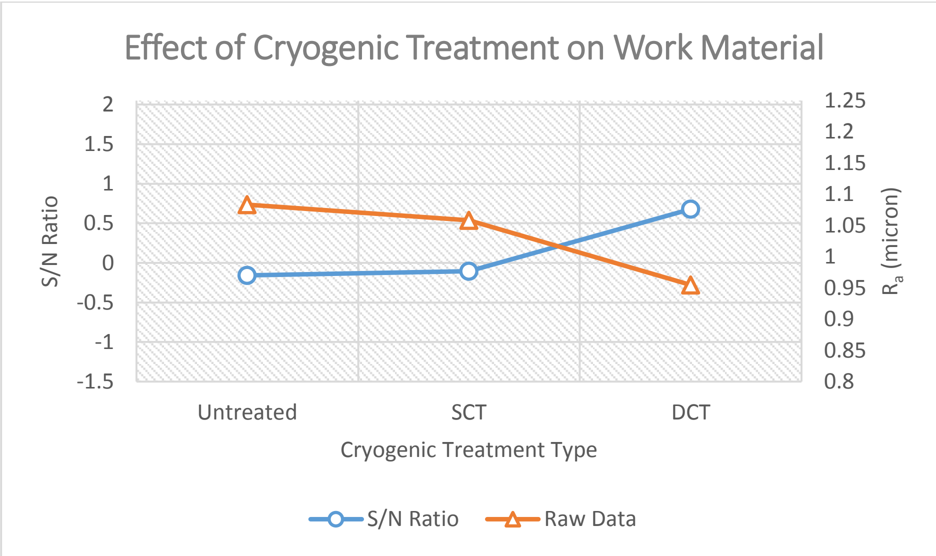

Figure 4.35 Effect of CT to workpiece on SR

Micro-hardness evaluation of samples prior and after the CT didn't reveal much difference. So the improved surface finish was probably not due to change in hardness but could be the result of some change in mechanical properties of the Ti alloy post deep cryogenic treatment. A comparison of SEM micrographs (Figure 4.36) of the machined region in DCT and UT samples indicate a difference in the cleavage of material from the work piece surface in the two types of samples. Figure 4.36 (a-b) correspond to untreated Ti-6Al-4V work-piece machined with higher power ratings and rather coarser grains while Figure 4.36 (c-d) correspond to DCT samples machined with low to moderate power with relatively finer grains. The deep and uneven cleavages in the former indicate total brittle fracture with cracks travelling deep beneath the surface while the presence of comparatively uniform and small micro-cavities indicate some ductile mode of fracture at surface in the later.

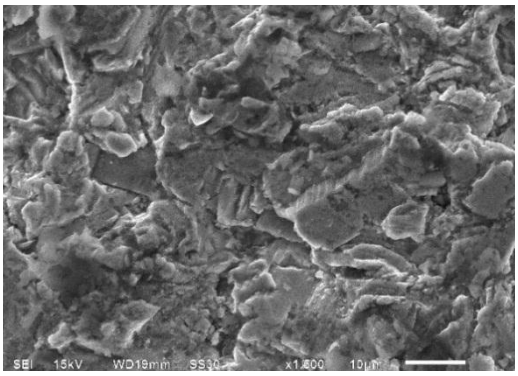 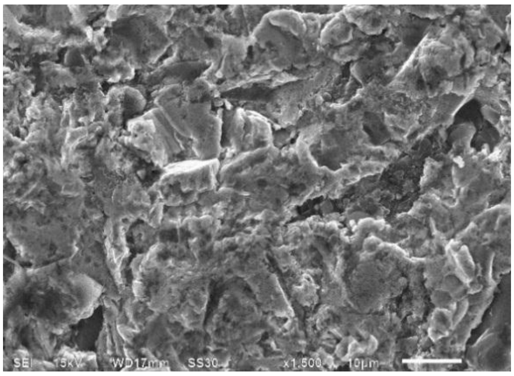

(a) (b)

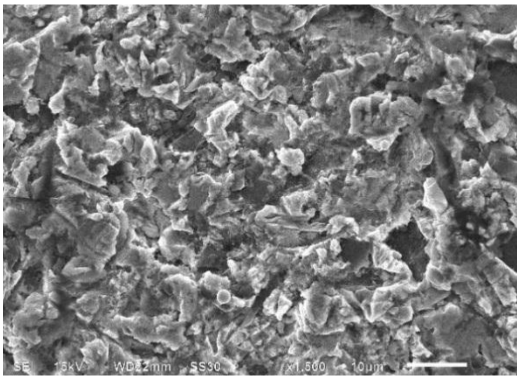 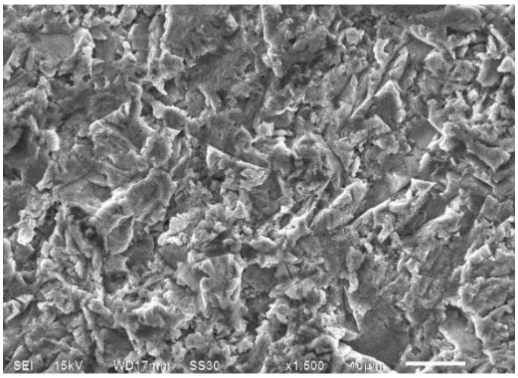

(c) (d)

Figure 4.36 SEM micrographs at 1500X corresponding to a) Exp. 14 b) Exp. 16 c) Exp. 13 d) Exp. 4

Ti-6Al-4V consists of α and β phases comprising of hexagonal closed pack and body centered cubic structure respectively, while the alloying elements stabilize the two phases. A careful glance at optical micrographs of the untreated and deep cryogenic treated samples of Ti-6Al-4V indicate a reduction in β-phase particles as shown in Figure 4.37. Gu et al. [101-102] have also reported improvement in plasticity, yield strength and hence ductility of the alloy after cryogenic treatment and have attributed the same to the phase transformations wherein metastable β-phase gets transformed to stable α and β phase due to variation in concentration of stabilizing alloying element. Superior plasticity and ductility of the material could have changed the fracture pattern of the material under the impact of grains and the mode of fracture may shift slightly from brittle towards ductile and thus leading to reduction in the size of indentation on the work-surface and hence improving the finish.

From the main effects plots of Figure 4.29-4.33 and Figure 4.35, it can be seen that the best setting for minimum SR, and hence maximum surface finish, can be obtained at $\mathbf{A_1B_3C_1D_3E_3F_3}$ which corresponds to aluminium oxide slurry, Ti tool, 100W power, abrasive grit size of 500 and deep cryogenic treated tool and workpiece. The confirmation experiment conducted at this setting resulted in an average SR of 0.28μm which is global minimum within the experimental space.

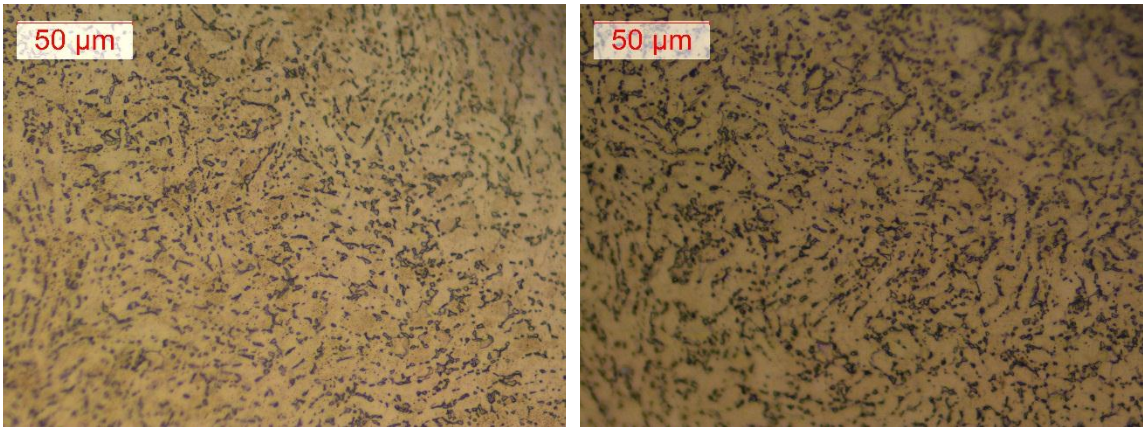

Figure 4.37 Optical micrographs at 500X of Ti-6Al-4V a) Untreated b) Deep Cryogenic Treated

4.6 DIMENSIONAL ACCURACY (HOLE OVERSIZE)

Hole oversize and thus dimensional in-accuracy is caused by influx of abrasive slurry between the tool and work-piece lateral surface as shown in Figure. 4.4.

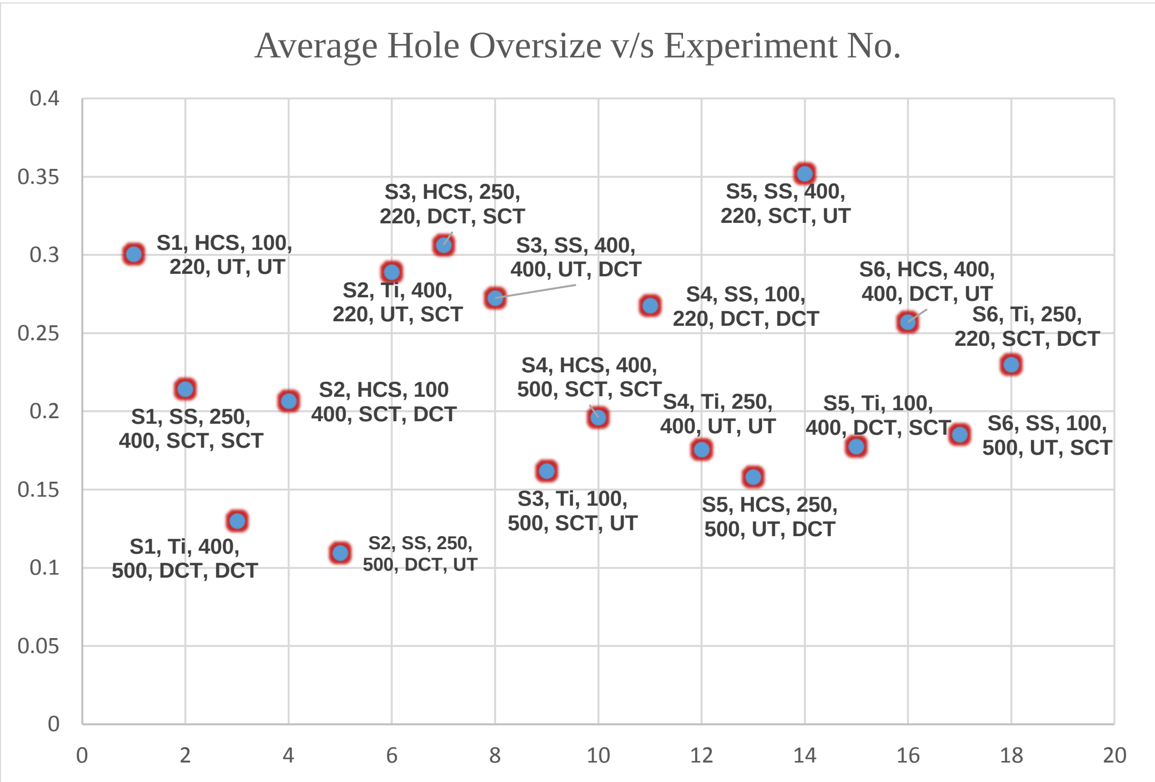

Data Label depict experimental setting and are in sequence of Slurry Type, Tool Type, USM Power, Grit Size, Type of Cryogenic Treatment to Tool and Type of Cryogenic Treatment to Workpiece

Figure 4.38 Average value of HOS corresponding to 18 experimental conditions

The average HOS corresponding to 18 experimental runs is shown in Figure 4.38. A glance at Table 4.25 indicates that Grit Size is the most significant and dominating factor in establishing the dimensional accuracy. The prominence of abrasive size in establishing dimensional accuracy has also been highlighted by other researchers in past [129, 130, 134]. HOS increases almost linearly (Figure 4.39) as the abrasive grit size changes from finer #500 size to coarser #220 size owing to relatively large difference in average particle sizes.

Table 4.25 ANOVA for Data Means (HOS)

Analysis of Variance for Means

Source	DF	Seq SS	Adj SS	Adj MS	F	P
Slurry	5	0.003662	0.003662	0.000732	3.00	0.269
Tool	2	0.006949	0.006949	0.003475	14.22	0.066*
Power Rating	2	0.007865	0.007865	0.003932	16.10	0.058*
Grit Size	2	0.054189	0.054189	0.027094	110.91	0.009†
Tool CT	2	0.001707	0.001707	0.000853	3.49	0.223
Workpiece CT	2	0.001077	0.001077	0.000539	2.20	0.312
Residual Error	2	0.000489	0.000489	0.000244		
Total	17	0.075937				

† Highly Significant * Significant

A coarser grit size leads to bigger gap between the tool surface and inside surface of the machined hole. These findings are in accordance with several published results on dimensional accuracy [15, 54, 129, 134, 155].

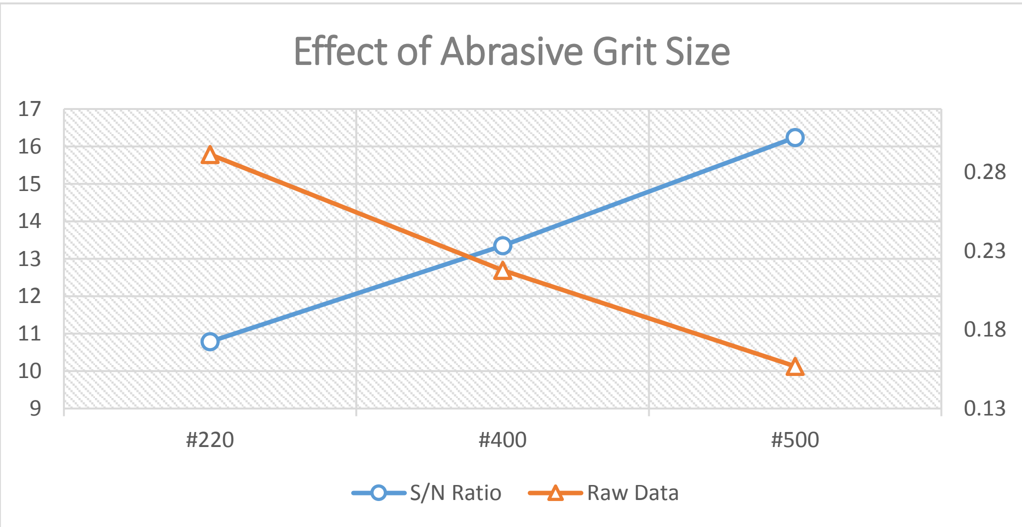

Figure 4.39 Variation of HOS with Abrasive Grit Size

The material removal mechanism in the lateral gap between tool surface and machined walls of the drilled hole (Figure 4.4) comprises of abrasion of slurry against the two surfaces and rolling of abrasive particles in the gap. Magnified intensity of lateral vibrations at higher power rating resulted in increased transfer of the momentum through the oscillating energized tool to the abrasives. Due to this increased momentum associated with abrasive particles in the lateral gap, there is hammering of abrasives against the workpiece surface in lateral gap which cause higher oversize. However the variation with power was not found to be linear (Figure 4.40) as was the case with grit size. Lower power ratings are associated with low rate of material removal in the frontal zone between tool and workpiece because of reduced momentum available with abrasive particles.

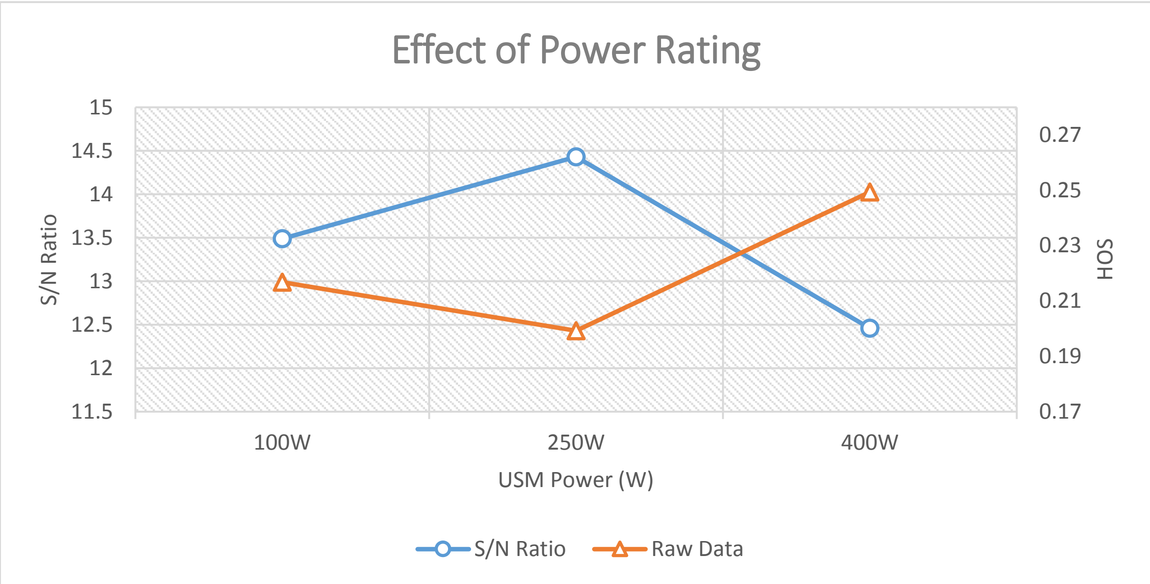

Figure 4.40 Effect of Power Rating on HOS

This slow down the machining in frontal zone. However the abrasive particles in lateral gap remain in action during this period and cause oversize. The minimum oversize is produced at moderate power ratings. These findings are in conformance with some of the similar studies [138]. Tool material has also been observed to affect the dimensional accuracy significantly.

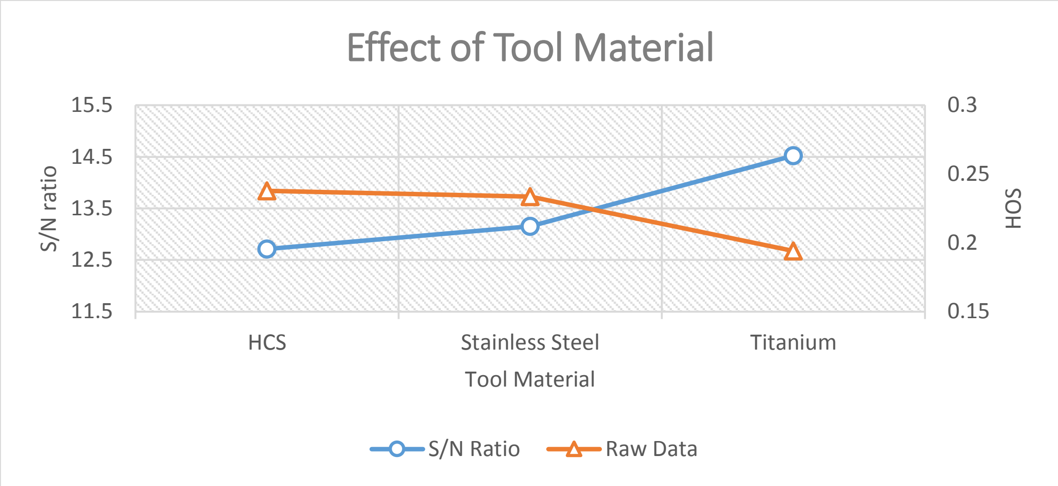

Figure 4.41 Effect of Tool Material on HOS

Figure 4.41 indicates that tools of HCS and SS due to their higher hardness resulted in more oversize owing to higher momentum transfer to abrasives in the lateral direction. Titanium on the other hand with relatively lesser hardness, also possesses superior fracture toughness and thus resists the tool wear and therefore displayed markedly improved results in reducing oversize and hence improving dimensional accuracy. An increased tool wear has been associated with poor dimensional accuracy by researchers in the past as well [129,134].

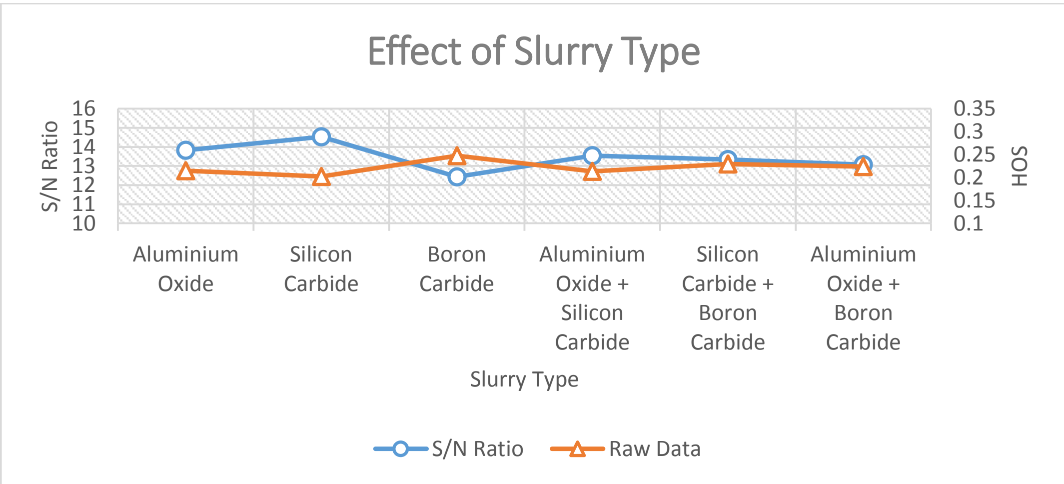

Figure 4.42 Effect of Slurry Type on HOS

Among the other parameters, improved accuracy with deep cryogenic treatment can also be attributed to reduced tool wear post cryogenic treatment. B_4C abrasive slurry with maximum knop hardness resulted in maximum oversize (Figure 4.42) due to stronger cutting action, although the effect on dimensional deviation due to change in slurry was not of much significance as has also been reported by Kuo et al. [54].

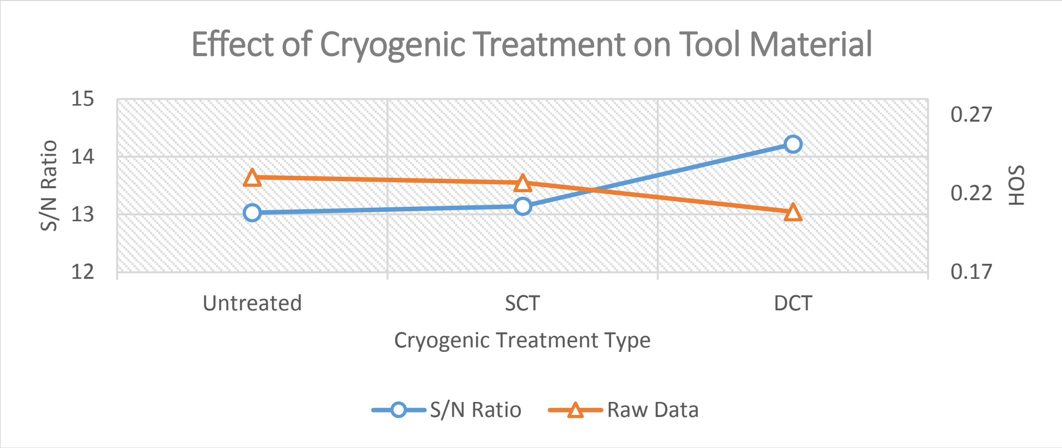

Figure 4.43 Variation in HOS with CT of Tool

However as was the case with power rating, relatively weaker abrasive slurry of Al_2O_3 resulted in slower rate of material removal under the frontal surface of tool and thus engaged the particles in lateral zone. The best result was thus obtained with SiC slurry having an optimum knop hardness from dimensional accuracy view point. However variation due to these parameters was statistically insignificant as was the case with cryogenic treatment of tool and work material (Figure 4.43-4.44).

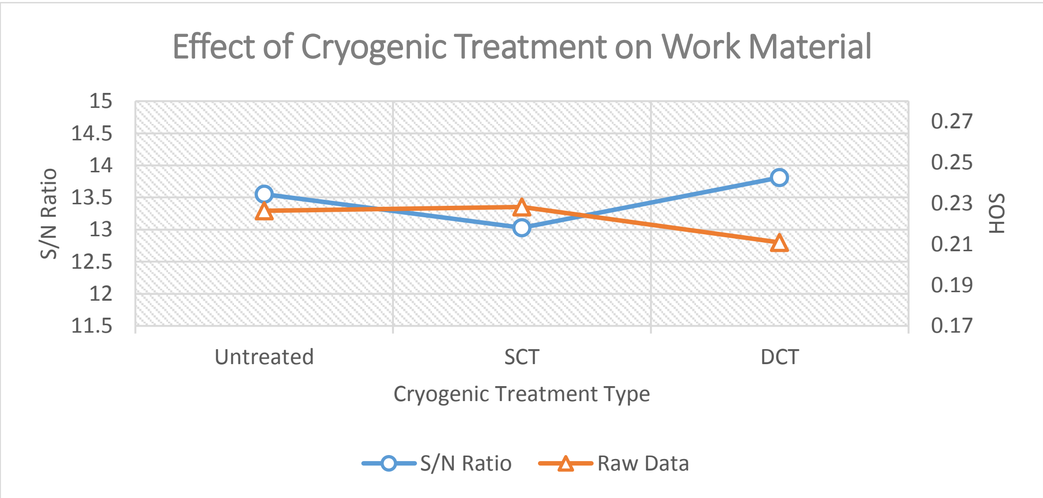

Figure 4.44 Effect of CT to Workpiece on HOS

Among the six parameters chosen for study, abrasive grit size, power rating and tool type were the statistically significant parameters for determining the hole oversize. From the above discussion, it is apparent that hole oversize is a function of abrasive particle size as well as rate of machining in frontal region. Factors contributing for higher machining rates such as grit size and high power rating also lend an increased momentum transfer in lateral direction. However at low power ratings when the machining rates were relatively lesser, abrasive particles continue to act in lateral direction causing oversize. The range of oversize obtained in the present study varied between 3.5 times to 8.5 times of the average particle size as against the theoretical value of twice the average particle size. Though the magnitude of hole oversize was more for coarser particles than finer particles but it was interesting to observe that when compared with respect to average particle size, mean hole oversize (mean HOS/Avg. particle size) was slightly more for finer particles as compared to coarser particles. This can also be attributed to slow machining rates associated with finer particles that keep several layers of these particles engaged in the lateral machining space between tool and workpiece. HOS in the present study ranged from 0.352mm to 0.109mm during the 18 set of experiments. The maximum HOS was observed corresponding to Experiment No. 14 while the least was found to occur during Experiment No. 5. The best setting for the three significant parameters for minimum oversize was recorded at abrasive grit size of 500 with Ti tool at 50% power rating.

SEM images of the machined zone indicated a good round profile corresponding to all the experimental conditions. The hole edges were found to be generally free from cracks and with minimal of burring. Typical edge quality can be seen from Figure 4.45 corresponding to Experiment 12.

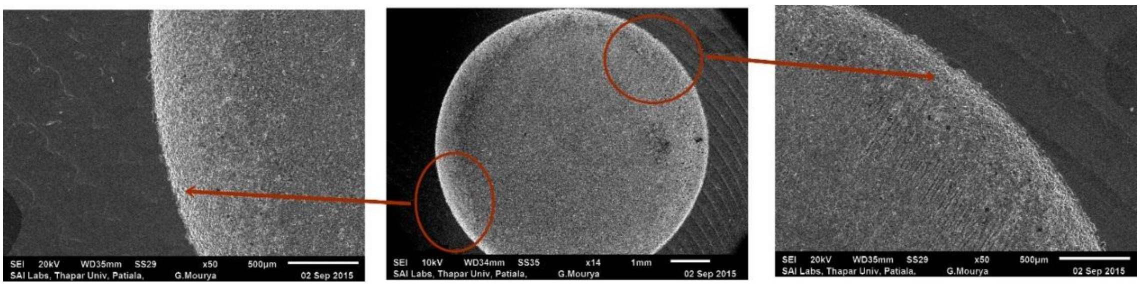

Figure 4.45 SEM images corresponding to entry of machined zone (Experiment No. 12)

A careful control of process parameters can minimize the hole oversize and can improve the edge quality as well. The effect of stringent lateral vibrations which are maximum at entry to hole, larger grit size and tool hardness on edge quality can be seen from the Figure 4.46. A finer grit size and optimum power rating generates a fine detailing at hole edge in comparison to higher power rating and coarser grit size.

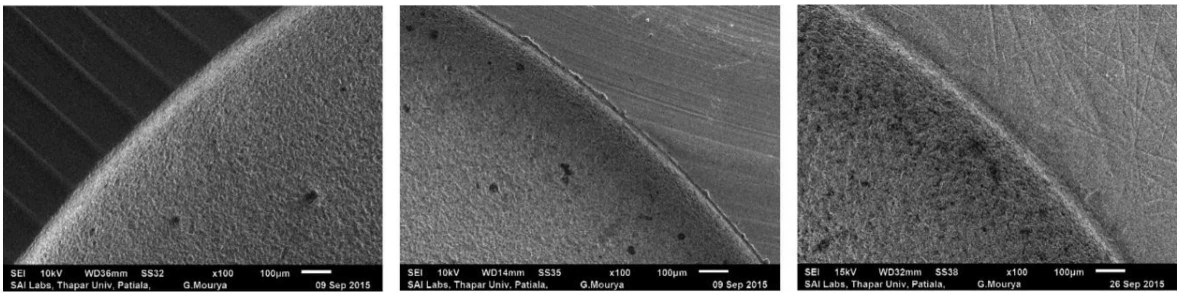

Figure 4.46 Edge quality corresponding to Experiment No. 4, 5 and 6.

At higher power ratings machining behavior sometimes becomes unstable and causes spattering of abrasive particles especially while using a harder tool due to excessive momentum transfer to the abrasive slurry as shown in Figure 4.47. Appropriate fixture is highly necessary to generate a true profile accordingly a suitable fixture was designed to ensure the work-piece doesn’t slip away. The effect of slipping, which is especially dominating at the entry, in the absence of an appropriate fixture can be seen from Figure 4.48.

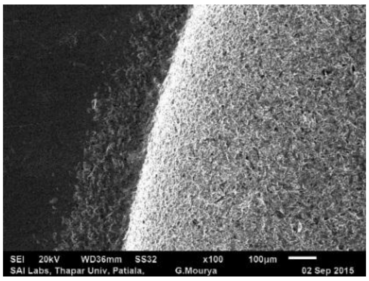

Figure 4.47 Spattering (Exp. 16)

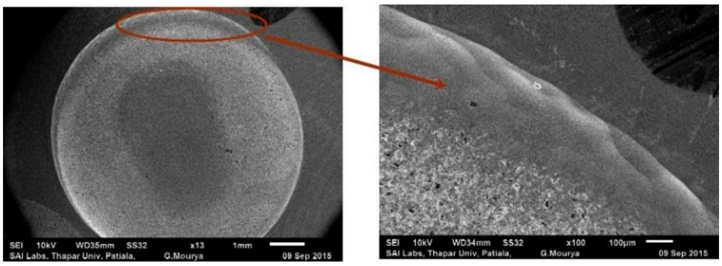

Figure 4.48 Effect of in-appropriate fixture

4.7 TOLERANCE GRADES

ANOVA table 4.26 and response table 4.27 indicate that abrasive grit size is the most significant factor in establishing the tolerance unit, and hence the tolerance grade, followed by power rating and tool type while the variation due to other parameters is statistically insignificant. Response Table indicates that least error in dimension, and thus maximum accuracy, corresponded to finer grit size of #500 while coarser grit size of #220 resulted in maximum oversize.

Table 4.26 ANOVA for Tolerance Unit n (raw data)

Analysis of Variance for Means

Source	DF	Seq SS	Adj SS	Adj MS	F	P
Slurry Type	5	4860	4859.8	972.0	3.00	0.269
Tool Type	2	9223	9223.4	4611.7	14.22	0.066*
Power	2	10439	10438.5	5219.3	16.10	0.058*
Grit Size	2	71923	71923.2	35961.6	110.91	0.009*
Cryo tool	2	2266	2265.6	1132.8	3.49	0.223
Cryo Work	2	1430	1429.9	714.9	2.20	0.312
Residual Error	2	649	648.5	324.3		
Total	17	100789				

* *Significant Parameters*

This is due to the inclusion of bigger gap between tool and workpiece while using coarser grains and the findings are in accordance with the established theories of ultrasonic machining [15,136,138,156-157]. Adithan and Venkatesh [129] have also reported abrasive grit size as the most influential parameter in determining the machining accuracy wherein finer grit size resulted in minimum oversize which was also found to be reduced with increased machining time due to abrasive wear and increased static load due to crushing of abrasives. Increased momentum transfer associated with higher intensity of lateral vibrations at 80% of power rating resulted in stronger impact of abrasive particles on the hole surface which led to oversize and higher tolerance unit in the present study.

Table 4.27 Response Table for Tolerance Unit n (Means)

Response Table for Means

Level	Slurry Type	Tool Type	Power	Grit Size	Cryo tool	Cryo Work
1	247.7	273.6	249.6	335.3	265.2	260.6
2	232.4	269.1	229.3	250.3	261.3	262.8
3	284.6	223.5	287.4	180.7	239.7	242.9
4	245.5					
5	264.1					
6	258.1					
Delta	52.2	50.1	58.1	154.6	25.5	19.9
Rank	**3**	**4**	**2**	**1**	**5**	**6**

The optimum power rating from dimensional accuracy view point was at 50% while slow machining that kept abrasives engaged in tool-workpiece gap on lateral direction was responsible for poor accuracy at relatively lesser power ratings. Relatively harder tools of HCS and SS resulted in higher momentum transfer and resulted in higher oversize on the hole periphery while titanium owing to its peculiar mechanical properties exhibits superior fracture toughness and resists erosion on the lateral side which led to minimum oversize.

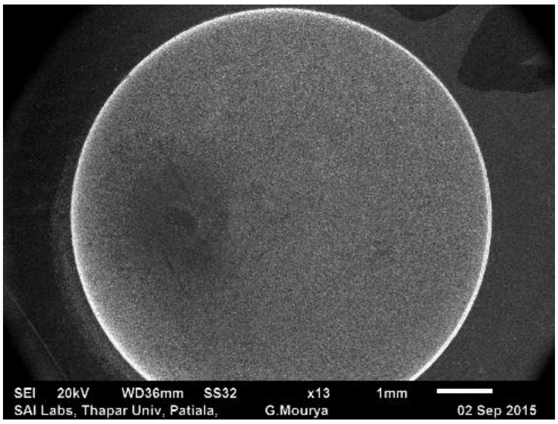

Figure 4.49 SEM image for machined zone

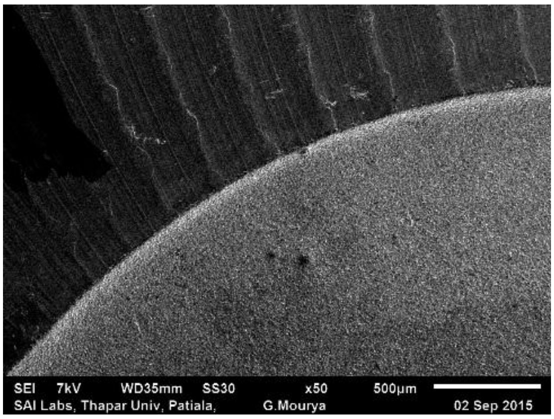

Figure 4.50 Edge profile of machined region

Figure 4.49 shows SEM images at the entrance of machined zone corresponding to high power of 400W, hard tool of HCS and medium abrasive size of 400 corresponding to Experiment 16 while Figure 4.50 shows edge profile corresponding to finer abrasive particles of 500, lower power of 100 W and titanium tool material (Experiment 9). Both the image indicate a good round profile at machined region and the hole edges were found to be free from cracks and burrs. Hole edge depicts a smooth surface and continuous profile.

CHAPTER - 5

MODELLING OF RESPONSE VARIABLES

5.1 ARTIFICIAL NEURAL NETWORK MODELLING

Estimation of response variables such as MRR, TWR and SR with variation in input process parameters is of prime importance for a manufacturing engineer to enable setting up of appropriate/optimal level values within a range for a required response value. The task becomes all the more difficult when the dependency is on a number of control factors as in ultrasonic machining. However, there are indicators which enable the experienced manufacturers to set the control values to requisite limits and attain results close to target. A more common approach that is followed by researchers is development of empirical relationships using extensive experimentation.

A good model or theory should satisfy two important criterion, firstly it should be able to describe a large set of observations corresponding to few arbitrary parameters and second, the predictions made out of the theory should be verifiable [158]. Physical models such as those of Shaw, Miller satisfy both the requirements [31] by basic analysis of theory of material removal from work surface with careful observation of phenomenon and physics involved in the process. In contrast, level one empirical relations such as a linear regression equation necessitate as many parameters as the variable number for description of experimental data with an uncertainty on physical justification. Data values are best fitted to some specific relationship, generally linear in nature. Regression analysis suffers from a couple of difficulties due to selection of relationship before analysis and the equation, once derived, is applied to entire span of input space which may not be too reasonable to assume [158]. Neural network based relations are however considerably advantageous over regression equation and are extremely useful in situations where physical models do not exist. The method also avoids the difficulties listed with regression analysis.

Neural Networks are the result of extensive research in Artificial Intelligence that attempts to model the human brain behavior. Barr and Feigenbaum [159] defined AI as the *part of computer science concerned with designing intelligent computer systems that exhibit characteristics associated with intelligence in human behavior*. Thus AI aims at making computers ‘think’ to enable them solve the problems requiring human human intelligence. Expert Systems, Neural Networks and Fuzzy Logic systems are three major technologies of AI. While the expert systems operating symbolically on a macroscopic scale need knowledge of relationships irrespective of their development, Neural networks use sub-symbolic processing at microscopic scale [160].

Some people may argue that neural network is just a technique of curve fitting as happens with any other empirical modelling method. However there are some notable differences between conventional empirical models and neural networks. The most prominent among them is that neural networks possess better filtering capacity due to micro feature nature of every node that encodes only a micro part of overall input-output pattern. The networks are massively parallel resulting in independent operation of every node. These networks are more adaptive compared to their counterparts in empirical modelling and are truly multiple-input, multiple-output (MIMO) systems thus making them far more effective and versatile.

Neural networks aim at mapping a given set of input patterns corresponding to a specific set of output patterns and this goal is accomplished by, firstly, learning from a series of available data sets of output parameters corresponding to given input parameters and subsequently, the developed network applies the learning to a new input pattern for predicting corresponding output. This is similar to what happens in human brain wherein the neurons within the nervous system have interaction in a very complex manner. The input signal through some sensory stimulus is transferred to brain exciting the other neurons and causing interaction amongst them. Brain responds with an output after reaching a conclusion based on interaction of neurons. The microscopic interactions among neurons, though invisible, but cause identifiable behavior. A simple example to explain this can be thought of in terms of brain’s response when humans touch a hot surface. The sensory stimulus of touch in this case transfers the signal to brain where it is processed within the neurons and output is generated in form of instruction to withdraw the hand immediately. Thus the input and output, touching the hot surface and withdrawing the hand respectively, happened because of complex invisible interaction among the neurons.

Neural Networks also use similar neuronal structure in computer modelling of intelligent behavior. Artificial Neural Networks (ANN) are massive parallel systems composed of several simple processing units called neurons. An ANN is a multilayered architecture having neurons grouped into three sets of input, hidden, and output layers. *Input layer* is where the information is received from an external source and then is passed on to network for further processing. This information is processed "quietly" in the *hidden layer* and the results are sent out to external receptor from the *output layer*. The neurons in adjacent layers are connected through certain weights that have to be established during ANN training. Characterization of ANN is done through their architecture, allocated weights and adjoined biases, and activation (transfer) functions which are used in the processing layers. Direct ANNs with supervised training and backpropagation (BP) are in common use to solve most of the practical problems.

5.1.1 Mathematical model of a neuron

An artificial neural network may be viewed as a function which shall map input variables into output variables. An artificial neuron is an information processing unit and is key towards operation of neural networks. The basic model of a neuron is as shown in figure 5.1 [161]. This Model forms the basis of an artificial neural network design.

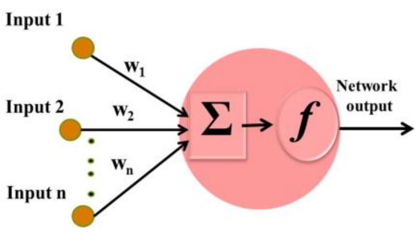

Figure 5.1 Basic neuronal model *[161]*

The three main elements of a neuronal model include a set of connecting links possessing some weights, an adder for summation of input signals and an activation function which will limit the amplitude of output neuron [162]. The summation function generates the net input coming to a cell by adding the weighted sum of inputs and is given by following equation:

$$IP_i = \sum_{i=0}^{n} w_{ij}x_j + w_{bi} \qquad \textit{Eq. 5.1}$$

where IP_i is weighted sum of input values, *i* and *j* are processing elements w_{ij} is weights associated with connections between processing elements, n is number of processing elements and x_j refers to output of jth processing element. In addition to this the network also has an externally applied bias denoted by w_{bi}which has the effect of controlling the net input to activation function, increasing or decreasing, depending upon its additive or subtractive character. Transfer function then, through an algorithm, converts the generated data of summation function into a real output. Logistic sigmoid, hyperbolic, step/signum, tangent sigmoid etc. are some of the commonly used transfer functions in ANN.

5.1.2 Network Architecture

Neural Network Architecture refers to arrangement of neurons in layers and pattern of synaptic connections within the neurons and among the layers. A layered network comprises of input layer of source nodes, computational nodes forming an output layer and one or more number of hidden layers of neurons between these two layers. Based on the connections between neurons, the two major classes of neural network architectures are Feed Forward Neural Networks and Recurrent Neural Networks. While in the former signal flow occurs in one direction between the layers without any connection between neurons of same layer, the later type of networks involve atleast one feedback loop containing unit delay operator making it a dynamic system with presence of both kinds of connections.

5.1.3 Learning Paradigms

Learning in in neural networks is a process of modifying the synaptic weights in the network corresponding to a specified input. Learning paradigms in Neural Networks can be classified into Supervised and Unsupervised mode. Supervised learning involves modification of synaptic weights to minimize the variation between actual and desired network output when network is presented with a training situation comprising of an input and desired output. However, unsupervised networks do not have any desired output. The synaptic weights are continuously modified till the time the network provides an output that is a good representation of input statistics.

5.2 MODELLING OF RESPONSE VARIABLES USING ANN

Use of artificial intelligence and soft computing in manufacturing for modelling and optimization has gained considerable momentum in last decade. Neural networks, genetic algorithms, particle swarm optimization etc. are being increasingly used with considerable success to create empirical relations and identify global optimal solutions. Complex problems with non-linear behavior have been successfully modeled with the use of single hidden layer with adequate number of neurons using ANN technique. Use of AHP for qualitative decision making is very popular and is in use for several years. However AHP has also been used successfully for arriving at quantitative decision making involving a number of decision variables. Kumar and Sait [163] have made the use of ANN for modelling the results of turning operation on bidirectional CFRP (bisphenol) pipe using carbide tool. ANN with BPNN algorithm was adopted for modelling and the number of layers and neurons in the layer were selected based on random trials with different combinations. A 3-25-25-1 network architecture was able to effectively model the results of cutting force with variation in feed, depth of cut and speed. Kara et al. [164] have suggested the use of 3-7-1 and 3-6-1 architecture for predictive modelling of cutting force and feed force during orthogonal turning of AISI 316L stainless. A 4-9-1 neural network architecture with feed forward back propagation algorithm was able to effectively model the surface roughness in dry cutting of AISI 1060 steel when *logsig* was used as activation function for hidden layer while *tansig* activation function was used for output layer Kant and Sangwan [165]. The model outperformed regression and fuzzy logic based models on account of better mapping between predicted and experimental values of the response variable [165]. ANN proved to be instrumental to fill the gaps of available experimental response data from Taguchi analysis in optimizing CO_2 laser welding parameters to establish penetration depth and zone width for fused and heat affected zones [166]. Rao et al. [167] have proposed ANN-GA hybrid models for predicting and optimizing surface roughness in electric discharge machining of the four materials including Ti-6Al-4V selected for the study. Feed forward neural network was used for modelling with 3 hidden layers in the architecture. Developed model was within the agreeable limits of error and significant reduction in MSE was obtained when GA was used to optimize the network.

A number of studies reported hitherto on ultrasonic machining, in general, and that of titanium, in particular, have made use of Buckingham – π theorem of dimensional analysis for modelling of response variables such as MRR and TWR [9,147,168]. An effort here has been made to model the response variables of this study viz MRR, TWR, SR and HOS by making use of ANN.

5.2.1 Modelling for Surface Roughness

An ANN model has several parameters such as number of layers, number of neurons in the layers, type of learning algorithm and transfer function that determine the overall architecture of the network and affect the modeling process. Prior to training a network these factors related to network architecture and structure which have to be determined to ensure a healthy and statistically controlled output from the network. An optimum combination is the one which will generate an output with minimum of error and hence maximum of correlation between training and test data

A number of published studies in use of ANN in manufacturing have sufficed the use of one hidden layer for modelling [162,164,169]. To complete the architecture, the number of neurons in the hidden layer were selected by trial and error method. Several networks with different number of hidden neurons were explored and the network that resulted in minimum mean square error was chosen which was found to be the network with 7 neurons in the hidden layer. Accordingly in the present study, an ANN model with one hidden layer comprising of 7 neurons has been chosen to model six input parameters for SR measurement thus giving a 6-7-1 architecture as shown in Figure 5.2. w_1, w_2, w_3….w_7 are the weights between hidden layer and output layer comprising of a single neuron. Additionally, biases are assigned to all the neurons of hidden and output layer. b_o is bias to output layer while b_1, b_2, b_3…b_7 are biases to hidden layer neurons.

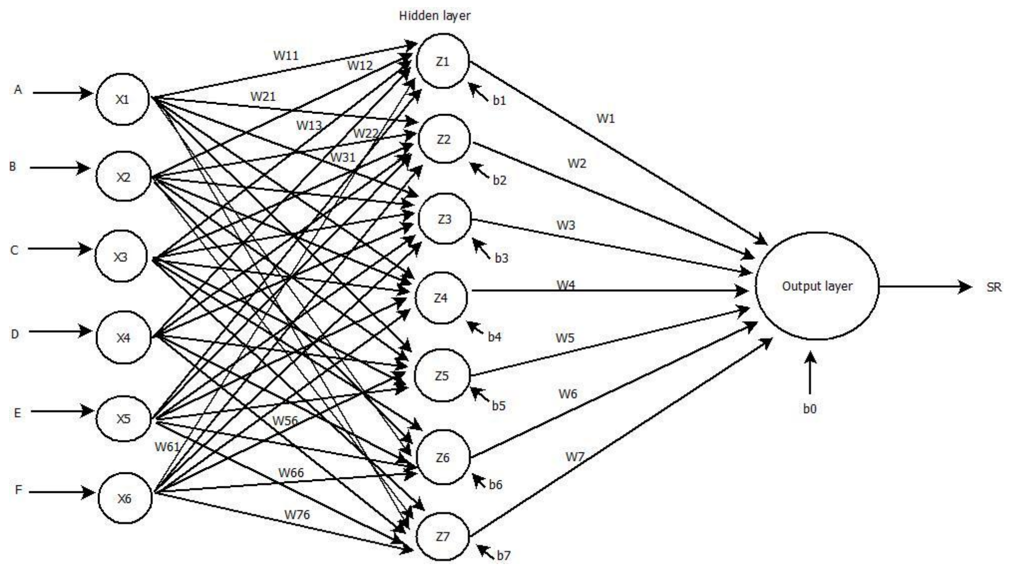

Figure 5.2 Neural Network 6-7-1 architecture used for modeling SR

Weights are assigned to each of the connecting link, 42 in number, between input layer and hidden layer neurons. The activation function used for the hidden layer is *log-sigmoid* while *pure linear* function is used for output layer and the two functions are characterized by the Eq. (5.2) and (5.3) respectively.

$$z_i = \frac{1}{1 + e^{NIP_i}} \qquad \textit{Eq. 5.2}$$

$$z_o = \sum_{i=1}^{p} z_i w_i + b_0 \qquad \textit{Eq. 5.3}$$

where z_i is the ouput of *i*th neuron in hidden layer and z_o is final result of output layer while *p* is number neurons in hidden layer.

Modeling is based on values of weights and bias given to the neurons in the two layers. The weights and bias are determined by training the network with input values of parameters and corresponding output values using neural network toolbox in MATLAB R2014a. The categorical factors in input parameters have been scaled to nominal value using 0-1 scale and accordingly the levels of slurry were coded as 1 to 6, while those of tool type and cryogenic treatment type were coded as 1 to 3.The training was carried out using Levenberg Marquadt (LM) algorithm that corresponds to *trainlm* function in MATLAB and works on back propagation network. The weights and biases thus determined from ANN training have been used to create mathematical model for surface roughness and is given below:

$$\begin{aligned} &Surface\ Roughness, SR \qquad \textit{Eq. 5.4} \\ &= 0.24989 z_1 + 0.26656 z_2 + 0.44295 z_3 + 0.1289 z_4 \\ &+ 0.0.61601 z_5 - 0.76117 z_6 + 1.1346 z_7 - 1.1681 \end{aligned}$$

where z_1, z_2.......z_7 are the outputs of hidden layer neurons and are determined by equation 5.1. Accordingly each of the z_i value is characterized by the following relations:

$$z_1 = \frac{1}{1+ e^{-m_1}} \qquad z_2 = \frac{1}{1+ e^{-m_2}} \qquad z_3 = \frac{1}{1+ e^{-m_3}} \qquad z_4 = \frac{1}{1+ e^{-m_4}}$$

$$z_5 = \frac{1}{1+ e^{-m_5}} \qquad z_6 = \frac{1}{1+ e^{-m_6}} \qquad z_7 = \frac{1}{1+ e^{-m_7}}$$

where m_1, m_2, m_3 …. m_7 are net inputs to hidden layer neurons and their values are determined by Eqs. (5.5-5.11):

$$m_1 = 0.92815x_1 - 2.1128x_2 - 0.022459x_3 - 1.5067x_4 + 2.3882x_5 + 0.48948x_6 - 4.3768 \quad \textit{Eq. 5.5}$$

$$m_2 = 0.42728x_1 + 0.45904x_2 + 2.1991x_3 - 3.6322x_4 - 0.28857x_5 + 1.8132x_6 - 1.3769 \quad \textit{Eq. 5.6}$$

$$m_3 = 1.5969x_1 + 0.97421x_2 + 0.97559x_3 - 2.0656x_4 + 2.6021x_5 + 0.16981x_6 - 1.3945 \quad \textit{Eq. 5.7}$$

$$m_4 = -2.0861x_1 - 0.25188x_2 - 1.6503x_3 + 0.79422x_4 - 1.3264x_5 + 1.9661x_6 - 0.5957 \quad \textit{Eq. 5.8}$$

$$m_5 = -2.461x_1 - 1.7965x_2 + 2.7711x_3 + 0.63393x_4 + 1.002x_5 + 0.52142x_6 - 0.61831 \quad \textit{Eq. 5.9}$$

$$m_6 = 0.98399x_1 - 0.53745x_2 - 0.80443x_3 + 2.8098x_4 + 2.7759x_5 + 2.6456x_6 + 1.2892 \quad \textit{Eq. 5.10}$$

$$m_7 = 1.7335x_1 - 3.4562x_2 - 0.57404x_3 - 0.5535x_4 - 1.3206x_5 + 0.30262x_6 + 4.9501 \quad \textit{Eq. 5.11}$$

where $x_1, x_2, x_3 \ldots\ldots x_6$ are values of input process parameters corresponding to slurry type, tool type, power rating, grit size and cryogenic treatment given to tool and workpiece respectively.

Based on the ANN modelling the predicted and actual values of SR are compared on line graph as shown in Figure 5.3 for the 54 outcomes of SR values and a highly close relation is evident from the coinciding line graphs. The model validation is evident from the correlation coefficients of test and validation data which stand at 0.99608 and 0.99388, respectively, as shown in Figure 5.4 (a-b) while the overall coefficient of the model is 0.9866 as shown in Figure 5.4 (c).

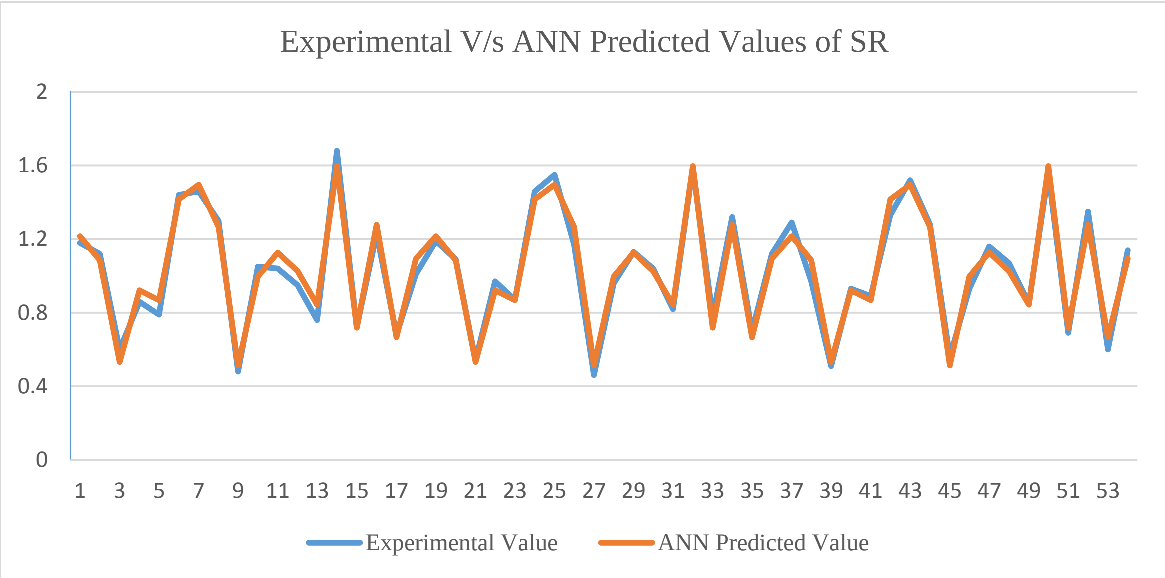

Figure 5.3 Comparison of experimental and predicted values of SR

To check the model for experimental validation, the average value of SR of eighteen experimental sets was plotted against the ANN predicted values as shown in Figure 5.5.

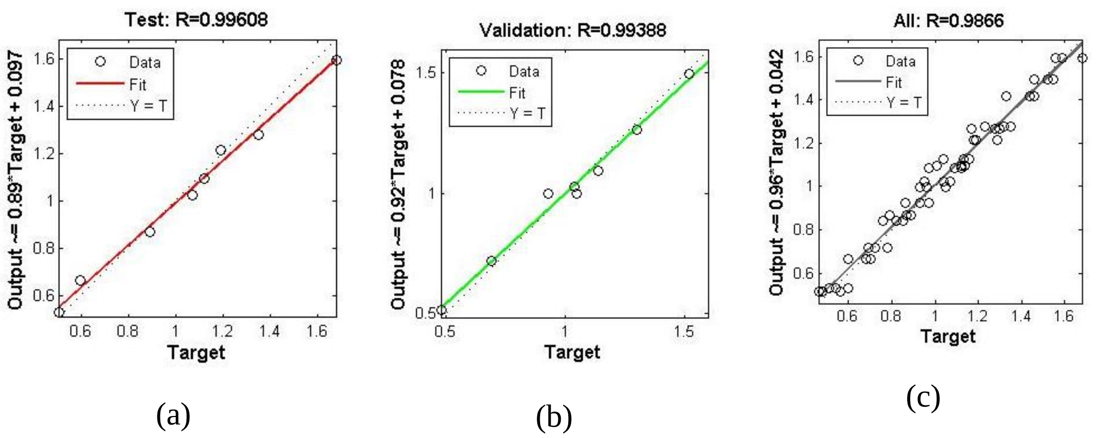

Figure 5.4 Correlation for a) Test data b) Validation data c) Overall coefficient

Corresponding values for percentage error percentage error and comparison of average SR and average value of ANN predicted SR are given in Table 5.1 The percentage error was calculated using Eq (5.12).

$$\%age\ prediction\ error = \frac{(Experimental\ Value - Predicted\ Value)}{Experimental\ value} * 100 \qquad Eq.\ 5.12$$

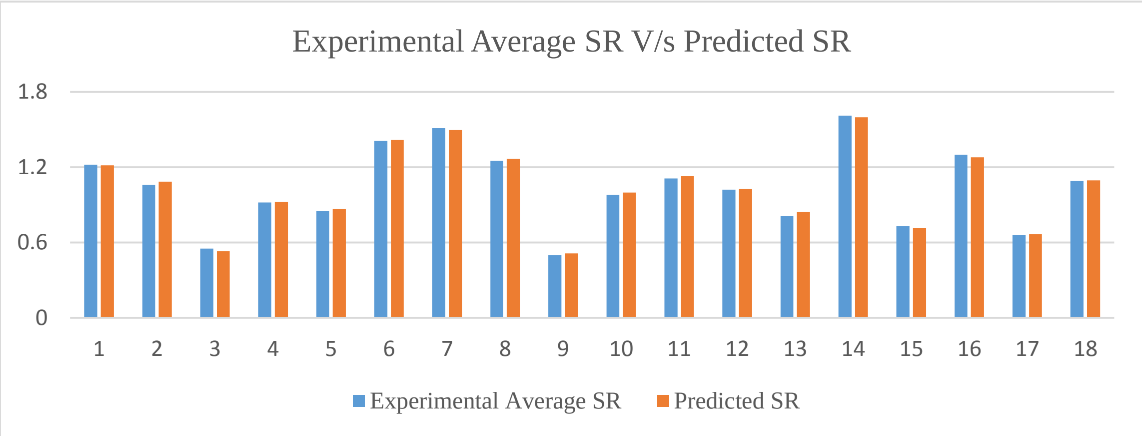

Figure 5.5 Comparison of experimental average and predicted SR

The maximum %age prediction error was found to be -4.14% corresponding to experiment no. 13, which indicates that the model is sufficiently accurate and hence can be used to predict the SR effectively.

Table 5.1 Comparison of experimental average SR and predicted average SR

Exp. No.	**1**	**2**	**3**	**4**	**5**	**6**	**7**	**8**	**9**	**10**	**11**	**12**	**13**	**14**	**15**	**16**	**17**	**18**
Avg. SR (Expt.)	1.22	1.06	0.55	0.92	0.85	1.41	1.51	1.25	0.50	0.98	1.11	1.02	0.81	1.61	0.73	1.30	0.66	1.09
Avg. SR (Predicted)	1.22	1.08	0.53	0.92	0.87	1.42	1.50	1.27	0.51	1.00	1.13	1.03	0.84	1.60	0.72	1.28	0.67	1.09
%age error	0.36	-2.34	3.28	-0.29	-2.14	-0.44	0.91	-1.29	-2.50	-1.77	-1.61	-0.55	-4.14	0.85	1.67	1.63	-0.90	-0.45

5.2.2 Modelling of MRR

From the ANOVA table 4.23, it can be seen that Material Removal Rate (MRR) was found to be significantly affected by abrasive grits size, USM power, abrasive type and tool material while the variation due to cryogenic treatment to tool and work material relatively less significant. An ANN model was formulated by selecting the similar 6-7-1 neural network architecture as was in the case of surface roughness (Figure 5.2). The data of 54 experimental runs was used for modelling of MRR. 70% of the data amounting to approximately 38 runs was used for training while 15% each was used for testing and validation that accounted for 8 experimental runs for each category. Mean Square Error (MSE) was selected as performance function to compare the modeled values with those of experimental ones. To minimize the variability within input data sets due to large range the variables were normalized using the following relationship:

$$y_{ij}^{*} = \frac{y_{ij}}{Max\ y_{ij}} \qquad \textit{Eq. 5.13}$$

where y_{ij}^{*} is the normalized value of the data set y_{ij} and maximum value in the data set is $Max\ y_{ij}$.

The activation function used in the hidden layer was *log-sigmoid* while *pure linear* function was used for output layer with LM algorithm and back propagation network. Accordingly, the following model for MRR resulted with satisfactory performance with regard to minimizing the error between experimental and predicted values.

$$\begin{aligned} &Material\ Removal\ Rate, MRR \qquad \textit{Eq. 5.14} \\ &= (-0.6397p_1 + 1.615p_2 - 0.39273p_3 + 1.5072p_4 \\ &+ 0.76816p_5 + 1.1719p_6 - 0.49792p_7 - 2.0127 \end{aligned}$$

where p_1, p_2.......p_7 are the outputs of hidden layer neurons and are determined by equation 5.1. Accordingly each of the p_i value is characterized by the following relations:

$$p_1 = \frac{1}{1+e^{-k_1}} \qquad p_2 = \frac{1}{1+e^{-k_2}} \qquad p_3 = \frac{1}{1+e^{-k_3}} \qquad p_4 = \frac{1}{1+e^{-k_4}}$$

$$p_5 = \frac{1}{1+e^{-k_5}} \qquad p_6 = \frac{1}{1+e^{-k_6}} \qquad p_7 = \frac{1}{1+e^{-k_7}}$$

where k_1, k_2, k_3 …. k_7 are net inputs to hidden layer neurons and their values are determined by Eqs. (5.15-5.21):

$$k_1 = 0.82743a_1 - 3.0505a_2 + 0.30744a_3 + 0.63553a_4 + 2.0272a_5 + 0.25124a_6 - 3.7845 \quad \textit{Eq. 5.15}$$

$$k_2 = 0.19333a_1 + 1.1859a_2 - 1.4122a_3 - 2.6346a_4 - 2.277a_5 + 0.36751a_6 + 1.8917 \quad \textit{Eq. 5.16}$$

$$k_3 = -1.3399a_1 + 1.0419a_2 - 2.4674a_3 + 1.1972a_4 - 1.8193a_5 + 1.7348a_6 + 0.76614 \quad \textit{Eq. 5.17}$$

$$k_4 = -0.21036a_1 - 2.9247a_2 + 2.6394a_3 + 1.229a_4 + 0.55221a_5 + 0.44784a_6 - 0.7165 \quad \textit{Eq. 5.18}$$

$$k_5 = 1.1954a_1 + 2.2809a_2 + 3.0434a_3 - 1.8681a_4 + 0.61101a_5 + 1.1437a_6 + 0.19063 \quad \textit{Eq. 5.19}$$

$$k_6 = 0.8047a_1 - 1.7411a_2 - 1.0961a_3 + 2.5916a_4 + 1.0301a_5 - 2.1213a_6 - 3.4343 \quad \textit{Eq. 5.20}$$

$$k_7 = 1.9289a_1 + 1.1547a_2 - 2.2639a_3 + 1.3653a_4 + 0.51811a_5 + 0.5796a_6 + 3.9692 \quad \textit{Eq. 5.21}$$

where $a_1, a_2, a_3 \ldots\ldots a_6$ are normalized values of input process parameters corresponding to slurry type, tool type, power rating, grit size and cryogenic treatment given to tool and workpiece respectively.

The best validation performance of the model was found at epoch 7 when Mean Square Error became 0.00041846 as shown in Figure 5.6.

Based on the developed model, the predicted and actual values of MRR are compared on line graph as shown in Figure 5.7 for the 54 outcomes of MRR values and a highly close relation is evident from the coinciding line graphs. The model validation is evident from the correlation coefficients of test and validation data which stand at 0.98283 and 0.93623, respectively, as shown in Figure 5.8 (a-b) while the overall coefficient of correlation for the model is 0.98792 as shown in Figure 5.8 (c).

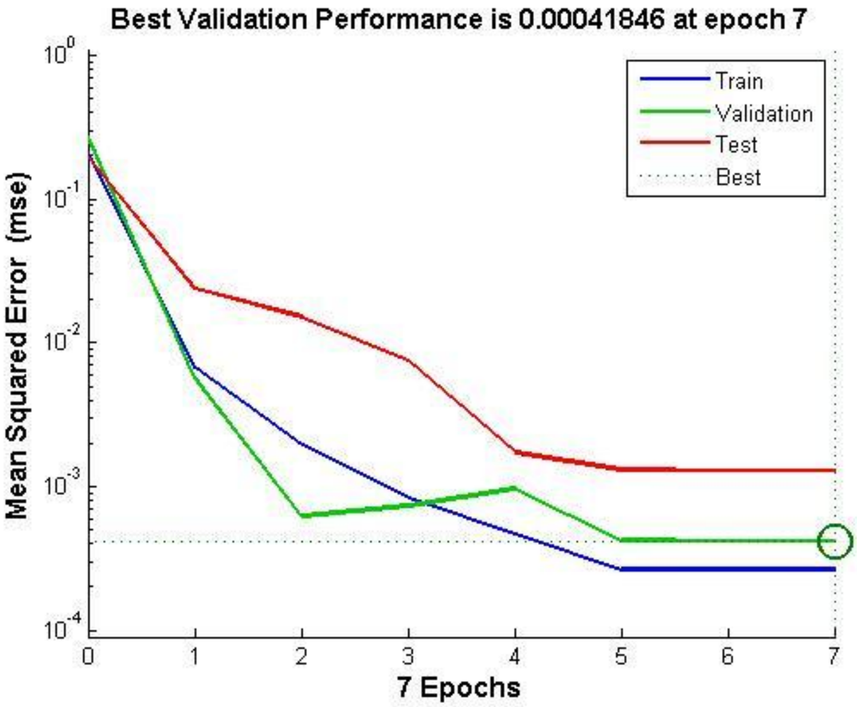

Figure 5.6 Best Validation performance for MRR model

Experimental validation of the model was checked by comparing the average value of MRR of the eighteen experimental sets against the ANN predicted values as shown in Figure 5.9. Corresponding values for percentage error and comparison of average SR and average value of ANN predicted SR are given in Table 5.2. The percentage error was calculated using Eq (5.12).

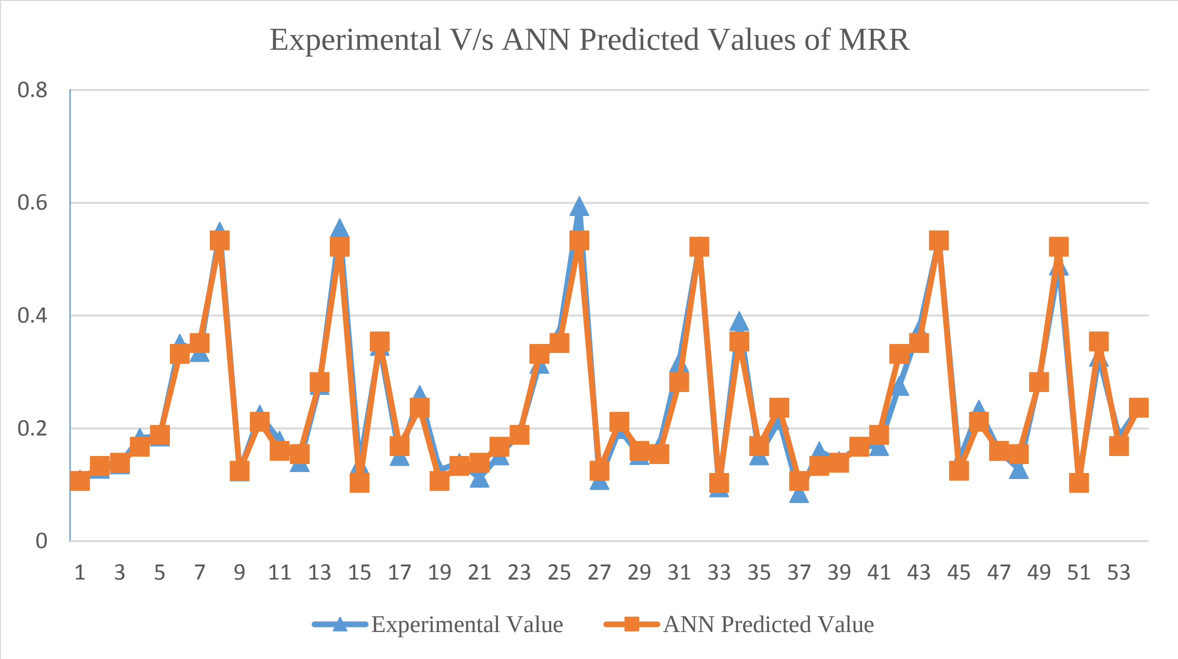

Figure 5.7 Experimental and Predicted Values of MRR

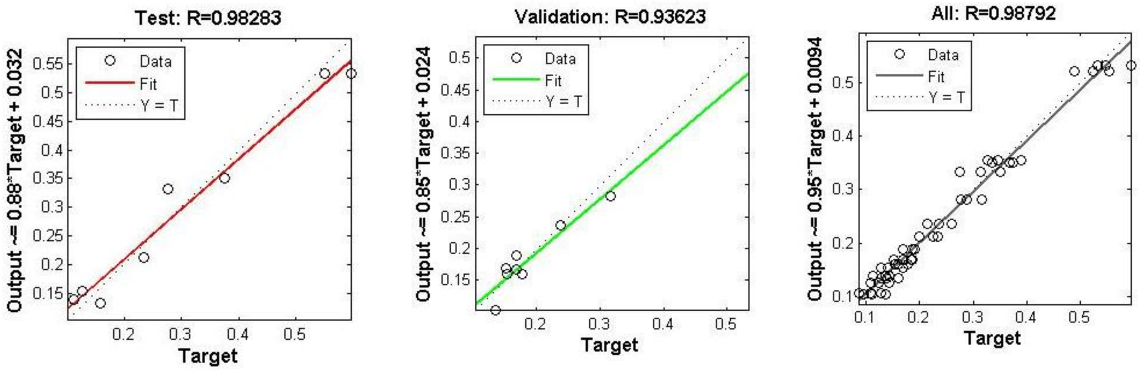

Figure 5.8 Correlation of a) Test Data b) Validation Data c) All Data for MRR

The maximum %age prediction error was found to be 9.73% corresponding to experiment no. 16, which indicates that the model is sufficiently accurate and hence can be used to predict the MRR effectively.

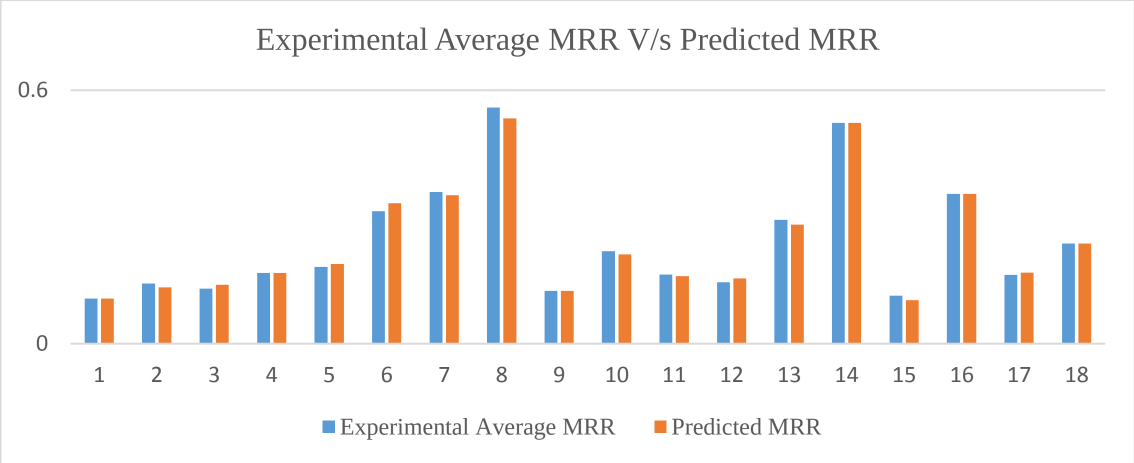

Figure 5.9 Comparison of experimental average and predicted MRR

Table 5.2 Comparison of experimental average MRR and predicted average MRR

Exp. No.	**1**	**2**	**3**	**4**	**5**	**6**	**7**	**8**	**9**	**10**	**11**	**12**	**13**	**14**	**15**	**16**	**17**	**18**
Avg. MRR (Expt.)	0.11	0.14	0.13	0.17	0.18	0.31	0.36	0.56	0.13	0.22	0.16	0.15	0.29	0.52	0.11	0.35	0.16	0.24
Avg. MRR (Predicted)	0.11	0.13	0.14	0.17	0.19	0.33	0.35	0.53	0.13	0.21	0.16	0.15	0.28	0.52	0.10	0.35	0.17	0.24
%age error	0.00	6.11	-6.85	0.05	-3.67	-6.06	2.12	4.57	0.00	3.33	2.22	-6.13	3.96	0.00	9.42	0.00	-3.60	0.00

5.2.3 Modelling of TWR

Table 4.24 indicates that TWR is significantly affected by USM power, abrasive grit size, abrasive type, tool material, type of cryogenic treatment imparted to tool and less significantly by type of cryogenic treatment given to workpiece. Six nodes in the input layer corresponding to six input parameters and one node in the output layer corresponding to tool wear rate constitute 6-7-1 architecture to model the tool wear rate with seven neurons in the hidden processing layer. Four categorical factors were scaled on nominal scale and thus the levels of slurry were coded as 1 to 6, while those of tool type and cryogenic treatment type were coded as 1 to 3.

Data available from the 54 experimental runs was used to develop the network by involving 70% of it for training and 15% each for testing and validation. The network architecture was similar to the one used for SR and MRR and hence is replica of Figure

5.2. The experimental input data was normalized to minimize the variability using equation 5.13. The resultant developed model for TWR is designated as follows:

$$Tool\ Wear\ Rate, TWR = (0.1514g_1 + 1.3435g_2 - 0.26613g_3 - 1.9844g_4 + 0.28758g_5 + 1.5664g_6 - 0.7803g_7 - 1.051) \qquad \textit{Eq. 5.22}$$

where g_1, g_2.......g_7 are the outputs of hidden layer neurons and are determined by equation 5.1. Accordingly each of the g_i value is characterized by the following relations:

$$g_1 = \frac{1}{1+e^{-s_1}} \qquad g_2 = \frac{1}{1+e^{-s_2}} \qquad g_3 = \frac{1}{1+e^{-s_3}} \qquad g_4 = \frac{1}{1+e^{-s_4}}$$

$$g_5 = \frac{1}{1+e^{-s_5}} \qquad g_6 = \frac{1}{1+e^{-s_6}} \qquad g_7 = \frac{1}{1+e^{-s_7}}$$

where s_1, s_2, s_3 …. s_7 are net inputs to hidden layer neurons and their values are determined by Eqs. (5.23-5.29):

$$s_1 = 0.43815a_1 + 2.3624a_2 + 0.9516a_3 + 0.7235a_4 - 1.244a_5 - 2.8313a_6 - 3.5848 \qquad \textit{Eq. 5.23}$$

$$s_2 = -3.4994a_1 - 0.1008a_2 - 1.4267a_3 - 2.4173a_4 - 1.9096a_5 - -0.9889a_6 + 2.2101 \qquad \textit{Eq. 5.24}$$

$$s_3 = -1.8203a_1 + 1.7821a_2 + 1.1966a_3 - 1.7507a_4 - 1.5172a_5 + 1.4258a_6 + 1.2411 \qquad \textit{Eq. 5.25}$$

$$s_4 = -2.6845a_1 - 0.55296a_2 - 1.509a_3 + 0.4489a_4 - 0.6624a_5 - 3.2268a_6 + 0.1178 \qquad \textit{Eq. 5.26}$$

$$s_5 = -1.9553a_1 - 2.1799a_2 + 2.343a_3 + 1.1715a_4 - 0.1588a_5 + 0.31903a_6 - 1.0704 \quad \textit{Eq. 5.27}$$

$$s_6 = 1.7496a_1 - 1.4642a_2 + 1.2566a_3 + 1.8341a_4 - 1.3926a_5 - 2.038a_6 + 3.4354 \quad \textit{Eq. 5.28}$$

$$s_7 = 1.4025a_1 + 0.5839a_2 - 0.8481a_3 + 1.8127a_4 - 1.5815a_5 + 3.143a_6 + 3.6542 \quad \textit{Eq. 5.29}$$

where $a_1, a_2, a_3 \ldots\ldots a_6$ are normalized values of input process parameters corresponding to slurry type, tool type, power rating, grit size and cryogenic treatment given to tool and workpiece respectively.

The best validation performance of the model was found at epoch 6 when Mean Square Error became 0.0027398 as shown in Figure 5.10. Based on the developed model, the predicted and actual values of MRR are compared on line graph as shown in Figure 5.11 for the 54 outcomes of MRR values and a highly close relation is evident from the coinciding line graphs.

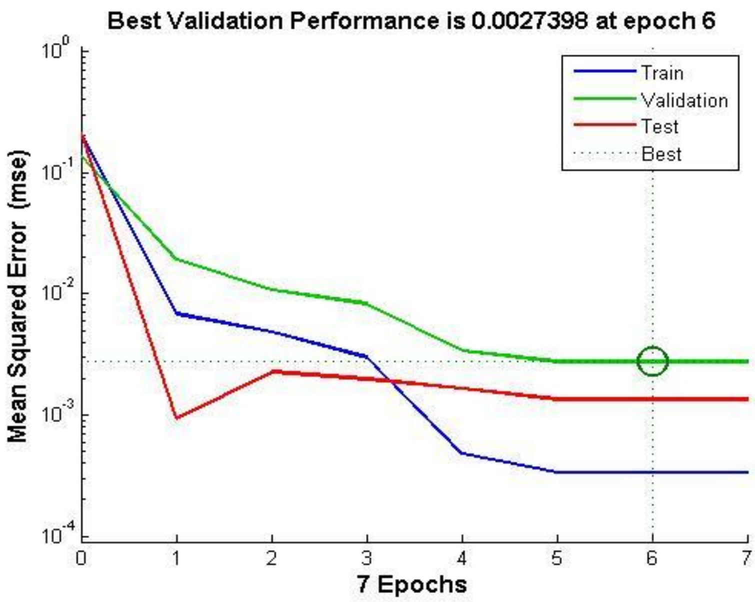

Figure 5.10 Best validation performance for TWR Model

The model validation is evident from the correlation coefficients of test and validation data which stand at 0.96181 and 0.95146, respectively, as shown in Figure 5.12 (a-b) while the overall coefficient of correlation for the model is 0.98051 as shown in Figure 5.12 (c). Experimental validation of the model was checked by comparing the average value of MRR of the eighteen experimental sets against the ANN predicted values as shown in Figure 5.13.

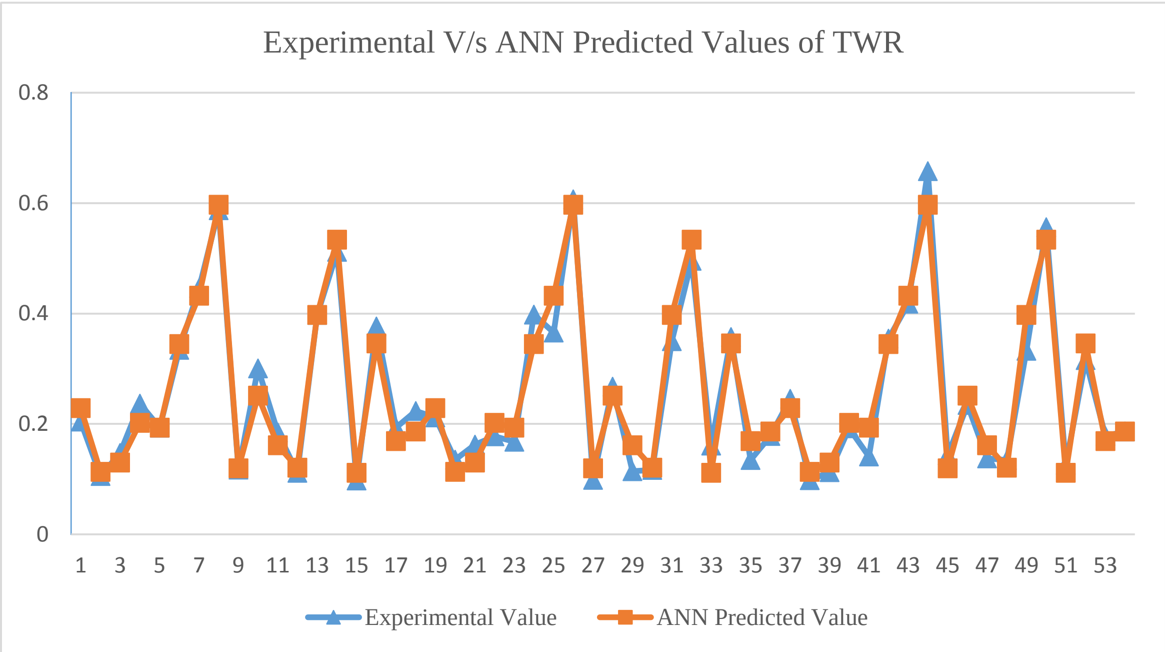

Figure 5.11 Experimental and Predicted Values of TWR

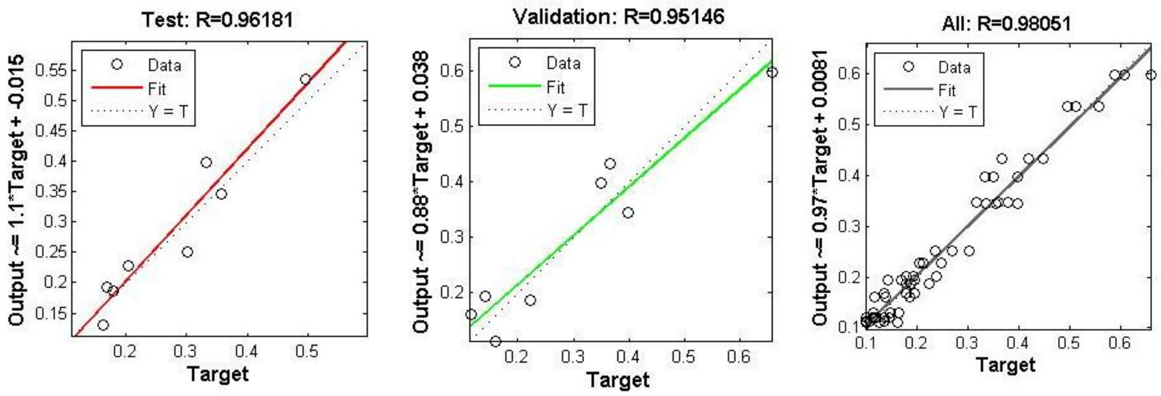

Figure 5.12 Correlation of a) Test Data b) Validation Data c) All Data for TWR

Corresponding values for percentage error and comparison of average SR and average value of ANN predicted SR are given in Table 5.3. The percentage error was calculated using Eq (5.12).

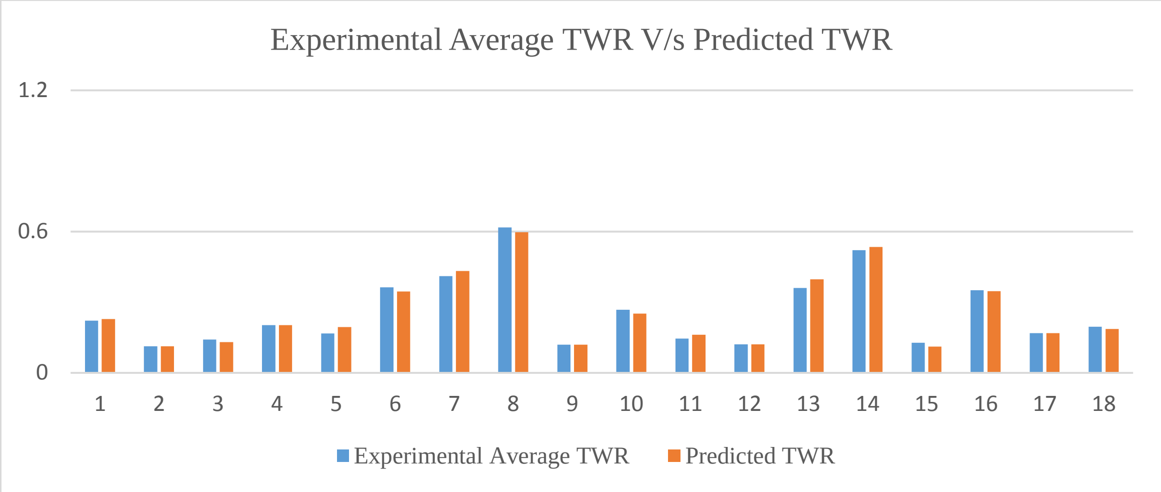

Figure 5.13 Comparison of experimental average and predicted TWR

Table 5.3 Comparison of experimental average TWR and predicted average TWR

Exp. No.	**1**	**2**	**3**	**4**	**5**	**6**	**7**	**8**	**9**	**10**	**11**	**12**	**13**	**14**	**15**	**16**	**17**	**18**
Avg. TWR (Expt.)	0.22	0.11	0.14	0.20	0.17	0.36	0.41	0.62	0.12	0.27	0.15	0.12	0.36	0.52	0.13	0.35	0.17	0.20
Avg. TWR (Predicted)	0.23	0.11	0.13	0.20	0.19	0.34	0.43	0.60	0.12	0.25	0.16	0.12	0.40	0.53	0.11	0.35	0.17	0.19
%age error	-3.66	0.00	7.72	0.00	-15.5	4.90	-5.42	3.29	0.00	6.17	-10.7	0.00	-10.4	-2.47	12.71	1.10	0.00	5.00

The maximum %age prediction error was found to be -15.5% corresponding to experiment no. 5, which indicates that the model is sufficiently accurate and hence can be used to predict the MRR effectively.

5.2.4 Modelling of HOS

Dimensional accuracy in ultrasonic machining of titanium in the present study was measured in terms of hole oversize from the diameter of the tool. It is evident from Table 4.26 that abrasive grit is the biggest contributing factor for establishing the hole oversize while tool type and USM power also had significant effect on the HOS. Remaining three factor did not have much effect in determining HOS. So it is proposed to create a model with only three input variables viz Abrasive grit size, tool type and USM power for predicting HOS. Use of one hidden layer has been found adequate in previous models and accordingly here also only one hidden layer is considered. 7 Neurons were fixed in hidden layer using trial and error method by exploring several combinations for minimum mean square error. Thus, a three layer 3-7-1 architecture, where the numbers refer to neurons in the input layer, hidden layer and output layer respectively, was selected for modelling in the present study as shown in Figure 5.14.

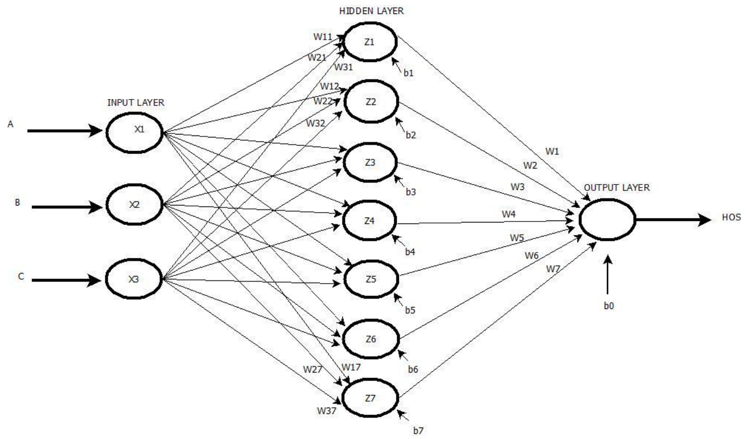

Figure 5.14 Neural Network 3-7-1 architecture used for modeling HOS

As shown, w_1, w_2, w_3….w_7 are the weights associated with connecting links between hidden layer and output layer. Bias is assigned to all the neurons of hidden and output layer. b_o is bias applied to output layer while b_1, b_2, b_3…b_7 are biases given to hidden layer neurons. Weights are also assigned to each of the 21 connecting links between input and hidden layer neurons. The activation function used for the hidden layer is *log-sigmoid* while *pure linear* function is used for output layer and the two functions are characterized by the Eq. (5.2) and (5.3) respectively.

Modeling is based on values of weights and bias given to the neurons in the two layers. The weights and bias are determined by training the network with input values of parameters and corresponding output values using neural network toolbox in MATLAB R2014a. Based on the ANOVA results for S/N rations, three critical-to-process parameters viz tool type, power rating and abrasive grit size were selected for modelling. Tool type being a categorical factor was initially assigned nominal value and Ti tool, SS tool and HCS tool were rated arbitrarily as 1, 2 and 3 respectively. With the operating range of process parameters being entirely different, it becomes important to scale or normalize the data. Normalization ensures effective training of the network and prevents any skewness in the results. Normalization in this case was done by mapping each term between -1 and +1 using Eq. (5.30).

$$N = \frac{(R - R_{min}) * (N_{max} - N_{min})}{(R_{max} - R_{min})} + N_{min} \qquad \textit{Eq. 5.30}$$

where R stands for real value of the parameter and N refers to normalized value and subscript *min* and *max* refer to minimum and maximum values, respectively, in the sequence. Accordingly N_{max} and N_{min} are equal to +1 and -1, respectively. Training was carried out using Levenberg Marquadt (LM) algorithm that corresponds to *trainlm* function in MATLAB and works on back propagation network. The weights and biases thus determined from ANN training have been used to create a model for hole oversize and is given below in Equation (5.31).

$$\begin{aligned} &\boldsymbol{Hole\ Oversize, HOS} \\ &= 0.99465h_1 + 0.10367h_2 + 0.25726h_3 + 0.37978h_4 \\ &- 1.2103h_5 - 0.88047h_6 + 0.31026h_7 + 0.23864 \end{aligned} \qquad \textit{Eq. 5.31}$$

where h_1, h_2.......h_7 are the outputs of hidden layer neurons and are determined by equation 1. Accordingly each of the z_i value is characterized by the following relations:

$$h_1 = \frac{1}{1+ e^{-u_1}} \qquad h_2 = \frac{1}{1+ e^{-u_2}} \qquad h_3 = \frac{1}{1+ e^{-u_3}} \qquad h_4 = \frac{1}{1+ e^{-u_4}}$$

$$h_5 = \frac{1}{1+ e^{-u_5}} \qquad h_6 = \frac{1}{1+ e^{-u_6}} \qquad h_7 = \frac{1}{1+ e^{-u_7}}$$

Where u_1, u_2, u_3 …. u_7 are net inputs to hidden layer neurons and their values are determined by Eqs. (5.32-5.38):

$$u_1 = 0.37233r_1 + 2.9328r_2 - 4.4093r_3 - 5.7949 \qquad \textit{Eq. 5.32}$$

$$u_2 = 0.82271r_1 - 4.4276r_2 - 2.5748r_3 - 3.1973 \qquad \textit{Eq. 5.33}$$

$$u_3 = 4.7033r_1 + 3.6465r_2 - 0.43196r_3 - 0.72824 \qquad \textit{Eq. 5.34}$$

$$u_4 = 4.9608r_1 + 0.81179r_2 + 1.9346r_3 + 1.8154 \qquad \textit{Eq. 5.35}$$

$$u_5 = -0.3978r_1 - 2.1962r_2 + 5.3282r_3 - 2.7877 \qquad \textit{Eq. 5.36}$$

$$u_6 = 2.3546r_1 + 5.1108r_2 + 0.07136r_3 + 3.4364 \qquad \textit{Eq. 5.37}$$

$$u_7 = 1.7421r_1 + 3.7108r_2 + 2.9409r_3 + 5.595 \qquad \textit{Eq. 5.38}$$

where r_1, r_2 and r_3 are normalized values of input process parameters corresponding to tool type, power rating, and grit size respectively.

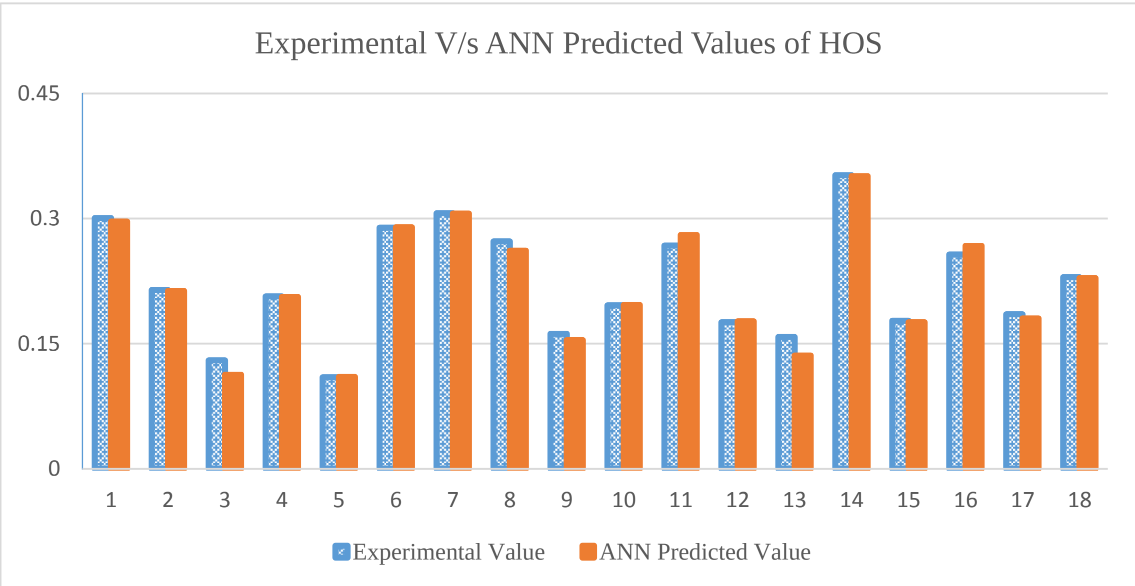

Figure 5.15 Comparison of Actual and ANN Predicted values of HOS

Based on the ANN modelling, the predicted and actual values of hole oversize are compared on bar graph as shown in Figure 5.15 for the 18 outcomes of average hole oversize values and a highly close relation is evident from the nearly identical bars.

The model validation is evident from the correlation coefficients of test and validation data which stand at 0.99773 and 0.99999, respectively, while the overall correlation coefficient of the model is 0.99399 as shown in Fig 5.16.

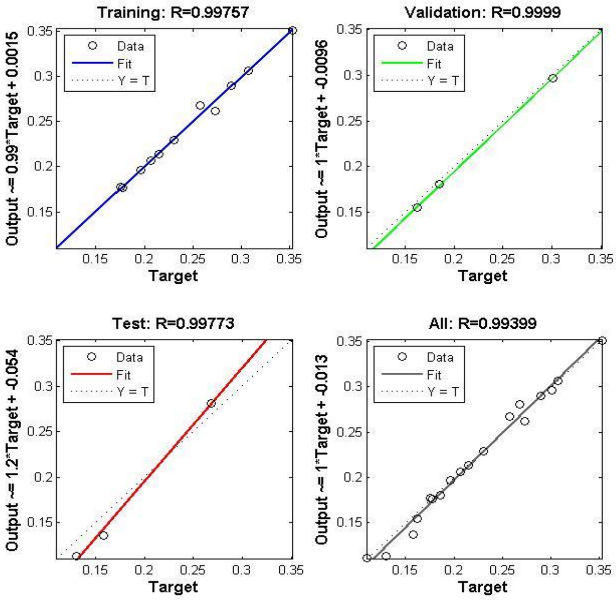

Figure 5.16 Correlation Coefficients for ANN Model of HOS

To check the model for experimental validation, the average value of HOS of eighteen experimental sets plotted against the ANN predicted values in Figure 5.15 were examined for the percentage error using Eq. 5.39 and the results have been tabulated in Table 5.4.

$$\%age\ prediction\ error = \frac{(Experimental\ Value - Predicted\ Value)}{Experimental\ value} * 100 \quad \textit{Eq. 5.39}$$

The error of prediction was found to lie between 0.15% to 13% and the mean percentage prediction error was found to be 2.9%.

Table 5.4 Comparison of experimental average HOS and predicted average HOS

Exp. No.	**1**	**2**	**3**	**4**	**5**	**6**	**7**	**8**	**9**	**10**	**11**	**12**	**13**	**14**	**15**	**16**	**17**	**18**
Avg. HOS (Expt.)	0.30	0.21	0.13	0.21	0.11	0.29	0.31	0.27	0.16	0.20	0.27	0.18	0.16	0.35	0.18	0.26	0.19	0.23
Avg. HOS (Predicted)	0.30	0.21	0.11	0.21	0.11	0.29	0.31	0.26	0.15	0.20	0.28	0.18	0.14	0.35	0.18	0.27	0.18	0.23
%age error	1.35	0.49	13.03	0.20	-0.55	-0.23	0.15	3.98	4.59	-0.33	-4.86	-0.81	13.94	0.33	0.87	-4.11	2.66	0.42

CHAPTER - 6

OPTIMIZATION OF RESPONSE VARIABLES

All the manufacturing processes operate on a particular principle and make use of certain material properties which lend them suitability for some application while at the same time putting limitations on their use. The processes are characterized by large number of process variables (parameters) making it crucial to have appropriate selection of the parameter setting for desired response output as each parameter may considerably affect the output.

Since, generally, a large number of process parameters are involved in any investigation, their random selection within the available range does not serve the purpose.

The situation becomes critical if more than one objectives (response variables) are involved in the process and even more so if the multiple objectives are conflicting in nature which means that increment in a parameter is favourable for one of the objectives and unfavourable for another one. It becomes imminent in such cases to look for an optimal setting for optimal outcome of involved response parameters. There are some methods available for optimization of parameters in such scenarios. One way of doing this is by converting multiple responses into a single objective function which could be minimized or maximized, as the need be. Here again there could be two different approaches. One approach is that of assigning equal preference or weightage to all the response parameters involved. Simple Grey relational analysis is one such method of doing the optimization. However many a times in one process certain parameter is more preferred over the other and selection here depends upon the desirability index of the different outcomes. For example in case of rough turning on a lathe machine the priority goal is that of increased production rates and surface finish is not of much importance. So the more weightage can be given to MRR for optimizing the process variables. However, same turning process if carried out for finishing operations, now require a good surface finish and the parameters need to be controlled accordingly. The optimization of parameters in such case will require more focus, and hence more weight, for surface finish as process and comparatively lesser weightage to MRR as response variable. However assigning of weights to a particular characteristic is not such a simple decision making criterion at all the time. For example in regular production scenario one has to make overall economic decision by minimizing tool wear rate for reducing production cost, minimize surface finish and dimensional inaccuracy to avoid rejections and at the same time have acceptable production rates to meet the consumer demand. The criterion of different objectives here has to be weighted after critical examination. Several techniques of assigning weights to variables have been reported by the researchers. In Grey Relational Analysis, use of measurement of entropy within the data sets has been made for deciding the weights [148,170]. In Analytical hierarchical process the judgment of experts may be used for fixing the priorities. Several studies have been reported with the use of multi response signal to noise ratio for converting multiple responses into weighted single response for multi objective optimization. Use of soft computing techniques such as genetic algorithms, artificial bee colony method, ant colony optimization, particle swarm optimization etc. has gained lot of momentum in past decade in use for optimization of responses in manufacturing processes. Two approached for optimization have been demonstrated in this thesis in the ensuing sections. Firstly the two responses MRR and TWR have been optimized using Entropy Based Grey Relational Analysis. The process is hybridized here with Taguchi's Design of Experiments by incorporation of S/N ratios for determining the grey relational grades. Subsequently, in the second approach, all the four responses viz MRR, TWR, SR and HOS have been together optimized using Analytical Hierarchical Process.

6.1 ENTROPY BASED GREY RELATIONAL ANALYSIS TO OPTIMIZE MRR AND TWR

6.1.1 Calculation of Entropy based Grey Relational Grade

In any machining operation it is very important to determine the optimal parameter setting for the desired machining output especially when the responses are of conflicting nature as in case of USM. It can be observed from the Main Effects Plots shown in Figures 4.6-4.9 and Figures 4.20-4.23 that the conditions favourable for higher MRR also lead to an increased TWR. Accordingly becomes pertinent to determine the optimal machine settings for a befitting solution for acceptable values of MRR and TWR. Grey Relational Analysis has been used by many researchers to determine the optimal solution of machining parameters. Here an entropy weight based GRA has been used to simultaneously optimize the conflicting machining responses. Sivasankar and Jeyapaul [170] have made use of entropy method for assigning weights to five response characteristics for optimization using grey relational analysis in electric discharge machining of hot pressed ZrB_2. Pre-processing of data was followed by generation grey relational coefficients. Weights were assigned to five response characteristics using entropy measurement method that determines the variability within data sequence to establish weight of a characteristic and subsequently grey relational grades were calculated for optimization. Jangra et al. [148] used Grey relational analysis together with Taguchi method and entropy measurement for optimizing the four machining characteristics viz MRR, SR, angular error and radial overcut in WEDM of WC-5.3% Co composite. Normalized S/N values were processed for generating grey relational coefficient. Grey relational grades were then calculated using entropy measurement method for assigning weight to all the machining characteristics and subsequently optimal setting was determined for all the four response characteristics together. The detailed procedure for the application of weight based GRA is shown in the Flow Chart in Figure 6.1.

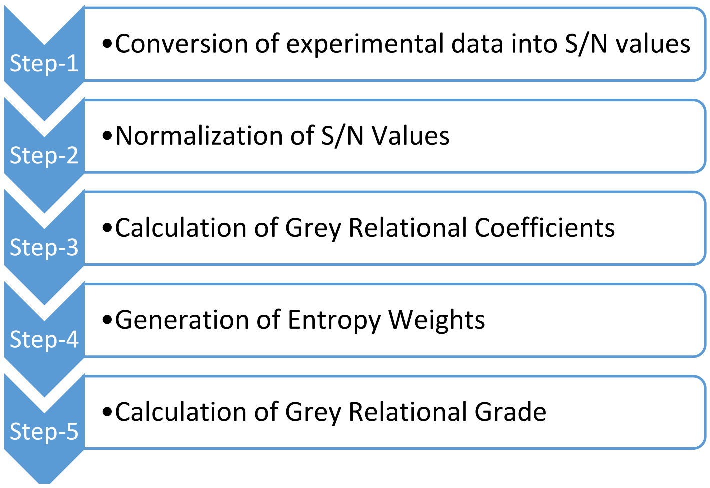

Figure 6.1 Steps in Entropy Weight based GRA

The calculated data for S/N ratios of MRR and TWR has been presented in 2nd and 3rd columns, respectively, of Table 6.1. Due to absence of comparability in the sequences of S/N ratios of MRR and TWR, normalization is carried out to convert the original sequence into measureable space. Since a higher value of S/N ratio is always a desirable feature, therefore normalization is accomplished using following equation (Eq. 6.1) recommended for higher the better problem:

$$x_i^*(k) = \frac{x_i^o(k) - \min x_i^o(k)}{\max x_i^o(k) - \min x_i^o(k)} \qquad \text{Eq. 6.1}$$

where $x_i^*(k)$ is the sequence generated as result of data pre-processing, $x_i^o(k)$ is the original sequence of S/N ratio and i and k denote no. of observations in each sequence and no. of sequences, respectively. Max $x_i^o(k)$ and min $x_i^o(k)$ are the maximum and minimum values of kth sequence.

Subsequently Grey Relational coefficients are calculated to determine the correlation among the optimal and actual normalized observation values using equation 6.2:

$$\gamma_{0,i}(k) = \frac{\Delta_{min} + \zeta.\ \Delta_{max}}{\Delta_{0,i}(k) + \zeta.\ \Delta_{max}} \qquad \textit{Eq. 6.2}$$

where $0 \leq \gamma_{0,i}(k) \leq 1$ is the Grey Relational coefficient for *i*th observation and *k*th sequence; $\Delta_{0,i}(k)$ is the deviation sequence given by absolute difference between reference sequence $x_i^*(k)$and comparability sequence $x_i^o(k)$; Δ_{min} is equal to min (min $\Delta_{0,i}(k)$) and Δ_{max} is equal to max(max $\Delta_{0,i}(k)$); ζ is distinguishing coefficient that displays relational degree between reference and comparability sequence and is such that $\zeta \in [0,1]$. $\zeta$is taken as 0.5 in the present study.

The average value of Grey Relational Coefficients is used to generate Grey Relational Grade. However this method results in giving equal importance to each response characteristic. In real life practical situations this is not very often. At times some of the response characteristics are more important than other. To address this issue, the concept of entropy measurement and subsequent weight generation for each response variable is accomplished based on relative importance and then grey relational grade is calculated by assigning the relative weight of each response variable to its Grey Relational coefficient [170]. The weight calculation is accomplished by entropy method. In information theory, and in thermodynamics, entropy is largely a measure of disorganization and randomness of the system. While applying the same concept of entropy for measurement of weights in the Grey Relational Analysis, a response attribute with higher entropy means the one having more diversity in responses and hence has more significant influence. Accordingly a higher weight will be assigned to such response variable. The mapping function used for entropy is $f_i : [0, 1] \longrightarrow [0,1]$ such that $f_i(0) = 0$, $f_i(x) = f_i(1-x)$ and the function $f_i(x)$ is monotonic increasing in $x \in (0, 0.5)$ [178]. Accordingly, equation 6.3 is used for entropy measure as a mapping function:

$$w_e\ (x) = xe^{1-x} + (1-x)e^{x} - 1 \qquad \text{Eq. 6.3}$$

$w_e(x)$ attains a maximum value of 0.6487 at x= 0.5.

Table 6.1 Calculation of Grey Relational Grade for MRR and TWR

Exp. No.	**SNRA1 MRR**	**SNRA2 TWR**	**Pre-processing MRR**	**Pre-processing TWR**	**GRC - MRR**	**GRC – TWR**	**GRG with entropy**	**Ranking based on GRG**
Reference Sequence $x_i^*(k)$			1.0000	1.0000				
1	-19.7564	13.0985	0.0000	0.6081	0.3333	0.5606	0.4470	18
2	-17.0401	18.8460	0.1851	1.0000	0.3803	1.0000	0.6902	1
3	-17.8278	16.9406	0.1314	0.8701	0.3653	0.7937	0.5796	8
4	-15.5786	13.8264	0.2847	0.6577	0.4114	0.5936	0.5025	15
5	-14.8340	15.4517	0.3354	0.7685	0.4293	0.6836	0.5565	9
6	-10.2047	8.7955	0.6509	0.3147	0.5888	0.4218	0.5053	14
7	-8.9216	7.7181	0.7383	0.2412	0.6564	0.3972	0.5268	13
8	-5.0811	4.1809	1.0000	0.0000	1.0000	0.3333	0.6666	2
9	-18.2140	18.3383	0.1051	0.9654	0.3584	0.9352	0.6469	4
10	-13.2572	11.4097	0.4429	0.4929	0.4730	0.4965	0.4847	17
11	-15.7764	16.5696	0.2712	0.8448	0.4069	0.7631	0.5850	7
12	-16.9026	18.3316	0.1945	0.9649	0.3830	0.9344	0.6588	3
13	-10.6876	8.8511	0.6180	0.3185	0.5669	0.4232	0.4950	16
14	-5.6746	5.6493	0.9596	0.1001	0.9252	0.3572	0.6411	5
15	-19.1308	17.6860	0.0426	0.9209	0.3431	0.8634	0.6033	6
16	-9.0794	9.0970	0.7276	0.3352	0.6473	0.4293	0.5383	12
17	-15.8799	15.3692	0.2641	0.7629	0.4046	0.6784	0.5415	11
18	-12.5838	14.1203	0.4888	0.6778	0.4944	0.6081	0.5513	10

Further, to ensure the value of entropy to rest between 0 to1, the modified function for entropy measurement was defined by Wen and Chang [171] , given as in equation 6.4:

$$W = \frac{1}{e^{0.5} - 1} \sum_{i=1}^{m} w_e(x) \quad \textit{Eq. 6.4}$$

The next step is calculation of weights for each of the response quality characteristic.

Sum of Grey relational coefficients corresponding to each sequence of response variables is given by equation 6.5:

$$D_k = n \sum_{i=1}^{m} y_i(k) \, , k = 1,2,3, \ldots . n \quad \textit{Eq. 6.5}$$

The normalized coefficient is then calculated as:

$$K = \frac{1}{(e^{0.5} - 1) \times m} = \frac{1}{(0.6487 \times m)} \quad \textit{Eq. 6.6}$$

Entropy of each response quality characteristic is given by

$$e_k = s \sum\nolimits_{i=1}^{m} w_e \left(\frac{\gamma i \ (k)}{\mathrm{Dk}} \right) \quad \textit{Eq. 6.7}$$

and the sum total entropy thus becomes

$$E = \sum_{k=1}^{n} e_k \quad \textit{Eq. 6.8}$$

Weight of each response variable is then calculated as follows:

$$w_k = \frac{\frac{1}{n - E} \ (1 - e_k)}{\sum_{k=1}^{n} \frac{1}{n - E} \ (1 - e_k)} \quad \textit{Eq. 6.9}$$

Grey Relational Grade is then calculated by summation of resultant obtained by multiplication of grey relation coefficient with the corresponding weight of each response characteristic and is given by:

$$\Gamma_{0,i} = \sum_{k=1}^{n} w_k \, \gamma_{0,i}(k) \, , i = 1,2,3 \ldots m \, ; k = 1,2,3, \ldots n \quad \textit{Eq. 6.10}$$

In the current study *m* is equal to 18 as the no. of observations for each sequence and *n* is 2 as the number of sequences. From the above equations the calculated value of entropies for MRR and TWR are 0.21399 and 0.21363 respectively and the relative weights for MRR and TWR are 0.4998 and 0.5001 respectively. Using these weights the value of grey relational grade is calculated and is presented in Table 6.1. It is evident from the data presented in Table 6.1 that the highest value of grey relational grade corresponds to Experiment 2. And therefore, from the point of view of optimizing both MRR and TWR, this experimental setting shall give the most optimum result. The average value of MRR and TWR found experimentally at the most optimum setting as suggested by GRG was 0.142mm^3/min and 0.113mm^3/min, respectively.

6.2 USE OF ANALYTICAL HIERARCHICAL PROCESS FOR OPTIMIZATION

A decision involve measurement of tangibles as well as intangibles, which though have to be measured, for evaluation of extent of purpose served for the decision maker. This requires allocation of different priorities to involved variables. Analytic Hierarchy Process (AHP) is an established theory of measurement developed by Prof. Thomas L. Satty in the 1970s. The process is based on pairwise comparisons of entities involved for measurement. The comparisons for deriving priority scales, which actually are a measure of degree of intangibility, are based on the judgment of experts. Use of absolute scale of judgment is made for drawing out the comparisons that represent dominating preference of one attribute over the other. Making of a good decision requires complete knowledge of the problem including various criterion of decision making, purpose of decision and available alternatives. Effort is then made to find the best alternative among the available alternative decisions. Similarly while dealing with resource allocation, it is required to establish priorities for the alternatives so as to allocate appropriate share of resources [172]. Evaluation of an entity, be it an object or a process, can be made either by studying it in absolute terms and drawing conclusions from the observations or other way around by studying it in relative terms by making comparisons with behavior of other entities of similar nature [172]. This is the fundamental aspect of the AHP which relies on pairwise comparisons among the different entities involved in decision making. To generate priorities for making an organized decision, the decision needs to be decomposed into the steps. AHP is a powerful tool for decision making and is used for many optimization problems related to manufacturing engineering. Bhattacharya et al. [173]used AHP to optimize MRR, TWR and SR during powder mixed electric discharge machining of three different work materials. The hierarchical tree was constructed with the goal to select parameter setting corresponding to each work material subject to criterion of optimizing MRR, TWR and SR by using different alternatives which were obtained by pairwise comparison of performance characteristics for each work material corresponding to different parametric setting. Pairwise comparison matrix for the three criterion was formulated based on the judgment of the experimenter while pairwise comparison matrices for alternatives were constructed on the basis of actual results obtained, thus bringing more objectivity to the problem. The process is capable for application to qualitative as well as quantitative attributes of measurement. The formulation of problem into a hierarchical structure facilitates deep insight into the problem. Several criterion and sub criterion can be accommodated simultaneously into the process. Any given decision making problem is decomposed into hierarchical criterion alongwith possible alternatives. Pairwise comparisons are made to establish relative importance of one criteria over the another and subsequently arranged in a hierarchical tree. Relative ranking of the available alternatives is then made by using expert judgment by deriving weights and establishing priorities. The process is summarized in the steps as mentioned here-under: [172-173].

1. Define the objective or goal of the problem
2. Identify the factors and criterion that directly or indirectly affect the decision making process
3. Construction of hierarchy structure with the objective being at the top level
4. Criterion and the sub-criterion that influence the decision making are placed in the next levels of the hierarchy in appropriate order
5. Lowest level comprises of available alternatives.
6. Construction of pairwise comparison matrix which is accomplished by comparing an element with the elements of next higher levels to find out the local priority weights.

A pairwise comparison matrix, [M], can be constructed as shown in equation 6.11:

$$[\mathrm{M}] = \begin{bmatrix} a_{11} & a_{12} & a_{13} & . & . & a_{1n} \\ a_{21} & a_{22} & a_{23} & . & . & a_{2n} \\ . & . & . & . & . & . \\ . & . & . & . & . & . \\ . & . & . & . & . & . \\ a_{n1} & a_{n2} & . & . & . & a_{nn} \end{bmatrix} \qquad \textit{Eq. 6.11}$$

where the values a_{ij} (for i, j = 1, 2, 3,…n) is the magnitude of preference of a_i over a_j corresponding to criterion ($a_{ij} = a_i/a_j$), $a_{ji} = 1/a_{ij}$ and a_{ii} = 1 for all values of i and j.

Table 6.2 Fundamental pairwise comparison scale [179]

Rating	Preferential Judgment
9	Extremely preferred; The support in favour of one over another is of the highest possible magnitude.
8	Between Very strong to extreme preference
7	Very strongly preferred; A decision favoured very strongly over another and dominance demonstrated in judgment.
6	Between strong tadmino very strong preference
5	Strongly preferred; Experience strongly favour one over another
4	Between moderate to strong preference
3	Moderately preferred; one activity slightly favoured over another
2	Between equally important to moderate preference
1	Equally preferred; Not a difference. Two activities equally important to the objective.

Satty's fundamental scale of absolute numbers for pairwise comparison (Table 6.2) is used to establish magnitude of preference, i.e. values of a_i and a_j in the matrix A. for example if a_1 has moderate preference over a_2, then a_{12} will become 3/1 = 3 and if a_2 is very strongly preferred over a_3, then a_{23} will be 7/1 = 7. Since $a_{ji} = 1/a_{ij}$, therefore, a_{21} and a_{31} will accordingly take the value of 1/3 and 1/7 respectively.

Once all the priorities are established and thus the pairwise matrix is complete, it is now important to check the matrix for consistency. The pairwise comparison matrix qualifies for being consistent if a_{ij} x a_{jk} = a_{ik} for all values of *i, j, k*. Therefore for consistent matrices $a_{ij} = a_i/a_j$ for all values of *i* and *j*. For example $a_{14} = a_1/a_4 = a_1/a_3$ x $a_3/a_4 = a_{13}$ x a_{34}.

If we consider the example just cited above, strength of preference of a_1 over a_2 was 3/1 and a_2 over a_3 was 7/1, which means priority of a_1 over a_3 should be 21/1 = 21 which is not possible since the pairwise comparison scale being used here has highest value of 9 only. Therefore in this example, $a_{13} \neq a_{12}$ x a_{23} and hence the comparison is not consistent.

Infact the matrix [M] is seldom consistent in most of the situations. Priority weight in such situations is then calculated by solving the eigen value equation (Eq. 6.12) given here-under:

$$Mw = \lambda w \Rightarrow (M - \lambda \mathrm{I})w = 0 \qquad \textit{Eq. 6.12}$$

where $w = (w_1, w_2, w_3 \ldots . w_n)^{\mathrm{T}}$

Equation 6.12 exhibits a non-zero solution when λ is the eigen value of A such that there is at least one non-zero eigen value alongwith maximum eigen value $\lambda_{max} \geq n$ where n is order of the matrix [M].

Consistency index for the pairwise matrix is then calculated as:

$$\text{Consistency Index, } CI = \frac{\lambda_{max} - n}{n - 1} \qquad \textit{Eq. 6.13}$$

Degree of inconsistency for an inconsistent matrix is determined by the value of consistency ratio (CR) which is ratio of CI and random index (RI) such that

$$CR = CI/RI \qquad \textit{Eq. 6.14}$$

Random index value corresponding to given order of matrix n can be determined from Table 6.3. For the assigned priority weights in the matrix to be acceptable CR$\leq$ 0.1 that is CR has to be less than or equal to 10%.

Table 6.3 Random Order (RI) corresponding to matrix order (n)

n	2	3	4	5	6	7	8	9	10
RI	0	0.56	0.9	1.12	1.25	1.34	1.42	1.45	1.51

Normalized eigen vector for maximum eigen value (λ_{max}) is then selected for priority weight (local weight) of the alternatives in the pair wise comparison matrix. The priority weights are thus obtained by raising the matrix to large powers and adding the elements of each row and subsequently dividing the sum obtained by the sum total of all the rows (normalization) [172]. Finally global weights are established by multiplying priority weights of every alternative for different criteria with the criteria weight which is actually the pairwise comparison matrix of the criteria. The optimum decision corresponds to maximum value of global weight.

6.2.1 Application of AHP to the current problem

The study presented here involved measurement of four response variables viz MRR, TWR, SR and HOS. The responses need to be optimized to determine the best setting that will give optimum performance from collective point of view of the four response variables. AHP was applied sequentially as per the procedures and steps mentioned in the preceding section. The average value of the four response variables as measured from the experimentation carried out using Taguchi's L18 OA are shown in Table 6.4

Table 6.4 Average response values obtained in the experimentation performed

Expt. No.	**Avg. SR**	**Avg. MRR**	**Avg. TWR**	**Avg. HOS**
1	1.22	0.1070	0.2206	0.3007
2	1.06	0.1423	0.1131	0.2144
3	0.55	0.1305	0.1407	0.1300
4	0.92	0.1678	0.2020	0.2066
5	0.85	0.1821	0.1675	0.1096
6	1.41	0.3134	0.3623	0.2891
7	1.51	0.3593	0.4099	0.3065
8	1.25	0.5589	0.6172	0.2726

9	0.50	0.1251	0.1197	0.1620
10	0.98	0.2189	0.2675	0.1959
11	1.11	0.1636	0.1455	0.2677
12	1.02	0.1457	0.1208	0.1756
13	0.81	0.2936	0.3599	0.1581
14	1.61	0.5224	0.5212	0.3521
15	0.73	0.1139	0.1280	0.1775
16	1.30	0.3545	0.3499	0.2571
17	0.66	0.1628	0.1686	0.1853
18	1.09	0.2370	0.1958	0.2299

The first step required here was to develop pairwise comparison matrix for the four response criterion involved in the study as per the relative preference of one over another using the Satty' comparison scale shown in Table 6.2. Now to establish the pairwise comparison matrix, the subjective judgment of priority of one variable over another has to be established. The machining of titanium has been a prime concern owing to the specific properties of the material as has already been discussed in section 1.3. Therefore MRR is the foremost thing of prime importance. Cost of machining directly depends, among other things, upon the rate of tool wear. So that can also not be neglected. However MRR definitely has moderate preference over TWR and accordingly the rating of 2 has been selected as preference of MRR over TWR. Similarly, MRR has been decided to be slightly strongly preferred over surface roughness and accordingly the index of preference has been selected as 4. Working on the similar lines, judgment has been used to decide preference of one variable over another and the complete priority matrix has been prepared as shown in Table 6.5. Criteria weight has been calculated as per the laid procedures specified in section 6.2 after checking the consistency of matrix which in this case was well below the upper limit of 0.1.

Table 6.5 Pairwise comparison matrix for the four criterion

	MRR	**TWR**	**SR**	**HOS**	**Criteria Weight**
MRR	1	2	4	6	**0.4948**
TWR	1/2	1	3	5	**0.3102**
SR	1/4	1/3	1	3	**0.1336**
HOS	1/6	1/5	1/3	1	**0.0614**

λ_{max} = 4.0792 CI = 0.0264 CR = 0.0293

Now the experimental plan had 18 experiments and orthogonality meant that corresponding to every level under each factor the number of trials/experiments would be same. For example if we consider the too material, there were three tool materials involved and corresponding to each tool material there were six experiments. Similarly there were six types of slurries and corresponding to each type of slurry there were 3 experiments within the DOE space. Once the criterion (response variable in this case) and their criterion weights have been determined, next is to identify the alternatives and their priority weights. Here since the problem has specifically been designed to understand the effect of cryogenic treatment, therefore we have selected cryogenic treatment given to the tool as the base over here and accordingly the goal has become selection of optimium paramters for each type of cryogenic treated tool. Thus three different settings will be obtained, one each for Untreated, Shallow Cryogenic Treated and Deep Cryogenic Treated tool material for optimizing the process parameters. The experimental space had six trials corresponding to each of the treatment condition given to the tool material. Therefore for each type of treatment given to tool material there are six alternatives available, that have been labeled as G1 to G6, in the given experimental design that will take us to three optimal solutions, one for each type of the treatment. The grouping of the 18 experimental trials for the purpose is shown in Table 6.6. The hierarchical structure for the present case designed here is thus shown in Figure 6.2 as suggested by Bhattacharya et al. [173].

Table 6.6 Grouping of experimental trials corresponding to type of cryogenic treatment given to tool material.

Type of CT to Tool	Exp. No.	Alternative code	Slurry Type	Tool Material	Power Rating (%age)	Grit Size	Type of CT to workpiece
UT	1	G1	Al_2O_3	HCS	20	220	UT
	6	G2	SiC	Ti	80	220	SCT
	8	G3	B_4C	SS	80	400	DCT
	12	G4	Al_2O_3+ SiC	Ti	50	400	UT
	13	G5	SiC + B_4C	HCS	50	500	DCT
	17	G6	Al_2O_3+ B_4C	SS	20	500	SCT
SCT	2	G1	Al_2O_3	SS	50	400	SCT
	4	G2	SiC	HCS	20	400	DCT
	9	G3	B_4C	Ti	20	500	UT
	10	G4	Al_2O_3+ SiC	HCS	80	500	SCT
	14	G5	SiC + B_4C	SS	80	220	UT
	18	G6	Al_2O_3+ B_4C	Ti	50	220	DCT
DCT	3	G1	Al_2O_3	Ti	80	500	DCT
	5	G2	SiC	SS	50	500	UT
	7	G3	B_4C	HCS	50	220	SCT
	11	G4	Al_2O_3+ SiC	SS	20	220	DCT
	15	G5	SiC + B_4C	Ti	20	400	SCT
	16	G6	Al_2O_3+ B_4C	HCS	80	400	UT

This way, selecting the alternatives from within the experimental design ensures the involvement of all the control parameters for finding the optimum solution. Another aspect here is that instead of using subjective judgment for pairwise ranking for comparisons within the alternatives, results obtained through actual experimentation for each of the response variable were used to formulate the pairwise comparison matrices, thus providing an objective evaluation of the alternatives and minimizing the subjectivity at this level of the hierarchy.

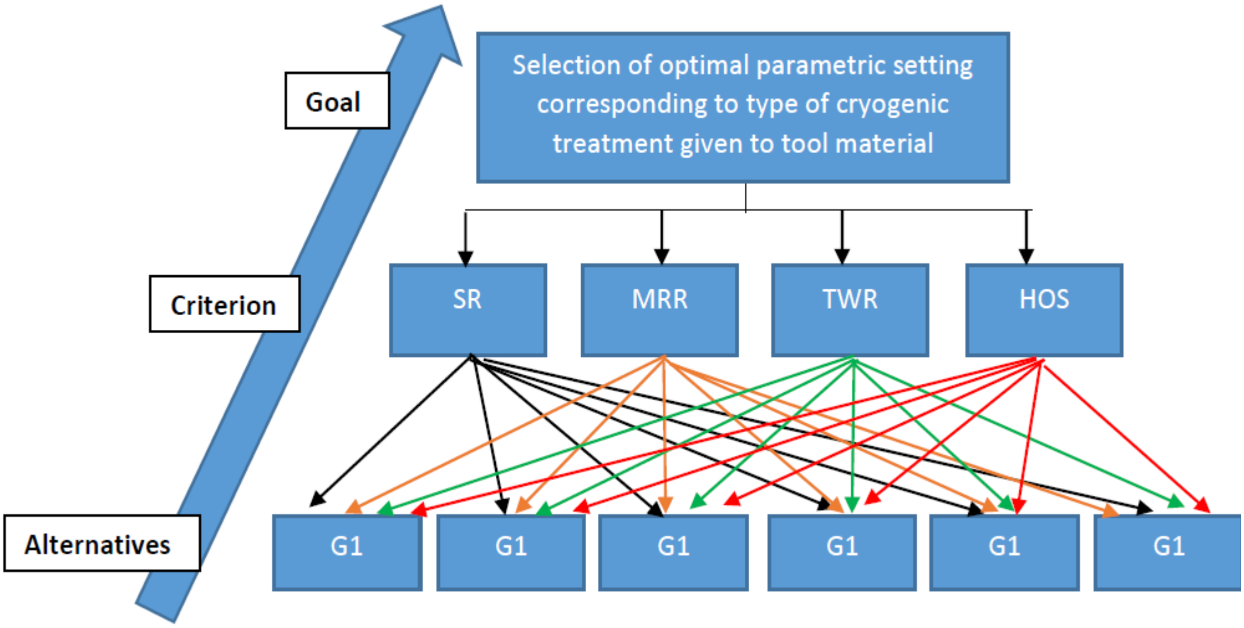

Figure 6.2 Hierarchy structure of the study

Accordingly a pairwise comparison matrix corresponding to each of the four response variables viz MRR, TWR, SR and HOS was constructed for each of the three levels of type of treatment given to tool materials viz UT, SCT and DCT. Thus there are 12 such comparison matrices which were formulated by comparing the results of experiment. For example corresponding to Untreated Tool and measurement of MRR from the table 6.6, there are six experiments corresponding to untreated tool in the experimental array. The priority of MRR for first over second is obtained by dividing the actual value obtained in the first experiment to that obtained in the second and then rounding off to nearest fraction from the data values provided in table 6.4. The procedure was repeated for all the six experiments and each result of the experiment was compared against every other result, thus leading to 15 such comparisons. The results were compiled in a matrix form and 6 x6 matrix have the comparisons listed along the rows and columns. The diagonal of the matrix comprises of all '1s' indicating the comparison of an alternative with itself. Thus, 3 matrices each were constructed for each of the four response variables. A MATLAB program was written to obtain the 12 comparison matrices.

Subsequently priority weights need to be calculated. This can be done by calculating the the normalized eigen vector for maximum eigen value (λ_{max}). Steps involved in computation of the required eigen vector are as follows:

1. Square the pairwise comparison matrix of alternatives.
2. Summation of all the elements within the row of the squared matrix.
3. Sum of the elements of the resultant column generated for normalization.
4. Normalize the elements generated in step 2 above.
5. Repeat the process from step one onwards, his time starting with the square matrix obtained at the first step, till the normalized elements stop showing any further change (In this case evaluation has been done upto four decimal places to establish the maximum eigen value and hence the required priority weights)
6. Check the consistency of the matrix by determining value of CR as per the procedure laid in preceding section.

   Following these steps, the pairwise comparison matrices with priority weight and CR values have been formulated are shown here from Table 6.7 to 6.18.

Table 6.7 Pairwise comparison matrix for alternatives on SR using Untreated Tool Material

	G1	**G2**	**G3**	**G4**	**G5**	**G6**	**Priority Weight**
G1	1	1	1	1	2	2	0.1994
G2	1	1	1	**2**	2	2	0.2261
G3	1	1	1	1	2	2	0.1994
G4	1	1/2	1	1	1	2	0.1622
G5	1/2	1/2	1/2	1	1	1	0.1131
G6	1/2	1/2	1//2	1/2	1	1	0.0997
λ_{max} = 6.0811			CI = 0.0162		CR = 0.013		

Table 6.8 Pairwise comparison matrix for alternatives on MRR with Untreated Tool

	G1	G2	G3	G4	G5	G6	Priority Weight
G1	1	1/3	1/5	1	1/3	1/2	0.0677
G2	3	1	1/2	2	1	2	0.1912
G3	5	2	1	4	2	3	0.3537
G4	1	1/2	1/4	1	1/2	1	0.0900
G5	3	1	1/2	2	1	2	0.1912
G6	2	1/2	1/3	1	1/2	1	0.1061
λ_{max} = 6.038			CI = 0.0077		CR = 0.0061		

Table 6.9 Pairwise comparison matrix for alternatives on TWR with Untreated Tool

	G1	G2	G3	G4	G5	G6	Priority Weight
G1	1	1/2	1/3	1/2	1/2	1	0.1061
G2	2	1	1/2	3	1	2	0.1912
G3	3	2	1	5	2	4	0.3537
G4	1/2	1/3	1/5	1	1/3	1	0.0677
G5	2	1	1/2	1	1	2	0.1912
G6	1	1/2	1/4	1	1/2	1	0.0900
λ_{max} = 6.0384			CI = 0.0077		CR = 0.00613		

Table 6.10 Pairwise comparison matrix for alternatives on HOS with Untreated Tool

	G1	G2	G3	G4	G5	G6	Priority Weight
G1	1	1	1	2	2	2	0.2222
G2	1	1	1	2	2	2	0.2222
G3	1	1	1	2	2	2	0.2222
G4	1/2	1/2	1/2	1	1	1	0.1111
G5	1/2	1/2	1/2	1	1	1	0.1111
G6	1/2	1/2	1/2	1	1	1	0.1111
λ_{max} = 6			CI = 0		CR = 0		

Table 6.11 Pairwise comparison matrix for alternatives on SR using SCT Tool Material

	G1	G2	G3	G4	G5	G6	Priority Weight
G1	1	1	2	1	1/2	1	0.1553
G2	1	1	2	1	1/2	1	0.1553
G3	1/2	1/2	1	1/2	1/3	1/2	0.0817
G4	1	1	2	1	1/2	1	0.1553
G5	2	2	3	2	1	2	0.2972
G6	1	1	2	1	1/2	1	0.1553
λ_{max} = 6.008			CI = 0.0016		CR = 0.0012		

Table 6.12 Pairwise comparison matrix for alternatives on MRR using SCT Tool Material

	G1	G2	G3	G4	G5	G6	Priority Weight
G1	1	1	1	1/2	1/4	1/2	0.0936
G2	1	1	1	1	1/3	1	0.1259
G3	1	1	1	1/2	1/4	1/2	0.0936
G4	2	1	2	1	1/2	1	0.1665
G5	4	3	4	2	1	2	0.3538
G6	2	1	2	1	1/2	1	0.1665
λ_{max} = 6.068			CI = 0.014		CR = 0.011		

Table 6.13 Pairwise comparison matrix for alternatives on TWR using SCT Tool Material

	G1	G2	G3	G4	G5	G6	Priority Weight
G1	1	1/2	1	1/2	1/5	1/2	0.0770
G2	2	1	2	1	1/3	1	0.1497
G3	1	1/2	1	1/2	1/4	1/2	0.0802
G4	2	1	2	1	1/2	1	0.1603
G5	5	3	4	2	1	3	0.3831
G6	2	1	2	1	1/3	1	0.1497
λ_{max} = 6.023			CI = 0.0046		CR = 0.0037		

Table 6.14 Pairwise comparison matrix for alternatives on HOS using SCT Tool Material

	G1	**G2**	**G3**	**G4**	**G5**	**G6**	**Priority Weight**
G1	1	1	2	1	1/2	1	0.0770
G2	1	1	1	1	1/2	1	0.1497
G3	1/2	1	1	1	1/2	1	0.0802
G4	1	1	1	1	1/2	1	0.1603
G5	2	2	2	2	1	2	0.3831
G6	1	1	1	1	1/2	1	0.1497
λ_{max} = 6.054			CI = 0.011		CR = 0.008		

Table 6.15 Pairwise comparison matrix for alternatives on SR using DCT Tool Material

	G1	**G2**	**G3**	**G4**	**G5**	**G6**	**Priority Weight**
G1	1	1/2	1/3	1/2	1	1/2	0.0924
G2	2	1	1/2	1	1	1/2	0.1420
G3	3	2	1	1	2	1	0.2363
G4	2	1	1	1	2	1	0.1977
G5	1	1	0	1/2	1	1/2	0.1105
G6	2	2	1	1	2	1	0.2211
λ_{max} = 6.083			CI = 0.0167		CR = 0.0134		

Table 6.16 Pairwise comparison matrix for alternatives on MRR using DCT Tool Material

	G1	**G2**	**G3**	**G4**	**G5**	**G6**	**Priority Weight**
G1	1	1	1/3	1	1	1/3	0.1050
G2	1	1	1/2	1	2	1/2	0.1355
G3	3	2	1	2	3	1	0.2728
G4	1	1	1/2	1	1	1/2	0.1200
G5	1	1/2	1/3	1	1	1/3	0.0938
G6	3	2	1	2	3	1	0.2728
λ_{max} = 6.059			CI = 0.0118		CR = 0.0095		

Table 6.17 Pairwise comparison matrix for alternatives on TWR using DCT Tool Material

	G1	G2	G3	G4	G5	G6	Priority Weight
G1	1	1	1/3	1	1	1/2	0.1118
G2	1	1	1/2	1	1	1/2	0.1200
G3	3	2	1	3	3	1	0.2943
G4	1	1	1/3	1	1	1/2	0.1118
G5	1	1	1/3	1	1	1/3	0.1047
G6	2	2	1	2	3	1	0.2573
λ_{max} = 6.037			CI = 0.0073		CR = 0.0059		

Table 6.18 Pairwise comparison matrix for alternatives on HOS using DCT Tool Material

	G1	G2	G3	G4	G5	G6	Priority Weight
G1	1	1	1/2	1/2	1	1/2	0.1105
G2	1	1	1/3	1/2	1/2	1/2	0.0924
G3	2	3	1	1	2	1	0.2363
G4	2	2	1	1	2	1	0.2211
G5	1	2	1/2	1/2	1	1	0.1420
G6	2	2	1	1	1	1	0.1977
λ_{max} = 6.083			CI = 0.0167		CR = 0.0134		

Next, priority weights of experiments for each of the four response variables (MRR, TWR, SR, HOS) were assigned to four columns of a priority matrix [P]. The resultant 6 x 4 matrix is then multiplied by the single column criterion weight matrix [C], obtained from the criterion weights compiled in Table 6.5, to generate a single column global weight matrix (6 x 1) such that

$$[P] \times [C] = [G] \qquad \textit{Eq. 6.15}$$

where [G] is the required global weight matrix in which G(i, 1) represents the global weight of ith experiment.

6.2.2 Sample Calculation to determine the global weight of MRR corresponding to untreated tool material:

6.2.2.1 Calculation of Priority Weight

Six response values of MRR for UT Tool constitute a response array R such that

$$R = \{0.10703\ 0.3134\ 0.55887\ 0.14567\ 0.29357\ 0.16283\}^T \qquad \textit{Eq. 6.16}$$

Pairwise comparison matrix can be formed by calculating various elements M (i, j) such that M (i, i) = 1; M (1,2) = R(1)/R(2) = 0.10703/0.3134 ≅ 1/3 where R_i is the ith element in the response array [R]. Similarly M(1,3) = R(1)/R(3) = 0.10703/0.55887 ≅ 1/5; M(3,4) = R(3)/R(4) = 0.5588/0.1456 ≅ 4/1 and all the elements of the pairwise comparison matrix can be calculated to complete the matrix. The bottom half of the matrix i.e. elements A(j, i) will be formed by inversing the elements of upper half i.e. A(j,i) = 1/A(i,j) as A(4,3) = 1/A(3,4) = 1/4 and so on. This makes the following pairwise comparison matrix for MRR in case of Untreated Tool:

$$[M] = \begin{bmatrix} 1 & 1/3 & 1/5 & 1 & 1/3 & 1/2 \\ 3 & 1 & 1/2 & 2 & 1 & 2 \\ 5 & 2 & 1 & 4 & 2 & 3 \\ 1 & 1/2 & 1/4 & 1 & 1/2 & 1 \\ 3 & 1 & 1/2 & 2 & 1 & 2 \\ 2 & 1/2 & 1/3 & 1 & 1/2 & 1 \end{bmatrix} \qquad \textit{Eq. 6.17}$$

Once the pairwise comparison matrix is formed, next the priority weight will be computed as per the procedure listed above. First the matrix [M] is squared and the rows are added and normalized which results in following calculation.

[B] = [M] * [M] =

Squared Pairwise Matrix						**Sum of Rows**	**Normalized Val.**
5.9998	2.1499	1.14995	4.6332	2.1499	3.9332	20.01595	0.067492806
17.5	5.9999	3.2666	13	5.9999	11	56.7664	0.191413529
32	11.1665	5.9999	24	11.1665	20.5	104.8329	0.353491419
8.25	2.8333	1.5333	6	2.8333	5.25	26.6999	0.090030759
17.5	5.9999	3.2666	13	5.9999	11	56.7664	0.191413529
9.6665	3.3332	1.8166	7.3332	3.3332	5.9999	31.4826	0.10615779
					TOTAL	296.56415	

[B] * [B] =

Square of the Squared Pairwise Matrix						Sum of Rows	Normalized
224.2867	77.77564	42.09392	167.9366	77.77564	142.3933	732.261795	0.067736
633.1057	219.5954	118.8374	474.142	219.5954	402.043	2067.31902	0.191233
1170.981	406.1203	219.7897	876.9196	406.1203	743.5213	3823.45222	0.353682
297.9786	103.3564	55.9342	223.1882	103.3564	189.2136	973.027405	0.090008
633.1057	219.5954	118.8374	474.142	219.5954	402.043	2067.31902	0.191233
351.2872	121.8408	65.93529	263.0461	121.8408	223.0891	1147.03931	0.106104
					TOTAL	10810.41879	

A further iteration will not show any change in the normalized values and therefore the process of determination of eigen vector is terminated here. The last column of Normalized values is the priority weight array of the MRR for Untreated Tool. Thus,

Priority Wt. = {0.06774 0.19123 0.35368 0.09001 0.19123 0.10611} *Eq. 6.18*

To check the consistency, consistency ratio has to be calculated which in this comes out to be 0.006 which is less than 0.1 as required for the matrix to be consistent.

Now global weights are to be calculated. This is explained using the case of Untreated Tool Materials. Priority Weights Matrix corresponding to all the four response parameters for Untreated tool material is multiplied with criteria weight matrix to generate global weights as specified in equation 6.15.

SR	MRR	TWR	HOS		Criterion weights		Global Weights
0.1994	0.0677	0.1061	0.2222				0.14748
0.2261	0.1912	0.1912	0.2222		0.4948		0.21037
0.1994	0.3537	0.3537	0.2222		0.3102		**0.26928**
0.1622	0.09	0.0677	0.1111	×	0.1336	=	0.12404
0.1131	0.1912	0.1912	0.1111		0.0614		0.14764
0.0997	0.1061	0.09	0.1111				0.10109

The maximum global weight of 0.26928 corresponds to experiment No. 8 in the Design of experiments.

Working on similar lines the global weight matrices are prepared for all the three types of treatment conditions to the tool material viz Untreated, shallow cryogenic treated and deep cryogenic treated and the results are given in Table 6.19 to 6.21.

Table 6.19 Global weights for alternatives of Untreated Tool

Alternatives for UT Tool	**Expt. No.**	**SR Priority weight**	**MRR Priority Weight**	**TWR Priority Weight**	**HOS Priority Weight**	**Global Weight**
G1	1	0.1994	0.0677	0.1061	0.2222	0.1475
G2	6	0.2261	0.1912	0.1912	0.2222	0.2104
G3	8	0.1994	0.3537	0.3537	0.2222	**0.2693**
G4	12	0.1622	0.09	0.0677	0.1111	0.1240
G5	13	0.1131	0.1912	0.1912	0.1111	0.1476
G6	17	0.0997	0.1061	0.09	0.1111	0.1011

Table 6.20 Global weights for alternatives of SCT Tool

Alternatives for SCT Tool	**Expt. No.**	**SR Priority weight**	**MRR Priority Weight**	**TWR Priority Weight**	**HOS Priority Weight**	**Global Weight**
G1	2	0.1553	0.0936	0.077	0.1630	0.1262
G2	4	0.1553	0.1259	0.1497	0.1418	0.1446
G3	9	0.0817	0.0936	0.0802	0.1280	0.0880
G4	10	0.1553	0.1665	0.1603	0.1418	0.1586
G5	14	0.2972	0.3538	0.3831	0.2836	**0.3254**
G6	18	0.1553	0.1665	0.1497	0.1418	0.1572

Table 6.21 Global weights for alternatives of DCT Tool

Alternatives for DCT Tool	Expt. No.	SR Priority weight	MRR Priority Weight	TWR Priority Weight	HOS Priority Weight	Global Weight
G1	3	0.0924	0.105	0.1118	0.1105	0.1000
G2	5	0.142	0.1355	0.12	0.0924	0.1340
G3	7	0.2363	0.2728	0.2943	0.2363	**0.2554**
G4	11	0.1977	0.12	0.1118	0.2211	0.1636
G5	15	0.1105	0.0938	0.1047	0.142	0.1065
G6	16	0.2211	0.2728	0.2573	0.1977	0.2405

6.2.3 Results of Optimization using AHP

The optimal solution is the one that corresponds to maximum global weight corresponding to given condition of the tool material. Accordingly, from Table 6.19, the maximum global weight of 0.2693 corresponds to experiment no. 8, from Table 6.20, the maximum global weight of 0.3254 corresponds experiment no. 14 and from Table 6.21, the maximum value of 0.2554 of global weight corresponds to experiment no. 7. Thus it can be concluded that experimental conditions corresponding to experiment no. 8, 14 and 7 deliver the optimum results for MRR, TWR, SR and HOS when the tool is untreated, shallow cryogenically treated and deep cryogenically treated, respectively.

CHAPTER - 7

CONCLUSIONS AND RECOMMENDATIONS

7.1 CONCLUSIONS

The current study was carried out to investigate the effect of cryogenic treated tool and work material in ultrasonic machining of Ti-6Al-4V. The machining characteristics were measured in terms of material removal rate, tool wear rate, surface roughness, hole oversize and production tolerance grades. Six process parameters associated with machine tool, abrasive slurry, tool material and type of cryogenic treatment were selected for investigation. Experiments were carried out using Taguchi's Design of Experiments with L18 orthogonal array. The results obtained were modeled using artificial neural network approach and optimized with entropy weight based GRA and analytical hierarchy process. SEM analysis was carried out to determine surface topography of the machined region. Following conclusions can be drawn from the study:

1. USM power rating, type of abrasive slurry, tool material and abrasive grit size were found to be the significant parameters affecting material removal rate in ultrasonic machining of Ti-6Al-4V in the order of percentage contribution starting from highest. Large momentum associated with higher power and coarser abrasives resulted in higher value of MRR while hard and strong boron carbide abrasives resulted in effective erosion from work surface. Stainless steel tool with the most favourable work hardening characteristics owing to superior tool-workpiece combination was found to result in maximum MRR. Accordingly the optimum combination resulted from the design of experiments for maximum MRR corresponded to 400W of USM power, Boron Carbide Slurry, Stainless Steel tool material with #220 abrasive grit size using untreated tool material and cryogenic treated work material and was found to be 0.6358 mm^3/min.
2. SEM Micrographs indicate the fracture pattern at the work surface comprising of ductile and brittle modes with the presence of dimples and depressions indicating plastic deformation making ductile mode as the dominant one corresponding to experimental conditions involving lower power ratings and finer abrasive particles, whereas craters of varying depth were observed indicating presence of brittle fracture with larger power and coarser abrasive particles.

3. Tool wear rate in USM was found to be strongly determined by relative tool work-piece hardening. The factors causing higher MRR were also responsible for larger TWR and accordingly higher USM power, stronger and coarser abrasive particles were found to be associated with higher tool wear rate. Further it was also found that the tool material that forms a superior pair with regard to relative work hardening resulted in minimum tool wear. Titanium, though the softest among the three tool materials used, was thus found to be the most effective for minimizing the tool wear. Cryogenic treatment of tool material enhanced wear resistance, caused grain refinement and improved plasticity and thus resulted in reduction of tool wear. The optimum setting for minimum tool wear rate was thus obtained corresponding to aluminium oxide slurry, titanium tool, 100W power, #500 abrasive grit size, deep cryogenic treated tool material and untreated work material and was found to be 0.0975mm^3/min.
4. Slurry grit size was found to be the most significant parameter affecting surface finish followed by power rating, tool type and cryogenic treatment of work material respectively. Coarser abrasives under the high impact energy at higher USM power and harder tool material resulted in deeper craters and hence maximum surface roughness while the improved finish with deep cryogenic treated work-piece could be because of improved ductility of the work material. Minimum surface roughness, and hence the best surface quality, was obtained when machining with aluminium oxide slurry, titanium tool, 20W power rating, #500 grit size and deep cryogenic treated tool and work-piece.
5. Abrasive grit size was observed to be the most significant and dominating parameter affecting dimensional accuracy. Coarser particles led to higher magnitude of HOS as compared to finer particles. USM Power rating and tool material also significantly affected the dimensional accuracy measured in terms of hole oversize. The hole oversize obtained in the study ranged from a minimum of 3.5 to a maximum of 8.5 times the average abrasive particle size. Hole oversize was found to depend on rate of machining. Factors such as high power and coarser abrasives that lead to increased MRR also resulted in increased HOS. On the other hand HOS was also relatively more corresponding to lower power rating as compared to moderate values due to slow rate of machining. This means an optimum machining rate is essential to obtain minimum HOS. The optimum condition for best dimensional accuracy and thus minimum oversize was obtained

with DCT workpiece using SiC slurry and deep cryogenic treated Ti tool at 250W power with an abrasive grit size of #500.

6. Abrasive Grit Size owing to directly involved in the lateral gap between tool and workpiece was the most significant factor in establishing the tolerance grades while USM power and mechanical properties of tool material also significantly affected the tolerance grade. Coarse grains, high power and hard tool material were associated with poor tolerance grades. The obtained tolerance grades ranged from IT 12 to IT 15. The best condition for the closest tolerances was obtained using SiC based slurry of 500 abrasive grit size on deep cryogenic treated work material with 50% of the rated USM power and untreated SS tool.
7. ANN is capable of modelling complex manufacturing problems involving large number of controlling process parameters with relative ease, simplicity and substantial accuracy and thus provides a good alternative to conventional modelling techniques. Single hidden layer 6-7-1 neural network architecture based on LM algorithm using log-sigmoid and pure linear activation function for hidden and output layer respectively was able to effectively model the MRR, TWR and SR. Being a range based model, the modelling results were found to be sufficiently accurate within the given extreme values of process parameters which necessitates a careful selection of the extent of the varied parameters. The validation coefficient of determination for the ANN Models for MRR, TWR, SR and HOS was found to be at 0.936, 0.951, 0.993 and 0.999 respectively while test data correlation coefficient was found to be at 0.982, 0.961, 0.996 and 0.997 respectively thus indicating that the results obtained from ANN modelling are within the acceptable error limits.
8. Optimization of the results obtained was carried out using Grey Relational Analysis and Analytical hierarchy process. Weights were generated using entropy method, wherein entropy was measured across the S/N ratios of MRR and TWR. Thus a hybrid Taguchi-Entropy Weight based GRA method was used to determine the most optimum setting for conflicting for the two responses which was found to correspond with Experiment no. 2 from the L_{18} OA constructed for the study having highest Grey relational Grade of 0.6902. AHP was used to find an optimal solution for all the four response variables. The pairwise comparisons were obtained first, for response variables and then for available alternatives.

7.2 SCOPE FOR FUTURE WORK

While mixing the slurries for exploration of the effect of the mixture, the study was carried out with equal proportions of slurries blended together in similar grit size. A further exploration can be carried out by preparing mixture of varied proportions and different grits sizes especially from economic point of view to get the leverage associated with strong abrasives such as boron carbide. Effect of parameters involved in cryogenic processing cycle such as holding temperature, cooling rates and post treatment tempering and positioning of cryogenic processing in the heat treatment cycle, can also be explored to determine optimum treatment cycle to yield maximum benefit. Use of magnetic abrasives has not found a mention in literature with regard to ultrasonic machining. Magnetic Abrasives together with applied magnetic field can assist stagnation of slurry in the machined zone and hence has the potential for improving the machining characteristics since the time of action of abrasives will improve.

REFERENCES

[1] H. El-Hofy, Advanced Machining Processes: Non Traditional and Hybrid Machining Processes, The McGraw Hill Company, 2006.

[2] P. K. Mishra, Nonconventional Machining, Narosa Publishing House, 2011.

[3] G. Benedict, Non-Traditional Manufacturing Processes, New York, 1987, pp. 67-86.

[4] R. Singh and J. Khamba, "Ultrasonic machining of Ti and its alloys: a review," *Journal of Material Processing Technology*, vol. 173, p. 125–135, 2006.

[5] T. Thoe, D. Aspinwall and M. Wise, "Review on ultrasonic machining," *J. Mach. Tools Manuf.*, vol. 38, no. 4, p. 239–255, 1998.

[6] J. B. Kobles, "Ultrasonic manufacturing process: ultrasonic machining (USM) and ultrasonic impact grinding (USIG).," *Carbide Tool*, vol. 16, no. 5, p. 12–15, 1984.

[7] S. Kuriakosea, P. P. K. Kumar and J. Bhatt, "Machinability study of Zr-Cu-Ti metallic glass by micro hole drilling using micro-USM," *Journal of Materials Processing Technology*, vol. 240, pp. 42-51, 2017.

[8] M. S. Cheema, A. Dvivedi and S. A. Kumar, "An Ultrasonic Micromachining Setup for machining of 3D geometries," in *Proceedings of the International Conference on Research and Innovations in Mechanical Engineering: Lecture Notes in Mechanical Engineering*, Springer India, 2014, pp. 253-260.

[9] V. Kumar, "Ultrasonic machining of tungsten carbide, satellite and diamond," Ph.D. Thesis Thapar University, Patiala, 2009.

[10] P. Legge, "Machining without abrasive slurry’," *Ultrasonics*, p. 157–162, 1966.

[11] N. J. Churi, Z. J. Pei and C. Treadwell, "Rotary ultrasonic machining of Ti alloy (Ti-6Al-4V):effect of tool variables," *Int. J. Precision Technology*, vol. 1, no. 1, pp. 85-96, 2007.

[12] N. J. Churi, Z. C. Li, Z. J. Pei and C. Treadwell, "Rotary ultrasonic machining of Ti alloy: a feasibility study," in *Proceedings of IMECE 2005 ASME*, Orlando, Florida, USA November 5-11, 2005.

[13] N. J. Churi, Z. J. Pei and C. Treadwell, "Rotary ultrasonic machining of Ti alloys: effect of machining variables," *Machining Science and Technology*, vol. 10, no. 3,

p. 301–321, 2006.

[14] M. Komaraiah and P. N. Reddy, "A study on the influence of workpiece properties in ultrasonic machining’," *Int. J. Mach. Tools Manuf.,* vol. 33, no. 3, p. 495–505, 1993.

[15] M. Komaraiah, M. A. Manan, P. N. Reddy and S. Victor, "Investigation of surface roughness and accuracy in ultrasonic machining," *Precis. Eng.,* vol. 10, no. 2, p. 59–65, 1988.

[16] L. A. Balamuth, "Ultrasonic assistance to conventional metal removal’," *Ultrasonics,* vol. 4, p. 125–130, 1966.

[17] T. J. Drozda and C. Wick, "Non-traditional Machining," in *Tool and Manufacturing Engineers Handbook,* vol. 1, Society of Manufacturing Engineers, 1983, p. 1–23.

[18] D. E. Brehl and T. A. Dow, "Review of vibration-assisted machining," *Precision Engineering,* vol. 32, p. 153–172, 2007.

[19] B. Azarhoushang and J. Akbari, "Ultrasonic-assisted drilling of Inconel 738-LC," *International Journal of Machine Tools and Manufacture,* vol. 47, p. 1027–1033, 2008.

[20] Z. Wansheng , W. Zhenlong, D. Shichun, C. Guanxin and W. Hongyu, "Ultrasonic and electric discharge machining to deep and small holes on Ti alloy," *Journal of Material Processing Technology,* vol. 120, p. 101–106, 2002.

[21] J. Zhixin, Z. Jianhua and A. Xing, "Principal research on machining and discharge characteristics of ultrasonic vibration in EDM," *Elect. Mach.,* vol. 6, p. 19, 1994.

[22] Y. C. Lin, B. H. Yan and Y. S. Chang, "Machining characteristics of Ti alloys (Ti–6Al–4V) using a combination process of EDM and USM," *J. Mater. Process. Technol.,* vol. 104, no. 3, p. 171–177, 2000.

[23] Y. F. Chen and Y. C. Lin, "Surface modifications of Al–Zn–Mg alloy using combined EDM with ultrasonic machining and addition of TiC particles into the dielectric," *Journal of Materials Processing Technology,* vol. 209, p. 4343–4350, 2009.

[24] Q. H. Zhang, R. Du, J. H. Zhang and Q. B. Zhang, "An investigation of ultrasonic assisted electrical discharge machining in gas," *International Journal of Machine Tools & Manufacture,* vol. 46, p. 1582–1588, 2006.

[25] S. F. Chang and G. M. Bone, "Burr size reduction in drilling by ultrasonic assistance," *Robotics and Computer-Integrated Manufacturing,* vol. 21, p. 442–450, 2005.

[26] J. Pujana, A. Rivero, A. Celaya and d. L. López, "Analysis of ultrasonic-assisted drilling of Ti6Al4V," *International Journal of Machine Tools & Manufacture,* vol. 49, pp. 500-508, 2009.

[27] J. P. Choi, B. H. Jeon and B. H. Kim, "Chemical-assisted ultrasonic machining of glass," *Journal of Materials Processing Technology,* vol. 191, p. 153–156, 2007.

[28] Z. Liang, Y. Wu, X. Wang and W. Zhao, "A new two-dimensional ultrasonic assisted grinding (2D – UAG) method and its fundamental performance in monocrystal silicon machining," *International Journal of Machine Tools and Manufacture,* vol. 50, p. 728–736, 2009.

[29] I. Yang, M. S. Park and C. N. Chu, "Micro ECM with ultrasonic vibrations using a semi-cylindrical tool," *International Journal of Precision Engineering and Manufacturing,* vol. 10, no. 2, p. 5–10, 2009.

[30] S. Elhami and M. Razfar, "Study of the current signal and material removal during ultrasonic-assisted electrochemical discharge machining," *Int J Adv Manuf Technol,* vol. 92, no. 5-8, p. 1591-1599, 2017.

[31] P. C. Pandey and H. S. Shan, Modern Manufacturing Processes, Tata Mc-Graw Hill, 2004.

[32] R. C. Dorf and A. Kusiak, Handbook of Design, Machining and Automation, Wiley IEEE, 1994, p. 235–240.

[33] R. Singh and J. S. Khamba, "Comparison of machining characteristics of Ti alloys: effect of slurry in ultrasonic machining process," *in Proceedings of the Global Congress on Manufacturing and Management,* 2004.

[34] R. Gilmore, "Ultrasonic machining of ceramics," *SME technical paper series,* 1990.

[35] D. Kremer, "The state of the art of ultrasonic machining," *Ann. CIRP,* vol. 30, no. 1, p. 107–110, 1981.

[36] L. D. Rozenberg, Physical Principles of Ultrasonic Technology, Vols. 1,2, Plenum Press New York, 1973.

[37] S. Das, B. Doloi and B. Bhattacharya, "Recent Advancement on Ultrasonic Micro

Machining (USMM) Process," in *Non-traditional Micromachining Processes: Materials Forming, Machining and Tribology,*, G. K. e. al., Ed., Springer International Publishing AG, 2017.

[38] J. J. Boy, E. Andrey, A. Boulouize and C. K. Malek, "Developments in micro-ultrasonic machining (MUSM) at FEMTO-ST," *Int. J. Adv. Manf. Technol.,* vol. 47, p. 37–45, 2010.

[39] H. Youssef, Theory of Metal Cutting, Dar-El-Maaref, Egypt: Dar-El-Maaref, 1976.

[40] SONIC-MILL 500 W model, Instruction manual for stationary ultrasonic machining, Albuquerque, U.S.A., 2010.

[41] R. Singh and J. S. Khamba, "Study of machining characteristics of Ti alloys in ultrasonic machining," in *Proceedings of the 21st AIMTDR Conference*, Vellore Institute of Technology (Tamilnadu), India., 2004d.

[42] E. A. Neppiras, "Report on ultrasonic machining," *Metalwork. Prod.,* vol. 100, p. 1283–1288, 1956.

[43] J. A. McGeough, Advanced Methods of Machining, Chapman & Hall, 1988, p. 170–198.

[44] D. Prabhakar and M. Haselkorn, "An experimental investigation of material removal rates in rotary ultrasonic machining," *Trans. NAMR1/SME,* vol. 20, p. 211–218, 1992.

[45] E. J. Weller, Non-traditional Machining Processes, Society of Manufacturing Engineers, 1984.

[46] M. Haslehurst, Manufacturing Technology, 3rd ed., 1981, p. 270–271.

[47] D. Goetze, "Effect of vibration amplitude, frequency and composition of the abrasive slurry on the rate of ultrasonic machining in Ketos tool steel," *J. Acoust. Soc. Am.,* vol. 28, no. 6, p. 1033–1037, 1956.

[48] M. C. Shaw, "Ultrasonic grinding," *Microtechnic*, vol. 10, no. 6, p. 257–265, 1956.

[49] E. A. Neppiras and R. D. Foskett, Ultrasonic machining, Philips Technical Review, 1956.

[50] H. Dam, J. Jensen and P. Quist, "Surface characterization of ultrasonic machined ceramics with diamond impregnated sonotrode," in *Proceedings of the International Conference on Machining of Advanced Metals*, Gaithersburg,

Maryland, 1993.

[51] S. Aggarwal, "On the mechanism and mechanics of material removal in ultrasonic machining," *International Journal of Machine Tools and Manufacture,* vol. 96, pp. 1-14, 2015.

[52] P. L. Guzzo, A. H. Shinohara and A. A. Raslan, "A comparative study on ultrasonic machining of hard and brittle materials," *Journal of Brazilian Society of Mechanical Sciences and Engineering,* vol. 26, no. 1, p. 56–61, 2004.

[53] G. S. Kainth, A. Nandy and K. Singh, "On the mechanics of material removal in ultrasonic machining," *International Journal of Machine Tools Des. Res.,* vol. 19, pp. 33-41, 1979.

[54] K. L. Kuo, H. Hocheng and C. C. Hsu, "Ultrasonic Machining," in *Advanced Analysis of Nontraditional Machining*, H. Y. Hocheng H. and Tsai, Ed., Springer Science+Business Media New York, 2013, pp. 325-357.

[55] V. Soundararajan and V. Radhakrishnan, "An experimental investigation on the basic mechanisms involved in ultrasonic machining," *International Journal of Machine Tool Design and Research,* vol. 26, no. 3, p. 307–321, 1986.

[56] Z. Y. Wang and K. P. Rajurkar, "Dynamic analysis of ultrasonic machining process," *ASME Journal of Manufacturing Science & Enggineering,* vol. 118, pp. 376-381, 1996.

[57] D. Kremer, G. Bazine and A. Moison, "Ultrasonic machining improves EDM technology," in *Proceedings of the Seventh International Symposium on Electro Machining*, Birmingham, UK, 1983.

[58] M. Rahman, Y. S. Wong and A. R. Zareena, "Machinability of Titanium alloys," *JSME International Journal Series C,* vol. 46, no. 1, pp. 107-115, 2003.

[59] K. Gupta and R. F. Laubscher, "Sustainable machninig of titanium alloys: A critical review," *Proceedings of the Institution of Mechanical Engineers, Part B: Journal of Engineering Manufacture*, pp. 1-18, 2016.

[60] E. Abele and B. Frohlich, "High speed milling of titanium alloys," *Advances in Production Engineering and Management,* vol. 3, no. 3, pp. 131-140, 2008.

[61] E. O. Ezugwu and Z. M. Wang, "Ti alloys and their machinability – a review," *Journal of Material Processing Technology*, vol. 68, pp. 262-274, 1997.

[62] J. R. Myers, H. B. Bomberger and F. H. Froes, "Corrosion behavior and use of Ti and its Alloys," *Journal of Metals,* vol. 36, pp. 50-59, 1984.

[63] L. Thornes, "Ti is difficult to machine fact or fiction," *Metalworking Production,* pp. 15-16, 2001.

[64] W. Konig, "Proc. 47th Meeting of AGARD Structural and Materials Panel," in *AGARD Conference Proceedings No. 256,* AGARD, CP256, London, 1979.

[65] H. C. Child and A. F. Dalton, "ISI Special Report 94," p. 139–142, 1968.

[66] B. B. Johnson, "Tips on Milling Titanium-and Tools to Do the job," in *Proc. Symp. Machining and Grinding of Titanium*, 1982.

[67] S. Y. Hong and Y. Ding, "Cooling approaches and cutting temperatures in cryogenic machining of Ti-6Al-4V," *International Journal of Machine Tools & Manufacture,* vol. 41, pp. 1417-1437, 2001.

[68] X. Zhang, R. Shivpuri and A. Srivastava, "Role of phase transformation in chip segmentation during high speed machining of dual phase titanium alloys," *Journal of Materials Processing Technology,* vol. 214, pp. 3048-3066, 2014.

[69] J. Khamba and R. Singh, "Effect of alumina (white fused) slurry in ultrasonic assisted drilling of Ti alloys (TITAN 15)," in *Proceedings of the National Conference on Materials and Related Technologies (NCMRT-2003),* TIET Patiala (Pb.), 2003.

[70] R. Singh and J. S. Khamba, "A framework for modeling the machining characteristics of Ti alloys using USM," in *in Proceedings of the International Conference on Digital-aided Modeling and Simulation*, CIT, Coimbatore, India,, 2003.

[71] R. Singh and J. S. Khamba, "Tool manufacturing technique in ultrasonic drilling machine," *The International Journal of Advanced Manufacturing Technology,* vol. 3, no. 1, pp. 5-7, 2004.

[72] R. Singh and J. S. Khamba, "Machining characteristics comparison of Ti alloys in ultrasonic assisted drilling," in *Proceedings of the International Conference on Recent Advances in Composite Materials,* Institute of Technology, B.H.U, India, 2004.

[73] R. Singh and J. S. Khamba, "Comparison of slurry effect on machining

characteristics of Ti in ultrasonic drilling," *Journal of Material Processing Technology,* vol. 197, pp. 200-205, 2008.

[74] P. S. Babu, P. Rajendran and K. N. Rao, "Cryogenic treatment of M1, EN19 and H13 tool steels to improve wear resistance," *IE(I) Journal – MM,* vol. 86, pp. 64-66, 2005.

[75] D. M. Lal, S. Renganarayanan and A. Kalanidhi, "Cryogenic treatment to augment wear resistance of tool and die steels," *Cryogenics,* vol. 41, pp. 149-155, 2001.

[76] A. Bensely, S. Venkatesh, D. M. Lal, G. Nagarajan, A. Rajadurai and K. Junik, "Effect of cryogenic treatment on distribution of residual stress in case carburized En 353 steel," *Materials Science and Engineering A,* vol. 479, pp. 229-235, 2008.

[77] P. Ghosh and N. Dhokey, "Optimization of Cryosoaking Period and Microstructural Transformation on Wear Mechanism of SAE8620 Gear Steel," *Tribology Transactions,* vol. 60, no. 6, p. 1070-1077, 2017.

[78] H. G. Nanesa, H. Touazine and M. Jahazi, "Influence of cryogenic process parameters on microstructure and hardness evolution of AISI D2 tool steel," *Int J Adv Manuf Technol,* 2016.

[79] K. Ray and D. Das, "Improved wear resistance of steels by cryotreatment: The current state of understanding," *Materials Science and Technology,* vol. 33 no. 3, p. 340-354, 2017.

[80] F. J. d. Silva, S. D. Franco, A. R. Machado, E. O. Ezugwu and J. A. M. Souza, "Performance of cryogenically treated HSS tools," *Wear,* vol. 261, pp. 675-685, 2006.

[81] D. Das, A. K. Datta, V. Toppo and K. K. Ray, "Effect of Deep cryogenic treatment on the carbide precipitation and tribological behavior," *Materials and Manufacturing Processes,* vol. 22, no. 4, pp. 474-480, 2007.

[82] F. R. Baron, "Yes – Cryogenic Treatment Can Save You Money! Here's Why," *Tapi,* vol. 57, no. 5, pp. 35-40, 1974.

[83] P. Paulin, "Frozen gears," *Gear Technology,* pp. 26-28, 1993.

[84] J. Y. Huang, Y. T. Zhu, X. Z. Liao, I. J. Beyerlein, M. A. Bourke and T. E. Mitchell, "Microstructure of cryogenic treated M2 tool steels," *Material Science Engineering* , vol. A399, pp. 241-244, 2003.

[85] Z. Yuan-zhi, Y. Zhi-min, Z. Yong, L. Quan-Feng and F. WenShang, "Effects of cryogenic treatment on material properties and microstructure of Fe-Cr-Mo-Ni-C-Co alloy," *Journal of Central South Univ Technology,* vol. 15, pp. 454-458, 2008.

[86] D. Das, A. K. Dutta and K. K. Ray, "On enhancement of wear resistance of tool steels by cryogenic treatment," *Philosophical Magazine Letters,* vol. 88, no. 11, pp. 801-811, 2008.

[87] F. Cajner, V. Leskovesk, D. Landek and H. Cajner, "Effect of deep cryogenic treatment on high speed steel properties," *Materials and Manufacturing Processes,* vol. 24, no. 7, pp. 743-746, 2009.

[88] J. Vimal, A. Bensely, D. M. Lal and K. Srinivasan, "Deep cryogenic treatment improves wear resistance of En31 steel," *Materials and Manufacturing Processes,* vol. 23, no. 4, pp. 369-376, 2008.

[89] D. Das and K. K. Ray, "On the mechanism of wear resistance enhancement of tool steels by cryogenic treatment," *Philosophical Magazine Letters,* vol. 92, no. 6, pp. 295-303, 2012.

[90] D. Senthilkumar and I. Rajendran, "Optimization of Deep cryogenic Treatment to reduce wear loss of 4140 steel," *Materials and Manufacturing Processes,* vol. 27, no. 5, pp. 567-572, 2012.

[91] K. Amini, A. Akhbarizadeh and S. Javadpour, "Effect of deep cryogenic treatment on formation of nano sized carbide and the wear behavior of D2 tool steel," *International Journal of Minerals, Metallurgy and Materials,* vol. 19, no. 9, pp. 795-799, 2012.

[92] A. Molinari, M. Pellizzari, S. Gialanella, G. Straffelini and K. H. Staisny, "Effect of deep cryogenic treatment on mechanical properties of tool steels," *Journal of Material Processing Technology,* vol. 118, no. 1-3, pp. 350-355, 2001.

[93] G. Prieto, J. E. P. Ipina and W. R. Tuckart, "Cryogenic treatments on AISI420 stainless steel: Microstructure and Mechanical properties," *Materials Science and Engineering A,* vol. 605, pp. 236-243, 2014.

[94] B. Podgornik, I. Paulin, B. Zajec, S. Jacobson and V. Leskovsek, "Deep cryogenic treatment of tool steels," *Journal of Materials Processing Technology,* vol. 229, pp. 398-406, 2016.

[95] J. W. Kim, J. A. Griggs, J. D. Regan, R. A. Ellis and Z. Cai, "Effect of cryogenic

treatment on nickel Ti endodontic instruments," *International Endodontic Journal,* vol. 38, no. 6, pp. 364-371, 2005.

[96] Y. Jiang, D. Chen, Z. Chen and J. Liu, "Effect of Cryogenic Treatment on the Microstructure and Mechanical Properties of AZ31 Magnesium Alloy," *Materials and Manufacturing Processes,* vol. 25, no. 9, pp. 837-841, 2010.

[97] X. Chuang-xian, Z. Xin-ming, D. Yun-lai, X. Yang, D. Zhen-zhen and C. Bu-xiang, "Effects of cryogenic treatment on mechanical properties of extruded Mg-Gd-Y-Zr (Mn) alloys," *Journal of Central South University of Technology,* vol. 14, no. 3, pp. 305-309, 2007.

[98] C. J. Isaak and W. Reitz, "The Effects of Cryogenic Treatment on the Thermal Conductivity of GRCop-84," *Materials and Manufacturing Processes,* vol. 23, no. 1, pp. 82-91, 2008.

[99] S. Kumar, A. Batish, R. Singh and T. P. Singh, "Machining performance of cryogenically treated Ti–5Al–2.5Sn titanium alloy in electric discharge machining: A comparative study," *Proc IMechE Part C, Journal of Mechanical Engineering and Sciences,* pp. 1-8, 2016.

[100] T. Vinothkumar, D. Kandaswamy, G. Prabhakaran and A. Rajadurai, "Effect of dry cryogenic treatment on Vickers hardness and wear resistance of new martensitic shape memory nickel titanium alloy," *European Journal of Dentistry,* vol. 9, pp. 513-517, 2015.

[101] K. Gu, H. Zhang, B. Zhao, J. Wang, Y. Zhou and Z. Li, "Effect of cryogenic treatment and aging treatment on the tensile properties and microstructure of Ti–6Al–4V alloy," *Materials Science & Engineering A,* vol. 584, pp. 170-176, 2013.

[102] K. Gu, J. Wang and Y. Zhou, "Effect of cryogenic treatment on wear resistance of Ti-6Al–4V alloy for biomedical applications," *Journal of mechanical behavior of biomedical materials,* vol. 30, pp. 131-139, 2014.

[103] S. S. Gill and J. Singh, "Effect of Deep Cryogenic Treatment on Machinability of Titanium Alloy (Ti-6246) in Electric Discharge Drilling," *Materials and Manufacturing Processes,* vol. 25, no. 6, pp. 378-385, 2010.

[104] J. Sun and Y. B. Guo, "Material flow stress and failure in multiscale machining titanium alloy Ti-6Al-4V," *International Journal of Advanced Manufacturing Technology,* vol. 41, p. 651–659, 2009.

[105] C. H. Che-Haron and A. Jawaid, "The effect of machining on surface integrity of titanium alloy Ti–6% Al–4% V," *Journal of Materials Processing Technology,* vol. 166, pp. 188-192, 2005.

[106] P. F. Zhang, N. J. Churi, Z. J. Pei and C. Treadwell, "‘Mechanical drilling processes for titanium alloys Literature Review," *Machining Science and Technology,* vol. 12, pp. 1-18, 2008.

[107] P. J. Arrazola, A. Garay, L. M. Iriarte, M. Armendia, S. Marya, F. Maître and Le, "Machinability of titanium alloys (Ti6Al4V and Ti555.3)," *Journal of Materials Processing Technology,* vol. 209, p. 2223–2230, 2009.

[108] P. Crawforth, B. Wynne, S. Turner and M. Jackson, "Subsurface deformation during precision turning of a near-alpha titanium alloy," *Scripta Materialia,* vol. 67, pp. 842-845, 2012.

[109] N. Khanna and J. P. Davim, "Design-of-experiments application in machining titanium alloys for aerospace structural components," *Measurement,* vol. 61, pp. 280-290, 2015.

[110] J. Kumar, J. S. Khamba and S. K. Mohapatra, "An investigation into the machining characteristics of Ti using ultrasonic machining," *International Journal of Machining and Machinability of Materials,* vol. 3, no. 1-2, p. 143–161, 2008.

[111] D. A. Dornfield, J. S. Kim, H. Dechow, J. Hewsow and L. J. Chen, "Drilling burr formation in Ti alloy Ti–6Al–4V’," *Ann. CIRP,* vol. 48, no. 1, pp. 73-76, 1999.

[112] A. L. Mantle and D. K. Aspinwall, "Single point turning of Ti aluminide intermetallic’, in Ti 95," in *Proceedings of the Eighth World Conference on Ti,* 1995.

[113] A. F. Kazantsev, "Ultrasonic cutting," in *Physical principles of Ultrasonic Technology,* vol. 1, L. D. Rozenberg, Ed., Plenum Press, New York, 1973, pp. 3-37.

[114] J. Kumar and J. S. Khamba, "‘Modeling the material removal rate in ultrasonic machining of titanium using dimensional analysis’," *Inernational Journal of Advanced Manufacturing Technology,* vol. 48, pp. 103-119, 2010.

[115] R. Singh, "Experimental investigations on machining characteristics of titanium in ultrasonic impact grinding," *International Journal of Computational Materials Science and Surface Engineering,* vol. 3, no. 1, pp. 24-33, 2010.

[116] R. Singh and J. S. Khamba, "Investigation or ultrasonic machining of Ti and its alloys," *Journal of Material Processing Technology,* vol. 183, pp. 363-367, 2007a.

[117] R. Singh and J. S. Khamba, "Macro model for ultrasonic machining of Ti and its alloys: designed experiments," *J. Eng. Manf.,* vol. 221, pp. 221-229, 2007b.

[118] R. Singh and J. Khamba, "Comparison of slurry effect on machining characteristics of Ti in ultrasonic drilling," *Journal of Material Processing Technology,* vol. 197, pp. 200-205, 2008.

[119] R. Singh and J. S. Khamba, "Mathematical modeling of tool wear rate in ultrasonic machining of Ti," *International Journal of Advanced Manufacturing Technology,* vol. 43, no. 5-6, pp. 573-580, 2009a.

[120] J. Kumar and J. S. Khamba, "An experimental study on ultrasonic machining of pure Ti using designed experiments," *Journal of the Brazilian Society of Mechanical Sciences & Engineering,* vol. 30, no. 3, pp. 231-238, 2008.

[121] J. Kumar, J. S. Khamba and S. K. Mohapatra, "Investigating and modeling tool wear rate in ultrasonic machining of Ti," *International Journal of Advanced Manufacturing Technology,* vol. 41, p. 1107–1117, 2009.

[122] A. Dvivedi and P. Kumar, "Surface quality evaluation in ultrasonic drilling through the Taguchi technique," *International Journal of Advanced Manufacturing and Technology,* vol. 34, pp. 131-140, 2007.

[123] G. K. Dhuria, R. Singh and A. Batish, "Ultrasonic machining of titanium and its alloys: a state of art review and future prospective," *International Journal of Machining and Machinability of Materials,* vol. 10, no. 4, pp. 326-355, 2011.

[124] J. Kumar, "Ultrasonic machining—a comprehensive review," *Machining Science and Technology: An International Journal,* vol. 17, no. 3, pp. 325-379, 2013.

[125] S. Patil, S. Joshi, A. Tewari and S. S. Joshi, "Modeling and Simulation of Effect of Ultrasonic Vibrations on Machining of Ti6Al4V," *Ultrasonics,* vol. 54, no. 2, pp. 694-705, 2014.

[126] R. Muhammad, A. Maurotto, M. Demiral, A. Roy and V. V. Silberschmidt, "Thermally enhanced ultrasonically assisted machining of Ti alloy," *CIRP Journal of Manufacturing Science and Technology,* vol. 7, no. 2, pp. 159-167, 2014.

[127] A. Roy and V. V. Silberschmidt, "Ultrasonically assisted machining of Titanium

alloys," *IN: Paulo Davim, J. (ed). Machining of Titanium Alloys,* pp. 131-147, 2014.

[128] J. Kumar, "Investigations into the surface quality and micro-hardness in the ultrasonic machining of titanium (ASTM GRADE-1)," *Journal of the Brazilian Society of Mechanical Sciences & Engineering,* vol. 36, no. 4, pp. 807-823, 2014.

[129] M. Adithan and V. C. Venkatesh, "Production accuracy of holes in ultrasonic drilling," *Wear,* vol. 40, pp. 309-318, 1976.

[130] M. S. Cheema, P. K. Singh, O. Tyagi, A. Dvivedi and A. K. Sharma, "Tool wear and form accuracy in ultrasonically machined microchannels," *Measurement,* vol. 81, pp. 85-94, 2016.

[131] S. R. Jadoun, P. Kumar, R. Mishra and B. Mehta, "Optimization of process parameters for ultrasonic drilling of advanced engineering ceramics using the Taguchi approach," *Engineering Optimization,* vol. 38, no. 7, pp. 771-787, 2006.

[132] R. S. Jadoun, P. Kumar, B. K. Mishra and R. C. S. Mehta, "Manufacturing process optimisation for tool wear rate in ultrasonic drilling of engineering ceramics using the Taguchi method," *International Journal of Machining and Machinability of Materials,* vol. 1, no. 1, 2006.

[133] V. Kumar and J. S. Khamba, "Parametric optimization of ultrasonic machining of co-based super alloy using the Taguchi multi-objective approach," *Production Engineering- Research and Development,* vol. 3, pp. 417-425, 2009.

[134] R. Jadoun, P. Kumar and B. Mishra, "Taguchi's optimization of process parameters for production accuracy in ultrasonic drilling of engineering ceramics," *Prod. Eng. res. Devel.,* vol. 3, pp. 243-253, 2009.

[135] H. Lalchhuanvela, D. Biswanath and B. Bhattacharyya, "Enabling and Understanding Ultrasonic Machining of Engineering Ceramics Using Parametric Analysis," *Materials and Manufacturing Processes,* vol. 27, no. 4, pp. 443-448, 2012.

[136] H. Lalchhuanvela, B. Doloi and B. Bhattacharyya, "Analysis on profile accuracy for ultrasonic machining of alumina ceramics," *International Journal of Advanced Manufacturing Technology,* vol. 67, p. 1683–1691, 2013.

[137] B. B. Shrikrushna, S. P. Raju and P. K. Brahmankar, "Effect of process Parameters on MRR, TWR and surface topography in ultrasonic machining of alumina-zirconia

ceramic composite," *Ceramics International*, vol. 40, no. 8, p. 12831–12836.

[138] R. Kataria, J. Kumar and B. S. Pabla, "Experimental Investigation into the Hole Quality in Ultrasonic Machining of WC-Co Composite," *Materials and Manufacturing Processes,* vol. 30, no. 7, pp. 921-933, 2015.

[139] R. Kataria, J. Kumar and B. S. Pabla, "Experimental Investigation and Optimization of Machining Characteristics in Ultrasonic Machining of WC-Co Composite Using GRA Method," *Materials and Manufacturing Processes,* vol. 31, no. 5, pp. 685-693, 2016.

[140] E. D. Marquardt, J. P. Le and R. Ray, "Cryogenic Material Properties Database," in *11th international Cryocooler Conference*, Keystone, Co., 2000.

[141] N. B. Dhokey and S. Nirbhavne, "Dry sliding wear of cryotreated multiple tempered D-3 tool steel," *Journal of materials processing technology,* vol. 209, pp. 1484-1490, 2009.

[142] A. Akhbarizadeh, A. Shafeyi and M. A. Golozar, "Effects of cryogenic treatment on wear behavior of D6 tool steel," *Materials and design,* vol. 30, pp. 3259-3264, 2009.

[143] S. S. Gill, R. Singh, H. Singh and J. Singh, "Wear behavior of cryogenically treated tungsten carbide inserts under dry and wet turning conditions," *International Journal of Machine tools and Manufacture,* vol. 49, pp. 256-260, 2009.

[144] S. Akincioğlu, H. Gökkaya and İ. Uygur, "A review of cryogenic treatment on cutting tools," *The International Journal of Advanced Manufacturing Technology,* vol. 78, no. 9, pp. 1609-1627, 2015.

[145] T. Barker, Engineering Quality by Design: Interpreting the Taguchi approach, New York, Marcel-Dekker, Inc.,, 1990.

[146] D. Byrne and S. Taguchi, "The Taguchi approach to parameter design," *Quality Progress,* vol. 20, pp. 19-26.

[147] J. Kumar, "Investigating the machining characteristics of Titanium using Ultrasonic Machining," Thapar University, Patiala, 2009.

[148] K. Jangra, S. Grover and A. Aggarwal, "Optimization of multi machining characteristics in WEDM of WC-5.3%Co composite using integrated approach of Taguchi, GRA and entropy method," *Frontiers of Mechanical Engineering,* vol. 7,

no. 3, pp. 288-299, 2012.

[149] R. Singh, R. Kumar, L. Feo and F. Fraternali, "Friction welding of dissimilar plastic/polymer materials with metal powder reinforcement for engineering applciations," *Composites Part B,* vol. 101, pp. 77-86, 2016.

[150] P. Ross, Taguchi technique for quality engineering, McGraw Hill Book Company, New York, 1988.

[151] T. Bagchi, Taguchi Methods explained: Practical steps to robust design, Prentice Hall of India Private Ltd., 1993, pp. 11-19.

[152] R. Roy, A primer on the Taguchi Method",, New York: Van Nostrand Reinhold, 1990.

[153] "UNI EN 20286-1 ISO system of limits and fits. Bases of tolerances, deviations and fits (1995)".

[154] W. Derek, Analysis for optimum decisions, New York: Wiley International, 1982.

[155] S. Das, S. Kumar, B. Doloi and B. Bhattacharyya, "Experimental studies of ultrasonic machiningon hydroxyapatite bio-ceramics," *Int J Adv Manuf Technol,* vol. 86, no. 1-4, p. 829-839, 2016.

[156] M. Ramulu, "Ultrasonic machining effects on the surface finish and strength of silicon carbide ceramics," *International Journal of Manufacturing Technology Management,* vol. 7, no. 2/3/4, pp. 107-125, 2005.

[157] H. Lalchhuanvela, B. Doloi and B. Bhattacharya , "Experimental Investigation based analysis on ultrasonic drilling of alumina," in *Proceedings of 2nd International and 23rd All India Manufacturing Technology, Design and Research (AIMTDR),* IIT Madras, 2008.

[158] H. Bhadeshia, "Neural networks in materials science," vol. 39, no. 10, pp. 966-979, 1999.

[159] A. Barr and E. A. Feigenbaum, The Handbook of Artificial Intelligence, William Kauffman Inc., Los Altos, California, 1981.

[160] D. Baughman, "Neural Networks in Bioprocessing and Chemical Engineering," Virginia Polytechnic Institute and State University, 1995.

[161] S. N. Sahu, "Neural Network Modelling and Multi-objective optimization of EDM process," NIT Rourkela, 2012.

[162] A. K. Pandey and A. K. Dubey, "Modeling and optimization of kerf taper and surface roughness in laser cutting of Ti alloy sheet," *Journal of Material Science and Technology,* vol. 27, no. 7, pp. 2115-2124, 2013.

[163] K. V. Kumar and A. N. Sait, "Modelling and optimisation of machining parameters for composite pipes using artificial neural network and genetic algorithm," *International Journal on Interactive Design and Manufacturing,* vol. 11, no. 2, pp. 435-443, 2017.

[164] F. Kara, K. Aslantas and A. Cicek, "ANN and multiple regression method based modelling of cutting forces in orthogonal machining of AISI 316L stainless steel," *Neural Comput & Applic,* vol. 26, pp. 237-250, 2015.

[165] G. Kant and K. S. Sangwan, "Predictive Modelling and Optimization of Machining Parameters to Minimize Surface Roughness using Artificial Neural Network Coupled with Genetic Algorithm," *Procedia CIRP,* vol. 31, p. 453 – 458, 2015.

[166] A. G. Olabi, G. Casalino, K. Y. Benyounis and M. S. J. Hashmi, "An ANN and Taguchi algorithms integrated approach to the optimization of CO_2 laser welding," *Advances in Engineering Software,* vol. 37, no. 10, pp. 643-648, 2006.

[167] G. K. M. Rao, G. Rangajanardha, D. H. Rao and M. S. Rao, "Development of hybrid model and optimization of surface roughness in electric discharge machining using artificial neural networks and genetic algorithm," *journal of materials processing technology,* vol. 209, pp. 1512-1520, 2009.

[168] R. Singh, "Investigating the machining characteristics of Titanium aloys using ultrasonic machining," Thapar Institute of Engineering and Technology, Patiala, 2006.

[169] H. L. Lin, "The use of the Taguchi method with grey relational analysis and a neural network to optimize a novel GMA welding process," *Journal of Intelligent Manufacturing,* vol. 23, no. 5, pp. 1671-1680, 2012.

[170] S. Sivasankar and R. Jeyapaul, "Application of Grey Entropy and Regression Analysis for Modelling and Prediction on Tool Materials Performance During EDM of Hot Pressed ZrB2 at Different Duty Cycles," *Procedia Engineering,* vol. 38, pp. 3977-3991, 2012.

[171] K. L. Wen and T. C. Chang, "The grey entropy and its application in weighting analysis," in *Proceedings of IEEE International Conference on System, Man and*

Cybernetics, 1998.

[172] T. L. Saaty, "Decision making with the analytic hierarchy process," *Int. J. Services Sciences,*, vol. 1, no. 1, pp. 83-98, 2008.

[173] A. Bhattacharya , A. Batish and G. Singh, "Optimization of powder mixed electric discharge machining using dummy treated experimental design with analytic hierarchy process," *Proceedings of the Institution of Mechanical Engineers Part B Journal of Engineering Manufacture,* vol. 226, no. 1, pp. 103-116, 2011.